# GEOMAGNETIC INVESTIGATIONS

# OF SOME

# RECENT BRITISH SEDIMENTS

Gillian M. Turner

Doctor of Philosophy

University of Edinburgh

1979

## DECLARATION

I hereby declare that the work presented in this thesis is my own, unless otherwise stated in the text, and that the thesis has been composed by myself.

Gillian M. Turner

ABSTRACT

In order to study the geomagnetic secular variation in Britain during the past 10000 years six metre and one metre long cores of post-Glacial sediment have been collected from three British lakes. Magnetic measurements were made on both the whole cores and on sub-samples from them. The natural remanent magnetization is stable, and records well defined declination and inclination swings of 40-50° and 15-20° peak-peak amplitudes respectively. There is also much between swing detail. Both the major swings and many finer details are readily correlated from core to core and lake to lake. Thirty radio-carbon age determinations, pollen analyses and correlations with observatory and archaeomagnetic records have been combined to derive a detailed time scale. This time scale has been transferred to all the cores by means of magnetic susceptibility and lithological correlations. Fourier analyses of declination and inclination, separately and combined as a complex pair, show that the variations are not simply periodic, nor is their spectrum constant with time. The geomagnetic vector has been looping in a clockwise sense for most of the past 10000 years. The records have been compared with other lacustrine and archaeomagnetic results from other countries, and various models for the non dipole field are discussed in the light of all these records.

Attempts to retrieve palaeointensities from the sediments have shown that ARM may provide an effective normalization parameter in some, but by no means all cases. Determining the suitability of sediments for palaeointensity studies is complicated.

Field tests were carried out to investigate the magnetic minerals in the soils of the drainage basin of one lake; soil and lake sediment samples were further analysed in the laboratory. In addition to magnetite an impure form of maghaemite appears to play some part in carrying the

NRM of this lake sediment.

Continental shelf sediment cores have also been collected from the Firth of Clyde. These have been correlated with each other by their susceptibility logs, and dated by correlation of their secular variation records with the lake sediment record.

ACKNOWLEDGEMENTS

I would like to thank Dr. Roy Thompson for suggesting the topic of my research, and for the encouragement and guidance he has given me throughout my work.

I am also grateful to the University of Edinburgh and Professor K.M. Creer for providing equipment and facilities, and to all members of the Geophysics Department for their friendship and generosity, and many hours of discussion, both technical and frivolous. My thanks go especially to Alex Jackson and Jennifer Neligan for help on fieldwork and in the laboratory.

I would also like to thank Drs. M.S. Baxter, J. Dickson, and D.A. Stewart of Glasgow University, Professor F. Oldfield and Jan Bloemendal of Liverpool University and Dr. W. Tutin of Leicester University for radiocarbon age estimates and pollen analyses.

My thanks also go to Dr. E. Hailwood of Southampton University for use of their Curie Balance, and his hospitality while I was there, to Mr. Moelwyn Williams for allowing us to dig holes in his fields, and to the Captain and crew of R.R.S. John Murray for all their help on board ship.

I am indebted to my husband and typist Malcolm Ingham for his endless help and patience.

This work was carried out while I was in receipt of a NERC studentship.

CONTENTS

LIST OF FIGURES

LIST OF TABLES

## ABBREVIATIONS

| | |
|---|---|
| AF | alternating field |
| ARM(C) | anhysteretic remanemt magnetization (AF cleaned) |
| B | magnetic field |
| $B_{CR}$ | coercivity of remanence |
| D | declination |
| $D_T$ | "transformed" declination |
| DRM | detrital remanent magnetization |
| dDRM | depositional DRM |
| pdDRM | post depositional DRM |
| FFT | fast fourier transform |
| I | inclination |
| $I_T$ | "transformed" inclination |
| IRM(C) | isothermal remanent magnetization (AF cleaned) |
| M | intensity of remanence |
| md | multi domain |
| MDF | median destructive field |
| NRM(C) | natural remanent magnetization (AF cleaned) |
| PIM | pulse induction meter |
| PPM | proton precession magnetometer |
| PT | preferred time |
| sd | single domain |
| SIRM | saturated isothermal remanent magnetization |
| SUSC or | magnetic susceptibility |
| TRM | thermoremanent magnetization |

UNITS - S.I. units are used throughout the thesis. A conversion table to c.g.s. is given in Appendix 2.

# CHAPTER 1: INTRODUCTION.

What is a magnetic field? It is invisible and intangible, penetrates some materials with difficulty, some more easily, and penetrates nothing easiest of all. Despite this enigma we are forever surrounded by the magnetic field of our own planet, and its effects are familiar parts of our everyday life. Indeed life would be quite different without it. But, what is its cause? Has it always existed? Will it ever end? Why is it continuously changing? Can we forecast its behaviour? Geomagnetists and palaeomagnetists worldwide are trying to answer these questions from the evidence of the past and present geomagnetic field.

In 1839 Gauss, by studying the radial dependance of successive spherical harmonic coefficients of the field, established that its source lies within the earth. Prior to this, William Gilbert (De Magnete, 1600) had noted the resemblance of the geomagnetic field to that of a uniformly magnetized sphere. Most models suggested since then have been based on a dipole placed at the centre of the earth. It is now known that the source cannot be a permanent remanent magnetization - it is too deep seated to be below the Curie point of any known magnetic materials. Nor is it an intrinsic property of rotating bodies, as suggested by Blackett (1947), as it increases in magnitude with depth (Runcorn et al., 1951). It is now believed to originate in the fluid motion of the iron/silicon outer core of the earth: the motion of a conducting fluid in an existing magnetic field induces currents, which themselves possess magnetic fields reinforcing the original ones. This is the general idea of the homogeneous, self-exciting dynamo, suggested by Elsasser (1946, 1947), Bullard

(1949) and Bullard and Gellman (1954). Lowes and Wilkinson (1951) have built a laboratory model dynamo which also reverses its polarity periodically (see below re reversals).

In addition to varying with global position, the magnitude and direction of the geomagnetic field also vary with time at any given site. This has been known since observatory records were first kept in the sixteenth century. These changes, the "secular variation", have a spectrum of periodicities extending from microseconds up to tens of thousands of years. The long period changes are of internal origin, probably an effect of features in the core growing, drifting and decaying. Some authors however, believe their origin to be in the relative solar and planetary motions; gravitational effects like the tides and precession and nutation of the earth's rotation axis (Malkus, 1963; Kawai et al., 1967). The most dramatic feature of the secular variation is the occassional complete reversal of the field. This has not occured during historical time, but has been inferred from palaeomagnetic records (see below). The time intervals between successive reversals seems to be quite random (Cox, 1968; Laj et al., 1979), but of the order of $10^5$ - $10^6$ years, a reversal taking place in about $10^3$ - $10^4$ years. Intensity changes accompany the direction reversal. The intensity remains very low for a period at least as long as the direction change (Dunn et al., 1971).

## 1.1: Description of the geomagnetic field.

Mathematically it is convenient to express the potential of the geomagnetic field, V, ($B = -\text{grad } V$), as an expansion of spherical harmonics. It is then possible to tabulate each

component and the annual variation in each component, and hence by linear or quadratic extrapolation to predict the magnetic field changes for navigational purposes. However, the extrapolation is inaccurate and frequent updating of charts is necessary. The first three terms of this spherical harmonic expansion represent a central axial dipole and account for about 90% of the total field. The first eight terms represent an eccentric dipole. However, the higher order multipoles have no physical interpretation. Palaeomagnetists prefer to divide the field simply into the "dipole" and "non-dipole" parts. The best fitting dipole for the present field is tilted at about $11.5^{\circ}$ to the rotation axis. The remainder of the field, the non-dipole part, consists of a number of foci of maximum and minimum intensity distributed over the globe. Both dipole and non-dipole fields contribute to the secular variation, though the non-dipole variation is much more marked. In the past 30 years, several more physically plausible models have been put forward for the geomagnetic fields of particular epochs. Lowes and Runcorn (1951) used about 12 axial dipoles at the core/mantle boundary, their latitudes and longitudes optimised to give the best fit to the non-dipole field. They argued that the sources must be at, or very close to, the core/mantle boundary; otherwise their effect would be screened by the highly conducting core material. They showed that the dipoles must be almost exactly vertical - in all their calculations the horizontal components were negligible. They therefore attributed their sources to small current loops, tangential to the core/mantle boundary, producing dipolar magnetic fields. They found that these sources tended to cluster around the equator. In 1964, Alldredge and Hurwitz took a similar approach, they placed

radially oriented dipoles beneath each of the foci of the non-dipole field, then altered their longitudes, colatitudes, amplitudes and radial distance until a best least squares fit to the 1955 British Admiralty Chart was obtained. Their dipoles turned out to be at 0.255 earth radii i.e. about half the radius of the core, (the actual sources are almost certainly closer to the core/mantle boundary, and of different form).

Recently Peddie (1979) has suggested that current loops should be considered rather than magnetic dipoles, as they are more closely related to core processes. A dipolar field is in effect produced by a current loop of infinitesimal radius; Peddie's model removes this restriction, and consequently changes the shape of the magnetic fields from the sources. Using different numbers of current loops of different radii, both constrained to the core/mantle boundary, and unconstrained, he produced a fit as close as the spherical harmonic expansion generally used. In all his models there is an approximately equatorial loop, corresponding to the main dipole field. The mechanics of the fluid motions necessary to produce such loops remain problems for the theoretician.

## 1.2: Secular variation from observatory records.

The present day secular variation of the magnetic field can be broken down into (after Cook, 1973):

1) A decrease in the main dipole moment of about 0.05% per year.

2) A decrease in the angle of tilt of the geocentric dipole of about $0.02^{\circ}$ per year.

3) An average westwards drift of features of the non-dipole field by $0.2^{\circ}$ per year.

4)A westwards rotation of the dipole by $0.05^{\circ}$ longitude per year.

5)A growth of some non-dipole features, and decay of others.

The predominant westward drift of both dipole and non-dipole features has been noticeable throughout the time records have been kept. Currently all but one of the world's observatories are recording westward drift. At Sitka, in Alaska, the field is drifting eastwards. Halley, who first noticed the westward drift at London in 1692, suggested that it was due to differential rotation of the outer and inner parts of the earth, the magnetic field having its source in the inner part. A similar model, incorporating a magnetic coupling between core and mantle, is still supported today, the difference in moments of inertia giving the core and mantle different angular speeds, (Bullard et al., 1950). Hide (1967, 1969, 1970) has suggested that "bumps" on the core/mantle boundary could leave eddies in the fluid behind them, which are the non-dipole field sources. It is a complex task however, to attempt to model the worldwide secular variation over any length of time. To model a static field, the representation used need not be physically realisable: if enough terms are evaluated, or sufficient sources incorporated, the required degree of accuracy can be obtained. But for a changing field, with a different pattern of variations at each site, the problem is much more complex. Creer and Hogg (Hogg, 1978) have tried to model the European secular variation curve by allowing each of the dipoles in the Alldredge and Hurwitz (1964) model to oscillate. The frequencies, amplitudes and initial phases of the oscillations were allowed to vary. Unfortunately there are insufficient well determined secular variation records to fix all the parameters uniquely.

## 1.3: Palaeomagnetism.

Our first hand knowledge of geomagnetic field behaviour extends back only to the advent of magnetic observatories in the sixteenth century. Beyond this we have to resort to the fossil records left in the world's rocks and sediments. Palaeomagnetists commonly work with two types of fossil records.

### 1.3.1: Thermoremanent magnetization (TRM).

As a magnetic material is cooled below its Curie point it acquires a magnetization in the same direction as the ambient field, and for a given material, proportional in intensity to the ambient field. Each magnetic grain becomes magnetized as the temperature drops below its own "blocking temperature", the value of which is dependant on the size, shape, domain state and environment of the grain in the material. TRM palaeomagnetic records are found in lava flows e.g. the successions of several hundred flows in Iceland have been used to develop the polarity time scale (Hospers, 1951; Cox et al., 1964; Dagley et al., 1967). Their relative chronology can be ascertained if they lie one on top of the other, and a few potassium-argon dates provide an absolute time frame. The TRM retained in fired pottery and bricks has also been used to obtain secular variation records on a shorter time scale, especially palaeointensity records (see Aitken, 1964). The most serious problem is that of dating individual specimens accurately, and obtaining a uniquely ordered series of measurements. Frequently also, there are time gaps when civilisations did not produce pottery, making the record discontinuous.

## 1.3.2:Detrital remanent magnetization (DRM).

A DRM is formed by the overall alignment of the magnetic moments of grains in a sediment, the individual grains having been magnetized during their previous histories, before deposition.

In order to understand the mechanism of DRM growth we need to know:

a)What forces act on a particle before, during and after deposition, which might aid alignment with the ambient magnetic field, or systematically or randomly oppose it.

b)At what stage in the formation of the sediment does the DRM become locked in i.e. whether on deposition (dDRM) or during compaction and consolidation (pdDRM).

c)How well does the DRM reflect the palaeofield direction, and what is the dependance of the remanent intensity on the palaeointensity of the geomagnetic field at the time of deposition.

It is a formidable task to model the mechanics of deposition mathematically and so produce theorectical answers to these questions, or to reproduce all the natural conditions in a laboratory and produce experimental answers.

Early workers (e.g. Nagata et al., 1943) proposed models of a purely physical nature, of spherical, and later elongated magnetized grains, falling in still water under gravity, to the lake or sea bed , and rolling or toppling into their final stable positions. This process was shown to result in an overall shallowing of the remanent inclination compared with the field value, (inclination error), a feature often observed in early work on varved clay sequences (Ising, 1942), and laboratory redeposition experiments (Johnson et al., 1948; King, 1955).

More recent work on a variety of deep sea, continental shelf and lake sediments, have however, not always found such an inclination error. It is now thought that some particles remain mobile in water filled voids between bigger particles well after deposition, and only become locked into position after a critical reduction in the water content. The buffeting of Brownian motion and/or the upward percolation of void water during compaction would keep the particles buoyant and able to realign. Such a post-depositional realignment process could allow the correction of any inclination error incurred during deposition. The time necessary, or the depth of overlying sediment needed before particles become locked in position is uncertain, but seems to depend on the physical properties of the particular sediment.

The first experimental support for a pdDRM is in some unpublished work of J. Lloyd (reported by Clegg et al., 1954). Lloyd powdered some British sedimentary rocks and a)redeposited them in water and b)resettled them from concentrated slurries. He found that if the initial water content of the slurry exceeded 50% a stable remanence of intensity comparable to that of the parent rock and with no detectable inclination error, was grown.

Subsequent experiments on reconstituted slurries of sediments have shown:

a)Inclination error is probably produced during deposition from still water, but can be removed by post-depositional realignment.

b)There is a critical water content, determined by the degree of sorting and grain size and shape distributions, above which a pdDRM can be grown, and below which it is locked in and becomes stable.

c)In deep sea and lake sediments this "locking" occurs some depth below the sediment/water interface. Thus stable remanences are frquently found in sediments whose uppermost layers are disturbed by bioturbation.

One advantage of working with sediments rather than with rocks or archaeological specimens is that a continuous, sequential data set is readily achieved. By choosing sediments with suitable deposition rates different aspects of geomagnetic behaviour e.g. reversals, broad or fine scale secular variation, can be studied. Deep sea sediments typically accumulate at a few mm/1000 years. The lacustrine and continental shelf sediments studied here settle at rates of about 0.5 - 1.0 mm/year.

## 1.4:Work included in this thesis.

Having seen the need for long, well dated, well determined sequences of secular variation data distributed worldwide, for the evolution of a reliable model, I have attempted to construct such a record for Britain over the past 10000 years from the DRM of lake sediments. The following five chapters describe the sample collection, laboratory measurements and results, dating of the sediments, attempts to derive palaeointensities, the production of the directional secular variation curves and their geomagnetic implications. They form the major part of the thesis.

Chapters 7 and 8 are related subsidiary projects. Chapter 7 is a study of the growth, development and movement of the natural magnetic minerals in the drainage basin of a lake - Llyn Geirionydd. Chapter 8 contains palaeomagnetic results from some continental shelf sediments from the Clyde estuary, covering a similar time span to the lacustrine sediments studied.

# CHAPTER 2:CORE COLLECTION AND MEASURING TECHNIQUES.

## 2.1:Core collection.

Cores of sediment were collected using pneumatically controlled piston corers (Mackereth, 1958), operated from a small boat. Two different 6m length corers were used, and in addition surface sediments were collected using 1m and 1.3m "mini-corers". Both 6m and mini-corers contain as little ferromagnetic metal as possible, to protect the NRM of the sediments during coring.

The 6m corer uses opaque pvc drainpiping of 54mm internal diameter and 60mm external diameter as coretubing. Before coring the coretube is housed inside a barrel of similar pvc tubing of 88 mm e.d. The tube is forced out of the barrel by increasing the air pressure above a piston, fixed to its top, which fits flush inside the barrel. Attached to the bottom of the barrel is a cylindrical aluminium anchor chamber 1m long and 60cm in diameter which is pneumatically pumped into the sediment before coring begins to stabilize the corer. A Kullenberg piston inside the core tube and initially at its base, is fixed in position relative to the core barrel and so moves up the coretube as the core is taken. This piston prevents the sediment slipping out of the coretube, and at the same time also avoids compression. After coring the corer is made buoyant by refilling the anchor chamber with air, and it floats to the surface for retrieval.

The mini-corer is basically a smaller version of the 6m corer, with the exception that the core tubes are transparent perspex and reusable. It was thought that the "pumping-in" of the anchor chamber of the 6m corer might disturb or remove the

uppermost 20cm or so of sediment. This prompted the design of the mini-corer, which anchors vertically under gravity only. The weight of the mini-corer can be adjusted so that the core contains a few centimetres of water and the sediment/water interface is preserved accurately. There is sufficient overlap between the mini-cores and the undisturbed part of the long cores from the same site to allow correlation and construction of a complete record to the present day.

In their original form, and as used for most of the cores in the project, the corers had no means of absolute orientation. Non-vertical penetration was sometimes suspected if the inclination was systematically higher or lower than expected or than that of other cores from the site. Attempts at correction are hazardous and imprecise as they rely on an assumption of the present day inclination of the geomagnetic field at the site, or its mean over the past few thousand years. Also there was no means of fixing absolute declination values, other than matching that of the uppermost sediment to the present day magnetic north. For this reason all declinations presented here are "relative declinations", taking the core mean as an arbitrary zero.

A camera and compass orientation device is now mounted to the anchor chamber of the 6m corer. A photograph of the compass and a pair of orthogonal spirit levels is taken once the corer has anchored on the lake bed, before coring begins. This was given its first field trials at Geirionydd in summer 1978, and after some improvements should be in routine use for future fieldwork.

In previous projects there has been a suggestion of the core tube twisting as it enters the sediment, seen as a trend

superimposed on the declination record. Various modifications have been attempted to prevent this twisting. The most successful, which is now used, is a keyway along the length of the coretube, in which a stationary pointer, attached to the anchor chamber is constrained as the core is taken. This is now used routinely, but again was not adopted until after the collection of cores for this project.

## 2.2:Choice of lakes and sites.

The suitability of both a lake and its surroundings must be considered when choosing a site for coring. The size and morphology of the drainage basin, the nature of the bedrocks, and the land use, all control the quantity, composition and degree of sorting of the material entering the lake and becoming its sediment.

Rocks likely to contribute magnetic fragments to the sediment include basic volcanic rocks, yielding magnetites or titanomagnetites, and red sandstones yielding haematite. However the effect of haematite in a lake sediment has rarely been proved conclusively beneath the much stronger ferrimagnetism of magnetite, (the saturation magnetic moments of haematite and magnetite are 2.2 and 48.0 $mA.m^{-1}$ respectively). It is also possible that the magnetic minerals in a sediment do not originate from the rocks, but are formed in the soils of the drainage basin. Hence the nature of the soils and the history of the land use may also be important factors, and land use changes over the centuries may be traced by the magnetic character of the sediment.

Since it is frequently desired to obtain radio-carbon age estimations on the sediments, it is important to eliminate

sources of carbon older than the sediment (Chap 5). The most common source of such contamination is drainage through limestone country to the lake. So drainage basins containing limestones should be avoided if radio-carbon dating is required.

Secondly, the characteristics of the lake itself are important. We require to sample fine grained sediment, deposited continuously at a suitable rate in a quiet environment. To fulfil these conditions a coring site should be in the centre of a deep, flat bottomed basin, where the finest material is likely to settle away from inflowing rivers or lake shores. The bed should be as near horizontal as possible so that the corer rests and penetrates vertically. Steeply sloping beds should be avoided because of the likelihood of sediment slumping, and sediment discontinuities. Channels, in which there are likely to be currents, also make poor sites, as the orientation in which non spherical grains settle may be controlled by the current direction, and so give an erroneous remanent direction.

Table 2.1 summarises the physical properties of the lakes sampled.

## 2.3:Lakes sampled.

All the lakes studied in detail are, at least partly, in mountainous regions, and owe their formation to glacial action during the last ice age.

### 2.3.1:Loch Lomond (fig 2.1).

Loch Lomond is divided naturally into two distinct parts. The northern part is a steep sided trench, running N-S, cut into resistant Dalradian schists and grits, to a maximum depth of

Table 2.1 Lakes Sampled

| | Grid ref. | Surface area ($Km^2$) | Drainage basin ($Km^2$) | $DB/_{SA}$ | Max. depth (m) | Coring depth (m) |
|---|---|---|---|---|---|---|
| Lomond | $56^{o}N$ $4.5^{o}W$ | 72.6 | 731.8 | 10.08 | trench 190m<br>S.basin 26m | RD 24<br>RD 26<br>TO 20 |
| Windermere | $54.3^{o}N$ $3^{o}W$ | 14.44 | 233.6 | 16.2 | S.basin 42m<br>N.basin 61m | 42 |
| Geirionydd | $53.1^{o}N$ $3.8^{o}W$ | 0.26 | 3.9 | 15.0 | 15 | 15 |

Figure 2.1 : Loch Lomond : Drainage basin, bathymetry and coring sites

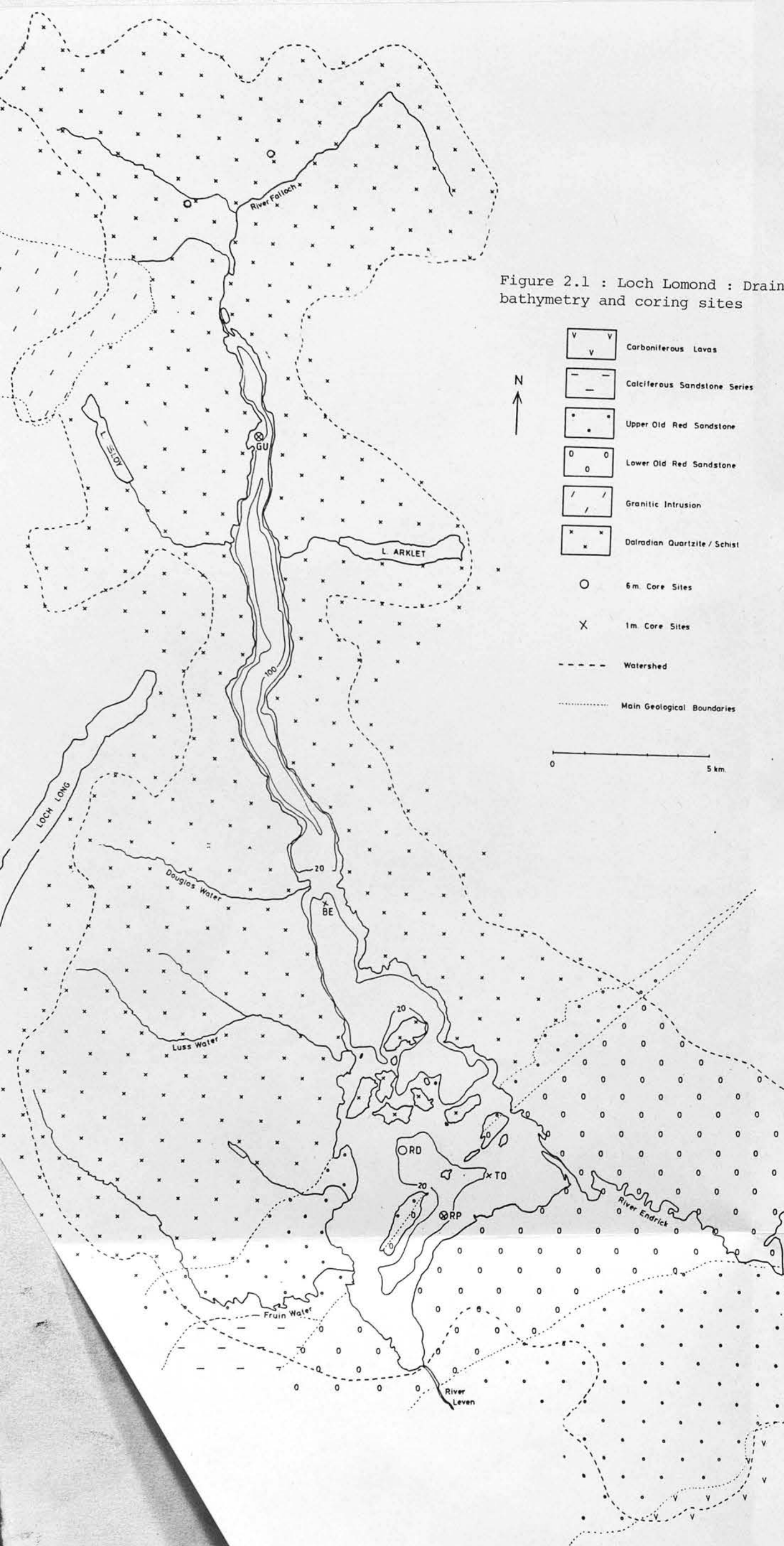

190m. Three main rivers, the Falloch, Fruin and Douglas Waters flow into the loch off these metamorphic rocks, from the north and west, through poor soils. These rivers are short and flow rapidly, so probably carry fairly coarse, poorly sorted material into the loch. To the south of the Highland Boundary Fault where the ice wore more easily into the softer Old Red Sandstone rocks, the loch opens out into a broad, relatively shallow basin . The loch here, particularly along the line of the fault, is dotted with islands, composed of more resistant conglomerate and schistose grit. The main inflow to the southern basin, and the most mature inflow to the loch is the River Endrick, which with its tributary the Blane rises in the basaltic lavas of the Campsie Fells, east of the loch, and flows over alluvial plains to the south-east corner. The outlet of the loch is the Leven, at the southernmost tip, which flows into the Clyde estuary at Dumbarton.

The main form of the lake basin was eroded by the glaciers of the last ice age, which had retreated by ca 12500BP (Sissons, 1974). After this the loch was marine, as many of the present day Scottish sea-lochs, until the glaciers of the Loch Lomond Readvance covered it once more, depositing moraine debris at its connection to the sea -the outflow of the Leven. This last ice load had retreated fully by ca 10500BP (Sissons, 1967), the age of the earliest organic sediments used in the project. The loch surface is now only 8 m o.d., and there is evidence to show that another post-Glacial marine transgression occured, between ca 6500 and 5000BP (Dickson et al., 1978), as the isostatic rebound of the land from its ice load was overtaken by the rising sea level, as the polar ice melted further.

Coring for palaeomagnetic purposes was concentrated in the southern basin, the deep trench being unsuitable. In May 1976 6m cores were taken from sites RD and RP, both at centres of flat bedded basins. Mini-cores TOM4 and BEM14, further north, were taken in 1977.The extreme north end of the loch, where the trench shallows again, proved difficult to core, as the hard Glacial clay was reached in only 3m.

The numbering system of the cores is incomplete as other cores in the series were used by Dr. D. M. Morton in a parallel sedimentological study (see appendix 1 for a complete list of cores).

2.3.2:Lake Windermere (fig 2.2).

Although the biggest freshwater lake in England, Windermere is appreciably smaller than Lomond, having a surface area of 14.4 $km^2$.

Windermere also occupies a glacially formed north- south trench, but is divided into two roughly equally sized basins by a shallow lip and islands. The north and south basins have maximum depths of 61m and 42m respectively. The major part of the drainage basin is north of the lake, and most of the inflowing rivers arise in the mountains of the Borrowdale volcanic series, and flow into the northern basin. One sizeable stream flows into the west side of the southern basin, through Esthwaite water. The outflow, to the Irish Sea, is via the River Leven (distinct from its Scottish namesake)at the south end. Windermere is also partly contained by glacially deposited moraines.

The rocks immediately surrounding the lake are mainly Ordovician and Silurian grits, shales and mudstones. However a

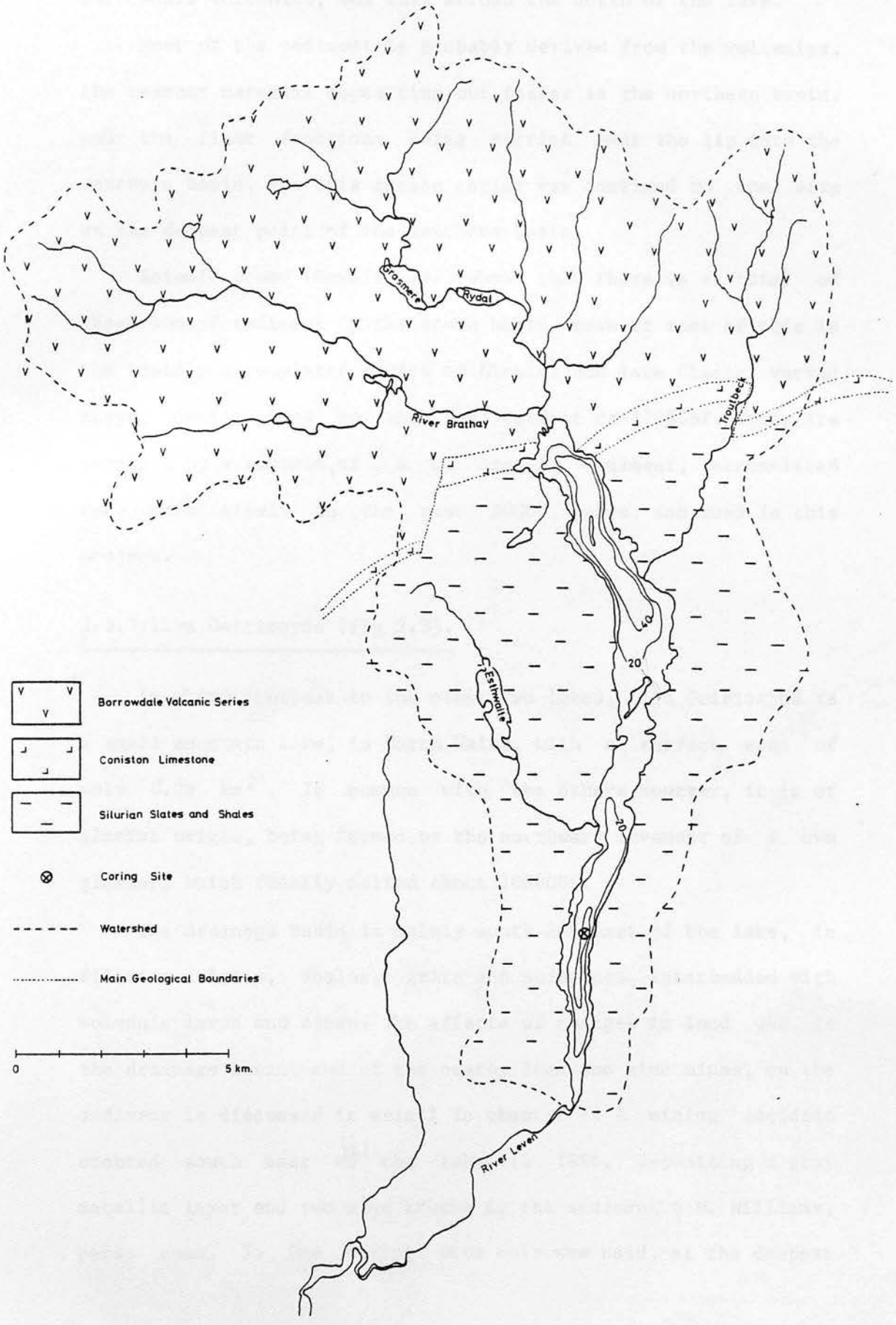


Figure 2.2 : Lake Windermere : Drainage basin, bathymetry and coring sites.

band of Coniston limestone outcrops between these and the Borrowdale volcanics, and cuts across the north of the lake.

Most of the sediment is probably derived from the volcanics, the coarser material depositing out faster in the northern basin, and the finer fractions being carried over the lip into the southern basin. For this reason coring was confined to one site at the deepest point of the southern basin.

Seismic study (Howell, 1971)shows that there is a total of about 40m of sediment in the south basin. However most of this is the rapidly accumulated series of Glacial and late Glacial varved clays, dating back to the ice retreat ca 17000BP. These are overlain by a maximum of 4 m of organic sediment, accumulated much more slowly in the past 10000 years, and used in this project.

### 2.3.3:Llyn Geirionydd (fig 2.3).

In sharp contrast to the other two lakes, Llyn Geirionydd is a small mountain lake, in North Wales, with a surface area of only 0.26 $km^2$. In common with the others however, it is of glacial origin, being formed by the northward movement of a cwm glacier, which finally melted about 10000BP.

The drainage basin is mainly south and east of the lake, in Silurian slates, shales, grits and mudstones, interbedded with volcanic lavas and ashes. The effects of changes in land use in the drainage basin, and of the nearby lead and zinc mines, on the sediment is discussed in detail in chapter 7. A mining accident occured south east of the lake in 1896, depositing a gray metallic layer and two mine trucks in the sediment ( M. Williams, pers. comm. ). One coring site only was used, at the deepest

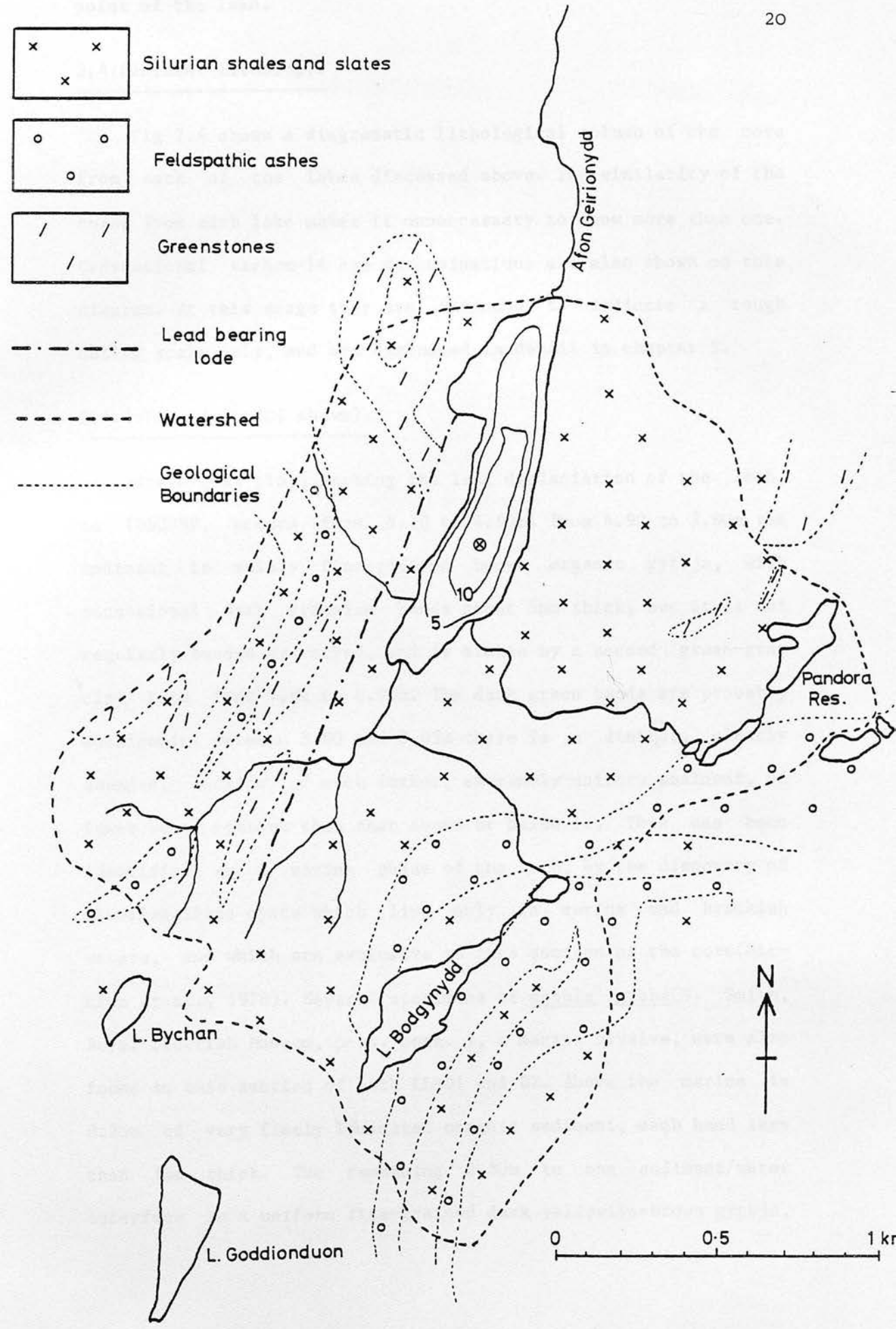


Figure 2.3 : Llyn Geirionydd : Drainage basin, bathymetry and coring sites.

point of the lake.

## 2.4:Sediment lithology.

Fig 2.4 shows a diagramatic lithological column of one core from each of the lakes discussed above. The similarity of the cores from each lake makes it unneccessary to show more than one. Conventional carbon-14 age determinations are also shown on this diagram. At this stage they are intended to indicate a rough dating scale only, and are discussed in detail in chapter 5.

### 2.4.1:Lomond (LLRD1 shown).

Green-gray clay, marking the last deglaciation of the loch, ca 10500BP, occurs from 5.10 to 4.90m. From 4.90 to 3.80m the sediment is mainly fine-grained brown organic gyttja, with occassional dark greenish bands about 5mm thick, but it is not regularly banded or varved, and is broken by a second green-gray clay band from 4.02 to 4.00m. The dark green bands are probably authigenic. Between 3.80 and 3.05m there is a distinct, clearly bounded, section of much darker, extremely uniform sediment, of lower water content than that above or below it. This has been identified as a marine phase of the loch, by the discovery of dinoflagellate cysts which live only in marine and brackish waters, and which are exclusive to this section of the core(Dickson et al., 1978). Several specimens of cobula gibba(S. Smith, Royal Scottish Museum, pers. comm. ), a marine bivalve, were also found in this section of both LLRD1 and D2. Above the marine is 0.25m of very finely laminated organic sediment, each band less than 1mm thick. The remaining 2.80m to the sediment/water interface is a uniform fine-grained dark yellowish-brown gyttja,

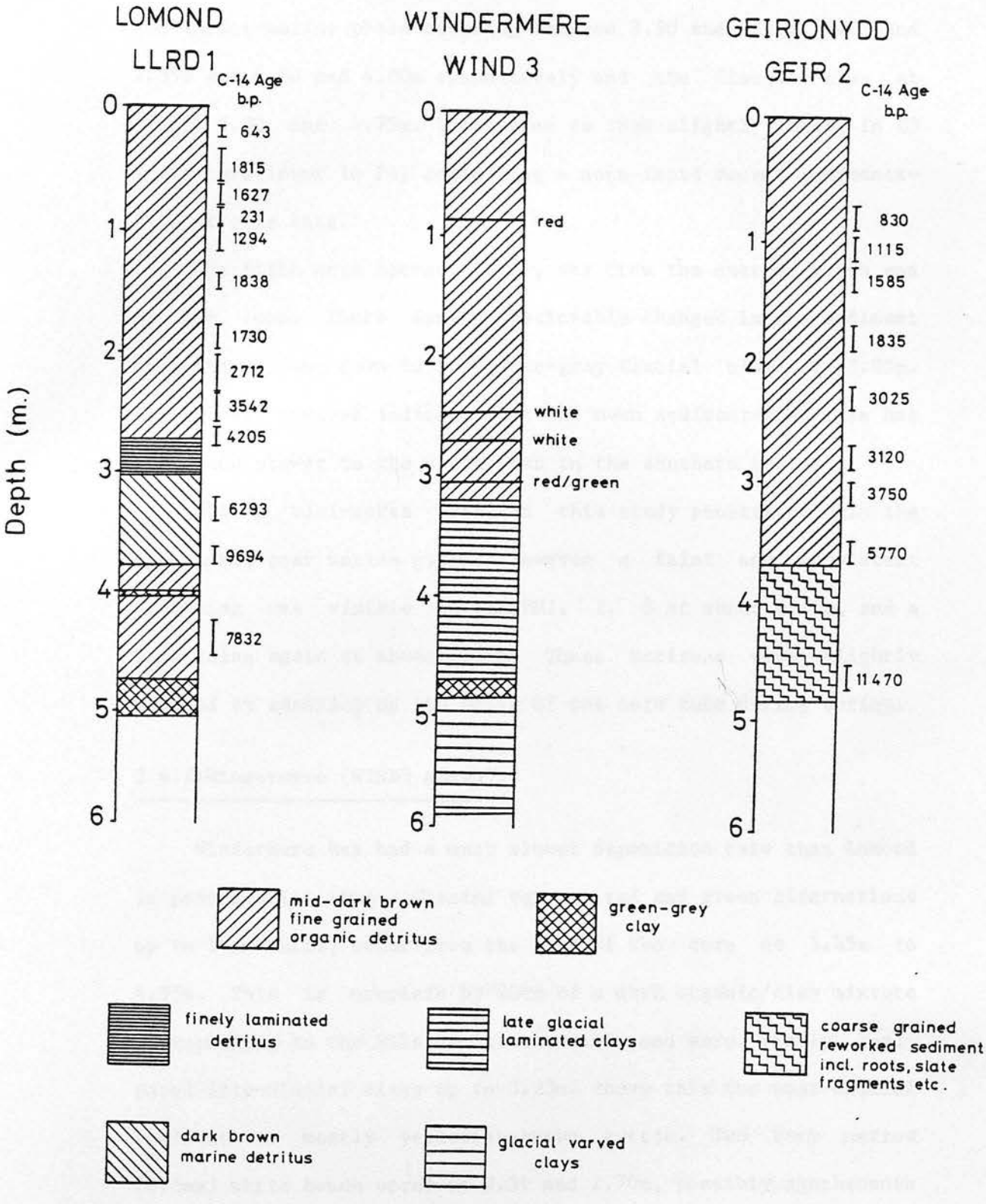


Figure 2.4: Core lithology and conventional C-14 age determinations.

similar to that below the marine.

The same stratigraphy was noted on opening D2, D3 and P4, the darker marine phase occuring between 3.90 and 3.10m, 4.05 and 2.95m and 4.50 and 4.00m respectively and the Glacial clay at 4.80, 5.03 and 4.75m. The marine is thus slightly longer in D3 and occurs lower in P4, indicating a more rapid recent sedimentation at this site.

The fifth core opened, LLGU9, was from the extreme north end of the loch. There were no noticeable changes in the sediment from the surface down to the green-gray Glacial clay at 3.05m. This does however indicate that the mean sedimentation rate has been much slower in the north than in the southern basin.

All 6 mini-cores used in this study penetrated only the uppermost, post marine gyttja. However a faint and consistent darkening was visible in LLRPM1, 2, 3 at about 0.15m, and a lightening again at about 0.38m. These horizons were slightly blurred by smearing up the walls of the core tube during coring.

### 2.4.2:Windermere (WIND3 shown).

Windermere has had a much slower deposition rate than Lomond in post-Glacial times. Glacial varves, red and green alternations up to 10cm thick, occur from the base of the core at 5.85m to 4.95m. This is overlain by 20cm of a dark organic/clay mixture corrsponding to the Alleröd interstadial, and more finely laminated late-Glacial clays up to 3.25m. Above this the post-Glacial sediment is mostly yellowish-brown gyttja. Two very narrow (0.5mm) white bands occur at 2.51 and 2.70m, possibly synchronous with lowerings of the lake level, and two similar red bands occur at 0.88 and 3.05m. These four bands in the post-Glacial gyttja

were found in all three cores. Their depths (in m) are tabulated in table 2.2, and were used in correlating between cores.

Table 2.2.

| | RED | WHITE | WHITE | RED | CLAY BOUNDARY |
|---|---|---|---|---|---|
| WIND1 | 0.77 | 2.29 | 2.46 | 2.98 | 3.12 |
| WIND2 | 0.79 | 2.38 | 2.56 | 2.97 | 3.22 |
| WIND3 | 0.87 | 2.50 | 2.68 | 3.04 | 3.26 |

The four mini-cores each contained 7 to 9cm of black, recently resuspended organic sediment, above the lighter, brown, uniform gyttja. The narrow red band at 0.88m in WIND3 was not visible in any of the mini-cores, probably again because of smearing up the walls of the tube through which the lithology is noted before extrusion of the sediment.

2.4.3:Geirionydd (GEIR2 shown).

Geirionydd has a deposition rate similar to that of Loch Lomond, Glacial clay being found at the base of only one core, GEIR8, which was not subsampled.

The bottom 1.20m had a very high water content, was rather coarse-grained and in places contained plant, root and slate fragments, and occasional distinct green banding. This section proved unsuitable for palaeomagnetic work and is probably marginal material, reworked during a lowering of the lake level.

From 3.80m to 4.0cm below the surface is a brown organic gyttja, very uniform in colour and texture, but still having a rather high porosity. Eight samples, from four horizons spaced down the core all had water contents of 78-80% by weight. The uppermost 4cm were a dark gray metallic colour, with some

orange/red oxidised specks, on exposed surfaces. This was probably brought into the lake very rapidly during the 1896 mining accident. The thickness of this layer is very variable between cores, and it does not occur at all in mini-cores from the north-west bay of the lake. Such variability would be expected in the rapid settling of a heavy input from one source.

In GEIR3 the gray metallic layer is disturbed, probably by plugging the core with paper towels for transport, however the useful record is longer, as the reworked lowermost sediment only extends up to 4.57m. GEIR4 has 4cm of metallic sediment at the top and the reworked sediment is reached at 4.35m.

In general the mini-cores from the sites of the long cores contain a greater thickness of metallic inwash: 10cm in GEIRM6 and 18cm in GEIRM2.This shows that with such porous sediments, there is appreciable loss ( up to 10cm ) of the uppermost layers during "pumping-in" of the 6m corer. However the base of the metallic inwash provides a good dated horizon from which to begin measurements.

## 2.5:Magnetic measurements.

Whole core scanning of 1) magnetic susceptibility and 2) the horizontal component of NRM, are routinely carried out on all cores while still in the coretube and the sediment untouched. These measurements are very rapid: about 5 minutes to measure the susceptibility of a 6m core, and 20-30 minutes for its NRM, depending on strength, so they provide valuable preliminary information on a core before it is subsampled and measured in detail.

## 2.5.1: Instrumentation.

### 1) Whole core susceptibility.

The whole core susceptibility bridge used is that described by Molyneux and Thompson(1973). The air-cored coil system has a cylindrical sample head of 8.5cm diameter through which the whole core is passed. As it does so the coretube passes over a roller attached to a slotted disc and photocell arrangement, which causes measurements to be taken at approximately 2.7cm intervals along the core. The sensor signal drops to 66% at about 3cm from the end of the sample, giving the response function a half width of 6cm. So the log obtained is a smoothed version of the true susceptibility pattern, features closer than about 6cm being unresolved. One could perform a deconvolution on the results obtained, since the response function can be plotted. However, since the results are only of a preliminary nature, and their correlation with subsequent single sample measurements is usually quite obvious, this is not done as a rule.

### 2) Whole core NRM.

The whole core NRM apparatus (Molyneux et al.,1972), is an adaptation of the Digico complete result spinner (Molyneux, 1971), used for single sample measurements. A fluxgate head of 7.5cm diameter is mounted horizontally at the centre of a coaxial mu-metal shield. The core is spun, with its axis horizontal, at a uniform frequency between 1 and 2 Hz. Rotating with it is a disc, having 128 slots around its circumference, and the analogue output from the fluxgate head is digitised each time a slot passes a photocell arrangement. After a predetermined number of

spins the results, stored in a M16V mini- computer, are compounded, and the resulting intensity and direction of the horizontal remanence(in the plane of the fluxgate ring) are printed out on a teletype. Measurements are usually made at 5cm intervals along the whole core.

Again there is an unavoidable smoothing effect over a finite length of sediment above and below the plane of the fluxgate. In addition to smoothing the intensity log, this also reduces the amplitude of the declination swings. As the calculation of inclination also requires a vertical component of remanence, it cannot be obtained using the whole core apparatus. Also, the intensity record obtained is not that of total intensity M, but only its horizontal componenet M.cos I - a little under 50% in Britain. Both M and I are measured when single samples are taken from selected cores.

It is sometimes inadvisable to perform whole core NRM measurement on a core, particularly if the sediment has a high porosity, when it may be disturbed by spinning, and "twist" the declination record. If the sediment does not reach the top of the coretube it is held in place by a plug of paper towels before spinning.

3)Subsampling.

i)6 metre cores.

After whole core measurements have been completed it is decided whether to subsample a core. An orientation line is drawn along the length of the coretube, and it is cut into 1.50m lengths. Each length is then cut into two halves lengthwise (fig

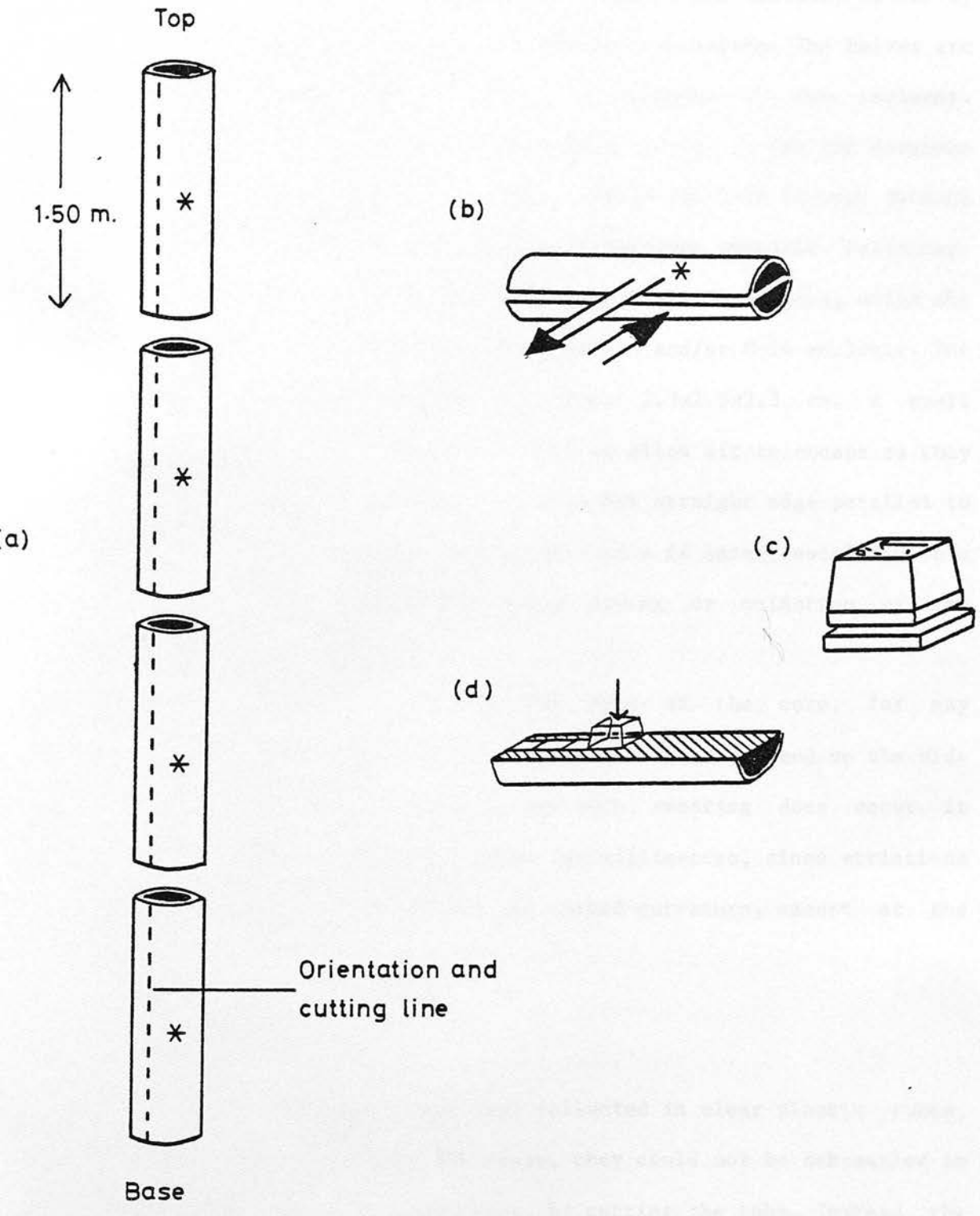


Figure 2.5 : Core cutting and sampling technique.

2.5). A circular saw is used to make two diametrically opposite cuts, one along the orientation line, nearly, but not quite, through the tube wall. The cuts are cleaned of any PVC shavings and slit right through with a sharp blade. The sediment is cut by sliding a nylon thread between the two halves. The halves are then slid apart, causing minimum disturbance to the sediment. Care is taken throughout to exclude slivers of the PVC coretube from the sediment, as these would affect the C-14 dating. Contact with ferrous metals is also avoided wherever possible. Palaeomagnetic samples are then taken from one half of the core, while the other (*) is stored for future pollen and/or C-14 analysis. The sample boxes are approximately cubic: 2.5x2.5x2.3 cm. A small hole is drilled in the top of each to allow air to escape as they are pressed into the sediment, with one straight edge parallel to the length of the coretube. This hole is later resealed with a patch of plastic tape to prevent drying or oxidation of the sediment.

Sampling the sediment at the edge of the core, for any purpose, is avoided, in case any sediment has smeared up the side of the tube during coring. If any such smearing does occur it must be restricted to the outer few millimetres, since striations in the sediment rarely show any marked curvature, except at the extreme edges.

ii)1 metre cores.

Since the mini-cores were collected in clear plastic tubes, which were required for reuse, they could not be subsampled in the same way as the long cores, by cutting the tube. Instead the sediment was extruded upwards, and sampled as it rose above the

top of the coretube. In the early cores a rubber bung was used as piston and a broom handle to push it up. Later a hydraulic pump was adapted for the purpose, which avoided the danger of twisting the sediment, encountered in the first method. The method is still not ideally suited for oriented samples, but quite adequate if no directional information is required. The amount of compression during extrusion is less than 2%.

4)Subsample NRM.

Subsample NRM measurements were made on a Digico complete result balanced fluxgate spinner magnetometer, interfaced to a M16V mini-computer(Molyneux, 1971). Two instruments were used, with fluxgate rings of 3.8cm and 4.8cm diameter, both having rotation frequencies of about 4Hz. A noise level of less than 0.1 $mA.m^{-1}$ was always ensured before beginning measurements. As with the long core spinner, at each measurement, two orthogonal components of the remanence in the plane of the fluxgate ring are recorded, by integrating over a preset number of spins of the sample;the weaker the remanence the more spins are needed to reach the required signal:noise ratio. A sample is measured upright and inverted in each of three orthogonal orientations, giving four estimates of each component of the remanence. Any static contribution, e.g from the sample platform of the spinner, is calculated and subtracted, and the best estimates of M, D and I calculated and printed out by a teletype. For samples with remanent intensities between 10 and 100 $mA.m^{-1}$, $2^5$ spins are allowed per measurement, and a whole sample can be measured in about two minutes. This time is increased by a factor of about 2 or 4 for weaker samples when $2^6$ or $2^7$ spins per orientation are

used.

5)Subsample susceptibility.

Initial (low field)reversible susceptibility was measured on an air-cored bridge, similar to the whole core scanning bridge but with a smaller, 3cm, diameter aperture, also interfaced to the M16V mini-computer. The noise level was about $2 \times 10^{-6}$ SI units. An oscilloscope was also used to monitor the output signal, and as an aid to placing the sample in the centre of the sensing head. This position is critical to within about 5mm for reliable, reproduceable results.

6)Alternating field demagnetization and ARM growth.

Alternating field (A.F.) demagnetization was carried out in a coil of 15cm diameter operating at 50Hz. The alternating field is gradually reduced by an automated variac and the decay time is variable between 50 s and 4.5 mins. The maximum peak field obtainable is 100mT, however it was not possible to reach this value many times in succession, due to heating effects, so the maximum used was 95mT. For A.F. demagnetization the coil is housed in a triple mu-metal shield 70cm long and 23cm in diameter, which reduces the field at its centre to 50nT, and ensures low field gradients in this region. When demagnetising in three orthogonal directions, 8 samples, taped into a cube were treated simultaneously. It was felt that this number made optimum use of the volume of uniform field inside the coil. Some experiments were also done using a two axis tumbler, with inner and outer rotation frequencies of 1.92 and 4.94Hz respectively. Six samples could be demagnetized together using the tumbler. The

same coil was used for ARM growth. When the Lomond and Windermere cores were analysed the coil had to be removed from its mu-metal shield, and aligned parallel to the ambient field in the laboratory, to obtain a direct field bias. It was later modified-(Geirionydd and John Murray cores)so that a fixed steady direct current could be switched into the main coil in addition to the rising and falling alternating current, and provide a bias field of 0.22mT.

Isothermal remanence was produced by a conventional electro-magnet having 5.5cm diameter, tapered pole pieces with a 3 cm air gap, capable of reaching a maximum field of 1.2T.

2.5.2:Objectives.

Whole core measurements can be used for the following tests on cores.

1)To test the suitability of a lake, if it is previously unsampled. This involves:

a)Testing whether the remanence is strong enough to be measur-ed readily and accurately. This can be gauged from susceptibility and horizontal intensity.

b)Testing whether the declination is controlled by geomagnetic field changes, or by some local phenomenon e.g current; or whether the sediment is unsuitable for recording a stable direction e.g. if too coarse grained, and the directions are scattered. Without an idea of the deposition rate it is sometimes difficult to distinguish a geomagnetic signature- in such cases correlation (3) becomes important.

2)To detect defects in the coring procedure e.g twisting of the coretube during penetration, resulting in a "twisted" declination

record. Sometimes one can also see clear-cut "jumps" in the declination record where whole sections of core have rotated with respect to adjacent sections.

3)To correlate magnetic parameters between cores.In view of the large number of natural processes which can disrupt or introduce spurious features into a palaeomagnetic record e.g. currents, slumping, coring defects, it is important to obtain duplicate records of the magnetic features. The sequence of correlation is three tiered.

a)Correlation between cores from the same site within a lake. Magnetic susceptibility is very useful here, as it is very sensitive to sedimentological changes affecting the magnetic mineralogy and concentration. This also identifies "one-off" defects in the coring process.

b)Correlation between cores from different sites in one lake. If the sites are close enough to have the same source of sediment, then the susceptibility logs show the same features, although differences in sedimentation rate result in a "concertina-ing" effect along the depth axis. Sometimes gradual sedimentological changes and source changes can be traced through a sequence of susceptibility logs along a lake (e.g. Lomond, Thompson and Morton, 1979). This, and a comparison of declination logs provide a means of isolating good and bad sites. Intensity logs may or may not correlate, depending on whether the remanence is controlled principally by the magnetic mineralogy and concentration or by the palaeomagnetic field strength, (this is discussed further in chap 4).

c)Correlation between different lakes. This is a later stage and is usually carried out on the dated single sample records of

declination and inclination (chap 6). It is the final stage in picking out the true geomagnetic features.

4)To decide whether lakes are suitable for further coring, and which cores are suitable for subsampling and detailed investigation.

The advantages of subsample measurements over those on whole cores are:

1)Inclination and total remanent intensity records are obtained as the vertical component of remanence can now be measured.

2)Each measurement is an average over 2.5cm of sediment, but there is no smoothing effect outside this range. When sampling, visible defects in the sediment e.g gaps, large stones or pieces of wood can be avoided. These factors result in a better resolution of features, and hence more accurate between core correlations.

## 2.6:Summary.

The following points summarise the procedures involved in collecting palaeomagnetic data from lake sediments.

1)The choice of a lake and coring sites depend on the geology, morphology and drainage of the land around the lake, and the bathymetry of the lake basins.

2)Long (6m) and short (1m) cores are collected from each site.

3) Whole core measurements are made of horizontal remanence and magnetic susceptibility, while the sediment is still in the coretube.

4)Correlation and comparison of the results from (3) are used to select suitable lakes, sites and cores for further study.

5)Selected long cores are subsampled. If the long core record

is incomplete mini-cores are subsampled also.

6)Detailed subsample measurements are made of NRM intensity, declination, intensity and magnetic susceptibility.

# CHAPTER 3:MAGNETIC RESULTS.

## 3.1:Lomond.

Whole core logs of susceptibility, horizontal intensity and declination for LLRD1, 2, 3, LLRP4, 7 and LLGU9 are shown in figures 3.1, 3.2 and 3.3 respectively. Subsample results for LLRD1, 2, 3 and LLRP4 are shown in figures 3.4 and 3.5. When LLRP4 was subsampled, the section between 3.60 and 3.00m was found to be spuriously remagnetized. As this was found in none of the other cores, nor in the whole core measurement, it was assumed to have happened between whole core and subsample measurements. Consequently the NRM direction record for this section(figure 3.5 ) is made up of whole core declination and interpolated inclination values. The correlation of all parameters between the five southern cores is striking.

### 3.1.1:Susceptibility and NRM intensity.

Both susceptibility and NRM intensity are stronger than in most European gyttjas studied, having mean values in the uppermost 3m of visibly uniform gyttja, of 500 x $10^{-6}$ SI units and 100 $mA.m^{-1}$ respectively. In this section there are marked variations of up to a factor of two, indicating large changes in the magnetic content of the sediment. Sixteen features: maxima, minima and points of inflection (labelled on LLRD1) are identified in the uppermost 3.5m of the whole core susceptibility log. These have been re-identified, with greater accuracy , on the single sample logs(figure 3.4 ), and used as a means of correlating between the cores, which is independent of the

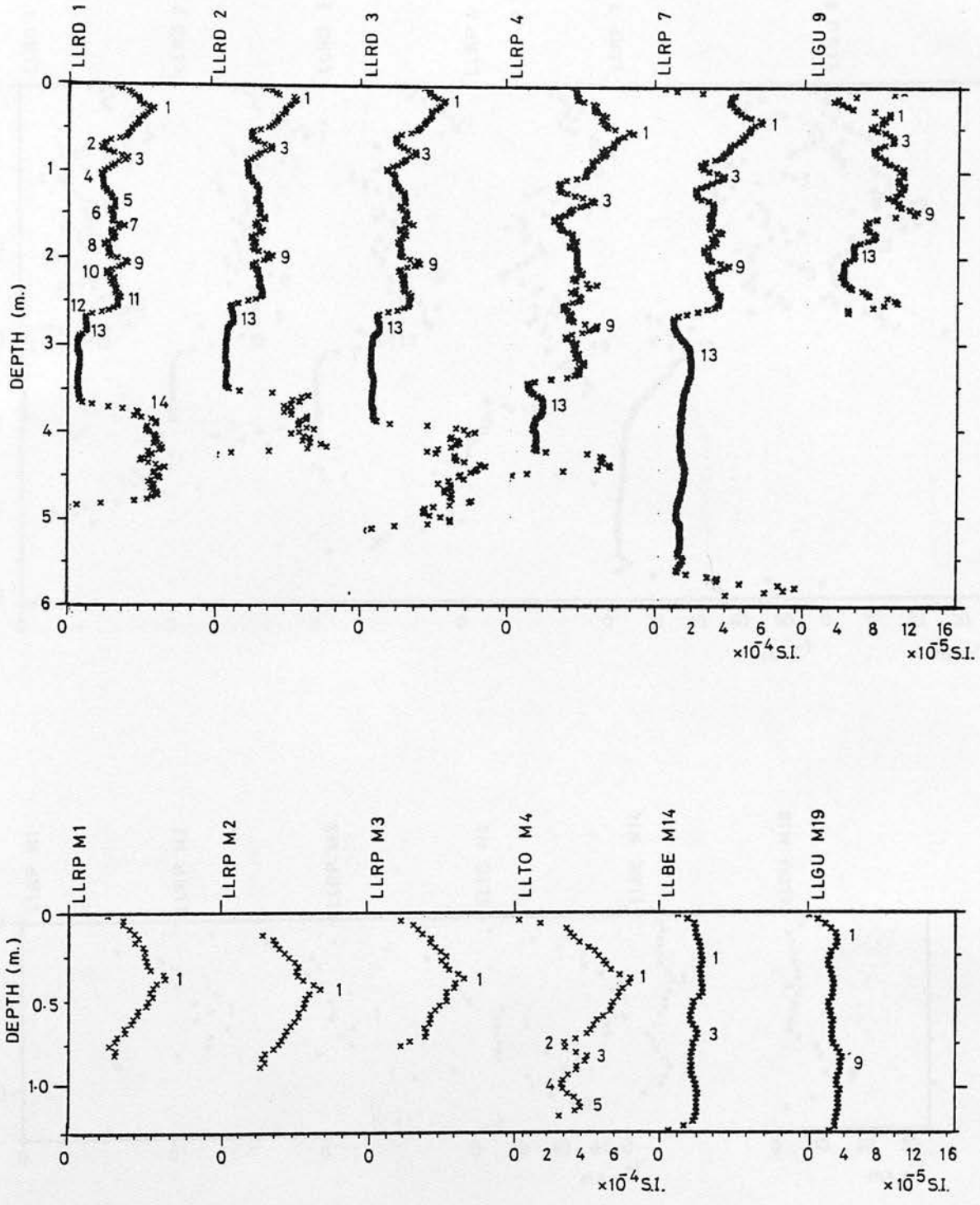


Figure 3.1 : Lomond long and mini cores ; whole core susceptibility logs.

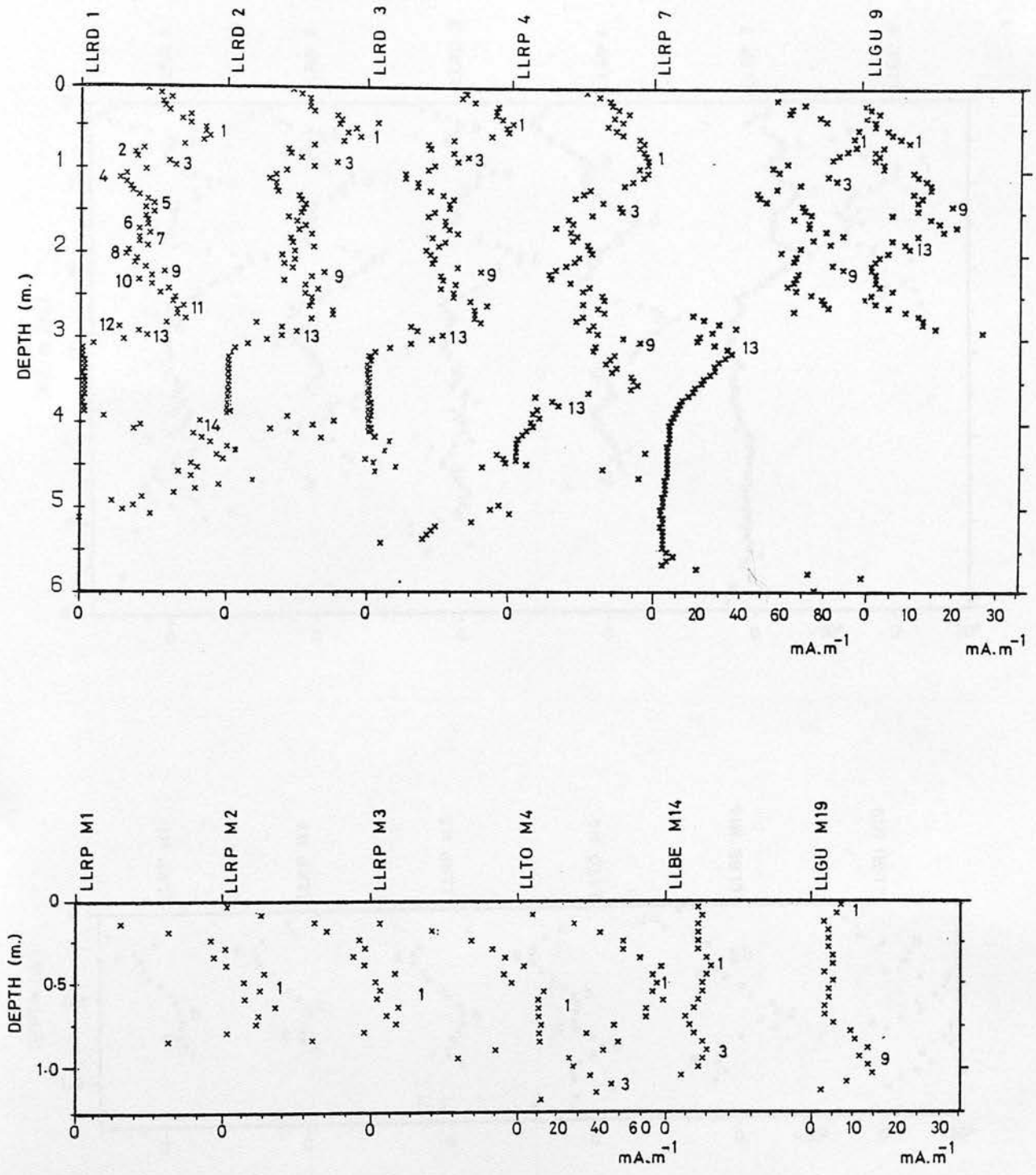


Figure 3.2 : Lomond long and mini cores : whole core horizontal remanent intensity logs.

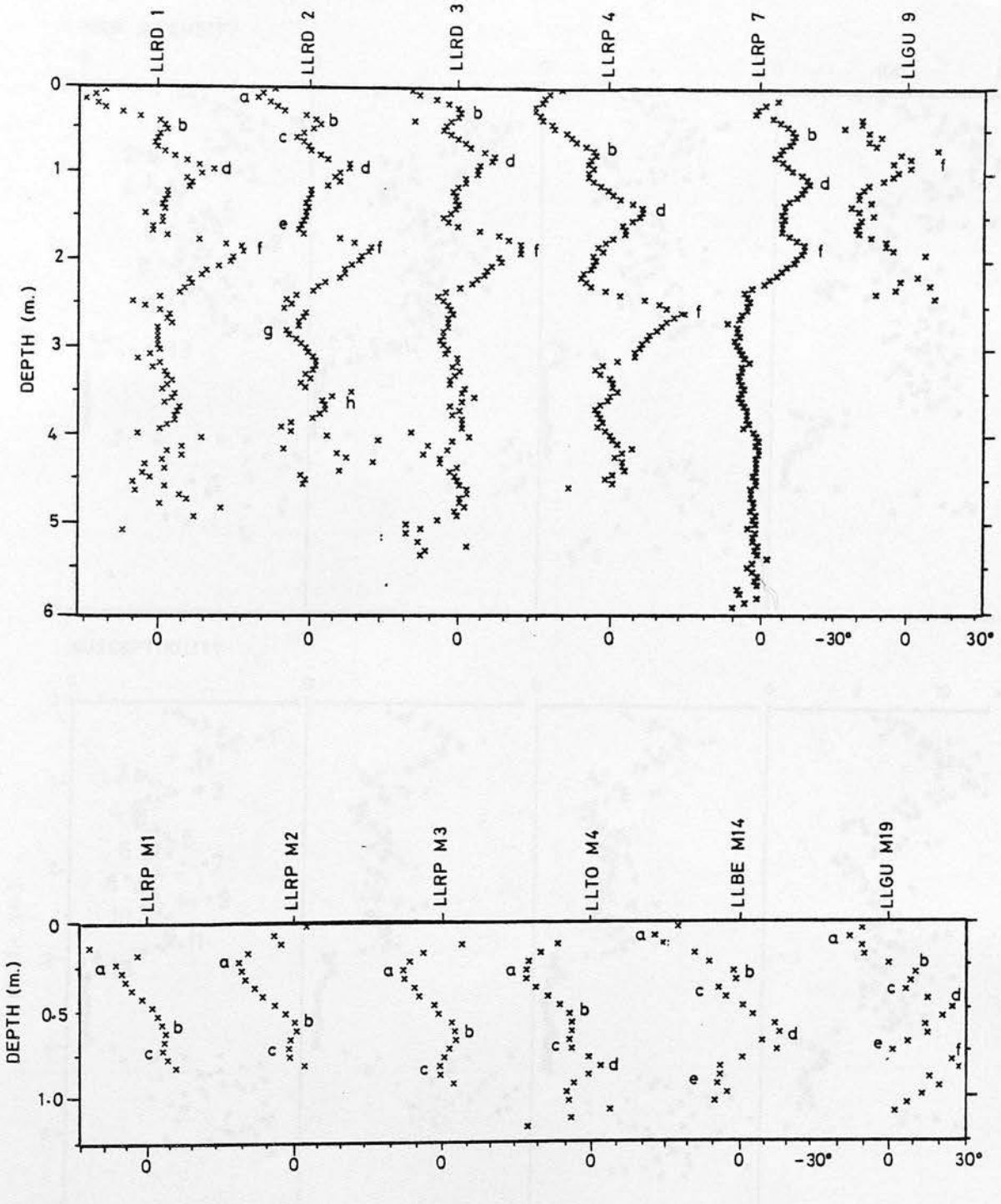


Figure 3.3 : Lomond long and mini cores ; whole core declination logs.

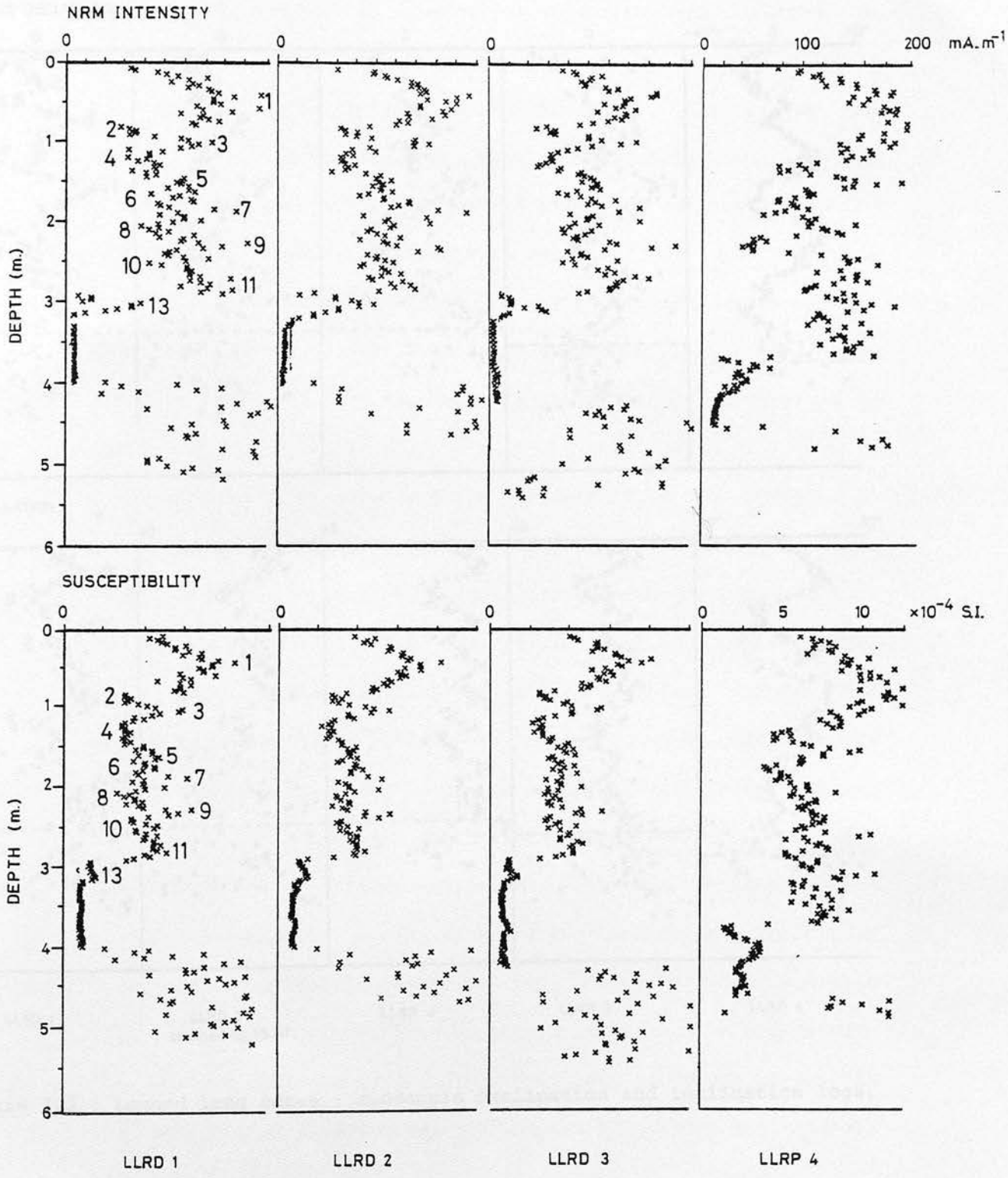


Figure 3.4 : Lomond long cores : subsample remanent intensity and susceptibility logs.

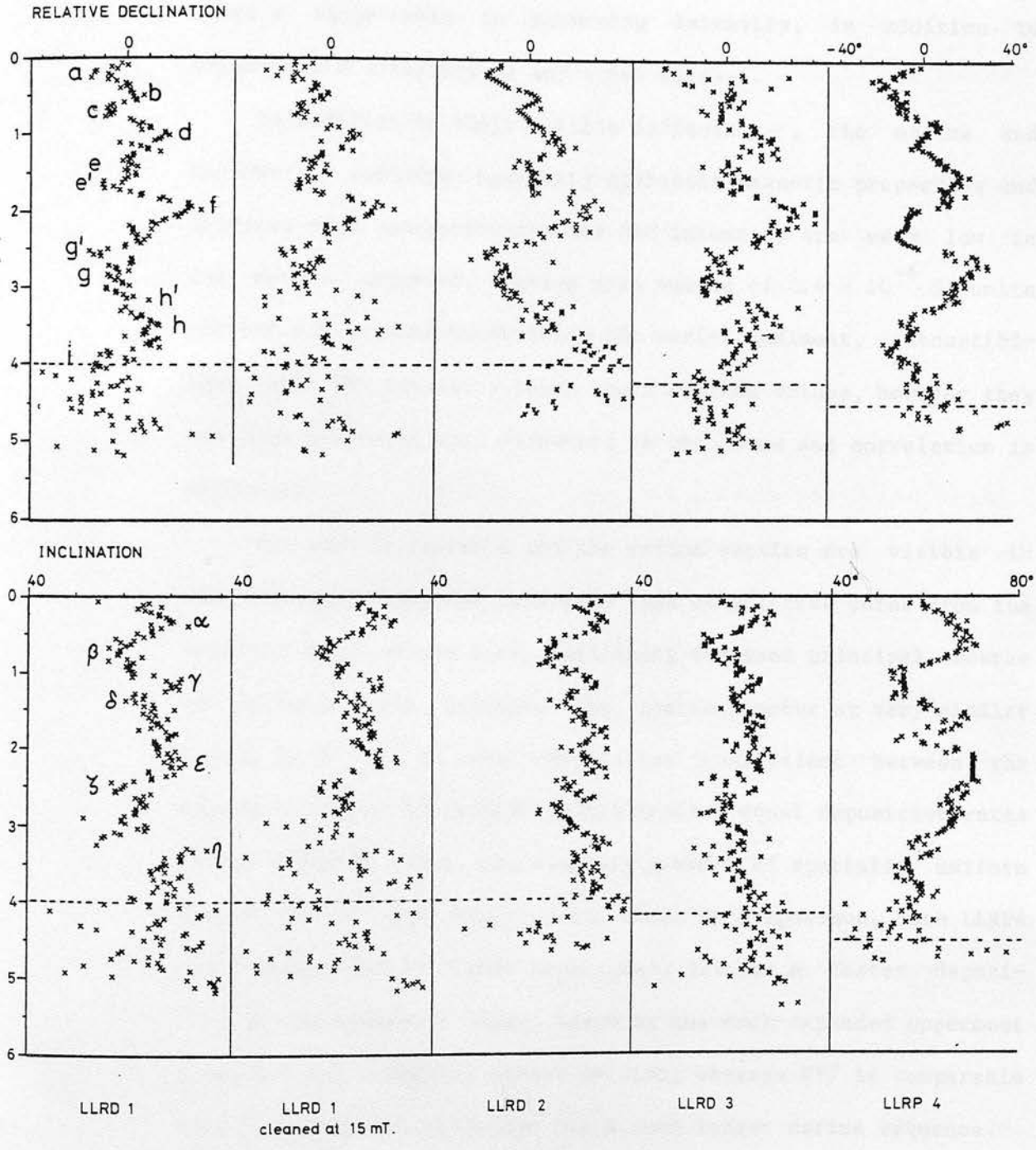


Figure 3.5 : Lomond long cores : subsample declination and inclination logs.

geomagnetic field. The same 16 features occur at the same depths in each of the remanent intensity logs, both long core horizontal intensity and subsample total intensity. This similarity between susceptibility and NRM intensity is a good indication that the remanence is of detrital origin, but shows that magnetic content plays a large role in governing intensity, in addition to palaeo-field intensity or any other factors.

In addition to their visible difference , the marine and freshwater sediments have very different magnetic properties and origins. Both susceptibility and NRM intensity are very low in the marine sediment, having mean values of $0.4 \times 10^{-6}$ SI units and $1 mA.m^{-1}$ respectively. Below the marine sediment, susceptibility and NRM intensity reach their maximum values, however they are more scattered than elsewhere in the cores and correlation is difficult.

The same 16 features and the marine section are visible in the susceptibility and intensity logs of all five cores from the southern basin of the loch, indicating the same principal source of sediment: the Endrick. The features occur at very similar depths in D1, 2, 3 (the correlation coefficient between the depths in D1 and D3 is 0.95). This implies equal deposition rates in all three RD cores, and suggests a model of spatially uniform deposition in this basin of the loch. By comparison, both LLRP4 and 7 have slightly higher amplitudes. RP4 has a faster deposition in the uppermost metre, shown by the much expanded uppermost peak, and has a shorter marine section, whereas RP7 is comparable with RD in the top 2.5m, but has a much longer marine sequence.

These variations in the deposition rate at RP may be due to the site being in a channel between the lake shore and islands,

and near the outflow. During the marine transgression the connection to the sea would have been at this end of the loch, whereas RD would have been more protected by the intervening islands.

LLGU9 is more difficult to compare. The bottom 3m of coretube contained green/gray clay. The correlation shown in the post Glacial is tentative, but is aided by the mini-core LLGUM19.

The three LLRP mini-cores, and the longer LLTOM4, are all easily correlated with their 6m counterparts, via the whole core logs. However, as they demonstrate the long records to be reliable to the surface, it was unnecessary to use them to complete the record.

### 3.1.2: NRM directions.

The Lomond direction records are amongst the finest quality records obtained on European lake sediments. The declination logs are similar in general form to other British lake records (Windermere, Mackereth 1971; Neagh, Thompson 1975; Shiel, Thompson and Wain-Hobson 1979) , and their peak-peak amplitude of 40-45° is in good agreement also. However the scatter is much lower, and much more fine scale detail between the major swings can be resolved than previously. For example, the broad double nature of westerly swings e and g is quite distinct from the sharpness of f. All four cores sampled in detail also have excellent, well-defined inclination records, of peak-peak amplitude 10-15°.

The stability of the remanence was demonstrated by stepwise alternating field demagnetization of sets of pilot samples spaced down selected cores. Sixteen samples were chosen from 12 horizons

in LLRD3 and 8 from 6 horizons in LLRD1. Demagnetization was at peak-peak intervals of 5mT to 50mT, then at 10mT intervals to 100mT. Zijderveld plots for the samples from LLRD1 are shown in figure 3.6. These plots are an alternative, more informative way than the stereogram(also shown for sample 13) for viewing tightly clustered directions; small changes in direction are picked out more easily. Also given are values of the circular standard deviation of the directions for each sample in the interval 0-50mT. With the exception of sample 18, in the uppermost, wetter sediment, for which $\vartheta_{63} = 1.79°$, all the samples from the post-marine gyttja have values of $\vartheta_{63}$ less than 1.25°, showing extremely stable remanence directions, as this discrepancy is within the measuring error of the Digico spinner. A value of $\vartheta_{63}$ up to 5° in this coercivity range is considered good and up to about 10° quite acceptable. No secondary components are visible from figure 3.6 for either the freshwater or the marine samples, although the directions at high fields are more scattered in the weaker marine pilot sample (129), probably because of the difficulty in measuring such weak remanences accurately.

Both the declination and the inclination logs have been compared with 1)the London magnetic observatory records for the last 250 years, 2)archaeomagnetic direction curves extending back to 1700 BP (Aitken, 1970;Thellier,1968), and 3)Mackereth's(1971) C-14 dated declination curve for Lake Windermere.

The 1820 westerly declination swing (a) and the 1720 inclination maximum ($\alpha$) from observatory data are visible in all four single sample records. b and c in declination and $\beta, \gamma, \delta$ in inclination also correlate with points on the archaeomagnetic curves. The archaeomagnetic "dark-ages" between Roman and Me-

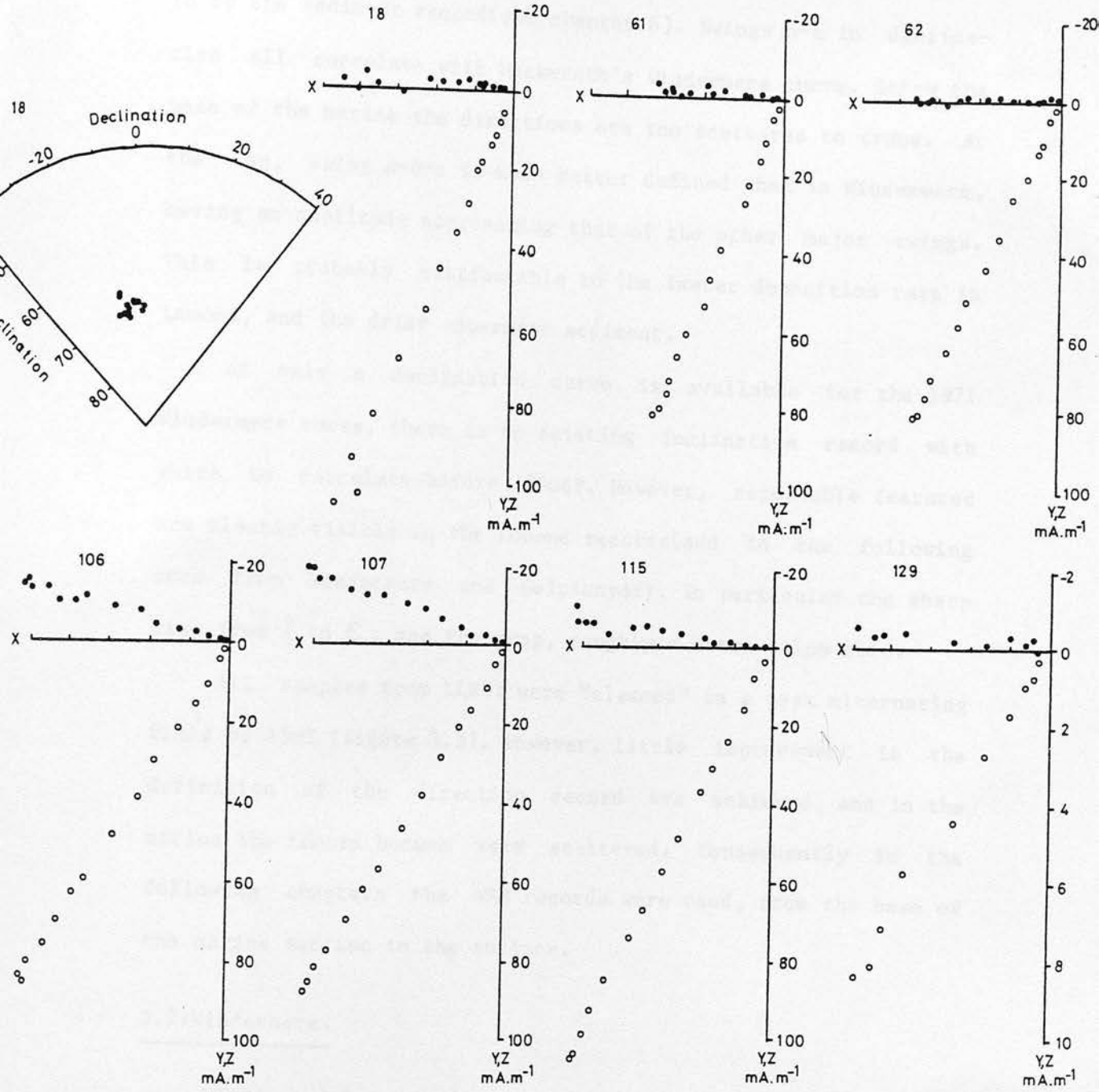


| Sample | 18 | 61 | 62 | 106 | 107 | 115 | 129 |
|---|---|---|---|---|---|---|---|
| Depth (m.) | 0·39 | 1·41 | 1·44 | 2·46 | 2·48 | 2·67 | 3·01 |
| M D F (mT.) | 26·0 | 38·5 | 36·0 | 38·0 | 36·0 | 37·0 | 20·0 |
| $\vartheta_{63}$ | 1·79 | 1·22 | 1·11 | 1·24 | 0·93 | 0·91 | 9·17 |

gure 3.6 : LLRD 1 pilot samples : Zijderveld plots of remanent directions during A.F. demagnetization.

● X vs Y  o Xvs Z

diaeval times, for which fired artifacts are scarce, are filled in by the sediment record(see chapter 6). Swings h-c in declination all correlate with Mackereth's Windermere curve. Below the base of the marine the directions are too scattered to trace. At the top, swing a-b-c is much better defined than in Windermere, having an amplitude approaching that of the other major swings. This is probably attributable to the faster deposition rate in Lomond, and the drier uppermost sediment.

As only a declination curve is available for the 1971 Windermere cores, there is no existing inclination record with which to correlate before 1700BP. However, repeatable features are clearly visible in the Lomond records(and in the following ones from Windermere and Geirionydd). In particular the sharp rise from $\zeta$ to $\varepsilon$, and the drop, roughly a metre below this.

All samples from LLRD1 were "cleaned" in a peak alternating field of 15mT (figure 3.5). However, little improvement in the definition of the direction record was achieved, and in the marine the record became very scattered. Consequently in the following chapters the NRM records were used, from the base of the marine section to the surface.

## 3.2:Windermere.

WIND1 and 2 were subsampled from the clay boundary only, as the varve sequence below has quite a different sedimentation rate and character from the gyttja above. WIND3 was sampled throughout. Wholecore measurements are shown in figures 3.7, 3.8 and 3.9 and subsample results in figures 3.10 and 3.11.

The characteristics of the Windermere records are quite different from either Lomond or Geirionydd.

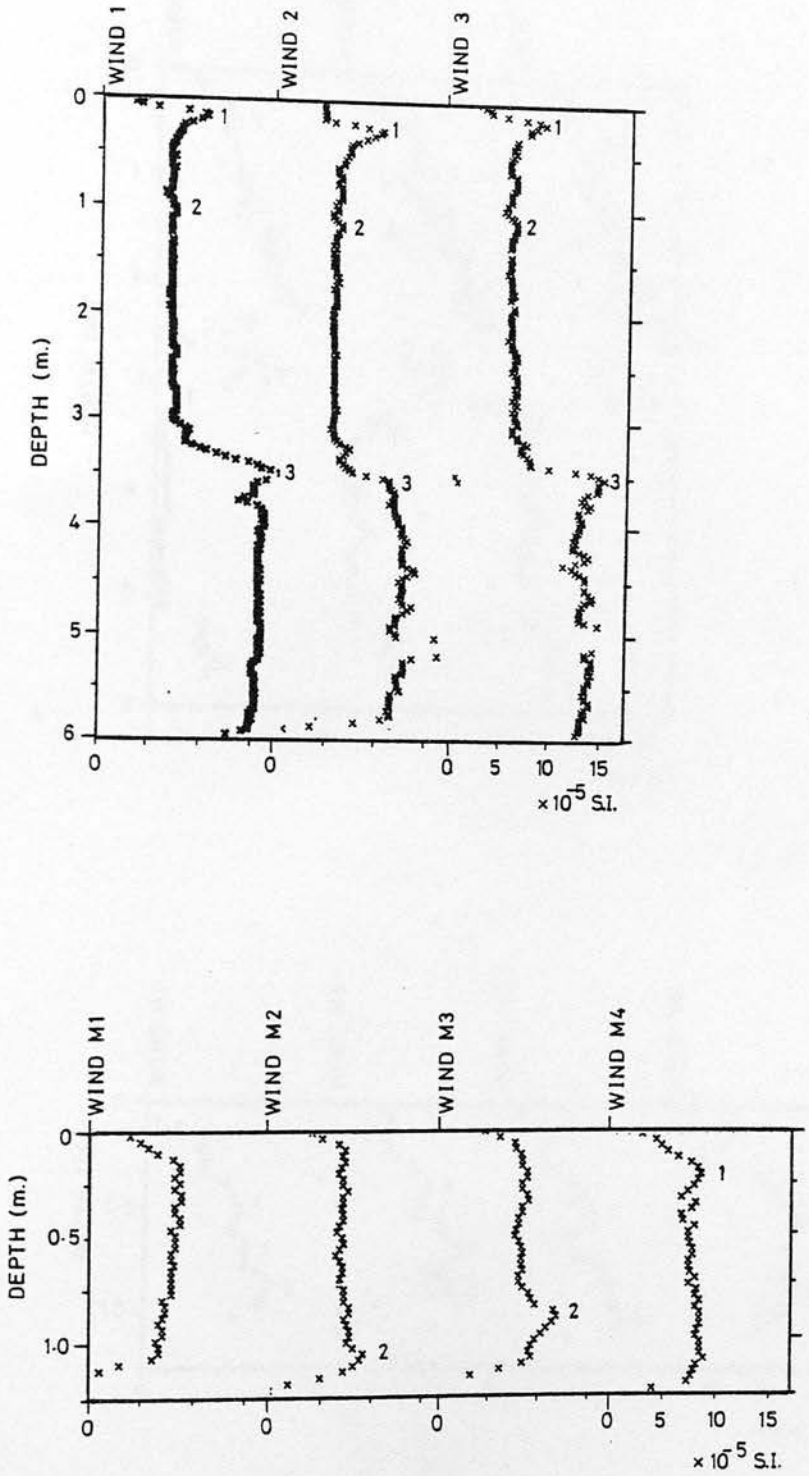


Figure 3.7 : Windermere long and mini cores ; whole core susceptibility logs.

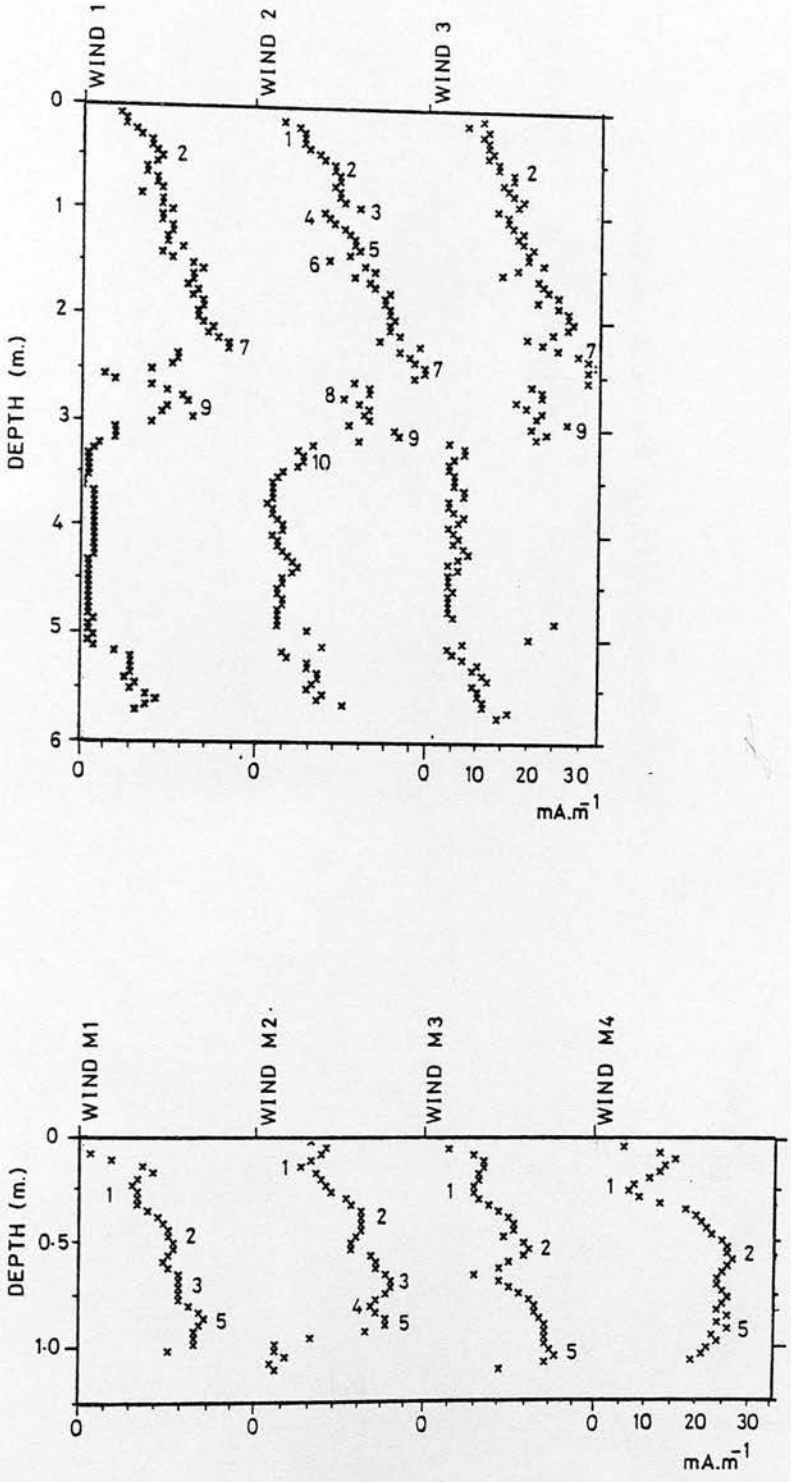


Figure 3.8 : Windermere long and mini cores : whole core horizontal remanent intensity logs.

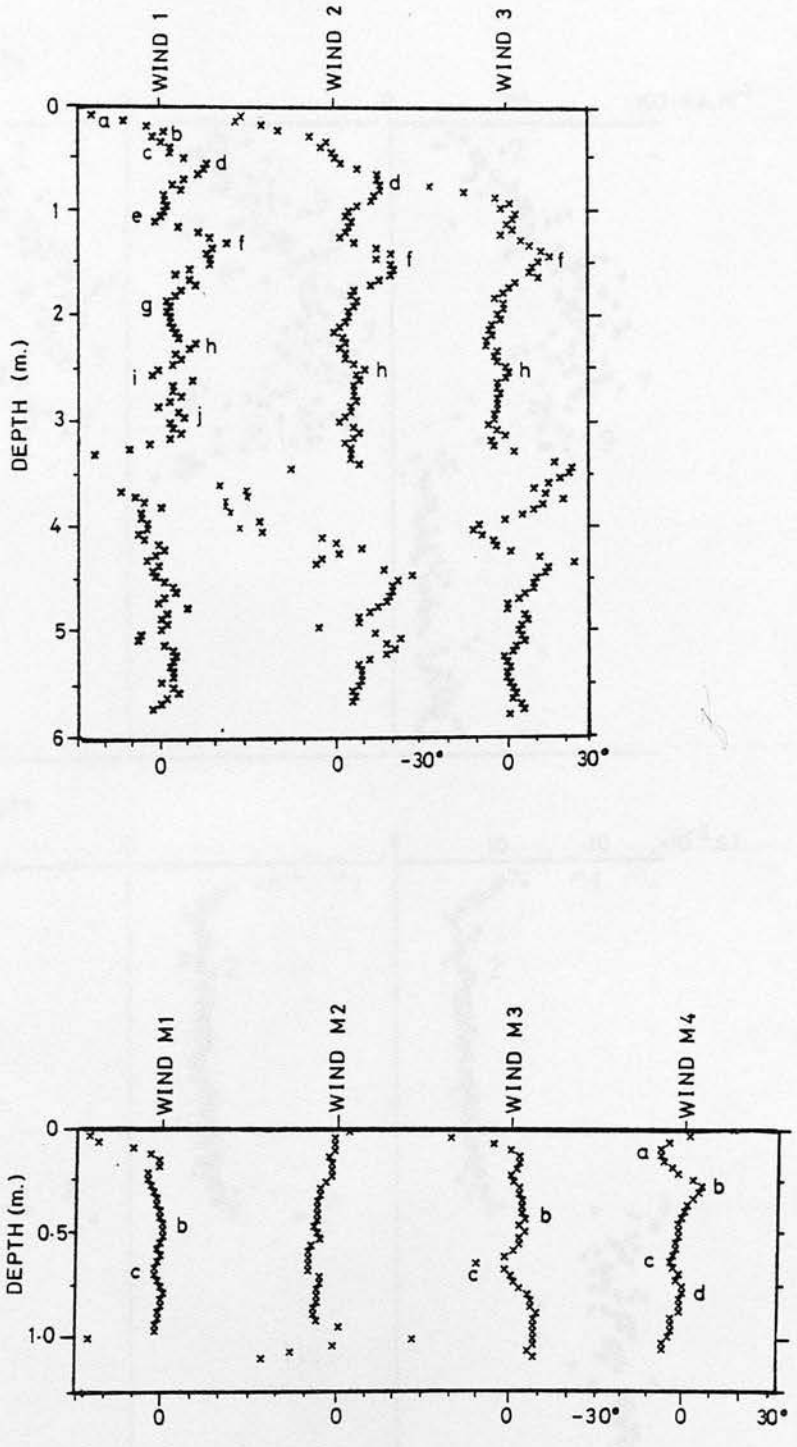


Figure 3.9 : Windermere long and mini cores : whole core declination logs.

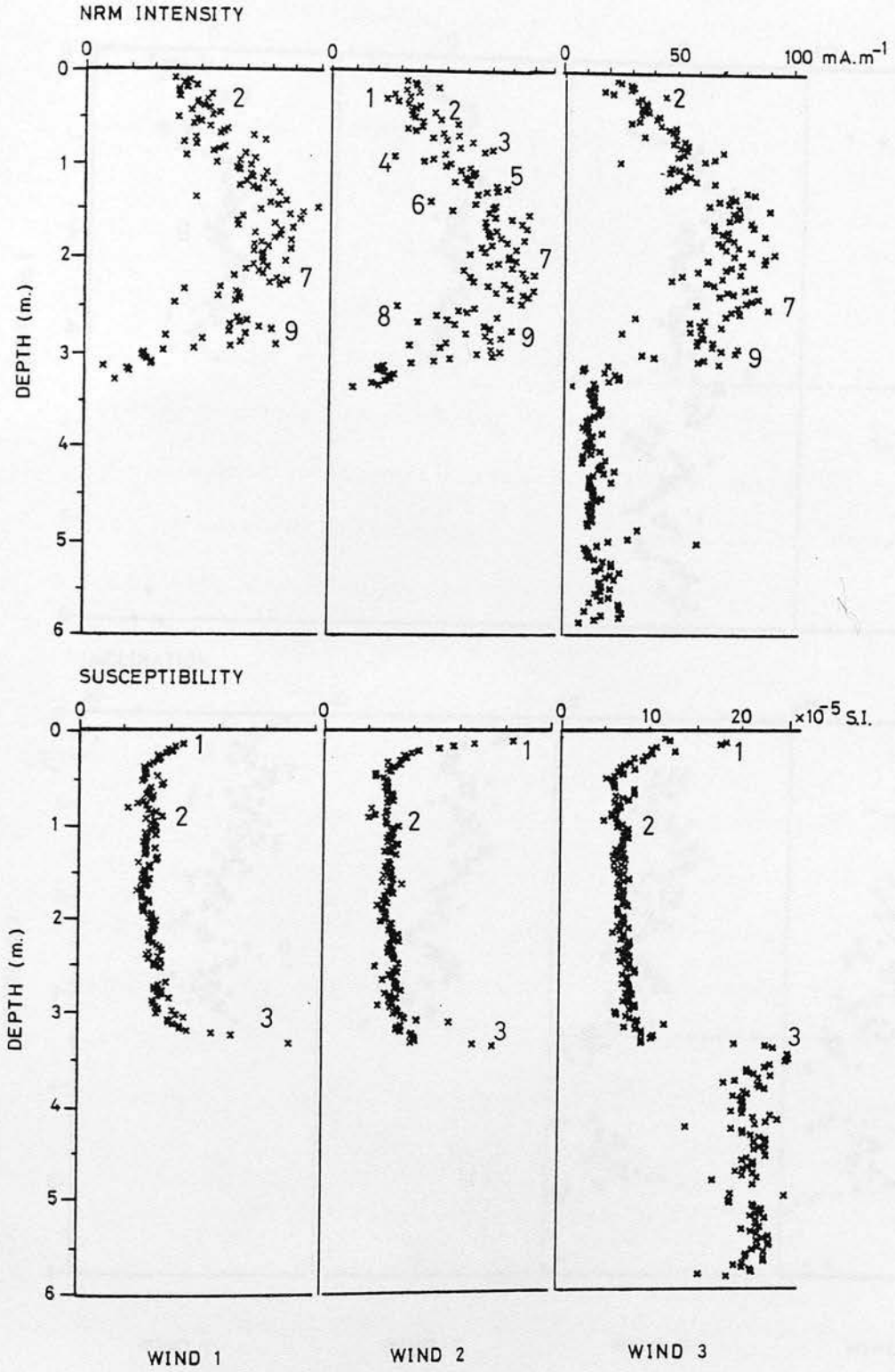


Figure 3.10 : Windermere long cores : subsample susceptibility and intensity logs.

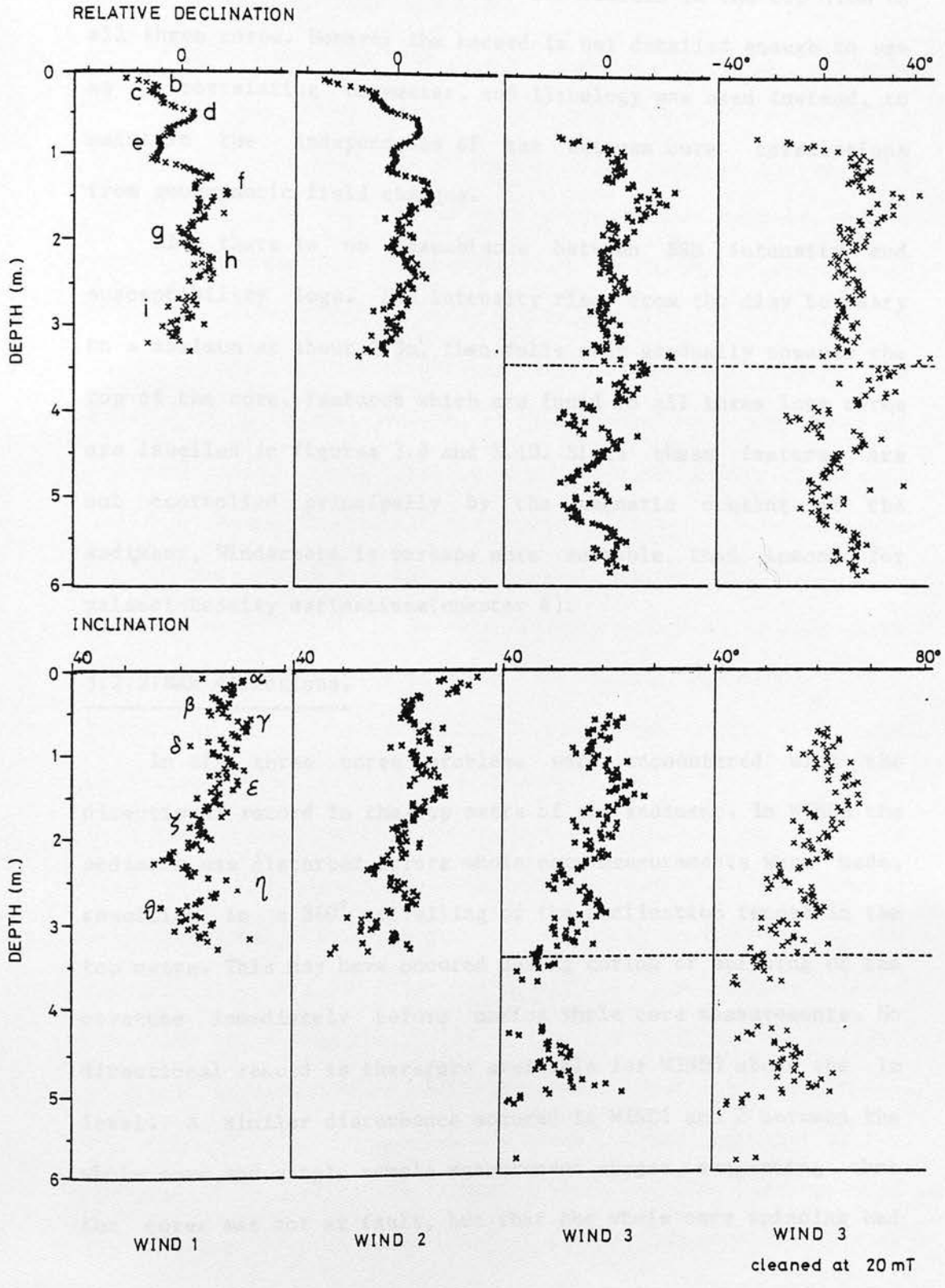


Figure 3.11 : Windermere long cores : subsample declination and inclination logs.

### 3.2.1: Susceptibility and NRM intensity.

Firstly, apart from the sudden change from high to low values across the clay/gyttja boundary, the susceptibility record is almost featureless. Two peaks are visible in the top 1.0m of all three cores. However the record is not detailed enough to use as a correlating parameter, and lithology was used instead, to maintain the independence of the between core correlations from geomagnetic field changes.

Also there is no resemblance between NRM intensity and susceptibility logs. NRM intensity rises from the clay boundary to a maximum at about 2.3m, then falls away gradually towards the top of the core. Features which are found in all three long cores are labelled in figures 3.8 and 3.10. Since these features are not controlled principally by the magnetic content of the sediment, Windermere is perhaps more suitable than Lomond for palaeointensity estimations(chapter 4).

### 3.2.2: NRM directions.

In all three cores problems were encountered with the directional record in the top metre of wet sediment. In WIND3 the sediment was disturbed before whole core measurements were made, resulting in a 360° spiralling of the declination record in the top metre. This may have occured during coring or spinning of the coretube immediately before making whole core measurements. No directional record is therefore available for WIND3 above the 1m level. A similar disturbance occured in WIND1 and 2 between the whole core and single sample measurement stages, suggesting that the corer was not at fault, but that the whole core spinning had

twisted the sediment. Fortunately the inclination records for WIND1 and 2 are reliable, shown by their agreement with the archaeomagnetic features $\delta$-$\alpha$. The whole core results have been used to make up the top metre of the subsample declination logs, resulting in a smoother appearance.

WIND1 carries the most complete declination record, although the uppermost swing, a-b-c, is not nearly as well defined as in Lomond. This was also true of Mackereth's Windermere record. The inclination records however are much better defined, and in better agreement with one another than the old Windermere curve. $\delta$ -$\alpha$ of the archaeomagnetic curve are discernable, as in Lomond, at corresponding depths with respect to the declination records. The rise $\zeta$ to $\varepsilon$ is also present, at approximately the same level as the declination swing from g to f. Below this level both declination and inclination are better defined in Windermere than Lomond, and extend back further. Several new features have been identified ($\eta$ - $\varepsilon$) in the lowermost metre of all three inclination records. The break in the inclination record just below the clay boundary is not of geomagnetic origin, but caused by a slump, also recorded by Mackereth(1971).

Eight pilot samples taken from four horizons in WIND3 were stepwise A.F. demagnetized to test the stability of the remanence. Zijderveld diagrams for six are shown in figure 3.12 (the remaining two were from the Glacial varves). The samples marked (*) were taken from the second half of the core, and so are from identical levels to the non-(*) samples. However the inclinations of each of the (*)-samples is 7-10° higher than that of its opposite. This must be the result of some sampling discrepancy. The samples are all more resistant to A.F. demagnetization than

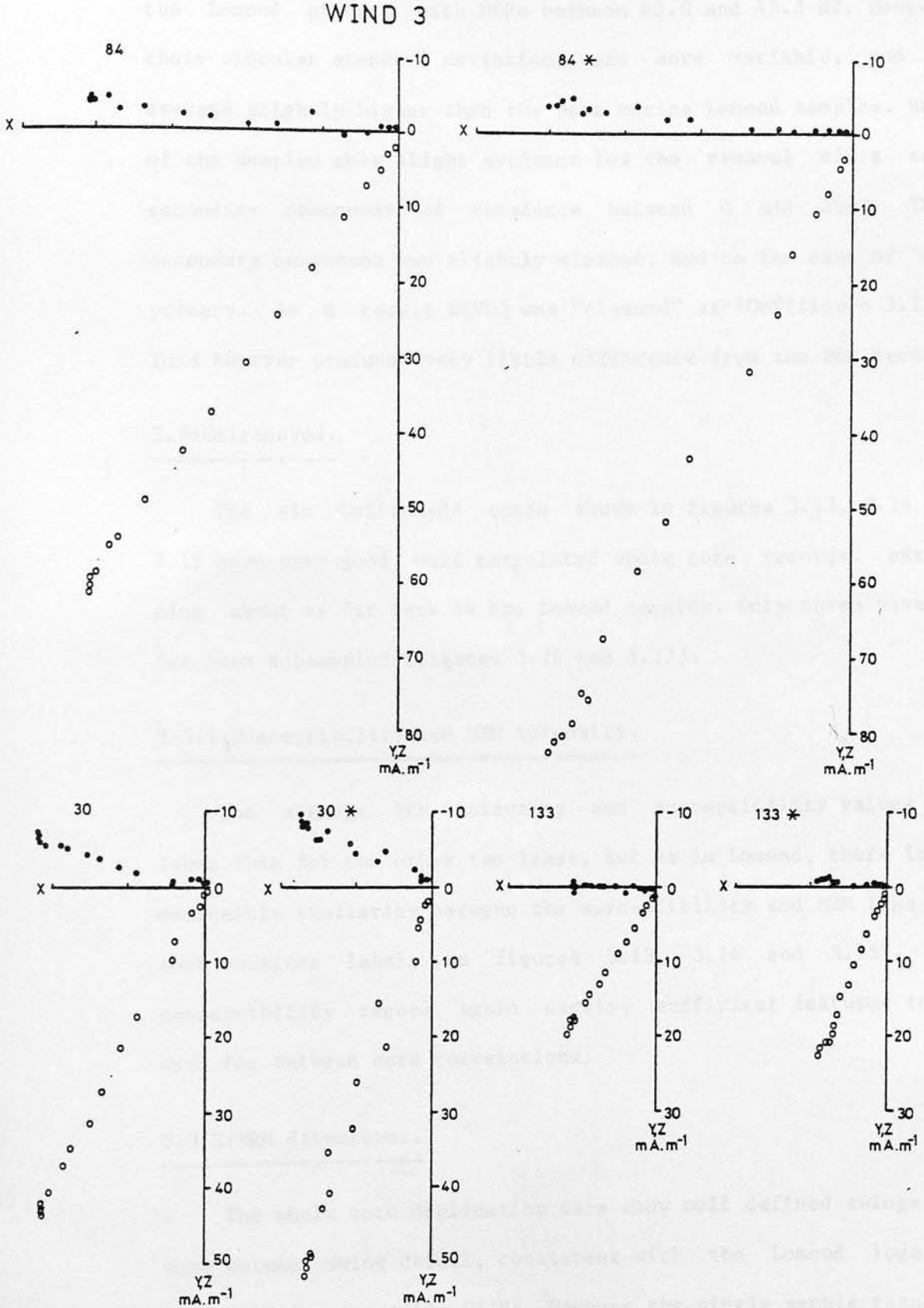


| Sample | 30 | 30 * | 84 | 84 * | 133 | 133 * |
|---|---|---|---|---|---|---|
| Depth (m.) | 0·69 | 0·69 | 1·98 | 1·98 | 3·14 | 3·14 |
| M.D.F. (mT.) | 44·5 | 45·5 | 45·0 | 46·0 | 43·0 | 43·0 |
| $\vartheta_{63}$ | 0·95 | 2·03 | 0·98 | 1·19 | 2 17 | 1·60 |

● X vs Y
○ X vs Z

Figure 3.12 : WIND 3 pilot samples : Zijderveld plots of remanent directions during A.F. demagnetization.

the Lomond pilots, with MDFs between 43.0 and 45.5 mT. However their circular standard deviations are more variable, and on average slightly higher than the post marine Lomond samples. Most of the samples show slight evidence for the removal of a soft secondary component of remanence between 0 and 20mT. This secondary component was slightly steeper, and to the east of the primary. As a result WIND3 was "cleaned" at 20mT(figure 3.11). This however produced very little difference from the NRM record.

### 3.3:Geirionydd.

The six Geirionydd cores shown in figures 3.13, 3.14 and 3.15 have very good, well correlated whole core records, extending about as far back as the Lomond records. Only three have so far been subsampled (figures 3.16 and 3.17).

#### 3.3.1:Susceptibility and NRM intensity.

The average NRM intensity and susceptibility values are lower than for the other two lakes, but as in Lomond, there is a noticeable similarity between the susceptibility and NRM logs for each core(see labels on figures 3.13, 3.14 and 3.15). The susceptibility record again carries sufficient features to be used for between core correlations.

#### 3.3.2:NRM directions.

The whole core declination data show well defined swings and some between swing detail, consistent with the Lomond logs of figure 3.3, especially GEIR4. However the single sample results, particularly GEIR4, are rather scattered in comparison with either Lomond or Windermere. It was thought that this scatter

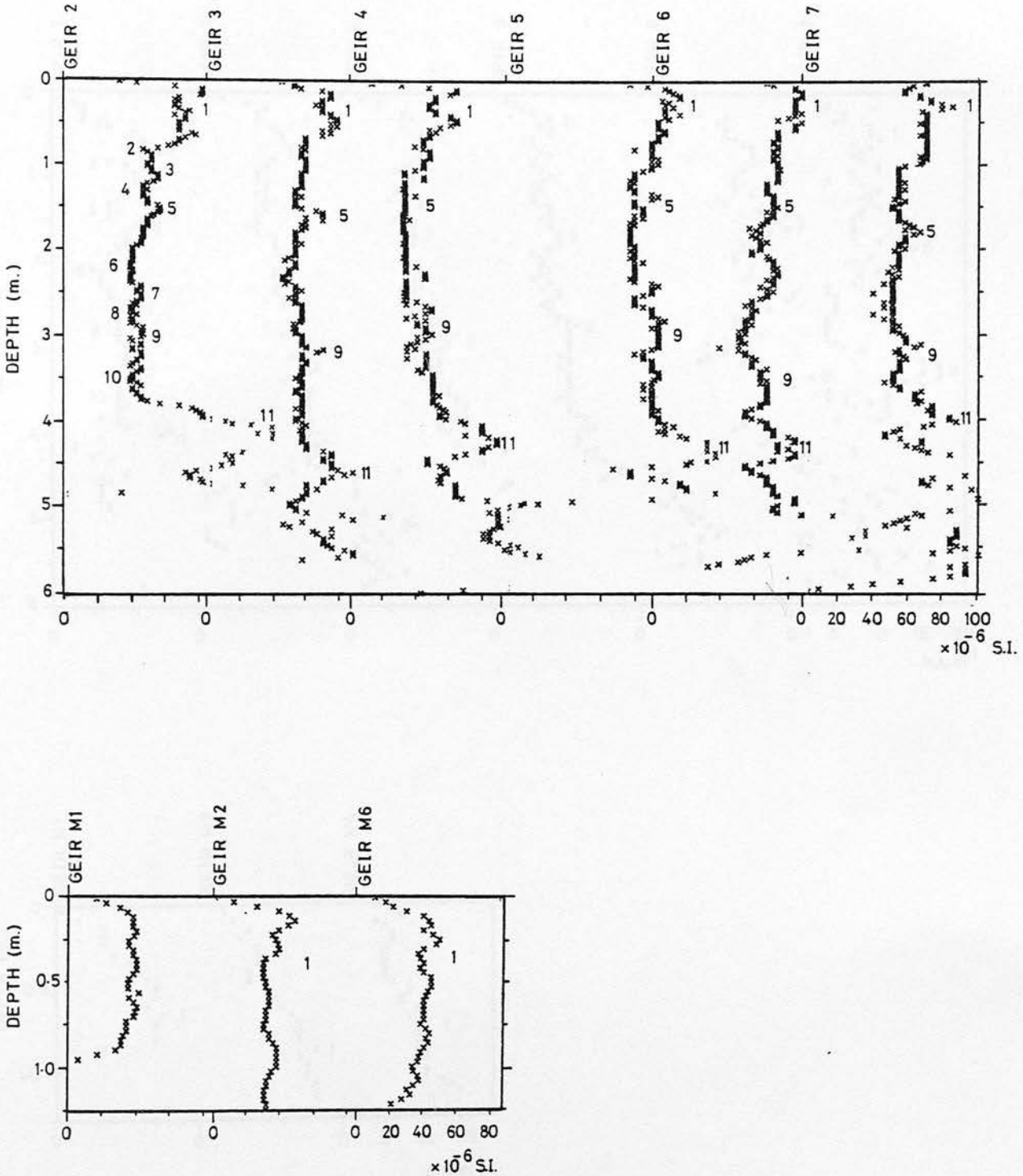


Figure 3.13 : Geirionydd long and mini cores : whole core susceptibility logs.

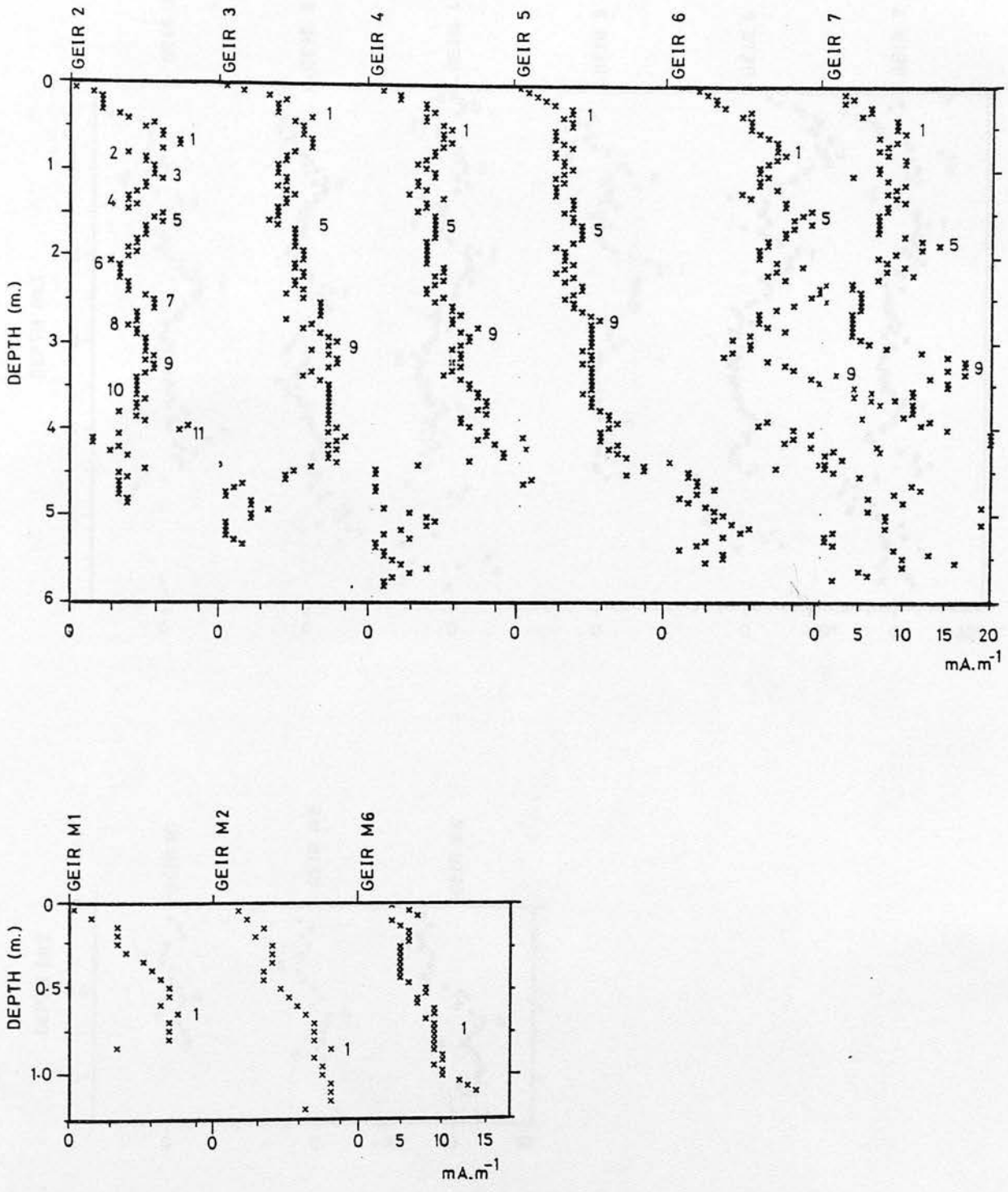


Figure 3.14 : Geirionydd long and mini cores : whole core horizontal remanent intensity logs.

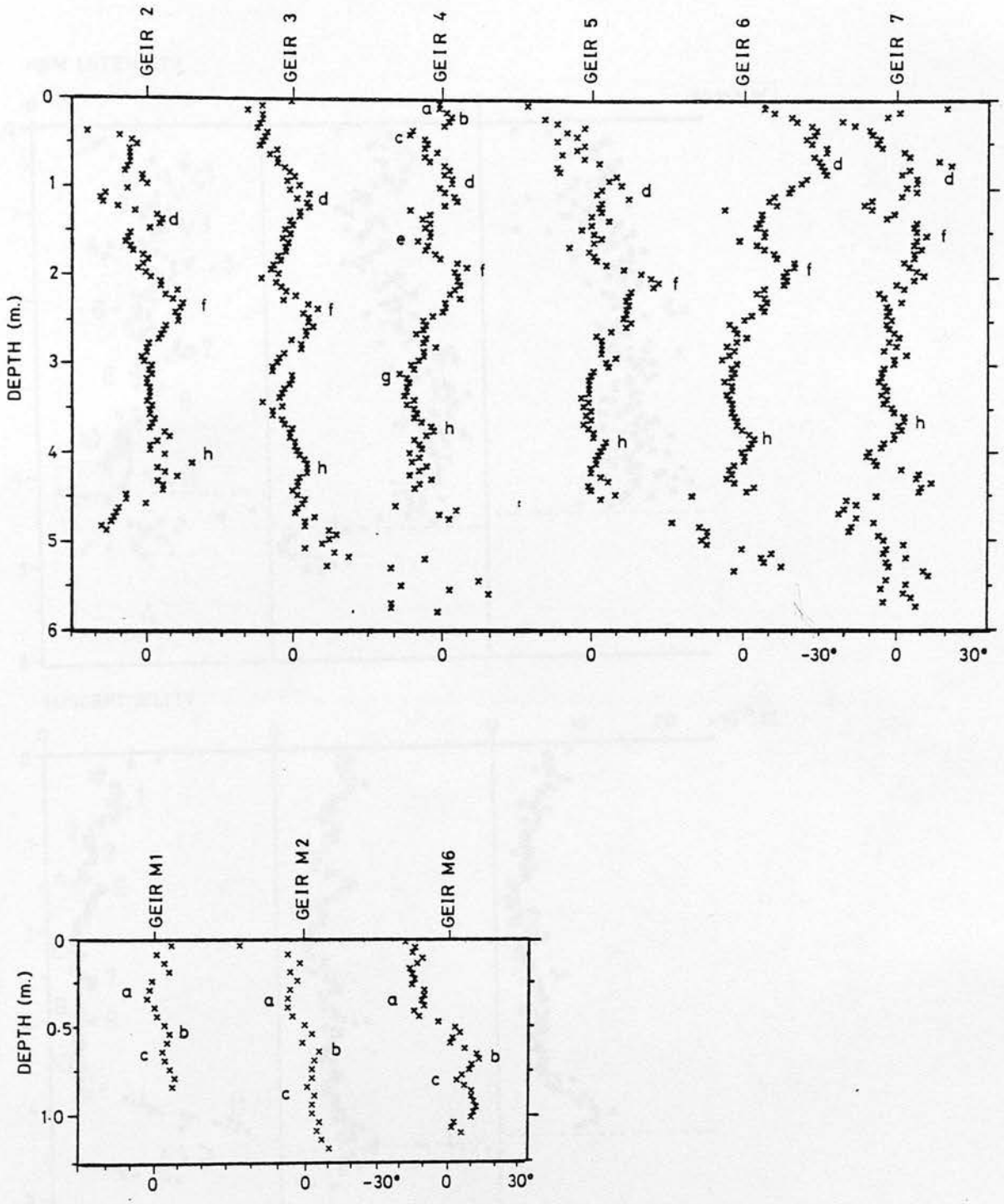


Figure 3.15 : Geirionydd long and mini cores : whole core declination logs.

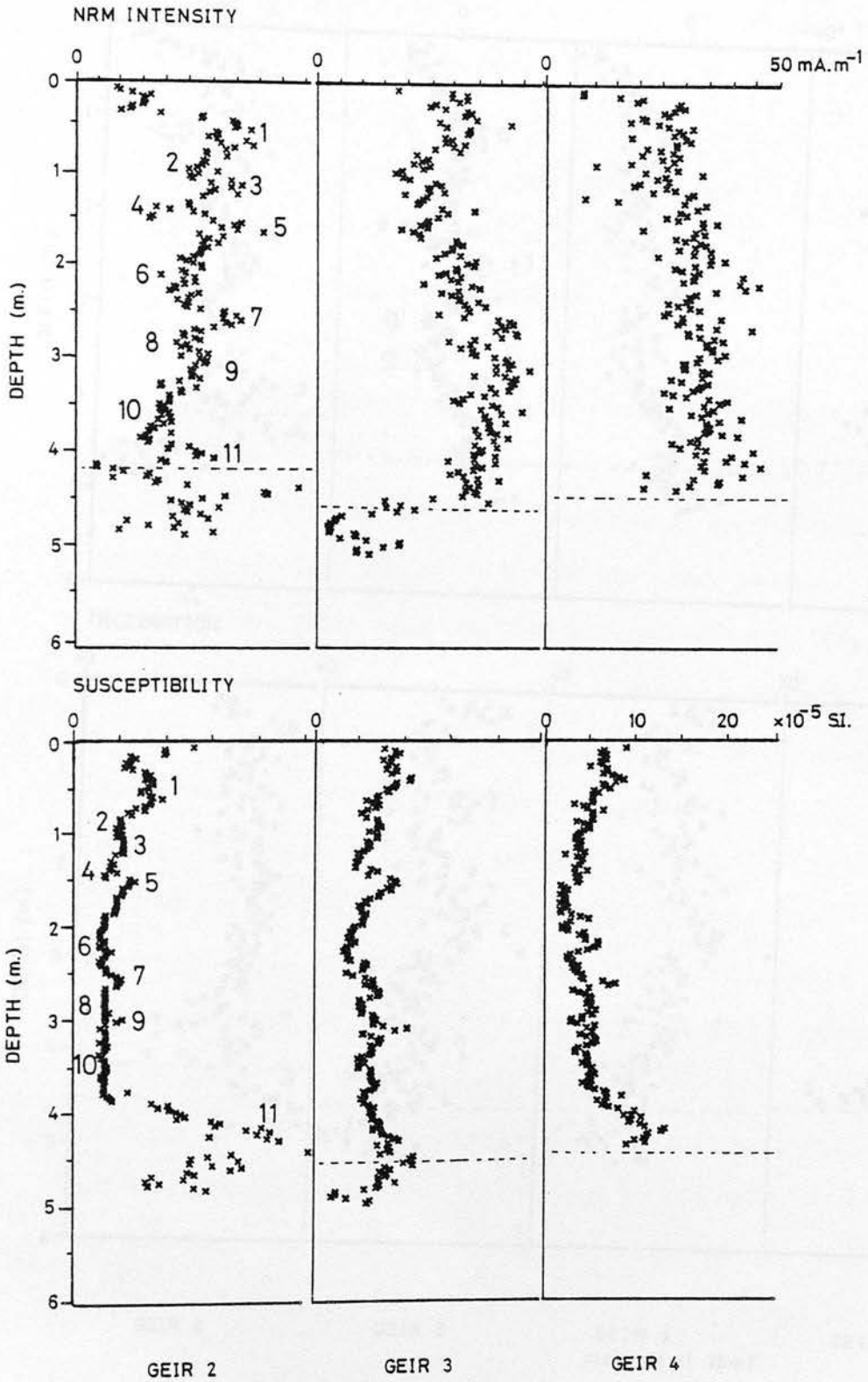


gure 3.16 : Geirionydd long cores : subsample remanent intensity and susceptibility logs.

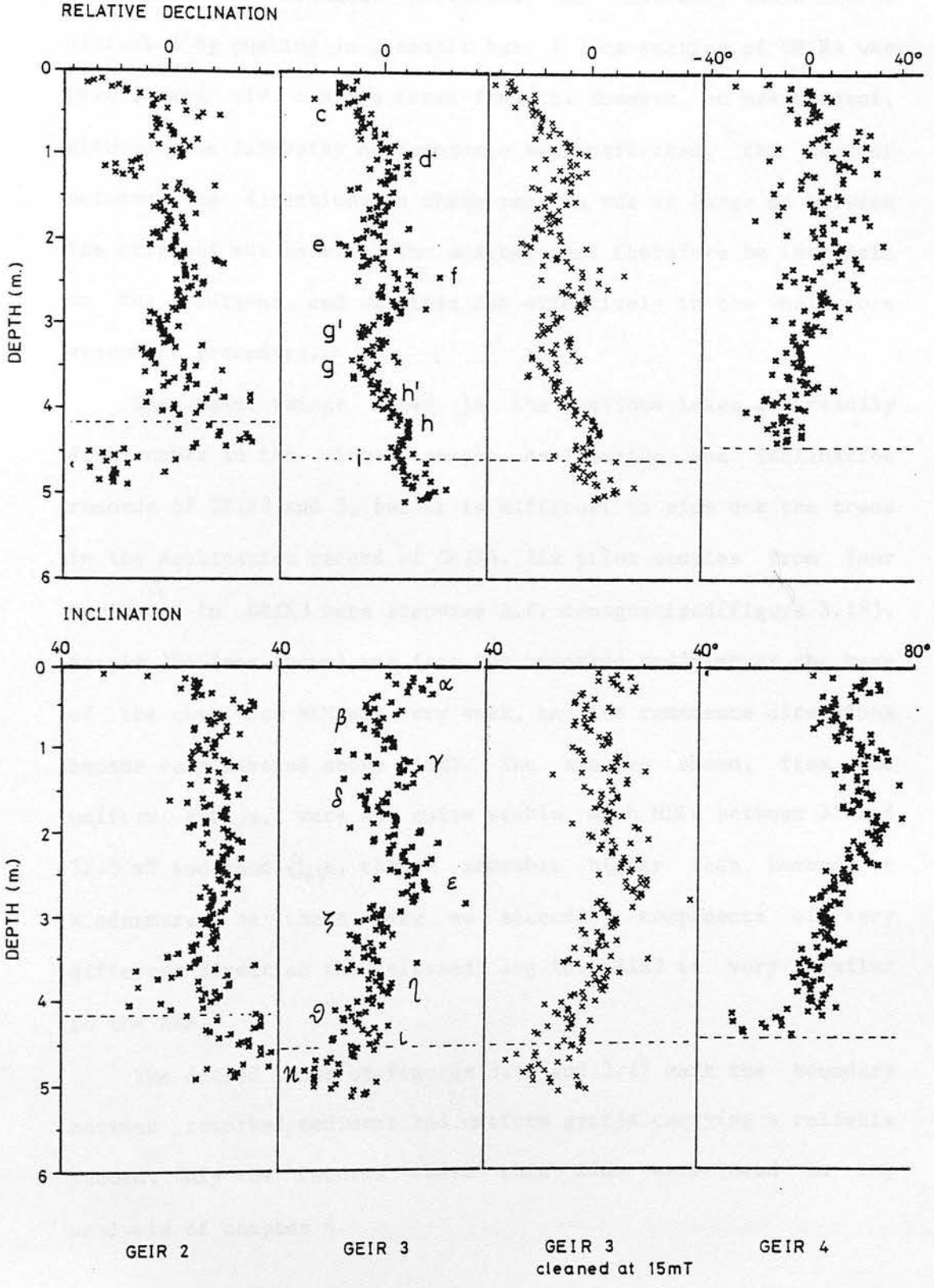


Figure 3.17 : Geirionydd long cores : subsample declination and inclination logs.

might have been introduced during sampling of the extremely wet sediment. Experiments were therefore tried in which the water was replaced by Carbowax 6000 (Greene-Kelly et al., 1970) before sampling from the coretube. It was hoped that this would immobilise the sediment particles, so that they would not be disturbed by pushing in a sample box. A 20cm section of GEIR4 was waxed, and six samples taken from it. However, on measurement, although the intensity of remanence was unaffected, the scatter between the directions in these samples was as large as between the original wet samples. The scatter must therefore be intrinsic to the sediment, and smoothed out effectively in the whole core measuring procedure.

The main swings noted in the previous lakes are readily discernable in the single sample declination and inclination records of GEIR2 and 3, but it is difficult to pick out the trend in the declination record of GEIR4. Six pilot samples from four horizons in GEIR3 were stepwise A.F. demagnetized(figure 3.18). Sample 184 (not shown) was from the reworked sediment at the base of the core, its NRM was very weak, and its remanence directions became very diverse above 10mT. The samples shown, from the uniform gyttja, were all quite stable, with MDFs between 31 and 32.5 mT and good $\vartheta_{63}$s, though somewhat higher than Lomond or Windermere. As there were no secondary components of very different direction the "cleaned" log for GEIR3 is very similar to the NRM.

The dotted lines of figures 3.16 and 3.17 mark the boundary between reworked sediment and uniform gyttja carrying a reliable record. Only the records above this line were used in the analysis of chapter 6.

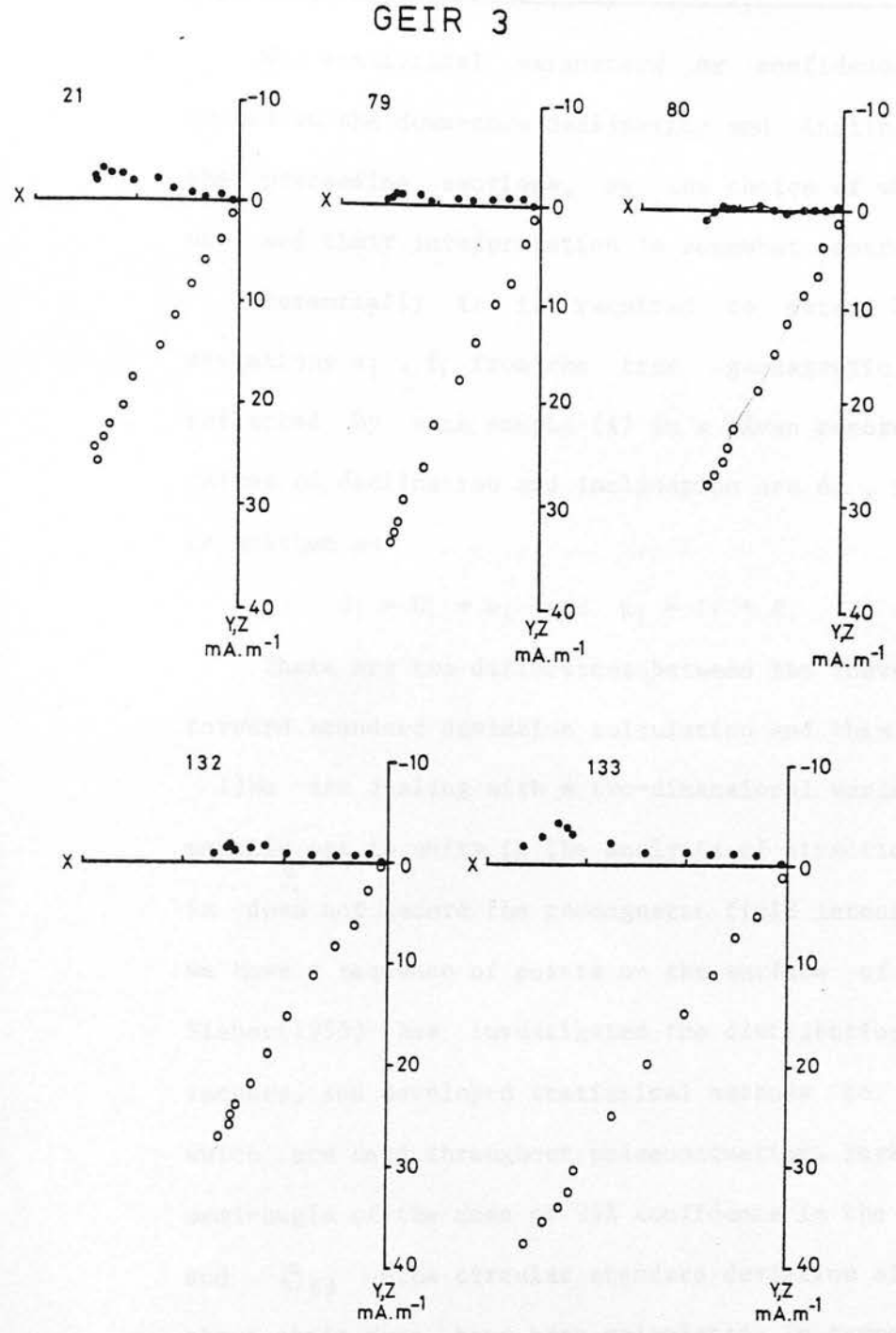


| Sample | 21 | 79 | 80 | 132 | 133 |
|---|---|---|---|---|---|
| Depth (m) | 0·53 | 2·12 | 2·15 | 3·42 | 3·44 |
| M.D.F. (mT.) | 32·5 | 31·0 | 31·0 | 32·0 | 31·0 |
| $\vartheta_{63}$ | 2·77 | 3·08 | 2·60 | 4·22 | 3·16 |

Figure 3.18 : GEIR 3 pilot samples : Zijderveld plots of remanent directions during A.F. demagnetization.

● X vs Y  o X vs Z

## 3.4: Statistics of directional records and confidence levels.

No statistical parameters or confidence limits have been quoted on the down-core declination and inclination records in the preceeding sections, as the choice of which parameters to use, and their interpretation is somewhat controversial.

Essentially it is required to obtain an estimate of the deviations $e_i$ , $f_i$ from the true geomagnetic signal $D_i$ , $I_i$ reflected by each sample (i) in a given record. If the measured values of declination and inclination are $d_i$ , $i_i$ , then they can be written as

$$d_i = D_i + e_i \quad \text{and} \quad i_i = I_i + f_i$$

There are two differences between the conventional straightforward standard deviation calculation and this problem:

1)We are dealing with a two-dimensional variable (intensity is usually set to unity in the analysis of directional records, as it does not record the geomagnetic field intensity directly). So we have a sequence of points on the surface of a unit sphere. Fisher(1953) has investigated the distribution of such a set of vectors, and developed statistical methods to deal with them, which are used throughout palaeomagnetism. Formulae for $\alpha_{95}$-the semi-angle of the cone of 95% confidence in the mean direction, and $\vartheta_{63}$ -the circular standard deviation of the measurements about their mean, have been calculated. In comparing records with different numbers of data points, $\vartheta_{63}$ should be used in preference to $\alpha_{95}$, as the latter is dependant upon the number of points.

2)We are studying the secular variation down a sediment sequence, hence $D_i$ and $I_i$ are not constant down the record but

vary with depth (and hence i). Parameters such as $\alpha_{95}$ and $\vartheta_{63}$ are calculated on the assumption that all the $d_i$ and $i_i$ are reflections of the same geomagnetic vector D, I, the best estimate of which is the mean vector of the core. So $\alpha_{95}$ and $\vartheta_{63}$ are calculated assuming the "error" in the $i^{th}$ measurement to be $e'_i$ , $f'_i$ , given by

$$d_i = \bar{D} + e'_i \quad \text{and} \quad i_i = \bar{I} + f'_i$$

This error $e'_i$ , $f'_i$ is really the sum of the secular variation $\bar{D}-D_i$ , $\bar{I}-I_i$ and the actual error in the measurement $e_i$ , $f_i$ . So the values of $\alpha_{95}$ and $\vartheta_{63}$ for a record reflect both the amplitude of secular variation and the amount of scatter.

An alternative approach is provided by Watson and Beran's "serial correlation" test (Watson and Beran, 1967). This computes a statistic dependant on the size of the angles between successive unit vectors in the record. The scalar products of each pair of adjacent vectors are taken and summed. The deviation of this statistic from its mean value over all permutations of the data points is then calculated. Formulae for calculating the statistic, and its mean and variance over a number of random permutations are given by Epp, Tukey and Watson(1971). The parameter calculated and quoted in table 3.1 is given by

$$A = (L-E)/V$$

in which L=observed sum of scalar products

E=mean sum of scalar product over a number of random permutations of the data points

V=variance of values used in calculating E.

The record is correlated at the 5% or 1% level if the value of A is greater than 1.645 or 2.326 respectively. The test shows significance if each measurement tends to be close to those

immediately above and below it i.e. it will discriminate between real vector movement and scatter if the sampling is close enough for the scatter to be greater than changes in $D_i$ and $I_i$ . Large real differences between adjacent samples will however still contribute to a poor serial correlation.

Values of A, $\alpha_{95}$ and $\vartheta_{63}$ for the sections of cores used for analysis in chapter 6 are shown in table 3.1.

1)Each value of A is very much above the 1% level of significance quoted above.This is probably because of the nature of the variations under investigation. Oberg(M.E.Evans, pers.comm.)has found similarly high values in some much older sediments from British Columbia.

2)On the average the Lomond cores have the highest significance levels, and visually they are undoubtedly the best defined of the records. The Windermere cores however have slightly lower $\vartheta_{63}$s, than Lomond. This is probably because, although Windermere is more scattered (lower serial correlation) the amplitude of the Lomond records is higher, increasing their $\vartheta_{63}$s.

The lower value of A for LLRD3 compared with the other Lomond cores is consistent with the higher scatter visible in the records.

The poor values of both A and $\vartheta_{63}$ for the "cleaned" LLRD1 record is largely due to the marine section, between approximately 4 and 3m, where there are very big angles between adjacent measurements.

The Geirionydd records are much more scattered visually than either of the other two, and have lower peak-peak amplitude than Lomond. This lower amplitude , in spite of increased scatter accounts for the lowest mean $\vartheta_{63}$. The scatter, especially in the

Table 3.1: Downcore Statistical Parameters

| CORE | N | $\alpha_{95}$ | $\theta_{63}$ | A | CORE | N | $\alpha_{95}$ | $\theta_{63}$ | A | CORE | N | $\alpha_{95}$ | $\theta_{63}$ | A |
|---|---|---|---|---|---|---|---|---|---|---|---|---|---|---|
| LLRD1 | 152 | 0.88 | 6.25 | 12.87 | WIND1 | 124 | 0.96 | 6.13 | 9.16 | GEIR2 | 124 | 0.87 | 5.56 | 10.04 |
| LLRD1 cleaned | 146 | 1.82 | 12.49 | 4.32 | WIND2 | 132 | 0.98 | 6.42 | 13.30 | GEIR3 | 158 | 0.82 | 5.90 | 9.98 |
| LLRD2 | 144 | 0.84 | 5.79 | 13.51 | WIND3 | 112 | 1.06 | 6.36 | 11.03 | GEIR3 cleaned | 158 | 0.84 | 6.07 | 9.51 |
| LLRD3 | 162 | 1.01 | 7.33 | 11.13 | WIND3 cleaned | 108 | 1.16 | 6.88 | 10.64 | GEIR4 | 142 | 0.83 | 5.67 | 8.44 |
| LLRP4 | 178 | 1.07 | 8.14 | 16.30 | Average except WIND3 cl. | | | 6.30 | 11.16 | average except G3 cl. | | | 5.71 | 9.49 |
| average except D1 cleaned | | | 6.88 | 13.45 | | | | | | | | | | |

Key: N = Number of data points

$\alpha_{95}$ = Circle of 95% confidence

$\theta_{63}$ = Circular standard deviation

A = Serial correlation parameter

declination record of GEIR4 keeps the serial correlation low also.

In conclusion: 1) Serial correlation would seem the better method for discriminating between random scatter and true direction changes, especially when comparing between different lakes, where different sediment types are likely to cause different recording abilities which will be reflected in both peak - peak amplitude and degree of scatter.However it is difficult to put any absolute interpretation on the significance level obtained.

2) $\vartheta_{63}$ may be of some value within a particular lake where cores contain the same sediment type, and the differnces between records are random, introduced during coring, sampling and measurement. $\vartheta_{63}$ should always be used in preference to $\alpha_{95}$.

A possible improvement on the type of statistic discussed above would be an approach involving the fitting of a smooth curve to each data set (or a single curve to a combination of all the data sets), and calculation of the confidence limits, or the variance from this. This has been done for declination and inclination taken separately, using a convolution parameter (Clark and Thompson, 1978), however the problem of treating declination and inclination together is more complex. Serial correlation has the advantage of encompassing the two-dimensionality of the problem quite simply.

## 3.5:Summary.

1)The quality and reproduceability of the results from each lake and the comparison between lakes is better than has previously been obtained.

2)Susceptibility features provide a within-lake correlation for

cores from Lomond and Geirionydd; lithology is used in Windermere.

3)The correlation between declination and inclination logs, within and between lakes and their correlation with existing historical and archaeomagnetic records show that they faithfully record geomagnetic field changes. As each of the 10 cores subsampled yields a complete set of paired declination and inclination values, further, more quantitative analyses , including spectral analyses were carried out (chapter 6).

4)There is little similarity between remanent intensity records from the different lakes: factors such as magnetic content overide the dependence of remanent intensity on geomagnetic field intensity. Chapter 4 discusses attempts to retrieve relative palaeointensities.

5)So far the data is logged in terms of depth below the sediment/water interface. A time scale is necessary to perform spectral analysis in the time domain, and for interpretation in terms of magnetic field models. Suites of radiocarbon dates were obtained on material from each lake for this purpose (chapter 5).

# CHAPTER 4: PALAEOINTENSITIES FROM LAKE SEDIMENTS?

## 4.1: Intoduction.

Twenty years ago Thellier and Thellier (1959) proposed a method for determining the intensity of the ambient magnetic field in which an igneous rock or a fired archaeological specimen had aquired its thermal remanence (TRM). Since then numerous improvements (e.g. Kono, 1977; Shaw, 1974) have been made to the original method, so accurate palaeointensities are now obtainable on many TRM bearing samples. However dating is frequently problematic in such cases, and it is sometimes impossible to place samples in chronological order with certainty. With a sediment record, although absolute dating is equally difficult, we at least have a uniquely ordered, and continuous sequence of measurements: the gaps between civilizations producing fired pottery are filled in, and the record extends back before the beginning of archaeomagnetic ones. So it would be valuable to produce, at least a record of relative changes in palaeointensity from sediments, which could then be calibrated using a few well determined and well dated absolute archaeomagnitudes.

However, it is possible to devise palaeointensity methods on TRMs, because they can be produced and studied in the laboratory. It is not possible to study the growth and behavior characteristics of the depositional or post depositional DRM of sediments in an analagous way for two reasons: 1)the difficulty of realistically scaling down lake bed conditions, and the way in which a sediment forms; and 2)the time necessary for a sediment to form and consolidate naturally. So whereas, for instance, it can be

shown that TRM intensity depends linearly on magnetic field strength, no such relationship has been conclusively proved in the case of the DRM of a lake sediment.

Collinson's (1965) theoretical treatment of non-interacting magnetized particles, settling through water in an applied field, disturbed only by Brownian motion, is an exact parallel with the Langevin theory of a paramagnetic gas, it predicts a linear relationship at low fields ( $mB_o \ll kT$ ). So does Stacey's treatment (1972), in which the grain magnetic moments have a uniform distribution up to some maximum value. In general results of resettling experiments on concentrated reconstituted slurries of both natural and synthetic sediments show a roughly linear trend up to about 0.4 mT (Kent, 1973; Barton, 1978; Papamarono-poulis, 1978). Barton, working on Australian sediment, reports this linearity extending up to 0.8 mT, however this is not so for Lomond (section 4.3). Barton also reports results of redepositing from "dilute slurries" or suspensions, in which the linear region does not extend beyond 0.1 mT, and there is a tendency towards saturation by 0.4 mT. From existing archaeomagnetic records (Kovacheva and Veljovich, 1977; Walton, 1979), however, it seems reasonable to assume that the field has not exceeded at most, 0.2 mT (i.e. five times its present value) in the past few thousand years, so to a first approximation a linear (P) DRM intensity vs. field relationship will be optimistically assumed.

Other factors upon which the remanence is likely to depend are

1)The concentration of NRM bearing material in the sediment.

2)The distribution of magnetic moments possessed by the magnetic particles in the sediment.

3)The number of grains able to align with the magnetic field, and the net degree of alignment. These will depend directly on the size and shape distributions of both magnetic and non-magnetic particles in the sediment. Also if the magnetic mineral is present as inclusions in larger particles of a non-magnetic matrix, the balance between magnetic and dynamical forces on NRM bearing particles will be quite different from the case of homogeneous magnetic particles.

4)Physical conditions e.g. temperature, hydrostatic pressure, water content under which sedimentation takes place. These are usually assumed constant, or of negligible effect. Barton (1978) does record drops in DRM intensity of as much as 85% between dilute suspensions settled at 6°C and 90°C. However, it is felt that lake bed temperatures, in the lakes studied, are unlikely to rise more than a few degrees above 4°C, where negligible effect is anticipated.

There are two classes of approach to normalising these factors:

1)To reproduce a remanence in each sample in exactly the same manner as the NRM was grown, but in a known magnetic field in the laboratory. Then all factors except the ambient fields are identical for NRM and laboratory grown remanences, and the ratio of the two intensities is equal to the ratio of palaeointensity to laboratory field. This is basically the approach taken by Thellier's method, where

$$\frac{\text{(partial) } TRM_{lab}}{\text{(partial) NRM}} = \frac{B_{lab}}{B_{anc}}$$

The equivalent for a sediment would be redeposition or reconstitution. As shown above, this is still too uncertain to

give quantitative results, and impractical at present.

2)To compensate for, or eliminate each factor (1-4) one at a time. The usual method is to neglect 2-4 in so far as they are independant of 1, to assess the concentration of NRM bearing magnetic material in each sample, and to normalise using these estimates. Various magnetic properties have been used to estimate this quantity. The first attempt was probably by Johnson et al. (1948) using IRM. Nesbitt (1966) and Harrison (1966) have used magnetic susceptibility. Nakajima and Kawai (1975) used saturation IRM on Lake Biwa sediments, while Johnson et al. (1975) and Levi and Banerjee (1976) have tried ARM. Susceptibility is not generally a good choice, as it is not a remanent property, but depends upon the existence of a magnetic field. Consequently it has contributions from superparamagnetic and large multidomain grains, in addition to those likely to carry the NRM. Similarly IRM, being grown in very high magnetic fields (100 mT, or 1000 mT for SIRMs) may also effect large multi-domain grains. The mechanism of growth and properties of ARMs in sediments is not absolutely clear, but as its use is becoming popular some tests were carried out on both organic and clay samples.

## 4.2:Properties of ARMs.

The variations of intensity and stability of ARM with 1)direct bias field and 2)peak alternating field, were investigated for selected samples from LLRP4 and WIND3. ARMs were produced in the same coil used for A.F. cleaning, removed from its mu-metal housing. The bias field was provided externally, using a set of three orthogonal pairs of Helmholtz coils 90 cm

square. The two components of the horizontal field were cancelled, and, by first opposing, then reinforcing the ambient vertical component, bias fields between 0 and 0.12 mT were achieved. A pair of circular 36 cm diameter Helmholtz coils were used for higher fields. However, as mutual induction effects were encountered between A.F. and bias coils, only transverse ARMs (A.F. perpendicular to bias field) could be grown, and are of limited value.

Figure 4.1 summarises the results of these experiments:

1)In LLRP4, and the organic WIND3 samples, longitudinal ARMs were saturated in 90 mT peak alternating field. No real saturation effect was observed for transverse ARMs up to 95 mT.

2)For peak A.F. of 90 mT and bias fields between 0 and 0.1 mT the ratio of transverse to longitudinal intensity is between 0.45 and 0.50 in Lomond, 0.55 in Windermere organic and 0.50 in Windermere clay samples.

3)Transverse ARMs were always less stable to A.F. demagnetisation than longitudinal. MDFs were 17% lower for LLRP4.

4)Little deviation from linearity was observed for longitudinal ARM intensity in 90 mT A.F. and 0-0.12 mT bias field. A slight upwards curvature is however persistent, and suggestive of a saturation at higher fields.

5)A.F.demagnetization curves for longitudinal ARMs grown in the range 0-0.12 mT bias field, are very similar, showing that a similar spectrum of grains are used at the different fields.

6)For higher bias fields, and transverse ARMs, the reduction in MDF from 29.5 to 27.5 mT between 0.1 and 0.4 mT is also very small.

In conclusion, since bias field has very little effect on

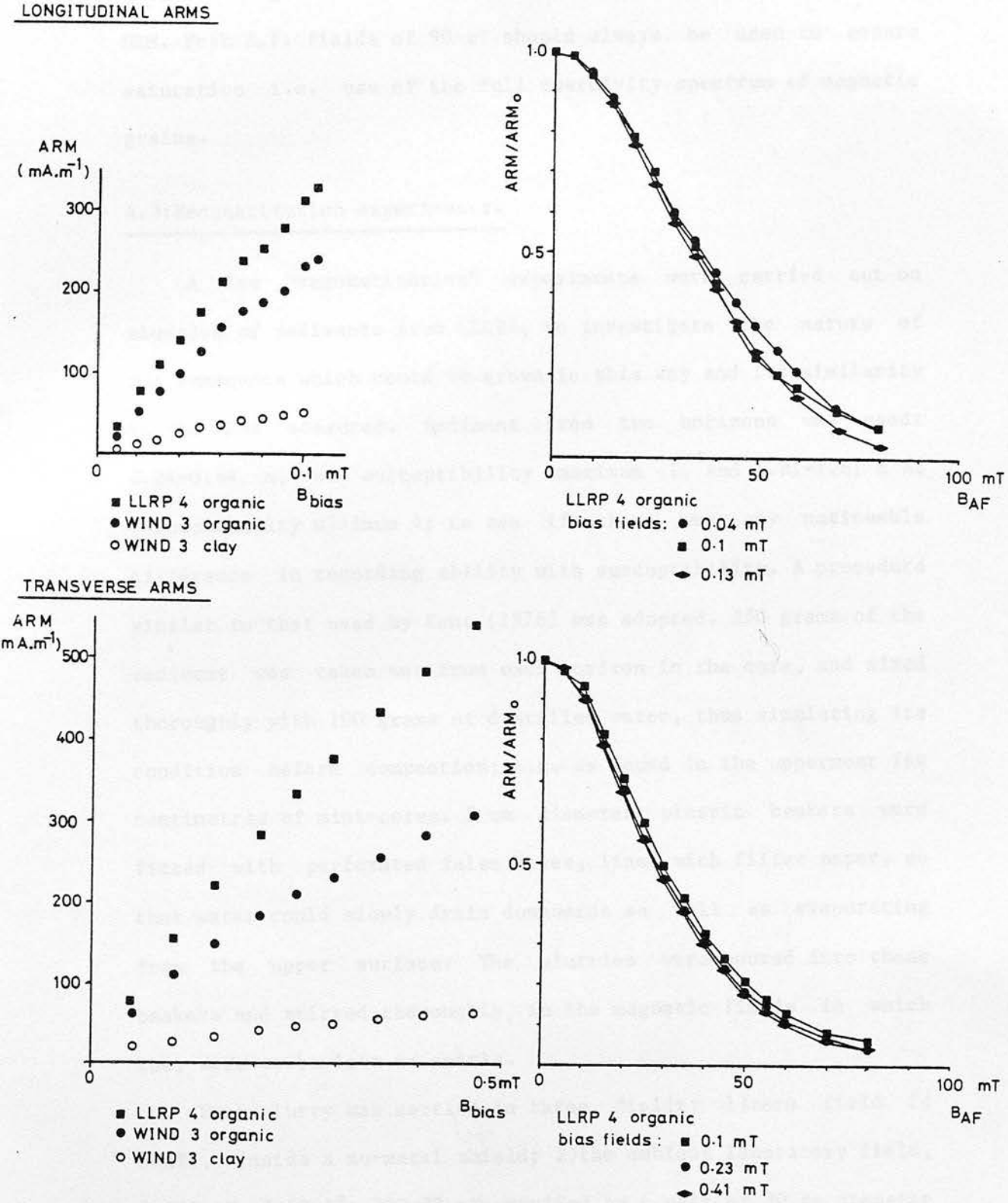


Figure 4.1 : Growth and A.F. demagnetization characteristics of ARM's in various samples.

ARM characteristics, and since the dependence of ARM intensity on $B_{bias}$ is roughly linear up to 0.1 mT, the choice of bias field within the range will not effect the efficiency of ARM to normalise NRM. Peak A.F. fields of 90 mT should always be used to ensure saturation i.e. use of the full coercivity spectrum of magnetic grains.

## 4.3:Reconstitution experiments.

A few "reconstitution" experiments were carried out on slurries of sediments from LLRP4, to investigate the nature of the remanence which could be grown in this way and its similarity to the NRMs measured. Sediment from two horizons was used: 0.84-0.64 m, at susceptibility maximum 1, and 1.81-1.61 m at susceptibility minimum 4; to see if there was any noticeable difference in recording ability with susceptibility. A procedure similar to that used by Kent (1976) was adopted. 250 grams of the sediment was taken wet from each horizon in the core, and mixed thoroughly with 100 grams of distilled water, thus simulating its condition before compaction; e.g. as found in the uppermost few centimetres of mini-cores. 5 cm diameter plastic beakers were fitted with perforated false bases, lined with filter paper, so that water could slowly drain downwards as well as evaporating from the upper surface. The slurries were poured into these beakers and stirred thoroughly, in the magnetic fields in which they were to be left to settle.

Each slurry was settled in three fields: 1)zero field (< 50nT), inside a mu-metal shield; 2)the ambient laboratory field, 0.038 mT, I=69.5°; 3)0.72 mT provided by a pair of 30 cm diameter Helmholtz coils aligned with the laboratory field. The beakers

were left uncovered for three days, allowing rapid drying, then covered with polythene for a further two days. They were then sampled in 2.5 cm cylindrical holders, noting the orientation to the applied field. The remanent intensities and directions were measured, and A.F. demagnetized, and anisotropy of susceptibility was investigated.

The results are summarised in table 4.2.

1)The remanent directions record the field directions within 5° in D and I. Although the inclinations are consistently shallow, there is insufficient evidence to suggest an inclination error.

2)In the laboratory field the high susceptibility sample grew a remanence 1.5 times the NRM intensity, whereas the low susceptibility sample was close to the NRM. This may be a result of a higher palaeointensity in the latter than the former sample.

3)The high field remanence of each sample is about 5 times the NRM intensity. If these two samples are representative this means that 0.72 mT is above the range of a linear remanence vs. field relationship for this sediment.

4)In all cases the remanences were quite stable to storage in zero field, and to A.F. demagnetization. Their MDFs were higher than those for the IRMs of parallel pilot samples investigated from LLRD1 (see next section), and were only about 25% lower than those of the NRMs. However there seemed to be a large high coercivity component. Over 10% of the remanence remained after A.F. demagnetization at 95 mT, compared with less than 5% for the NRMs. On demagnetization up to 60 mT, the directions were stable within 2°.

5)No evidence was found of anisotropy of susceptibility. It was originally thought that preferential alignment of the long axes

Table 4.2

Magnetic results on reconstituted sediment from LLRP4

| | NRM ($mA.m^{-1}$) | Susc. (SI) | Field (mT) | M ($m\ A.m^{-1}$) | D | I | Susc. (S.I.) | NRM / Susc. ($mA.m^{-1}$) | Rec.RM / Susc. ($mA.m^{-1}$) | rec. MDF (mT) | NRM / Rec.RM |
|---|---|---|---|---|---|---|---|---|---|---|---|
| χ max. | | | 0 | 2.3 | - | - | 905 | | | | |
| .84 - .64m | 197.4 | 1066 | 0.038 | 318.4 | 358.1 | 64.0 | 930 | 0.185 | 0.342 | 21.0 | 0.62 |
| | | | 0.72 | 1002 | 354.0 | 63.1 | 1169 | | 0.857 | 22.0 | |
| χ min. | | | 0 | 2.8 | - | - | 390 | | | | |
| 1.81 - 1.61 | 81.2 | 437 | 0038 | 78.0 | 356.5 | 65.9 | 390 | 0.186 | 0.20 | 27.5 | 1.04 |
| | | | 0.72 | 400.7 | 5.5 | 67.7 | 465 | | 0.862 | 29.0 | |

of magnetic particles parallel to the magnetic field might cause some anisotropy of magnetic properties.

## 4.4:Relative palaeointensity attempts.

Since the effects of magnetic and non-magnetic particle size and shape distributions on remanent intensity cannot be estimated, we must try to ensure that only sequences in which these factors do not change significantly are used for palaeointensity studies. This was pointed out by Levi and Banerjee (1976) in their condition that the section used be " magnetically homogeneous". Working on lake sediments from Minnesota, they used the similarity of the coercivity spectra of the NRMs of selected pilot samples through the section as a check of magnetic homogeneity. They then compared the NRM coercivity spectra with those of laboratory grown ARMs and IRMs in the same pilot samples, to select a normalising parameter which resides in the same spectrum of magnetic grains as the NRM.

### 4.4.1:Pilot samples.

A similar approach was undertaken on one core from each lake studied: LLRD1, WIND3, GEIR3. The following procedures were carried out on each of the pilot samples for which directional results were presented in section 2.

1)Stepwise alternating field partial demagnetization of the NRM at increments of 5mT peak field up to 50mT and at 10mT increments thereafter until the remanence was less than 10% of the original (this was usually attained before reaching 100mT, the maximum peak field attainable with the coil). The sample was held stationary and demagnetized consecutively in three orthogonal

directions. Then, to minimise any parasitic ARMs grown, due to impurities in the waveform of the coil, the final direction was reversed with the peak field halved (Snape, 1971). This procedure for A.F. demagnetization was chosen in preference to the two axis tumbler also available as it was more efficient and reproduceable, and also more compatible with the way in which ARMs were grown.

2)Growth of ARM in a bias field of 0.042 mT (0.25 mT for GEIR3 samples) superimposed on and parallel to a smoothly decaying alternating field of peak value 95 mT.

3)Stepwise A.F. demagnetization of this ARM as for NRM.

4)Growth of IRM in 100 mT direct field, measurement of coercivity of back IRM.

5)Stepwise A.F. demagnetization of IRM as for NRM.

Figures 4.2, 4.3 and 4.4 show the results for pilot samples from LLRD1, WIND3 and GEIR3 respectively. The uppermost figure for each sample shows normalised demagnetization plots for NRM(squares), ARM(circles) and IRM(diamonds), against peak alternating field. The lower figure is a plot of normalised NRM against normalised ARM (circles) and IRM(diamonds) with A.F. demagnetization. If the two remanences have identical coercivity spectra i.e. they lose equal fractions of the original remanence in each demagnetization stage, a straight line of unit gradient, through the origin will be obtained (dotted line in each plot). If the spectra are identical over only a restricted range of coercivities, a straight line will be obtained for this section, but not necessarily of unit gradient. An upward curvature indicates that the artificial remanence is softer than the NRM, a downward one that it is harder.

Table 4.1 gives the magnitudes of the remanences and their demagnetization characteristics. Also tabulated are the percentage differences between artificial and NRM demagnetization curves, in the coercivity range 0-50 mT. The fraction of each remanence lost in each demagnetization step is calculated and the difference between natural and artificial remanences obtained.The moduli of these values are summed and halved to give the percentage difference;

$$\Delta = \sum_{i=1,10} \left| \frac{NRM_i - NRM_{i-1}}{NRM_i} - \frac{ARM_i - ARM_{i-1}}{ARM_i} \right| \qquad \begin{array}{l} i = 1 \equiv 5\,mT \text{ AF Field} \\ \vdots \\ i = 10 \equiv 50\,mT \quad " \end{array}$$

The usual way of comparing coercivity spectra is to look at the spread in the NRM/A(I)RM values obtained during the demagnetisation stages (e.g. Levi and Banerjee, 1976). Such a comparison is, however, biased towards high coercivity components e.g. the >50 mT component is included in each NRM/ARM value, the 45-50 mT component in all but the last etc. In a method which compares the fractions lost at each demagnetization stage, the contribution of the grains in each coercivity range is counted only once. So the figures quoted are regarded as a better indication of the similarity of coercivity spectra between 0 and 50 mT.

### 4.4.2:Results.

#### 1)LLRD1.

Due to the obvious difference in sediment source and type between the marine and freshwater phases, only the postmarine, freshwater gyttja was suitable for palaeointensity work. Consequently, sample 129, although tested for directional purposes, is not shown in figure 4.2.

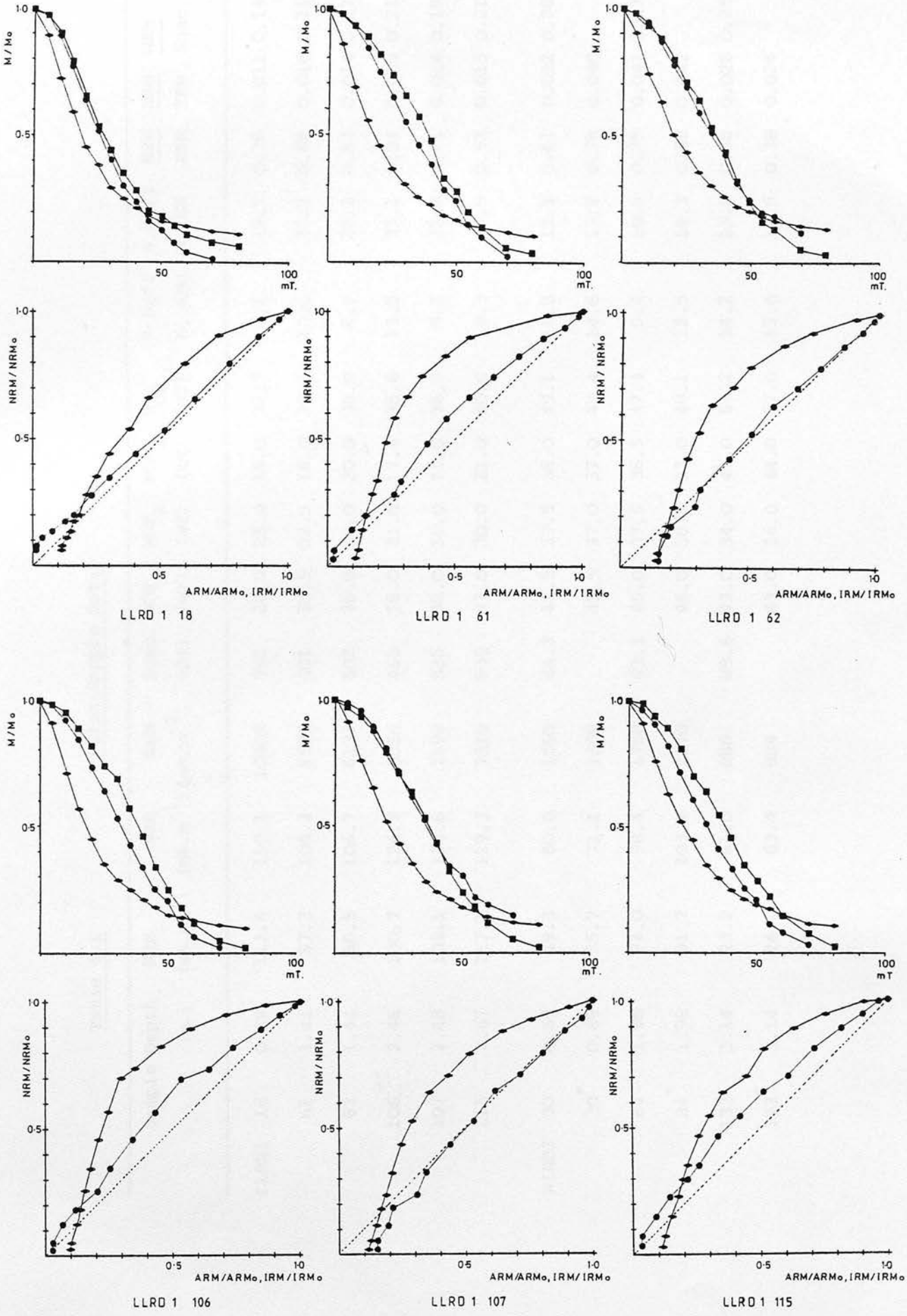


.gure 4.2 : LLRD 1 pilot samples : A.F. demagnetization of NRM, ARM and IRM.

■ NRM ● ARM , $NRM/NRM_o$ vs $ARM/ARM_o$ ◆ IRM , $NRM/NRM_o$ vs $IRM/IRM$

Table 4.1 Pilot Sample Data

| | Sample | Depth (m.) | NRM ($mA.m^{-1}$) | ARM ($mA.m^{-1}$) | IRM ($mA.m^{-1}$) | Susc. (SI) | $MDF_N$ (mT) | $MDF_A$ (mT) | $MDF_I$ (mT) | $B_{cr}$ (mT) | % Diff N, ARM | % Diff N, IRM | NRM/ARM | NRM/IRM | NRM/Susc. |
|---|---|---|---|---|---|---|---|---|---|---|---|---|---|---|---|
| LLRD1 | 18 | 0.39 | 113.4 | 150.1 | 10002 | 792 | 26.0 | 25.0 | 18.0 | 33.5 | 4.1 | 19.5 | 0.76 | 0.011 | 0.143 |
| | 61 | 1.41 | 87.3 | 104.2 | 5585 | 401 | 38.5 | 32.5 | 18.0 | 39.9 | 10.6 | 32.2 | 0.84 | 0.016 | 0.218 |
| | 62 | 1.44 | 88.5 | 106.7 | 6133 | 502 | 36.0 | 35.0 | 20.0 | 36.0 | 8.1 | 28.2 | 0.83 | 0.014 | 0.176 |
| | 106 | 2.46 | 100.7 | 124.3 | 6826 | 469 | 38.0 | 31.5 | 17.5 | 38.6 | 13.5 | 35.1 | 0.81 | 0.015 | 0.215 |
| | 107 | 2.48 | 103.1 | 126.6 | 7598 | 536 | 36.0 | 36.0 | 21.0 | 36.5 | 9.2 | 25.0 | 0.81 | 0.014 | 0.192 |
| | 115 | 2.67 | 117.1 | 129.3 | 7816 | 539 | 37.0 | 30.0 | 21.0 | 40.0 | 9.3 | 26.9 | 0.91 | 0.015 | 0.217 |
| WIND3 | 30 | 0.69 | 49.3 | 80.6 | 1565 | 64.3 | 44.5 | 37.5 | 38.0 | 49.1 | 11.8 | 13.1 | 0.61 | 0.032 | 0.767 |
| | 30* | 0.69 | 55.7 | 71.1 | 1399 | | 45.5 | 37.0 | 37.0 | 49.4 | 14.6 | 17.8 | 0.78 | 0.040 | |
| | 84 | 1.98 | 74.0 | 98.4 | 1768 | 63.1 | 45.0 | 37.5 | 36.5 | 47.4 | 9.4 | 10.8 | 0.75 | 0.042 | 1.170 |
| | 84* | 1.98 | 91.7 | 103.7 | 2170 | | 46.0 | 38.0 | 37.0 | 48.1 | 12.5 | 14.3 | 0.88 | 0.042 | |
| | 133 | 3.14 | 23.2 | 61.0 | 886 | 89.6 | 43.0 | 34.0 | 45.0 | 57.2 | 14.2 | 13.9 | 0.38 | 0.026 | 0.259 |
| | 133* | 3.14 | 24.0 | 63.4 | 984 | | 43.0 | 34.0 | 44.0 | 57.0 | 13.6 | 12.5 | 0.38 | 0.024 | |

Table 4. 1 continued.

| | Sample | Depth (m.) | NRM ($mA.m^{-1}$) | ARM ($mA.m^{-1}$) | IRM ($mA.m^{-1}$) | Susc. (SI) | $MDF_N$ (mT) | $MDF_A$ (mT) | $MDF_I$ (mT) | $B_{cr}$ (mT) | % Diff N,ARM | % Diff N,IRM | NRM / ARM | NRM / IRM | NRM / Susc. |
|---|---|---|---|---|---|---|---|---|---|---|---|---|---|---|---|
| GEIR3 | 21 | 0.53 | 29.1 | 339.5 | 1095 | 65.3 | 32.5 | 26.5 | 20.0 | 38.2 | 12.6 | 26.7 | 0.086 | 0.027 | 0.446 |
| | 79 | 2.12 | 36.6 | 331.2 | 1124 | 33.4 | 31.0 | 26.0 | 22.0 | 41.8 | 10.8 | 21.4 | 0.111 | 0.033 | 1.096 |
| | 80 | 2.15 | 30.2 | 292.2 | 896 | 30.9 | 31.0 | 26.0 | 21.0 | 40.1 | 11.7 | 23.7 | 0.103 | 0.034 | 0.977 |
| | 132 | 3.42 | 32.0 | 483.2 | 1620 | 45.1 | 32.0 | 27.5 | 22.0 | 41.6 | 15.8 | 26.6 | 0.066 | 0.020 | 0.710 |
| | 133 | 3.44 | 45.7 | 542.8 | 1714 | 58.6 | 31.0 | 28.0 | 22.0 | 41.4 | 10.2 | 24.0 | 0.084 | 0.027 | 0.780 |

In general the ARMs are of the same order of magnitude as the NRMs, whereas the IRMs are some 80 times larger. The NRMs and ARMs generally have similar coercivity spectra, with a mean percentage difference of 9.1% and 3.5 mT difference in mean MDFs. All the lower, normalised plots, lie very close to the line of unit gradient. The IRMs were considerably softer in all cases, with MDFs averaging 16 mT lower than for NRMs, and a mean percentage difference of 27.8%. The lower coercivity spectra of IRM compared with ARM suggests the remanence carriers to be single or pseudo-single domain, this inference is based on the "modified Lowrie-Fuller test" (Johnson, Lowrie and Kent, 1975). In the original Lowrie-Fuller test the stabilities to A.F. demagnetization of a low field TRM and a high field IRM are compared to distinguish between SD (TRM harder than IRM) and MD (IRM harder than TRM) magnetite or maghaemite. Since Dunlop and West (1969) found ARM and TRM in elongated magnetite grains to have similar A.F. demagnetization characteristics, Johnson,Lowrie and Kent suggest using a low bias field ARM in place of TRM for sediments in which growth of a TRM may cause alteration.

Sample 18 is slightly atypical of the set, each of the three remanences being softer than in the other samples. This can probably be attributed to the higher water content and incomplete compaction in the uppermost sediment, making the grains more mobile, rather than to a sedimentological difference. The remaining five samples are all very similar (table 4.1), showing that the nature and distribution of magnetic material does not change significantly between them. This suggests that the magnetic fraction is "internally homogenous", although its concentration varies by a factor of two in the top three metres, (from the

susceptibility logs).

2)WIND3.

The samples from parallel horizons in WIND3 are very consistent, but there is a slight variation between horizons, especially between the upper four samples and 133, 133*, 12 cm above the clay boundary. All three remanences are harder to A.F. demagnetization than in the Lomond samples. NRM, ARM and IRM have mean MDFs of 44.5, 36.3 and 39.6 mT respectively. Neither ARM nor IRM is particularly similar to NRM; they have mean percentage differences of 12.7% and 13.7% between 0 and 50 mT, and neither lies particularly close to the line of unit gradient in the lower plots. It is therefore difficult to choose a normalising parameter on this basis. In the upper four samples, ARM and IRM demagnetization curves lie very close to each other so it is also difficult to reach a conclusion from the modified Lowrie-Fuller test. This could mean that there is a distribution of SD, PSD and MD grains, though not all necessarily contributing to the NRM. Alternatively, since the modified Lowrie-Fuller test has only been substantiated for magnetite and maghaemite, a small amount of haematite might account for this difficulty. The coercivity of back IRM values are higher than those for Lomond, averaging 48.5 mT in the uppermost four samples and 57 mT in 133 (for which IRM is also slightly harder than ARM). This might suggest a second magnetic mineral. A small amount of haematite would however contribute little to the NRM intensity, and affect its demagnetisation characteristics little. So a broader distribution of grains than in Lomond seems the most likely explanation.

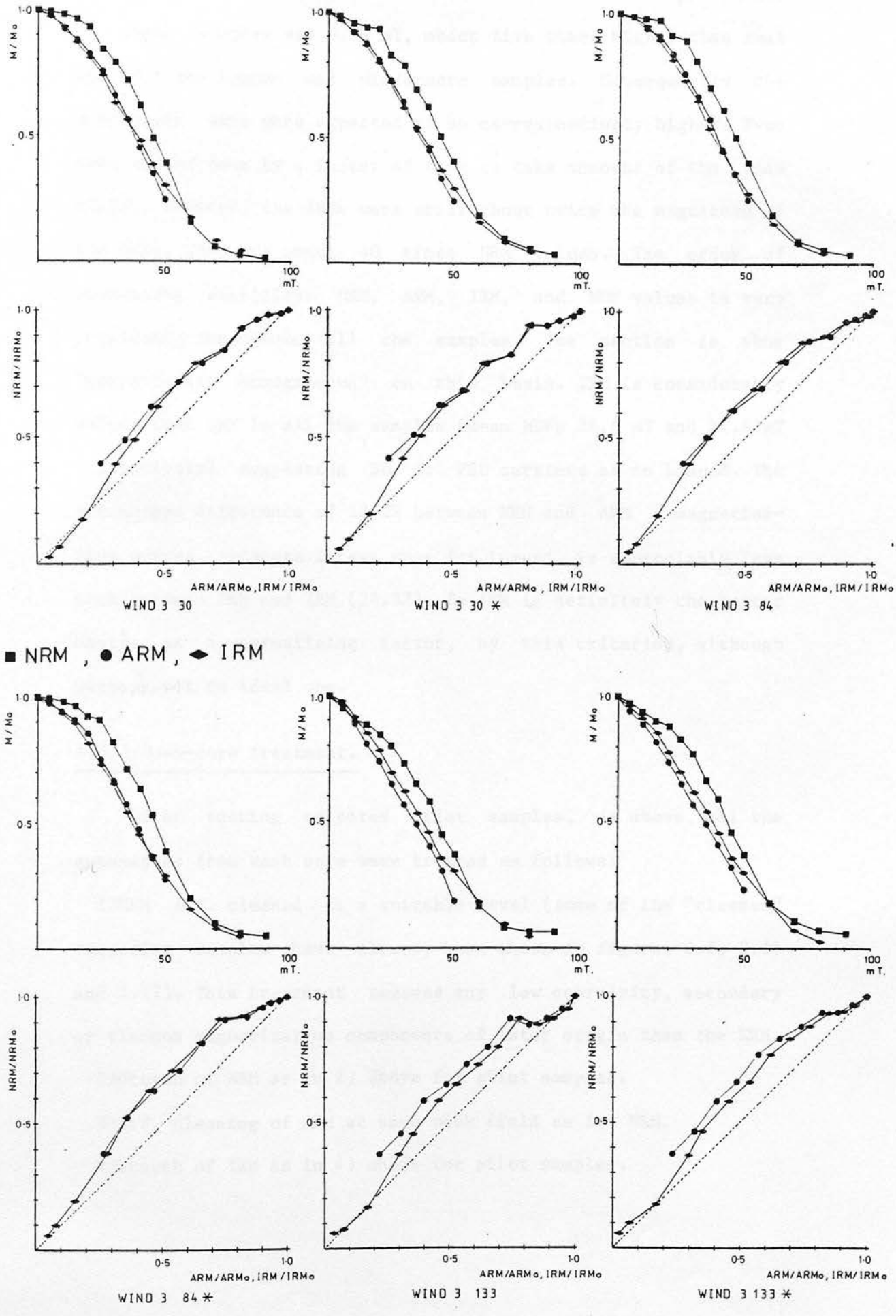


Figure 4.3 : WIND 3 pilot samples : A.F. demagnetization of NRM, ARM and IRM.

3)GEIR3.

As mentioned above, the bias field used for ARM production in these samples was 0.25 mT, about five times higher than that used for the Lomond and Windermere samples. Consequently the Geirionydd ARMs were expected to be correspondingly higher. Even when scaled down by a factor of five to take account of the bias field, however, the ARMs were still about twice the magnitude of the NRMs. IRMs are about 40 times NRM values. The order of decreasing stability: NRM, ARM, IRM, and MDF values is very consistent throughout all the samples. The section is thus "magnetically homogeneous" on this basis. IRM is considerably softer than ARM in all the samples (mean MDFs 26.8 mT and 21.4 mT respectively) suggesting SD or PSD carriers as in Lomond. The percentage difference of 12.2% between NRM and ARM demagnetisation curves, although larger than for Lomond, is appreciably less than between NRM and IRM (24.5%). So ARM is definitely the better choice as a normalising factor, by this criterion, although perhaps not an ideal one.

### 4.4.3:Down-core treatment.

After testing selected pilot samples, as above, all the subsamples from each core were treated as follows:

1)NRM A.F. cleaned at a suitable level (some of the "cleaned" direction results have already been shown in figures 3.5, 3.11 and 3.17). This treatment removes any low coercivity, secondary or viscous magnetization components of later origin than the NRM.

2)Growth of ARM as in 2) above for pilot samples.

3)A.F. cleaning of ARM at same peak field as for NRM.

4)Growth of IRM as in 4) above for pilot samples.

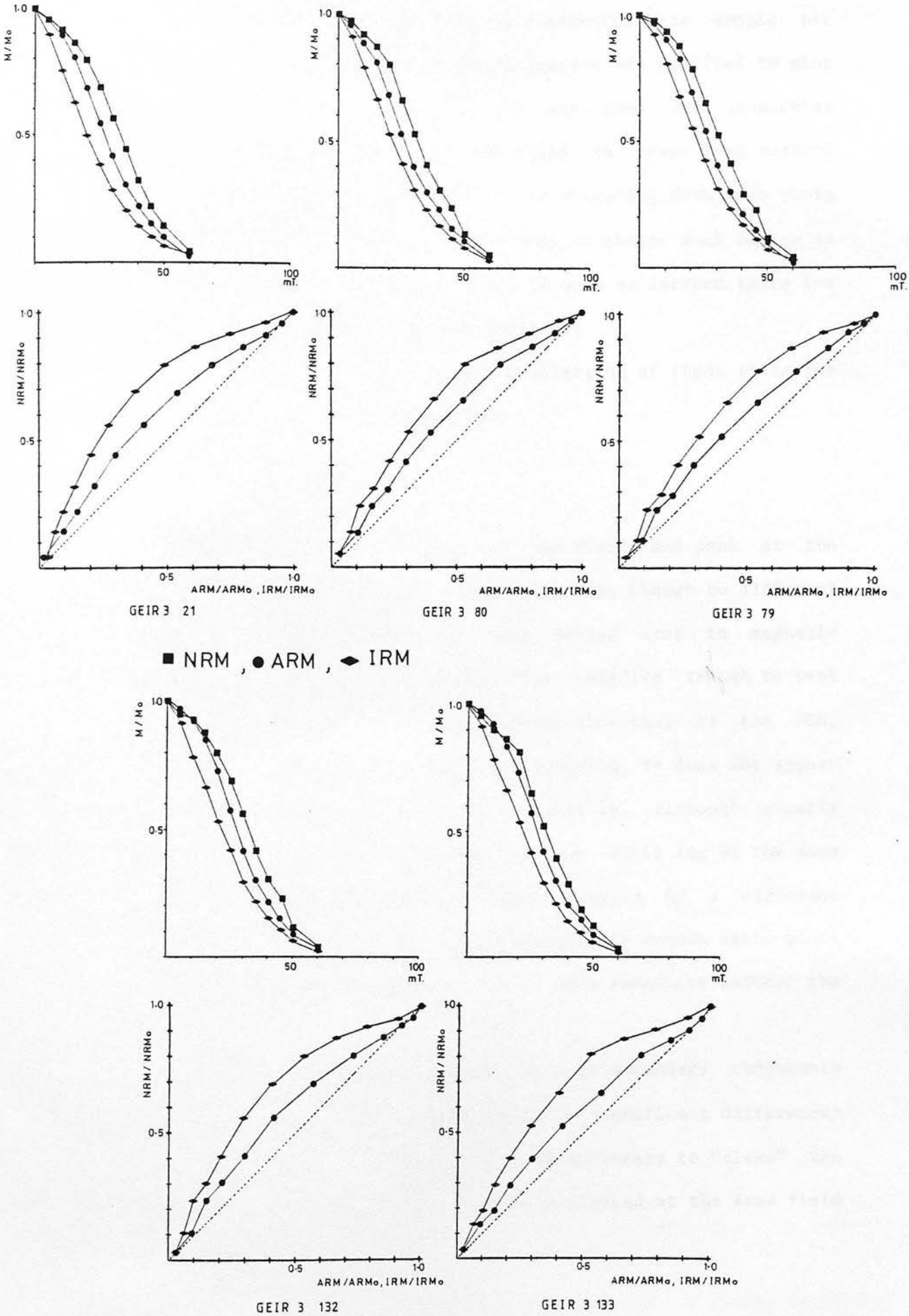


Figure 4.4 : GEIR 3 pilot samples : A.F. demagnetization of NRM , ARM and IRM.

5)A.F. cleaning of IRM as for ARM and NRM.

These results were all filed on a computer- one sample per card, and our standard core plotting program was modified to plot any single property, or the ratio of any two. The properties and/or ratios required were specified in prece ding control statements. In this way, in addition to obtaining down core plots of NRM/ARM and NRM/IRM, it was easy to obtain such ratios as NRMC/NRM, IRM/SUSC etc., which could be used as further tests for the down core homogeneity of the sediment.

Figures 4.5, 4.6 and 4.7 show a selection of these plots for LLRD1, WIND3 and GEIR3 respectively.

1)LLRD1 (post-marine).

Both ARM and IRM logs show the same trends and peak at the same horizons as NRM and susceptibility, though to different extents. Both also reflect the very marked drop in magnetic content in the marine section. The relative trough to peak amplitude of the ARM variations is lower than that of the NRM, and despite the promising coercivity spectrum, it does not appear to normalise the magnetic content completely. Although greatly attenuated, peaks still appear in the ratio log at the same horizons. IRM however, even though carried by a different spectrum of grains, does give a deceptively smooth ratio plot. NRM/SUSC (modified Königsberger ratio) lies somewhere between the two.

In the case of LLRD1, as there were no secondary components present in the NRM, cleaning produced no significant differences from the uncleaned logs shown. If it is necessary to "clean" the NRM, then ARM and IRM should also be cleaned at the same field

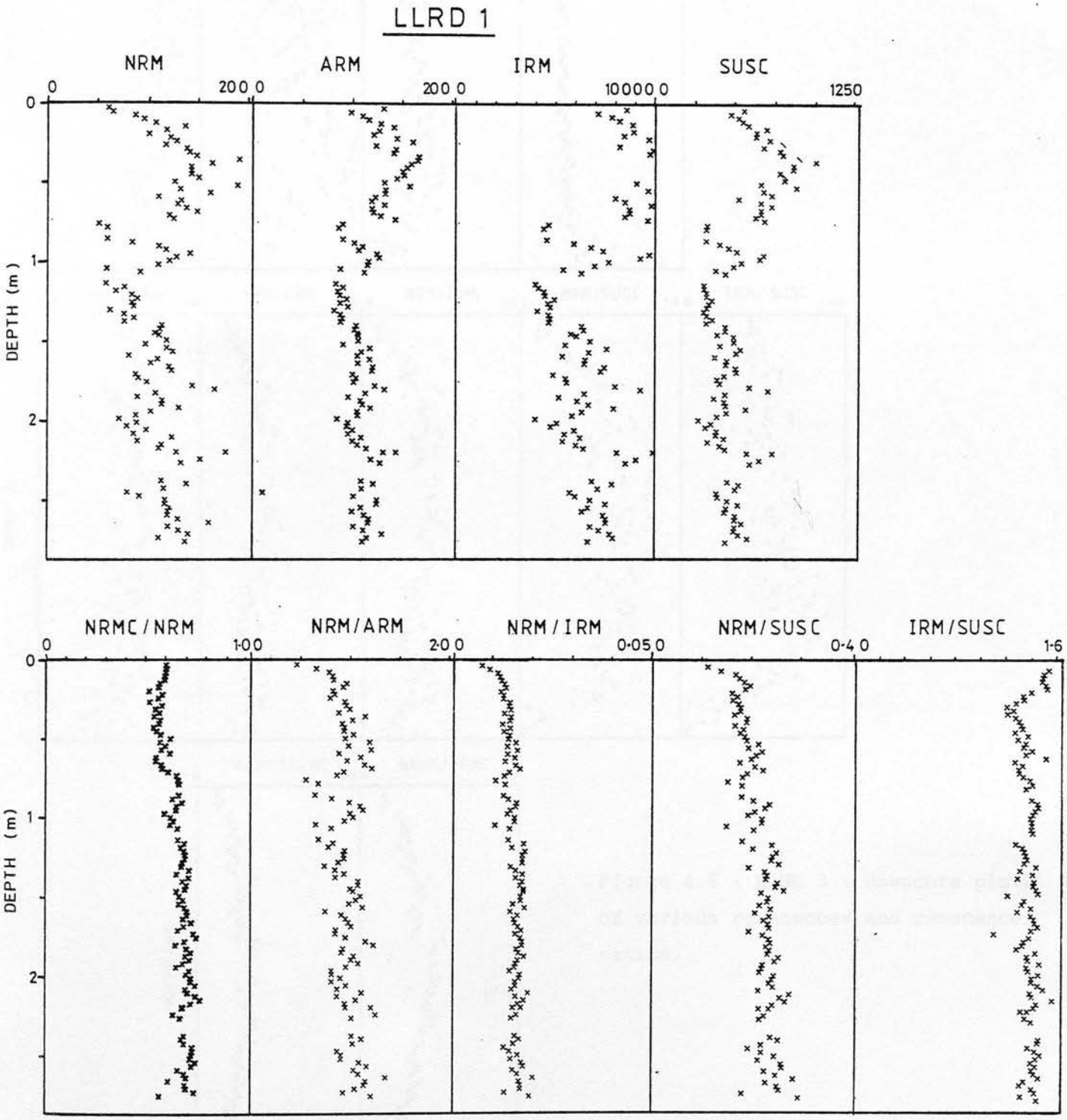


Figure 4.5 : LLRD 1 : downcore plots of various remanences and remanence ratios.

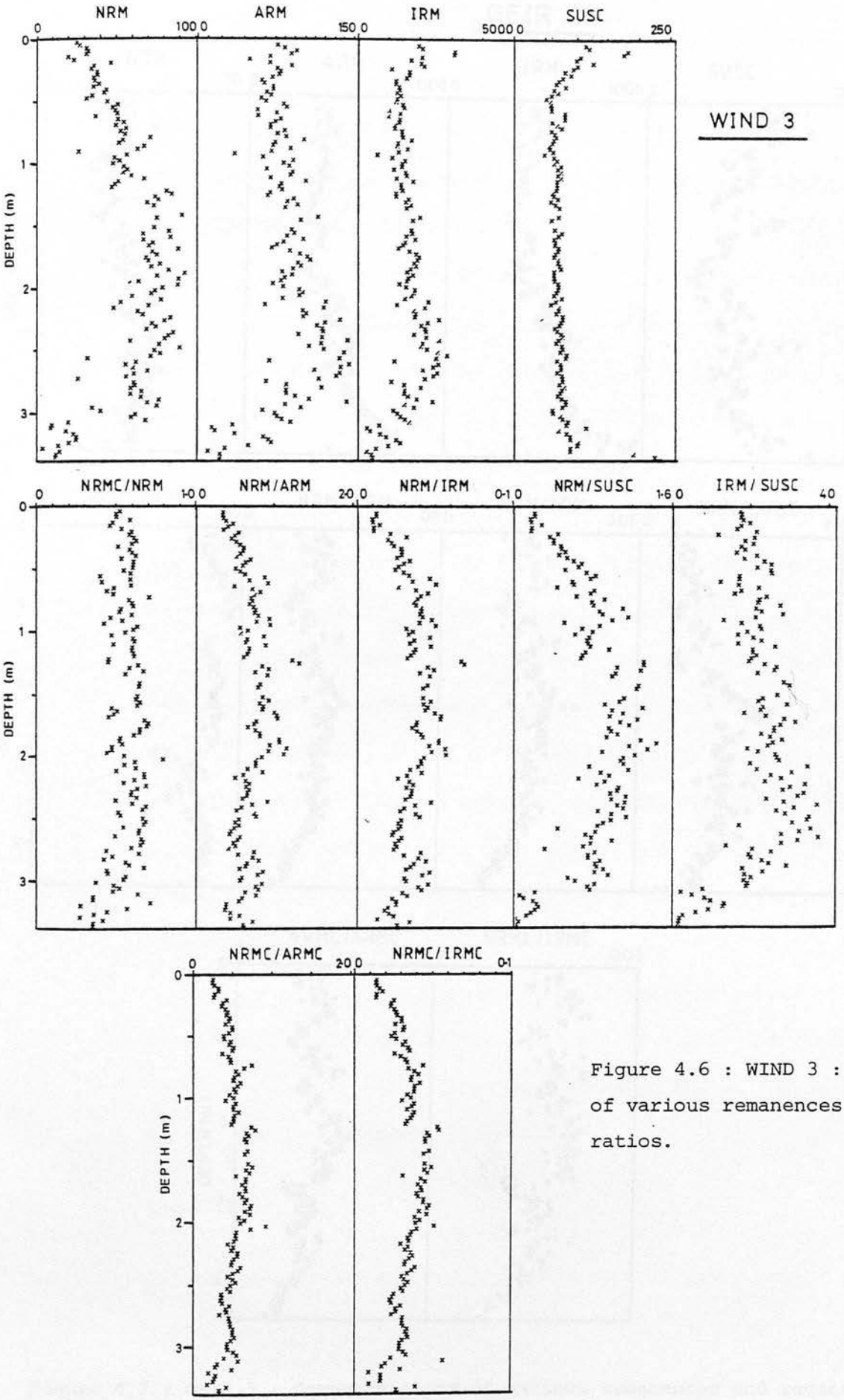


Figure 4.6 : WIND 3 : downcore plots of various remanences and remanence ratios.

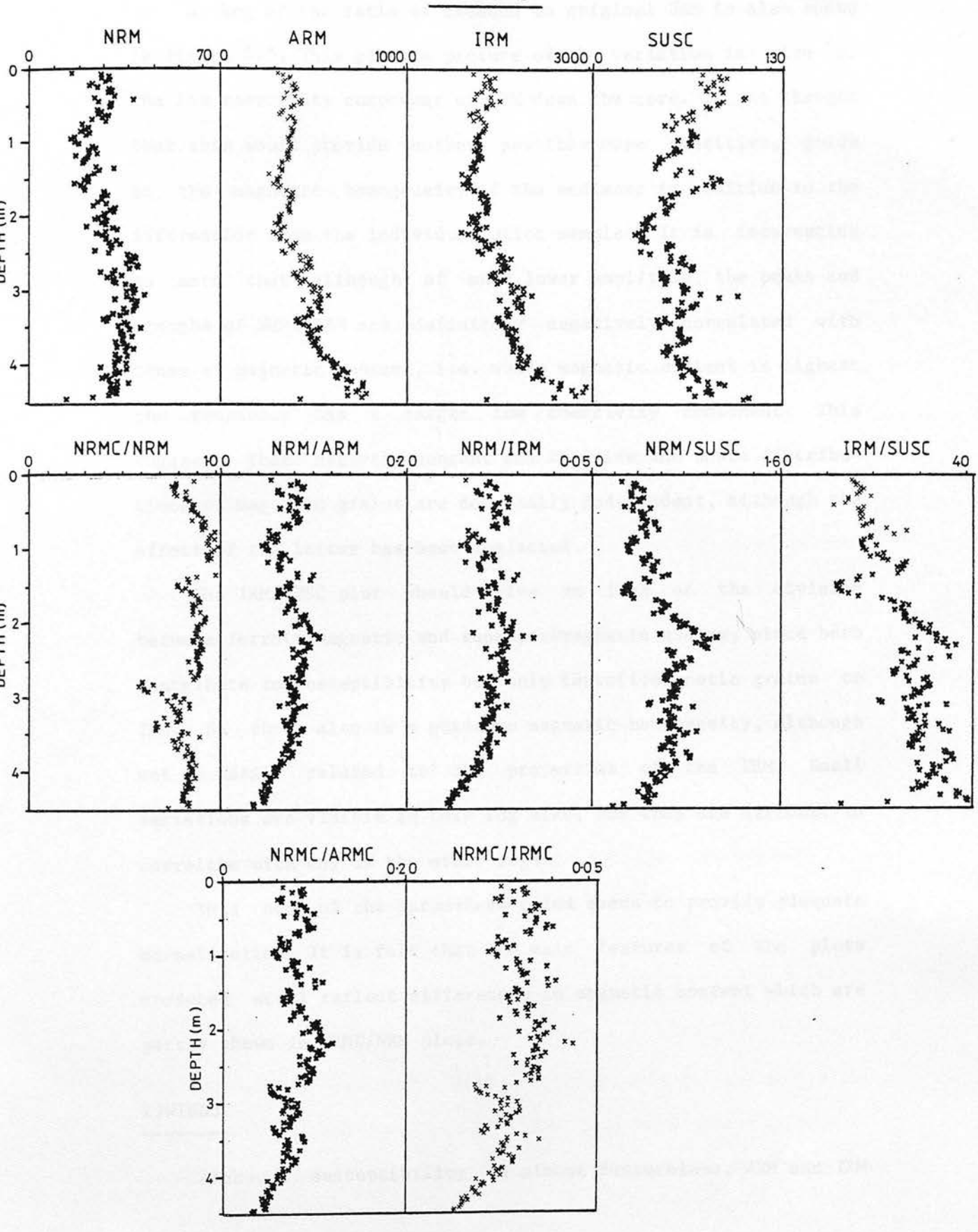


Figure 4.7 : GEIR 3 : downcore plots of various remanences and remanence ratios.

before computing ratios, so the same range of grain coercivities is used in each case.

A log of the ratio of cleaned to original NRM is also shown in figure 4.5. This gives a picture of the variation in size of the low coercivity component of NRM down the core. It was thought that this would provide another, possibly more sensitive, guide to the magnetic homogeneity of the sediment in addition to the information from the individual pilot samples. It is interesting to note that although of much lower amplitude, the peaks and troughs of NRMC/NRM are definitely negatively correlated with those of magnetic content, i.e. where magnetic content is highest the remanence has a larger low coercivity component. This suggests that magnetic content and the size and shape distributions of magnetic grains are not really independent, although the effect of the latter has been neglected.

The IRM/SUSC plot should give an idea of the division betweem ferro(i)magnetic and superparamagnetic grains, since both contribute to susceptibility but only ferro(i)magnetic grains to IRM. So this also is a guide to magnetic homogeneity, although not as easily related to the properties of the NRM. Small variations are visible in this log also, but they are dificult to correlate with any of the other logs.

Thus none of the parameters tried seems to provide adequate normalisation. It is felt that the main features of the plots produced still reflect differences in magnetic content which are partly shown in NRMC/NRM plots.

2)WIND3.

Although susceptibility is almost featureless, ARM and IRM

have very similar, distinctive trends. Both rise sharply in the bottom metre, then drop gradually over about 2m and rise again in the uppermost 20 cm. A few smaller features also occur in both records. These logs do not parallel NRM either, so normalisation with either ARM or IRM changes their form significantly. Both NRM/ARM and NRM/IRM have minima at 2.50m, then a broad maximum and fall in the upper part. This is quite distinct from the NRM/SUSC log which resembles NRM, owing to its almost constant susceptibility.

NRMC/NRM is again variable, although in this case there is more scatter and generally less systematic fluctuation. This is partly because some samples showed evidence of slight secondary remagnetization, which was removed on cleaning at 30 mT. Thus the logs of NRMC/ARMC and NRMC/IRMC are much better defined, but otherwise show the same general trends as the uncleaned ratios. The IRM/SUSC log is similar to IRM. This shows that, though the total of ferro(i)magnetic and superparamagnetic components has remained roughly constant (susc), the ferromagnetic component has decreased and the superparamagnetic increased in the top 2.5m.

So, the NRM log is definitely recording something more than magnetic content, and despite the dissimilarity between the coercivity spectra of artificial and natural remanences, the (cleaned) NRMC/ARMC and NRMC/IRMC plots are felt, in some way, to reflect geomagnetic field changes.

3)GEIR3.

Again ARM and IRM logs are very similar, having similar degrees of variation as in Windermere. Both have some features in common with the NRM, but they are not always of the same relative

amplitude. In the bottom metre of core, where NRM is rising gradually, from around its mean value, ARM and IRM both drop by about 50% from their maximum values. This difference produces a broad swing in the lower 3m of the normalised NRM/ARM and NRM/IRM logs, similar to the swing in the Windermere record.

In spite of the similarity of the pilot samples investigated, the NRMC/NRM plots show differences which suggest substantial downcore variations in the NRM coercivity spectra. The main areas of the magnetic inhomogeneity are around 1.50m and from 3.50 to 3.00m. In these areas the cleaned ratios also differ from the uncleaned ones, but the main trend with a broad peak around 2.5m is still prominent.

### 4.5.1:Comparison with other palaeointensity results.

In chapter 5 a detailed time scale for each lake is drawn up from C-14 age estimations. These have been used in figure 4.8 to plot NRM/ARM ratios against "preferred time" (see section 5) for each core, and to enable comparison with other palaeointensity curves. In the older sediments the dates are probably accurate only to about 500 years. Also shown are two recently published archaeomagnetic palaeointensity curves: that for S.E.Europe from 8500 to 2050 BP (Kovacheva and Veljovich, 1977) and for Greece between 4000 and 1500 BP (Walton, 1979). These are not the only available records but others are not as reliably dated.

The records from all three lakes show a maximum around 2000 BP. It is known that the dipole moment has been decreasing on average since about this date (Smith, 1970), so this is probably a feature of the main field.

There is little more of geomagnetic significance in the

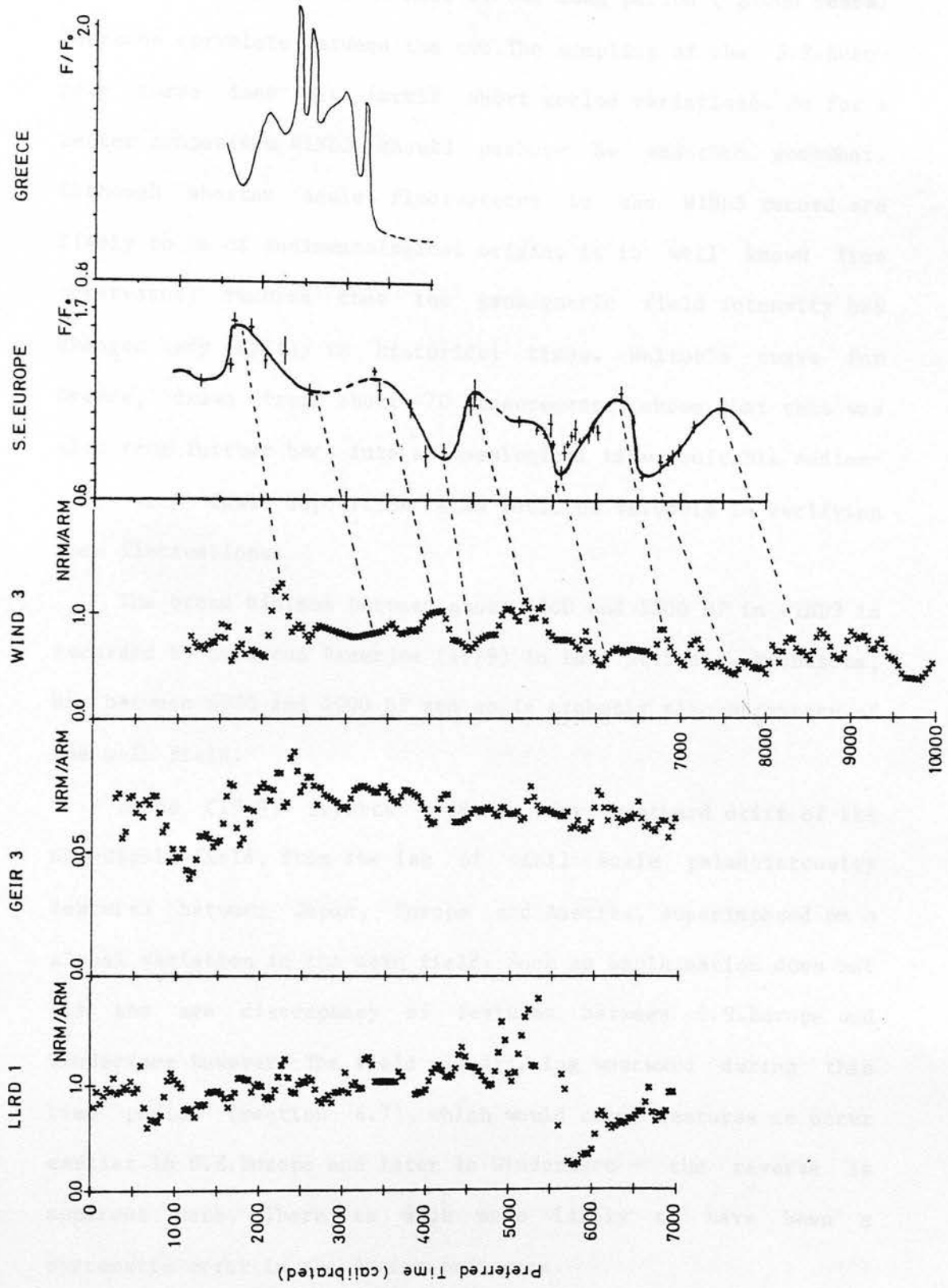


Figure 4.8 : NRM/ARM logs vs.'preferred time' for cores LLRD 1, GEIR 3 and WIND 3. Palaeointensity curves for Southeast Europe (Kovacheva and Veljovich, 1977) and Greece (Walton, 1979).

LLRD1 record. However, if the WIND3 dating is too old by about 500 years a very good correspondence emerges between WIND3 and the S.E. European curve. Most of the long period ( $\geqslant$1000 years) features correlate between the two.The sampling of the S.E.European curve does not permit short period variations. So for a better comparison WIND3 should perhaps be smoothed somewhat. Although shorter scale fluctuations in the WIND3 record are likely to be of sedimentological origin, it is well known from observatory records that the geomagnetic field intensity has changed very rapidly in historical times. Walton's curve for Greece, drawn from about 70 measurements, shows that this was also true further back into archaeological time. Suitable sediments, with fast deposition rates would be valuable in verifying such fluctuations.

The broad minimum between about 8000 and 5500 BP in WIND3 is recorded by Lund and Banerjee (1979) in Lake St.Croix, Minnesota, as between 8000 and 4000 BP and so is probably also a feature of the main field.

Bucha (1970) reports evidence for westward drift of the non-dipole field, from the lag of small scale palaeointensity features between Japan, Europe and America, superimposed on a global variation in the main field. Such an explaination does not fit the age discrepancy of features between S.E.Europe and Windermere however. The field was drifting westward during this time period (section 6.7), which would cause features to occur earlier in S.E.Europe and later in Windermere - the reverse is apparent here. There is much more likely to have been a systematic error in the dating processes.

With hindsight it is possible to see some of the features of

the S.E.European and Windermere records in GEIR3, but the correlation is not clear.

4.5.2:Possible weaknesses of the method.

Two possible reasons for the apparent unreliability of the above method to give palaeointensities in all cases are considered:

1)The effect of the size and shape distributions of both magnetic and non magnetic grains on the ability of the magnetic particles to align with the magnetic field.

2)The possibility of the magnetic mineral being present, not as single grains, but as inclusions dispersed in larger particles of a paramagnetic matrix (like currants in a bun).

1)Grain size distributions.

If the magnetic mineral is present as single, homogeneous grains, then any difference in the grain size distribution of the magnetic fraction should be reflected as differences in the coercivity spectra of the various remanences. Differences in the non magnetic fraction will not however show up, although, by controlling the degree of compaction and size of voids between grains they will affect the efficiency of alignment of the magnetic grains. Such effects have been reported in redeposition experiments on extracts from different grain sizes by C.Amerigan (1977). It is possible that testing a few pilot samples, selected down a core gives insufficient coverage and misses small, between sample inhomogeneities in magnetic mineralogy. Perhaps a down - core log, such as NRMC/NRM, covering all samples might be more reliable. This ratio records variations in the fraction of the

remanence carried by bigger, low coercivity grains, and so displays inhomogeneities in the NRM bearing grain component. In LLRD1 (and to a smaller extent in the other two cores) an inverse correlation was visible between NRMC/NRM, and the magnetic content indicators, suggesting (if lower coercivity is linked with bigger grains) a rise in the mean grain size when magnetic content increases, possibly due to faster erosion and less natural sifting and sorting (section 3.1). Particle size analyses, using a coulter counter do in fact show higher mean grain sizes in the uppermost susceptibility peaks of both LLRD1 and GEIR3, than lower down in the cores (table 4.3).

The following paragraph, and figure 4.9, show how down-core differences in particle size distribution might lead to erroneous palaeointensity results. a)Specific variation of a property X e.g.susceptibility, ARM, IRM, NRM with magnetic grain size. b)Magnetic grain size distribution in sediment. e)Product of a)and b) gives the contribution to the bulk property X from the different grain sizes. The bulk value is given by the area under the curve e).

In estimating palaeointensities a property, X, is required for which curve a) and therefore curve e) resembles that for NRM, so, in effect the NRM carried by each grain size fraction is normalised individually.

A small difference between curve a) for NRM and the chosen property X may be magnified by small down-core variations in curve b) to produce substantial differences in c) and invalidate the normalisation procedure.

2)"Currant bun" particles.

If the magnetic grains are present as inclusions then c),

Table 4.3 : Sediment particle sizes: Coulter counter results.

| | Depth | Susc | Grain size (μm.) Mean | Range including 70% * lower | upper |
|---|---|---|---|---|---|
| LLRD 1 | 32.5 | 1007 | 15.9 | 5.3 | 30.5 |
| | 75.1 | 329 | 10.6 | 5.0 | 20.1 |
| | 91.4 | 686 | 11.4 | 5.1 | 22.0 |
| | 112.5 | 318 | 11.7 | 4.9 | 21.1 |
| WIND 3 | 0.0 | 116 | 9.3 | 5.1 | 26.5 |
| | 35.0 | 82 | 12.0 | 6.0 | 30.1 |
| | 235.0 | 75 | 9.6 | 4.7 | 20.5 |
| GEIR 3 | 31.6 | 103 | 16.1 | 5.4 | 35.7 |
| | 121.4 | 43 | 10.9 | 4.5 | 20.1 |
| | 217.1 | 29 | 11.2 | 3.6 | 22.3 |
| | 300.2 | 99 | 10.5 | 3.8 | 21.1 |

* Range: 15% of particles are smaller than lower limit

15% of particles are larger than upper limit.

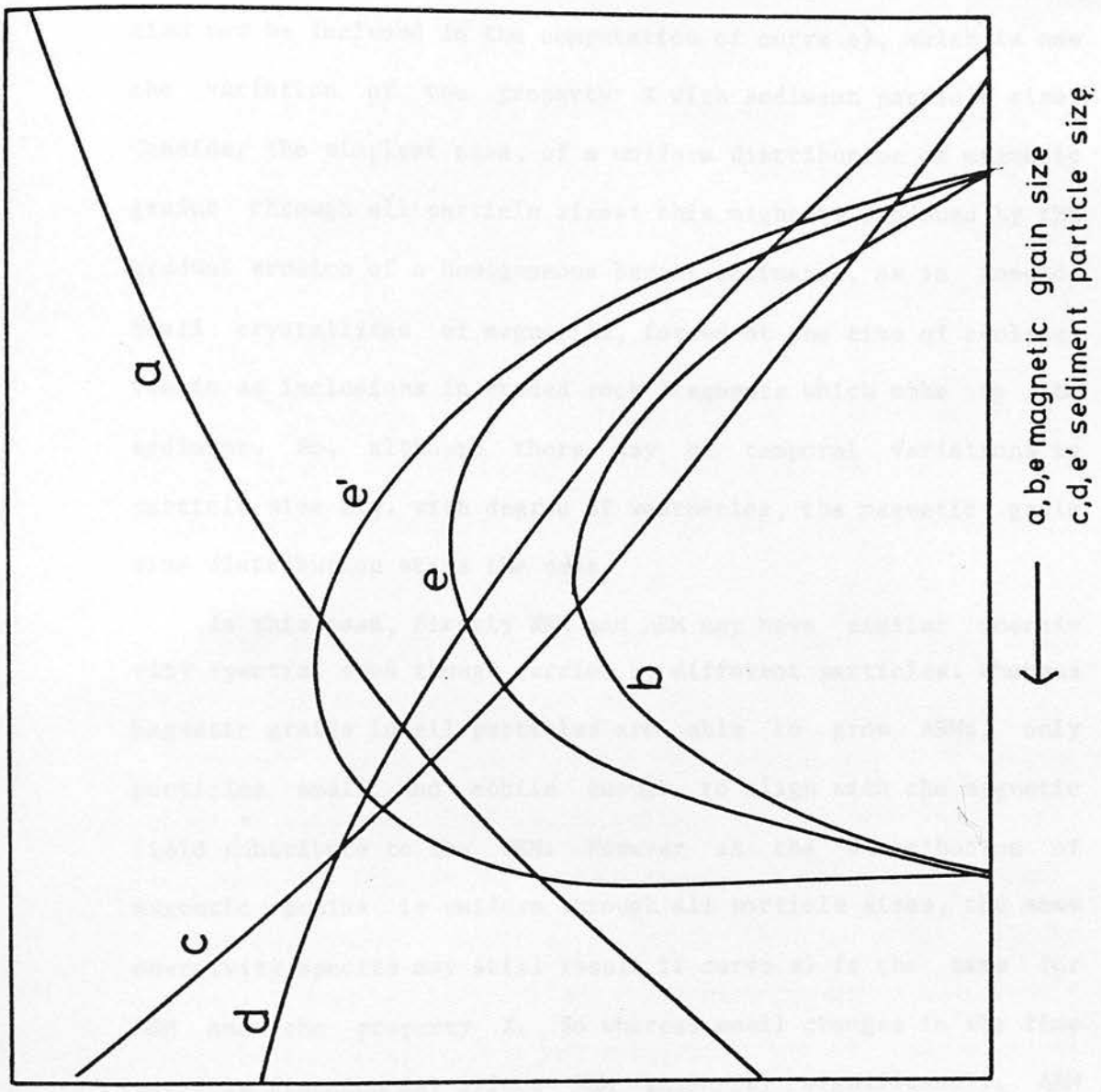


a) magnetic property X
b) number of magnetic grains
c) number of magnetic grains of a given size
d) magnetic property X for a given magnetic grain size
e) bulk magnetic property X.

Figure 49: Hypothetical dependance of the bulk value of a magnetic property X with magnetic grain and sediment particle size distributions.

their distribution through the different sediment particle size ranges and d) the dependence of X on sediment particle size, must also now be included in the computation of curve e), which is now the variation of the property X with sediment particle size. Consider the simplest case, of a uniform distribution of magnetic grains through all particle sizes: this might be produced by the gradual erosion of a homogeneous basalt intrusion, as in Lomond. Small crystallites of magnetite, formed at the time of cooling, remain as inclusions in eroded rock fragments which make up the sediment. So, although there may be temporal variations in particle size e.g. with degree of weathering, the magnetic grain size distribution stays the same.

In this case, firstly NRM and ARM may have similar coercivity spectra, even though carried by different particles. Whereas magnetic grains in all particles are able to grow ARMs, only particles small and mobile enough to align with the magnetic field contribute to the NRM. However as the distribution of magnetic grains is uniform through all particle sizes, the same coercivity spectra may still result if curve a) is the same for NRM and the property X. So whereas small changes in the fine particle fraction may affect NRM intensity significantly, ARM intensity would be affected much less. This would lead to bigger variations in the NRM than in ARM. So NRM/ARM ratio will give incomplete normalisation and will also reflect down- core variations in the fraction of magnetic grain bearing sediment particles able to align with the magnetic field.

Secondly, the down-core NRMC/NRM log would not necessarily show any inhomogeneities, as the magnetic grain distribution

would still be uniform throughout the section.

## 4.6:Summary and conclusions.

1)It is very difficult to choose a sediment sequence suitable for palaeointensity work, since we are still uncertain about how a sediment acquires and holds a remanence. The homogeneity of both magnetic and non magnetic fractions must therefore be tested as stringently as possible.

2)Similarly the choice of normalisation property is not straightforward and may differ from sediment to sediment. In the above cases ARM seems to have been the best choice. Redeposited or reconstituted remanence was not used, as, although its mode of formation may be similar to the NRM, insufficient is known about reproduction and regulation of conditions.

3)One of the sediments tested, Windermere, was felt uniform enough in magnetic properties to enable palaeointensity retrieval, and its NRM/ARM log is very similar to the archaeomagnetic S.E.European record. However, although the qualities of the magnetic component of the other two sediments were not obviously inhomogeneous, their quantities definitely varied too much to give reliable detailed results.

# CHAPTER 5: DATING AND CONSTRUCTION OF A TIME SCALE.

## 5.1: Introduction.

In the previous chapters continuous, ordered sequences of data points have been produced. However, an absolute time scale, taking into account possible variations in sedimentation rate must now be constructed for them, so that temporal features of the secular variation can be investigated.

Methods of dating materials can be classified as primary or secondary. Primary methods include all the isotopic techniques e.g. potassium-argon, radiocarbon, caesium-137, lead-210 : a property of the material which depends directly upon its age is measured (in these cases, the extent of decay of certain radioactive nuclides). Secondary methods involve finding and identifying certain features or horizons which have already been dated absolutely in other specimens. This class includes pollen analysis, and also the correlation of archaeomagnetic and magnetic observatory records of declination and inclination. It is hoped that the preferred time scale developed here is accurate and detailed enough to make "magnetic dating" of British and European sediments a viable secondary method.

## 5.2: Radiocarbon dating.

Natural carbon consists of a mixture of three isotopes: the stable isotope ${}_6C^{12}$ is overwhelmingly predominant, but there is a minute trace of ${}_6C^{13}$ , and about 1 part in $10^{12}$ ${}_6C^{14}$ , which is radioactive and used in dating. This ${}_6C^{14}$ is formed by the interaction of cosmic ray neutrons with nitrogen atoms in the

upper atmosphere.

$$_7N^{14} + _0n^1 \longrightarrow _6C^{14} + _1H^1$$

It is oxidized to $CO_2$, and mixes into the atmosphere, reaching an equilibrium concentration with the stable isotopes. This mixture of isotopes is then absorbed by plants and passed between all living organisms. However, once an organism is dead, it ceases to take up more carbon, so the existing $_6C^{14}$ in it decays away without being replenished.

$$_6C^{14} \longrightarrow _7N^{14} + _{-1}e^0 \quad \beta \text{ emmission}$$

The half life of this decay is 5730 years (although Libby's original estimate of 5568 years is still used for compatibility of results) i.e. the $C^{14}$ decays to half its original concentration in this time, and since the decay rate is exponential, this too drops to half its original rate after one half life. So, by monitoring the decay process of a known weight of carbon from a sample, the extent of its decay, and hence its age, can be determined. Experimental details of sample preparation and the method are given in Ergin et al. (1970). A half life process of 5700 years is ideal for our sediments, having maximum ages of about 10000 years, as the radioactivity of the oldest samples is still strong enough to be readily measurable.

Radiocarbon age determinations are usually quoted as "radiocarbon years" before present (present = 1950 A.D.) : bp, calculated assuming a constant equilibrium concentration of $C^{14}$ in the atmosphere throughout time. However, there have almost certainly been fluctuations in the atmospheric $C^{14}$ level, as the cosmic ray flux has varied e.g. due to changes in geomagnetic field intensity. Both annual varves in sediments, and tree ring sequences have been individually counted and C-14 dated in

attempts to provide a calibration from C-14 years bp to calendar years BP. The longest sequences have probably been provided by the rings of the Bristlecone pine - a species which grows only at high altitudes in the south-west U.S.A.. Some living specimens are 4000 years old, and dead wood dates back 8000 years. Sequences from dead and living trees have been overlapped by matching signatures of climatic change. The data have many short fluctuations of 10-20 year duration, whose authenticity is strongly debated. However, as these "kinks" are insignificant on the time scale of this work, the smooth curve, computed by Clark(1975), has been used to calibrate the dates obtained here. Objections to such dendrochronological calibration have been raised on the grounds of 1) its restricted location, as result of which it may not record worldwide fluctuations and 2) diffusion between adjacent tree rings. Other species of trees e.g. Irish Oak, and varve sequences are currently under investigation. The discrepancy between bp and BP is small for the past 2000 years, but increases to about 800 years at 5000 bp. Unfortunately the calibration extends only to 8000 bp, and it is controversial how one should calibrate earlier dates. Estimates for the radiocarbon error at the beginning of the Holocene range from 0 to 950 years (discussed at INQUA, Birmingham, 1977). The procedure adopted here is to extrapolate back to zero correction at 10000 bp, in the belief that the magnetic field intensity and cosmic ray flux had approximately their present day values then.

## 5.3:C-14 results.

Thirty radiocarbon age estimates have been obtained on four of the cores studied, and in addition pollen analysis has been

performed on one core from each lake. All the sediments studied have relatively low organic carbon contents, which meant that a large thickness of sediment had to be used, usually 20cm, to extract the 0.5-1 gm of carbon necessary for each date. Dating was carried out at two laboratories- Glasgow University (LLRD1), (Drndarsky, 1976), and at SURRC, East Kilbride (GEIR2, GEIR4 and WIND1).

Most of the samples were taken at specific declination or inclination features (table 5.1), aiming to date the features. Towards the bases of the cores, where the features are more widely spaced, extra dates have been interspersed. The errors quoted in table 5.1 are just the random statistical counting errors. No estimate can be made of systematic errors, such as those caused by the contamination of samples with ancient or modern carbon, which are discussed below, if suspected, nor from the averaging effect of using such a large thickness of sediment. Details of all the dates obtained are given in table 5.1, and plots against depth for LLRD1 and GEIR2 in figure 5.1. Prior to this work the only dated palaeomagnetic curve available for Britain was Mackereth's declination curve for Windermere (Mackereth, 1971). This is compared with the new results below.

### 5.3.1:Lomond, LLRD1 (GU 900 -912).

Thirteen age estimates were made, spaced along the core LLRD1, rather more closely near the top than the bottom, due to the greater detail in the magnetic variations. Differing lengths of sediment were used to obtain the required amount of organic carbon( > 0.5 gm).

The age estimates in the uppermost metre are rather erratic.

Table 5.1 Radiocarbon Age Estimates

| | Depth in core (cm) | Magnetic feature | Rawage ± σ bp. (counting error) | Calibrated age. BP. |
|---|---|---|---|---|
| LOMOND LLRD1 GU 900-912 | 17 - 27 | D a W | 643 ± 52 | 600 |
| | 35 - 59 | D b E | 1815 ± 78 | 1750 |
| | 60 - 84 | D c W | 1627 ± 51 | 1585 |
| | 85 - 99 | D d E | 231 ± 55 | 315 |
| | 99 - 121 | I γ H | 1294 ± 69 | 1260 |
| | 140 - 154 | D e W | 1838 ± 59 | 1760 |
| | 182 - 202 | D f E | 1730 ± 59 | 1690 |
| | 207 - 235 | I ε H | 2712 ± 78 | 2890 |
| | 235 - 259 | I ξ L | 3542 ± 55 | 3910 |
| | 264 - 280 | D g W | 4205 ± 59 | 4865 |
| | 322 - 342 | D g-h | 6293 ± 102 | 7160 |
| | 364 - 380 | | 9694 ± 156 | |
| | 428 - 456 | | 7832 ± 131 | |

Table 5.1 continued.

| | Depth in core (cm) | Magnetic feature | Raw age ± σ bp. (counting error) | Calibrated age. BP. |
|---|---|---|---|---|
| WINDERMERE | | | | |
| WIND1 | 91 - 111 | D e W | 1930 ± 120 | 1870 |
| SRR 1451-1453 | 116 - 136 | D f E | 2680 ± 140 | 2855 |
| | 146 - 166 | D f-g | 3520 ± 110 | 3870 |
| GEIRIONYDD | | | | |
| GEIR2 | 75 - 95 | D b E | 830 ± 60 | 760 |
| SRR 1270-1278 | 100 - 120 | D c W | 1115 ± 60 | 1085 |
| | 125 - 145 | D d E | 1585 ± 65 | 1545 |
| | 175 - 195 | D e W | 1835 ± 65 | 1750 |
| | 225 - 245 | D f E | 3025 ± 60 | 3295 |
| | 275 - 295 | D f-g | 3120 ± 60 | 3310 |
| | 305 - 325 | D g W | 3750 ± 55 | 4180 |
| | 355 - 375 | D g-h | 5770 ± 65 | 6560 |
| | 460 - 480 | reworked material | 11470 ± 330 | |

Table 5. 1 continued

| | Depth in core (cm) | Magnetic feature | Rawage ±σ bp. (counting error) | Calibrated age. BP. |
|---|---|---|---|---|
| GEIRIONYDD | | | | |
| GEIR4 | 176 - 196 | D f E | 2670 ± 60 | 2850 |
| SRR 1460-1464 | 301 - 321 | D g W | 4560 ± 70 | 5330 |
| | 356 - 376 | D h E | 6050 ± 80 | 6925 |
| | 396 - 416 | | 11270 ± 340 | |
| | 416 - 436 | | 8540 ± 150 | |

Key: D = declination: W = west, E = east

I = inclination: H = maximum, L = minimum.

Figure 5.1: Magnetic and conventional C-14 age determinations.

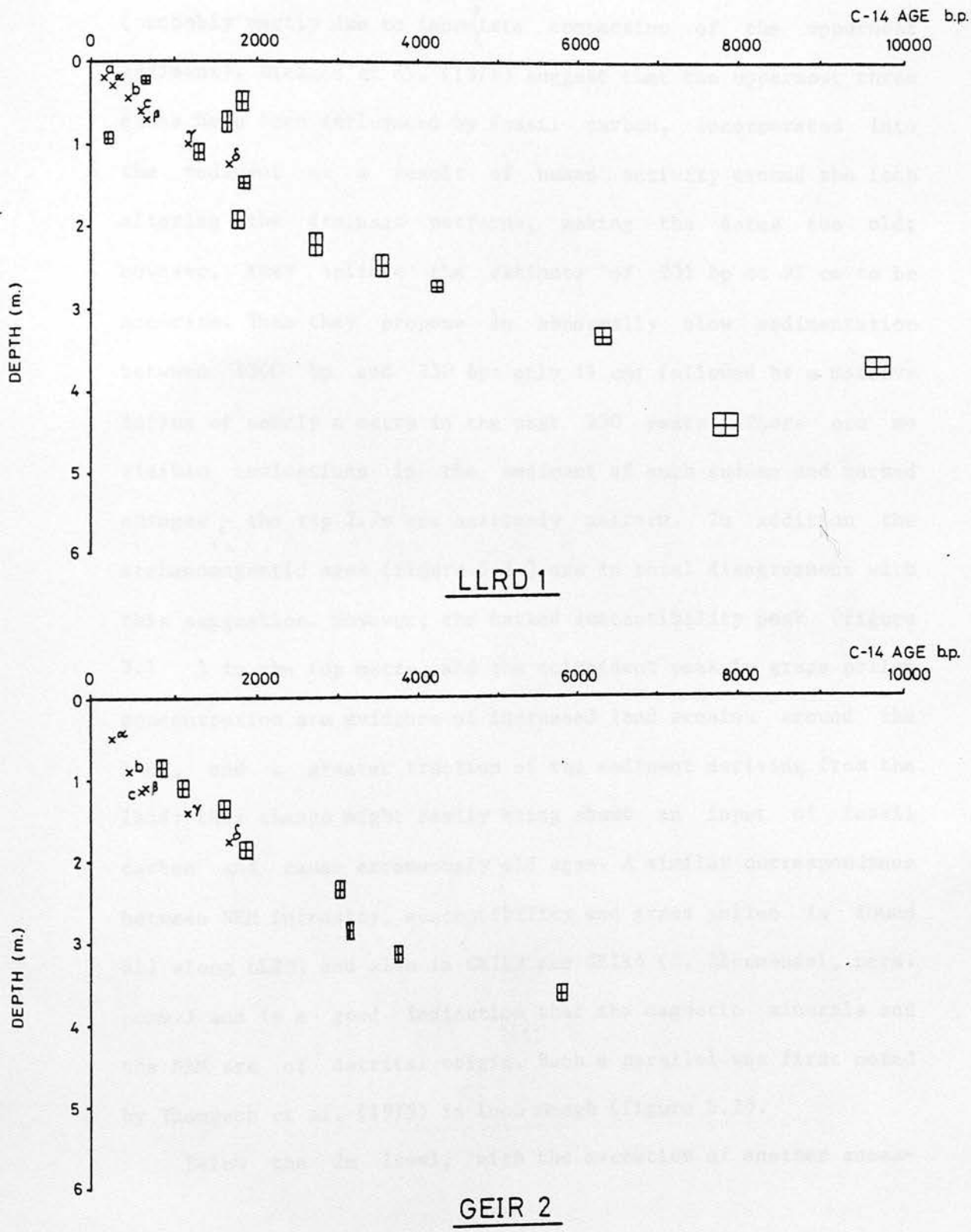

They neither describe a smooth deposition rate, nor do they agree with the ages inferred by correlation of declination and inclination features with archaeomagnetic and observatory records (chapter 3). This latter correlation indicates a smooth sedimentation over the last 1600 years, accelerating gradually to the present (probably partly due to incomplete compaction of the uppermost sediment). Dickson et al. (1978) suggest that the uppermost three dates have been influenced by fossil carbon, incorporated into the sediment as a result of human activity around the loch altering the drainage patterns, making the dates too old; however, they believe the estimate of 231 bp at 92 cm to be accurate. Thus they propose an abnormally slow sedimentation between 1300 bp and 230 bp: only 14 cm; followed by a massive influx of nearly a metre in the past 230 years. There are no visible indications in the sediment of such sudden and marked changes - the top 2.7m are extremely uniform. In addition the archaeomagnetic ages (figure 5.1 ) are in total disagreement with this suggestion. However, the marked susceptibility peak (figure 3.1 ) in the top metre, and the coincident peak in grass pollen concentration are evidence of increased land erosion around the loch, and a greater fraction of the sediment deriving from the land: this change might easily bring about an input of fossil carbon and cause erroneously old ages. A similar correspondence between NRM intensity, susceptibility and grass pollen is found all along LLRD1 and also in GEIR2 and GEIR4 (J. Bloemendal, pers. comm.) and is a good indication that the magnetic minerals and the NRM are of detrital origin. Such a parallel was first noted by Thompson et al. (1975) in Loch Neagh (figure 5.2).

Below the 2m level, with the exception of another anoma-

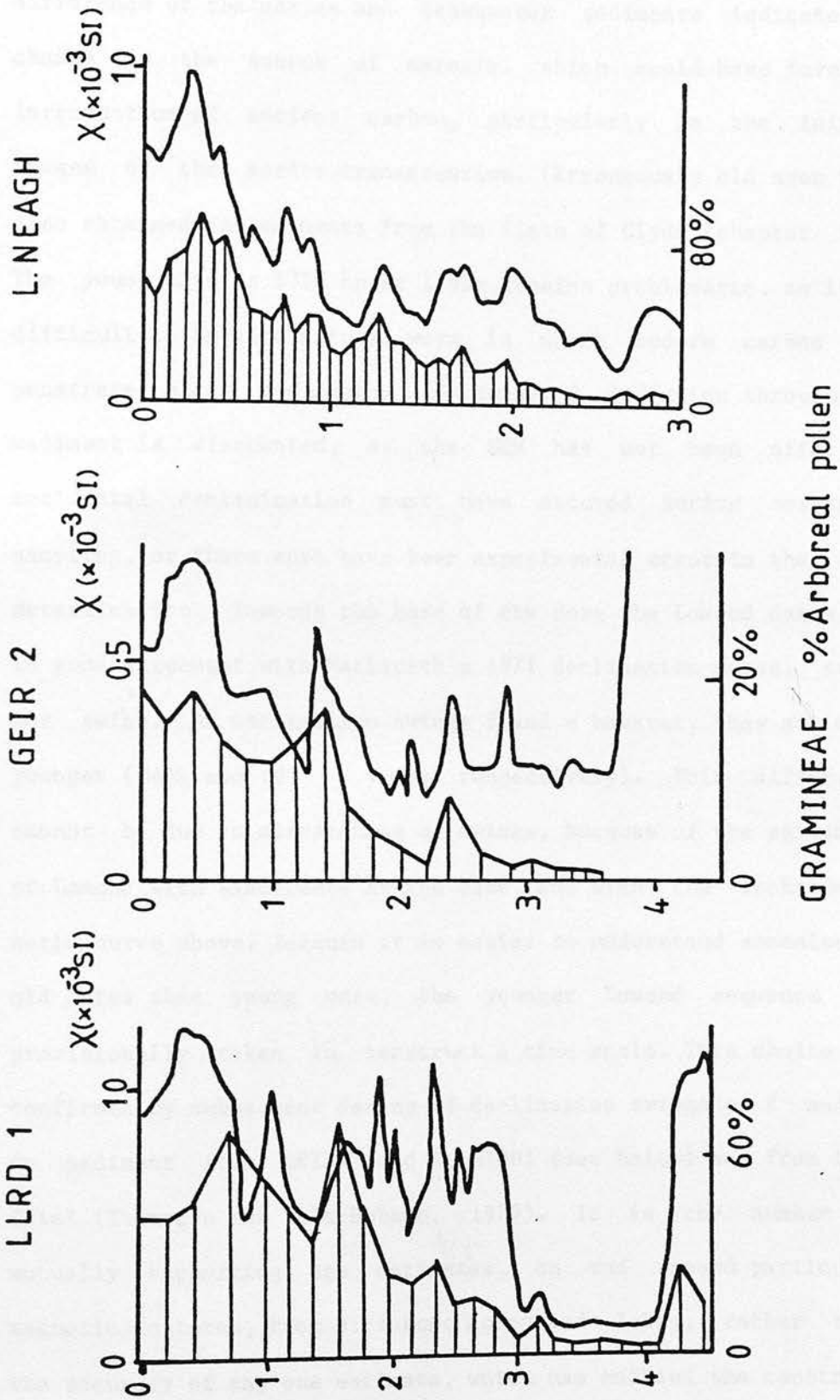


Figure 5.2 : Comparison of susceptibility and grass pollen logs (unshaded) (horizontal bars) LLRD 1, GEIR 2, and L.Neagh (from Thompson et al. 1975)

lously young date at 1.92m, and a very old one at 3.71m, in the marine sediment, the dates form a smooth progression. The large error in dating the marine sample is easily understood, as the difference of the marine and freshwater sediments indicates a change in the source of material which could have involved introduction of ancient carbon, particularly in the initial stages of the marine transgression. (Erroneously old ages were also obtained in sediments from the Firth of Clyde (chapter 8).) The young date at 1730 bp at 1.92m remains problematic, as it is difficult to imagine natural ways in which modern carbon can penetrate older sediments. If downward diffusion through the sediment is discounted, as the NRM has not been affected, accidental contamination must have occured during coring or sampling, or there must have been experimental error in the C-14 determination. Towards the base of the core the Lomond dates are in good agreement with Mackereth's 1971 declination curve, swing for swing. At declination swings f and e however, they are much younger ( 1600 and 600 years respectively). This difference cannot be due to mismatching of swings, because of the agreement of Lomond with Windermere at the base, and with the archaeomagnetic curve above. Because it is easier to understand anomalously old dates than young ones, the younger Lomond sequence was provisionally taken to construct a time scale. This choice was confirmed by subsequent dating of declination swings e, f and g on sediment from GEIR2 and 4, WIND1 (see below) and from Loch Shiel (Thompson and Wain-Hobson, 1979). It is the number of mutually supporting age estimates, on and around particular magnetic features, from different cores and lakes, rather than the accuracy of any one estimate, which has enabled the construc-

tion of the "preferred time scale" (section 5.5).

5.3.2:Geirionydd, GEIR2 and GEIR4 (SRR 1270-1278, SRR(1460-1464).

Declination swings b to g were dated in GEIR2, and f, g and h in GEIR4. In addition two samples were taken from the lower sections of each core for C-14 dating. Due to the low carbon content a 20cm length of sediment was used for each date.

The GEIR2 dates form a smooth monotonic sequence (figure 5.1). The uppermost three dates are a little older than the archaeomagnetic estimates. A similar explaination to that of the Lomond case is given here- the broad susceptibility and NRM intensity peaks in the top metre (figure 3.13) correlate with a similar peak in grass pollen and indicates increased land use and erosion in the drainage basin introducing ancient carbon. The date on declination swing e agrees well with the Lomond estimate. The date on f is possibly too old, both with respect to the Lomond estimate, and the other dates in the Geirionydd sequence- it is the only point not falling on the smooth sedimentation curve (figure 5.1 ). With the exception of the lowermost date, from the reworked marginal material, which would be expected to be old, the remaining estimates agree well with the Lomond and Windermere time scale prior to ca 4000 bp.

GEIR4 provides a valuable date on swing f in support of the new, younger time scale. In addition g and h are in good general agreement with the dates given above. The fourth date is probably influenced by the reworked sediment, but the lowermost may be accurate, since the Glacial clay expected at circa 10000 bp and found in GEIR8 was absent from this core.

### 5.3.3:Windermere, WIND1 (SRR 1451-1453).

Only three age estimates were possible on Windermere material, so samples were chosen from points at which the 1971 Windermere dates differ most from the new time scale developed: declination e-g. Again 20 cm lengths of sediment were used.

The results clearly support the new time scale (table 5.1), the date on f being very close to the LLRD1 and GEIR4 values, and over 700 years younger than the 1971 estimate of 3400 years bp. The effect of ancient carbon contamination thus seems to be localized and not encountered in every core from a particular site.

### 5.4:Pollen analysis.

Two aspects of the pollen analysis on LLRD1 (Stewart, 1978) and GEIR2 and 4 (J. Bloemendal, pers. comm.) were useful in this project:

1)The correlation of grass pollen concentration and magnetic susceptibility logs discussed above and illustrated in figure 5.2, again indicates that the magnetic minerals and remanence are of detrital origin.

2)The identification of pollen horizons. The elm decline- a sudden drop in the elm population which swept the whole of Britain very rapidly about 5000 bp (possibly similar to the effect of Dutch Elm Disease in the 1970's), has been identified in the 3 cores mentioned above, and in WIND1 (W. Tutin, pers. comm.). The elm decline has been identified and C-14 dated in several peat bogs close to the lakes studied. Peat generally has a much higher carbon content than lacustrine sediment, and often therefore, yields more accurate age estimates. Table 5.2 gives

the positions at which the elm decline was found in the cores, and relevant extra C-14 dates. In each core the elm decline occurs approximately half way between declination swings g and h, confirming the magnetic correlation between the three lakes. Hence, as susceptibility provides within lake correlations independent of the magnetic field, pollen analysis can provide such correlations between different lakes. This is used in constructing consistent preferred time scales for the lakes. Unfortunately the elm decline is the only suitable horizon in the period of interest.

Table 5.2:The elm decline.

| Core | Depth of elm decline (m.) | Relevant extra dates |
|---|---|---|
| LLRD1 | 3.15 - 3.00 | |
| GEIR2 | 3.50 | ( 4755±90 bp Melynllyn |
| GEIR4 | 3.40 | ( (Walker, 1977) |
| WIND1 | 2.30 - 2.20 | 5200 -5100 bp (Lake District). |

## 5.5:Construction of preferred time scale.

The method of choosing which age estimates to use in constructing a time scale is, of necessity, rather subjective. We want to maintain the independence of the magnetic records in the different cores as much as possible, so comparison of the ages of features in each is valid; and so that the Fourier spectra of each (chapter 6) is independent. Calibrated ages will be used from this point on, so that Fourier spectra etc. are computed in terms of calendar years. A time scale was first drawn up for LLRD1, using its age estimates listed in table 5.3, and the observatory and archaeomagnetic correlations, which are accura-

Table 5.3 Time Scale for Declination & Inclination features.

| Magnetic feature | Observatory archaeomag. or C-14 age.(bp) | Source of age | Calibrated age (B.P.) |
|---|---|---|---|
| D a W | 150 | O | 150 |
| I α H | 250 | O | 250 |
| D b E | 450 | a | 450 |
| D c W | 600 | a | 600 |
| I β L | 650 | a | 650 |
| D d E | 1150 | a | 1150 |
| I γ H | 1250 | a,L | 1250 |
| I δ L | 1650 | a | 1650 |
| D e W | 2000 | L,$G^2$,$W^1$ | 1950 |
| D f E | 2500 | S,$W^1$,$G^4$ | 2705 |
| I ε H | 3000 | | 3270 |
| I ξ L | 4000 | L,$W^1$,$G^2$ | 4545 |
| D g W | 4200 | L,$G^2$,$G^4$ | 4860 |
| I η H | 5000 | | 5785 |
| I θ L | 6100 | | 6980 |
| D h E | 6300 | L,$G^4$,$G^2$,W | 7165 |
| I ι H | 6600 | | 7465 |
| I ϰ L | 7000 | | 8000 |
| D i W | 7400 | W | 8400 |
| I λ H | 9000 | | 9500 |
| D j E | 10600 | W | 10600 |

Key: D = declination: W = west, E = east
I = inclination: H = maximum, L = minimum

Sources: O = magnetic observatory
a = archaeomagnetic
L = LLRD1 C-14
$G^2$ = GEIR2 C-14
$W^1$ = WIND1 C-14
S = Loch Shiel C-14
$G^4$ = GEIR4 C-14
W = 1971 Windermere C-14

tely dated. This time scale was transferred to the other Lomond cores using correlation of susceptibility features only. Since susceptibility variations have no dependence on the geomagnetic field, this preserves the independence of the 4 declination and inclination data sets. The correlation is accurate to within 3cm. The time scales on WIND1 and GEIR2 were evolved by combining the reliable C-14 dates on these two cores respectively, (table 5.3), and correlations with LLRD1 at the present, and the elm decline, and by "stretching" the records to fit around declination swings e-f-g. Unfortunately there are not enough suitable pollen horizons to avoid this last step which involves the geomagnetic field. The other Windermere cores were dated from WIND1 by lithological correlations (table 2.2), the Geirionydd cores from GEIR2 by susceptibility, as for Lomond.

The best combined dates on each of the declination and inclination swings are listed in table 5.3, the sources of declination swing dates are given, the inclination swings below are dated by interpolation between declination swings. Most of the swings consist of a single turning point or extremity (a, b, c, d, f) and so are clear to label. However, declination swings e, g and h are more complex. In these cases the mid point of the portion of the record on the positive or negative side of the vertical axis is labelled. Additional features, repeated in several cores are also labelled e.g. g', h' (figures 3.5, 3.17).

The sedimentation curves deduced using these "preferred time scales" are plotted in figure 5.3. In general they all show a gradual increase in deposition rate towards the tops of the cores. At the very top this apparent acceleration can be explained by incomplete compaction, but lower down it is probably

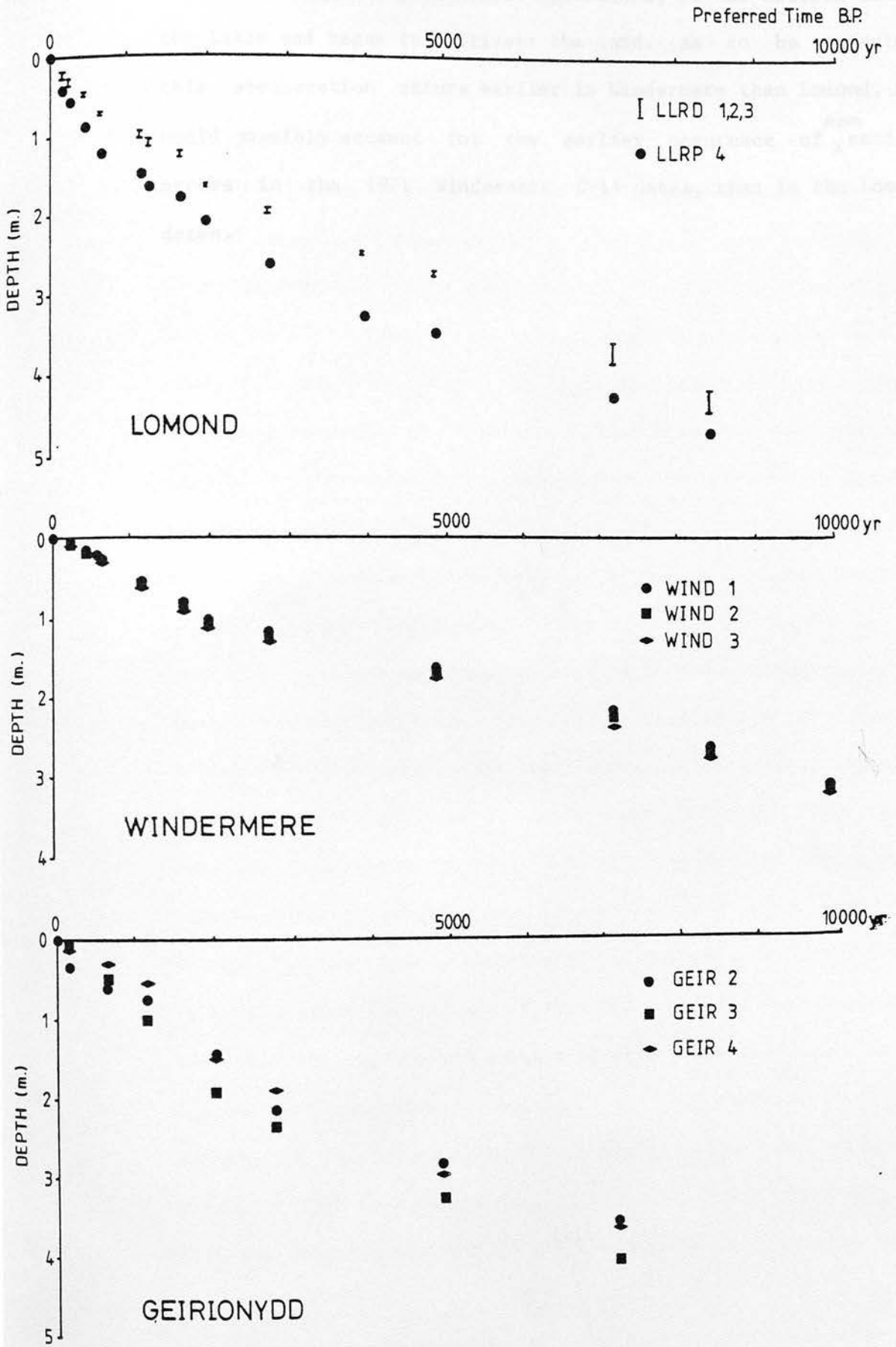


Figure 5.3: Deposition rates vs. preferred time scales.

real, and due to agricultural operations, as man settled around the lakes and began to cultivate the land. As to be expected, this acceleration occurs earlier in Windermere than Lomond, and could possibly account for the earlier occurence of more serious errors in the 1971 Windermere C-14 dates, than in the Lomond dates.

# CHAPTER 6: SECULAR VARIATION OF THE DIRECTION OF THE GEOMAGNETIC FIELD.

## 6.1: Introduction.

The previous chapter dealt with the complex, and still poorly understood, relationship between the intensity of the NRM of a sediment and the intensity of the magnetic field in which it was formed. Fortunately it is much more straightforward to interpret and assess the reliability of the directional records, as no correction or normalization procedures are generally necessary, other than occasional A.F. "cleaning". It is logical, therefore, to study the magnitude and direction of the palaeomagnetic field separately, remembering however, that the geomagnetic field is a three dimensional vector.

The quality and compatibility of the directional data from the four Lomond cores lead to a more quantitative approach to their treatment. This was the first time four sets of paired declination and inclination values, each covering 7000 years, from two different sites in a lake, could be treated together. In this case the correlation, and the time scale of the variations is easily visible on inspection of the raw records. However this is a subjective method, not reproducible, and its accuracy cannot be assessed. So the treatment discussed below was first carried out on the Lomond data, when it could be checked by visual examination of the records, before applying it to the Windermere and Geirionydd data, where the quality was not as high, but valuable information could still be obtained with careful treatment.

Further experiments were also done on one or more sets of

the Lomond data (section 6.6).

## 6.2:Data conditioning.

### 6.2.1:Co-ordinates.

As we were dealing with directions only, the magnitude of each remanence vector was set to unity i.e. the vectors were constrained to the surface of a unit sphere. In doing this the problem was reduced to a two-dimensional one: two sets of variables are sufficient to describe all the remaining information. These two variables can be angles, declination and inclination, or cartesian or polar co-ordinates on a projection e.g. on a stereographic projection. Both choices are used in the following sections: a "transformed" version of D and I in the straightforward spectral analysis (section 6.4), and components in section 6.6 where the vectors are mapped onto a complex plane. Because of the two-dimensionality it was decided not to revert to three components, x, y and z, or direction cosines, as this would complicate the interpretation of the spectra.

### 6.2.2:Interpolation of data sets to equal intervals of time.

In chapter 5 "preferred time" horizons were fitted to each core studied. The data points are, however, at arbitrary and variable intervals of time. Most spectral analysis methods require uniformly spaced data points. This was achieved by two stages of linear interpolation. Firstly, assuming uniform deposition between consecutive PT horizons, depths were calculated at 40 year intervals of PT. A time interval of 40 years was chosen to give approximately the same number of new as raw data points

in Lomond: this ensures optimum use of the data available- neither wasting nor over-using any. A more sophisticated form of interpolation e.g. polynomial or natural cubic-spline fitting, could have been used here, but it was felt the accuracy of the dating did not warrant the extra complication involved. The second step was linear interpolation between the two raw data points above and below each 40 year PT horizon, to obtain the new, equally spaced data. This was done separately for declination and inclination. Linear interpolation was chosen at this stage in order to preserve the maximum independence between new data points. Any higher order method (e.g. Parker and Denham, 1979, fitting cubic splines) would involve the use of more than two raw data points in computing each new one, and consequently more than two new points would depend on information from each raw one. In the computation of spectra it is desirable to avoid unnecessary mixing of data up and down the record.

### 6.2.3:Rotation of axes to a standard frame of reference.

Finally, the cartesian axes to which D and I are referred, were rotated for each core, first about y, then about z, to bring the new x axis along the main remanence direction of the core. This mean direction was calculated by averaging the direction cosines of the individual vectors with respect to the original axes. In this way then, the mean "transformed declination", $D_T$, and "transformed inclination", $I_T$, are both zero.

This procedure has three immediate advantages: 1) firstly, since the corer is not oriented during coring, the original z axis is taken along the length of the core-tube, and is not necessarily vertical. The spread of mean down core inclination

values shown in table 6.1 suggests that non-vertical penetration has probably occurred in most cores (the higher the latitude and the larger the angle of tilt, the inclination is more likely to be shallowed than steepened).

Table 6.1:Mean down-core inclinations.

| | | | | | |
|---|---|---|---|---|---|
| LLRD1 | 66.0° | WIND1 | 72.0° | GEIR2 | 69.6° |
| LLRD2 | 72.2° | WIND2 | 62.8° | GEIR3 | 61.9° |
| LLRD3 | 63.2° | WIND3 | 53.4° | GEIR4 | 66.4° |
| LLRD4 | 59.9° | | | | |

average 64.7°± 5.5°

The expected inclination at latitude 54.5°for an axial geocentric dipole = 70°.

The new reference axes are fixed relative to the mean remanence direction in the core, or the mean geomagnetic direction over the time spanned by the core.

2)Secondly, in comparing results from different latitudes (> 10° apart), the effect of latitude on the relative amplitudes of declination and inclination swings becomes apparent. In the records studied here declination has an amplitude about three times that of inclination. When corrected to zero mean D and I, these become standardized and roughly equal.

3)Finally, after transformation we are dealing with only small angles (usually <15°), so objective smoothing techniques such as that of Clark and Thompson (1978) can be applied to D and I separately with little error.

### 6.3.1:"Transformed" secular variation curves.

Figure 6.1 shows the effect of axis rotation and plotting against preferred time on the directional records from Lomond and

Geirionydd, figure 6.2 shows the corresponding Windermere curves.

In all cores the main effect of the axis rotation is to lower and roughly equalise the amplitudes of the declination and inclination variations. The same features $k-\alpha$ & $\nu-\alpha$, noted in section 3.1 are still just as easily picked out. Plotting against PT instead of depth, however, has a marked effect - it removes the periodic appearance of the main swings. In all three lakes the main declination swings are now seen to have decreased in duration with time, from several thousand years at the base of LLRD1 to about 700 years for the most recent declination oscillation. The same is true of the "transformed" inclination records, and is shown particularly clearly in GEIR3 and WIND2. Many of the details noted previously e.g. the recent westerly declination swing a, the sharp easterly swings d and f and the complex e and g are still present and make good identifying features. These records appear smoother than the raw data - an unavoidable consequence of the interpolation between raw data points in producing the new ones. This smoothing is especially pronounced in the Windermere records, as the post-Glacial sediment was only 3m deep, and the same PT interval of 40 years was used ,as for Lomond and Geirionydd, for consistency.

Figure 6.3 is drawn from the same data as figures 6.1 and 6.2, but the values at each time horizon have been averaged over the cores from each lake, to give a single curve. This procedure is sensitive to correlation discrepancies between the cores, and so will only give a good result if the PT scales have been transformed accurately. This may account for the slight loss of sharpness and lower amplitude of the Windermere curve compared to the Lomond one. The Geirionydd curve shows the ability of the

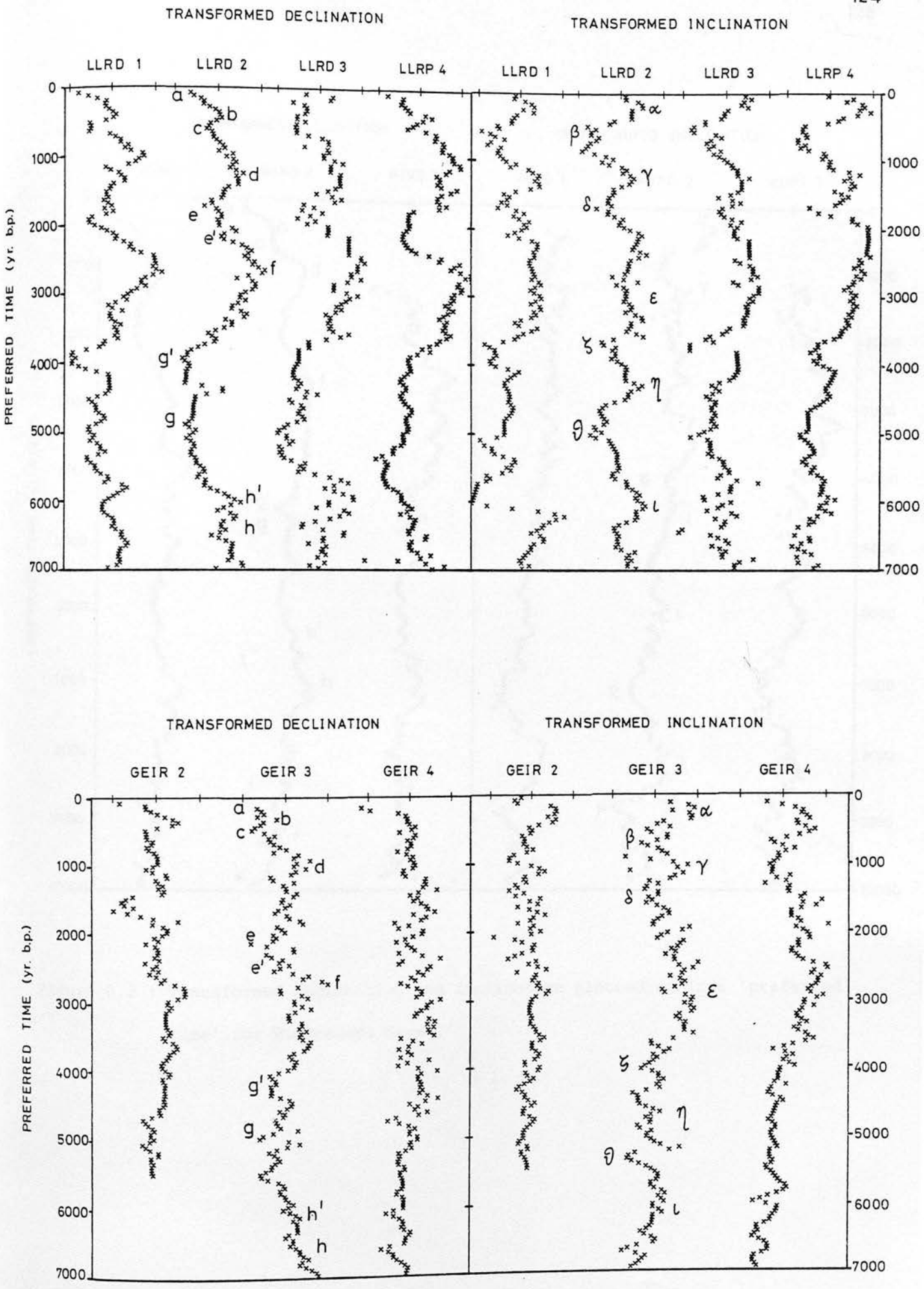


Figure 6.1 : Transformed declination and inclination plotted against 'preferred time' for Lomond and Geirionydd cores.

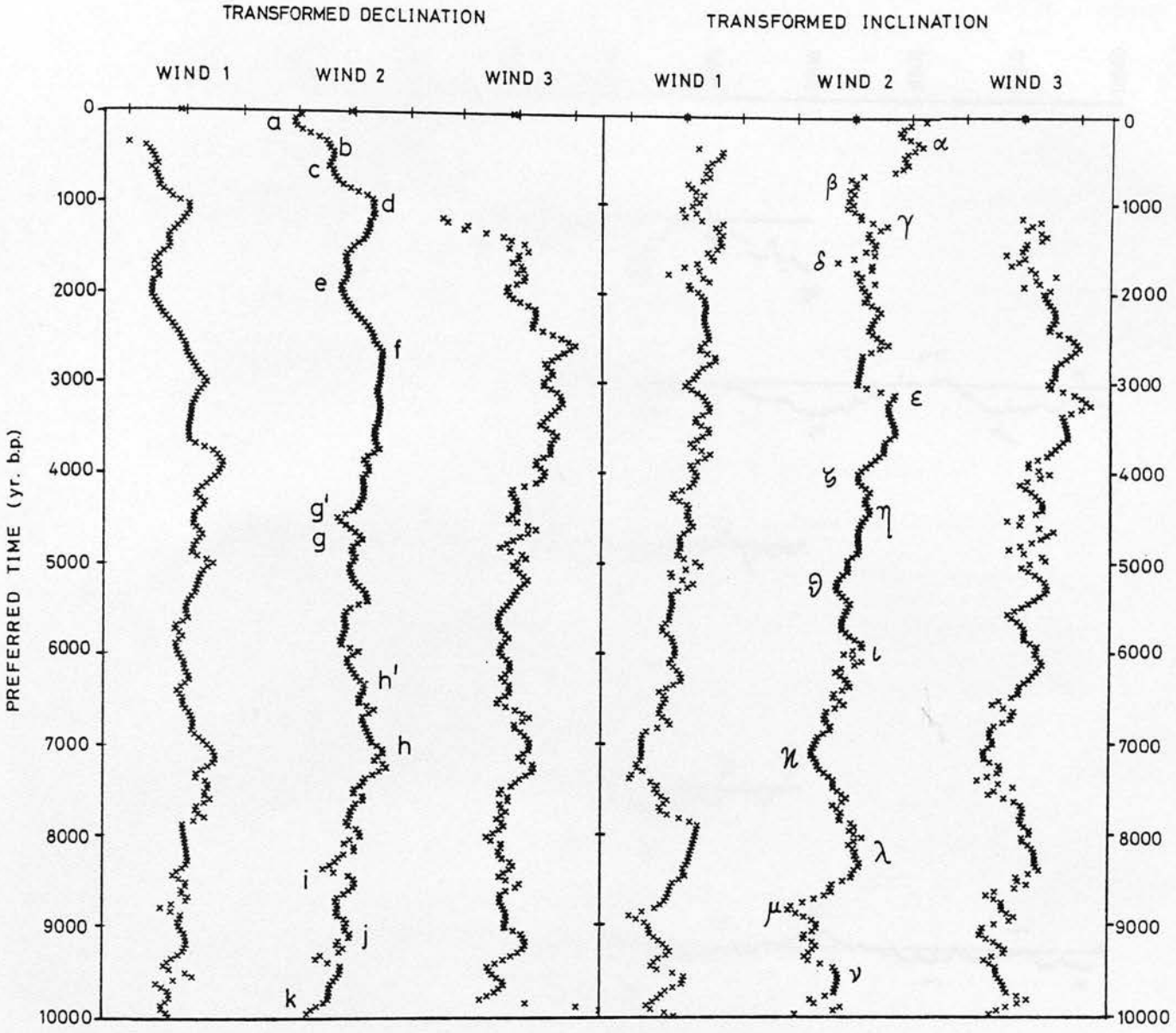


Figure 6.2 : Transformed declination and inclination plotted against 'preferred time' for Windermere cores.

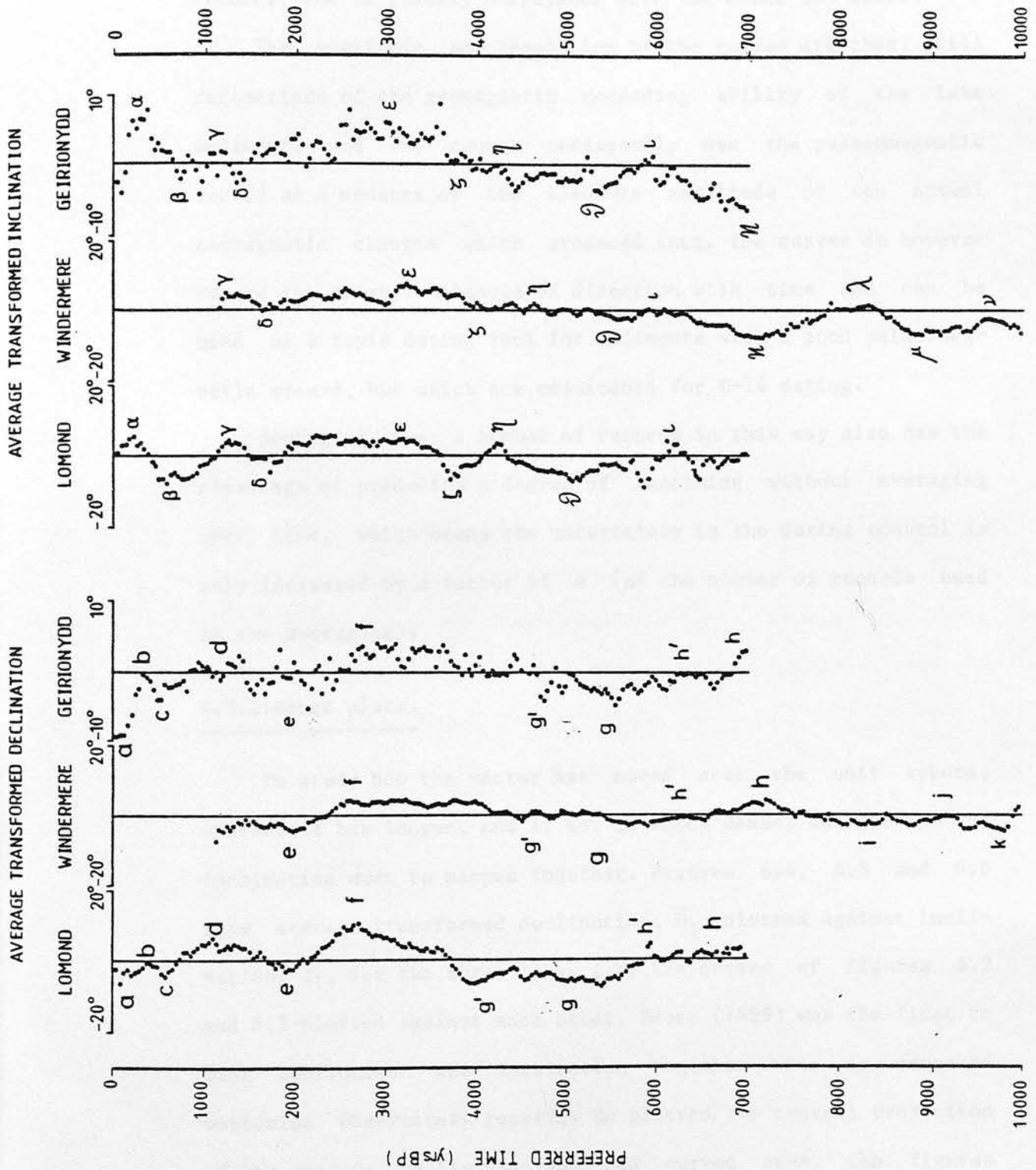


Figure 6.3 : Average transformed declination and inclination for each lake, plotted against 'preferred time'.

procedure to deal with random noise. Although also of low amplitude, and noisy compared with the other two curves, the composite curve is much better defined than any of the individual records, and is readily correlated with the other two lakes.

The amplitude and resolution of the curves are then, still reflections of the geomagnetic recording ability of the lake sediments and one cannot necessarily use the palaeomagnetic record as a measure of the absolute amplitude of the actual geomagnetic changes which produced them. The curves do however record the relative changes of direction with time and can be used as a rapid dating tool for sediments with a good palaeomagnetic record, but which are unsuitable for C-14 dating.

Averaging over a number of records in this way also has the advantage of producing a degree of smoothing without averaging over time, which means the uncertainty in the dating control is only increased by a factor of n (n= the number of records used in the averaging).

### 6.3.2:Bauer plots.

To study how the vector has moved over the unit sphere, whether it has looped, and if so, in which sense, declination and inclination must be mapped together. Figures 6.4, 6.5 and 6.6 show average transformed declination, $\bar{D}_T$, plotted against inclination, $\bar{I}_T$, for the three lakes i.e. the curves of figures 6.2 and 6.3 plotted against each other. Bauer (1895) was the first to plot declination and inclination together when he compared worldwide observatory records. He plotted the central projection of the vectors, so his diagrams had curved axes. the figures plotted here take the core mean as the origin, due to the axis

rotation, and are plotted with rectangular axes. As the angles involved are small there is little difference between this and a polar projection centered on the core mean direction. To facilitate visual inspection, the curves are plotted in 1500 year sections.

1)Lomond (figure 6.4).

1)The clockwise loop over the last 600 years (Lomond and Windermere) is in agreement with recent observatory records and archaeomagnetic data. In the mini-core results this loop is broader and does not contain the shorter anticlockwise kink of the long cores, which is probably due to sedimentological disturbance.

2)A definite anticlockwise loop occurs from 1500 - 600 BP The first and last parts of this loop occur in the Roman and mediaeval sections of the archaeomagnetic records (Aitken, 1970; Clark, 1979), but the "dark ages" section is missing from their records. All three lakes show that the anticlockwise looping persisted right through the dark ages.

3)The remainder of the Lomond curve is 1 1/3 clockwise loops from 4500 - 1500 BP preceded by a tighter, but still mainly clockwise loop.

2)Windermere (figure 6.5).

The Windermere Bauer plots for the period 5500 - 0 BP are very similar to those from Lomond. The amplitudes are lower, as noted in section 6.3.1. The origins of the Lomond and Windermere Bauer plots are not coincident, as the Lomond origin is the mean vector over 7000 years, whereas the Windermere origin is the mean

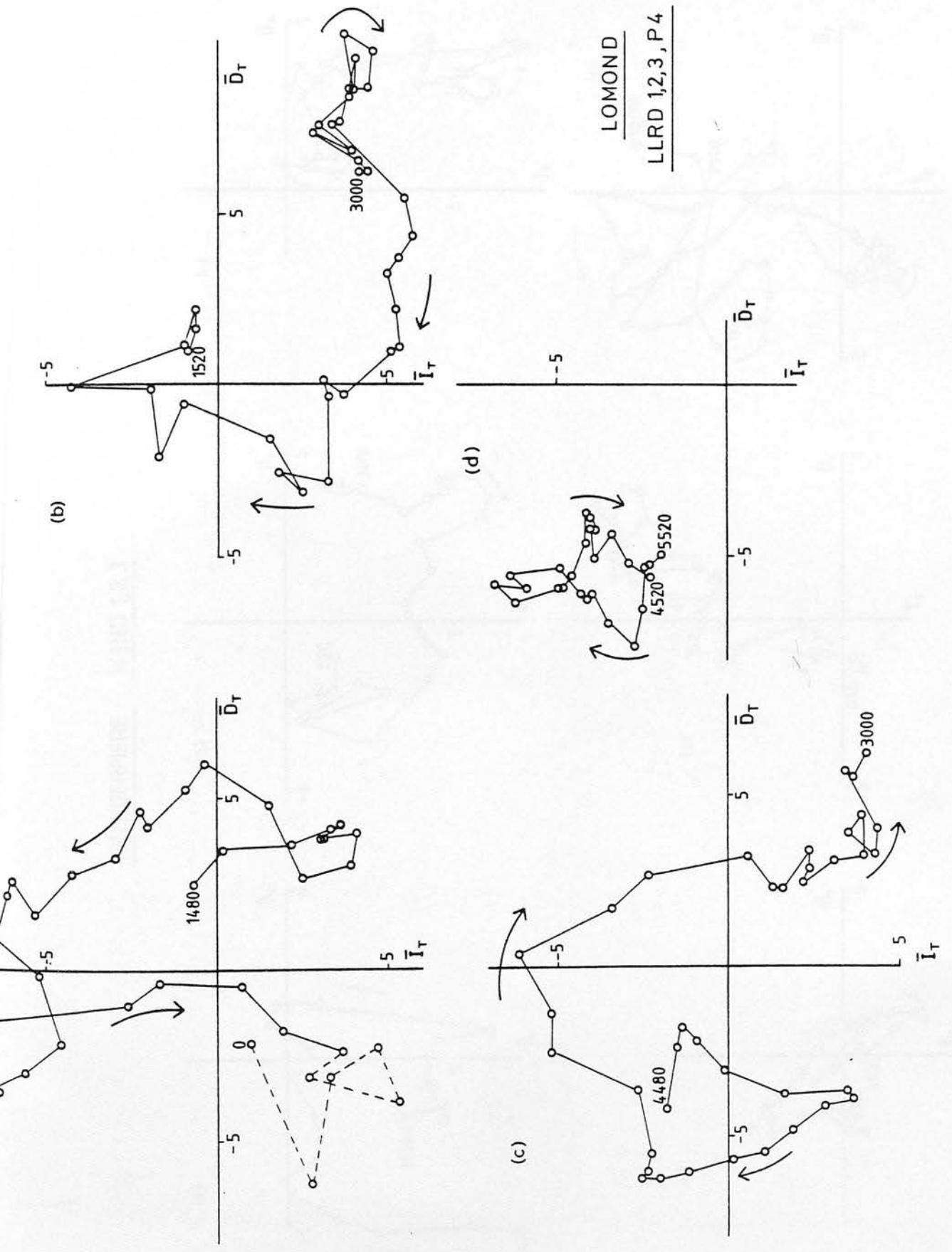


Figure 6.4 : Bauer plots of average transformed declination against inclination for Lomond cores

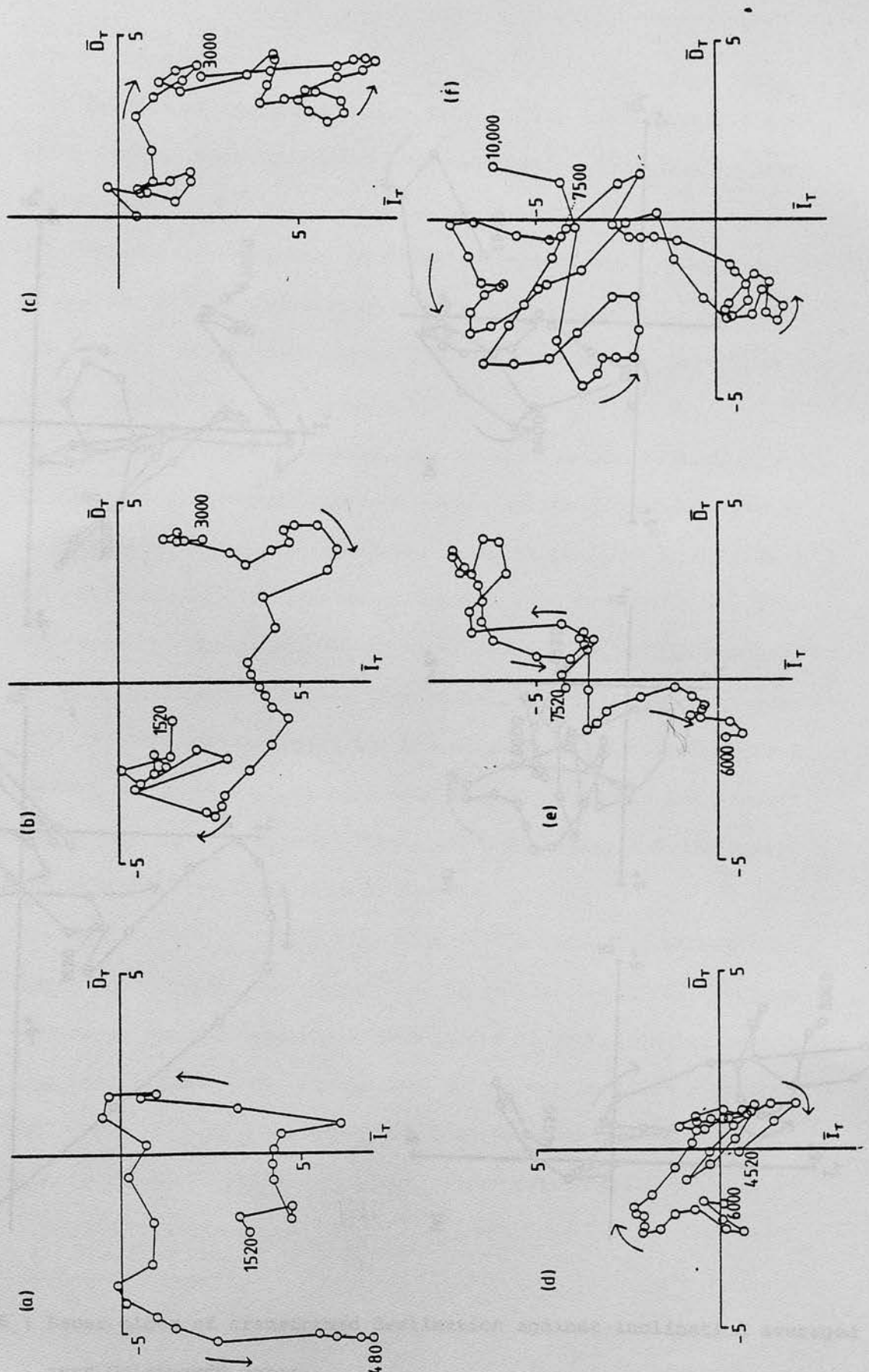


Figure 6.5 : Bauer plots of average transformed declination against inclination for Windermere cores.

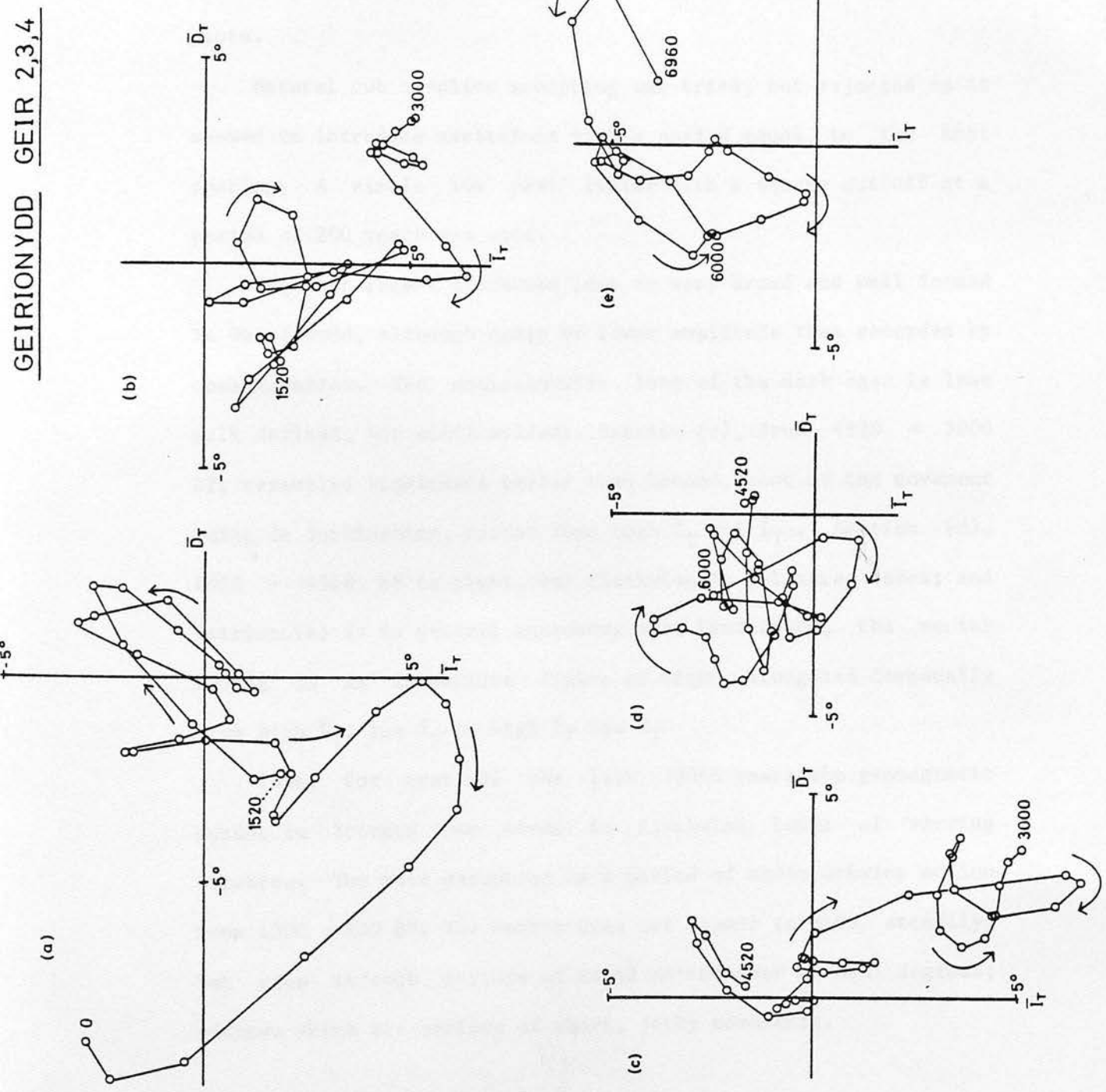


Figure 6.6 : Bauer plots of transformed declination against inclination averaged over Geirionydd cores.

vector over 10000 years.

3)Geirionydd (figure 6.6).

Because of the higher noise level in the Geirionydd composite curve, some smoothing was necessary before drawing Bauer plots.

Natural cubic spline smoothing was tried, but rejected as it seemed to introduce variations with a period equal to the knot spacing. A simple low pass filter with a square cut off at a period of 200 years was used.

The most recent clockwise loop is very broad and well formed in Geirionydd, although again of lower amplitude than recorded by observatories. The anticlockwise loop of the dark ages is less well defined, but still evident. Section (c), from 4520 - 3000 BP, resembles Windermere better than Lomond, most of the movement being in inclination, rather than both $\bar{D}_T$ and $\bar{I}_T$ . Section (d), 6000 - 4520 BP is tight, but clockwise in all three lakes; and section (e) is in general agreement with Windermere, the vector moving in an incomplete figure of eight, elongated diagonally from high $\bar{D}_T$, low $\bar{I}_T$ to high $\bar{I}_T$ low $\bar{D}_T$.

Thus, for most of the last 10000 years the geomagnetic vector in Britain has moved in clockwise loops of varying duration. The main exception is a period of anticlockwise motion from 1500 - 600 BP. The vector does not appear to move steadily, but goes through periods of rapid motion over several degrees, between which are periods of short, jerky movements.

6.4.1:Spectral analysis.

Frequency domain analysis of time varying data is popular in

many disciplines, and can be a powerful tool when used carefully. It is again important to demonstrate agreement between several records, as a spurious feature in a single record, which may be identifiable in the time series, may cause much less obvious errors in the spectrum.

Several authors have reported periodicities in palaeomagnetic data e.g. Thompson (1975) reported a 2700 year declination cycle from the English Lake District, Opdyke et al. (1972) a 6000 year inclination period from the Aegean Sea, and Creer (1974) a 2800 year inclination period from the Black Sea. The limiting factor in such work has always been the number and accuracy of the dating controls. Sometimes workers have had to study sequences with only two dated horizons available. In such cases one must either 1) assume uniform deposition between, above and below the horizons, to assign a time scale, and then perform spectral analysis (e.g. Oberg and Evans, 1977) or 2) assume the secular variation swings to be periodic and calculate their "period" from the number of cycles and the two dates (e.g. Creer, Gross and Lineback, 1976). In view of the spread of age estimates on a single declination feature presented in chapter 5, both approaches seem to place rather too much confidence in two dates. Also, although uniform deposition may be fairly assumed in deep sea sediments, section 5 demonstrates clearly that it could not be assumed in any of the lakes studied here, and section 6 shows that periodic secular variation cannot be explicitly assumed either.

The following sections examine the spectral components of the variations recorded for any underlying periodicities not obvious visually, or any systematic pattern to the secular

variation of both declination and inclination.

### 6.4.2:Fast Fourier Transform.

R.Singleton's Fast Fourier Transform (FFT) algorithm was used to compute all spectra presented in this chapter. This method is particularly suited to intransient data sets, such as palaeomagnetic ones, as its only restriction on data set length is to products of powers of prime numbers. In practice this means that rarely more than 2 or 3 data points have to be discarded, and nearly all the data is used. Another option would have been to use an algorithm such as that of Cooley and Tukey (1965), and make up the data set length to the required power of two by the addition of zeros. Such extension is permissible for transient data, but unrealistic for palaeomagnetic secular variations. Also, Singleton's FFT will accept complex data, and so could easily be incorporated into a program to analyse the total direction as a complex number pair (section 6.6).

### 6.4.3:Pretransform data treatment.

All data sets were reduced to zero mean value, detrended and cosine tapered prior to the application of FFT, whether straight forward, on a maximum entropy extended data set, or on complex data. (A slight modification was necessary to enable the subroutines to accept complex data.)

The F.T. of a continuous time function f(t) is defined by

$$F(w) = \int_{-\infty}^{\infty} f(t)\, e^{iwt}\, dt \qquad (i)$$

In practice f(t) is not defined continuously but at a finite number of points in a restricted range say between t=0 and t=T. The discrete nature of the data results in the transform being a

line spectrum with a "folding" or Nyquist frequency of $f_N = 2T/N$ above which the spectral components are aliases of those below. However, in our case $f_N$ corresponds to a period of about 80 years, which is well below the range of interest.

However the finite length of data means we have to approximate (i) by

$$\bar{F}(w) = \int_0^T f(t)\, e^{iwt}\, dt \qquad \text{(ii)}$$

which is equivalent to

$$\bar{F}(w) = \int_{-\infty}^{\infty} f(t)\, z(t)\, e^{iwt}\, dt$$

where $z(t) = 0 \qquad -\infty < t < 0 \qquad t > T$

$z(t) = 1 \qquad 0 \leqslant t \leqslant T$

i.e. we are effectively sampling an infinite data set by multiplying it by a "box-car" function in the time domain (figure 6.7). This is equivalent to convolving the F.T. of f(t), F(w), with the F.T. of z(t), Z(w), in the frequency domain.

i.e. $\bar{F}(w) = F(w) * Z(w) = \int_{-\infty}^{\infty} F(\chi)\, Z(w-\chi)\, d\chi$

Figure 6.7 shows the "box-car" z(t) and its F.T. Z(w)

$$Z(w) = 2T \sin(wT)/wT = 2T \operatorname{sinc}(wT)$$

The large side lobes of Z(w) - 24% in the first negative lobe, 13% in the first positive lobe, allow leakage of power from the main peak and cause spectral distortion. This leakage is especially important if there is substantial power in the zero and fundamental frequencies, hence it is important to minimize these. The standard procedure adopted was to remove any linear trend from the data sets. This was always small, but may be caused by twisting of the sediment. The mean (d.c.) level should already have been set to zero during the axis rotation process, but this was checked again at this stage. The side lobes of Z(w) can also be reduced considerably by applying a half cosine bell taper to

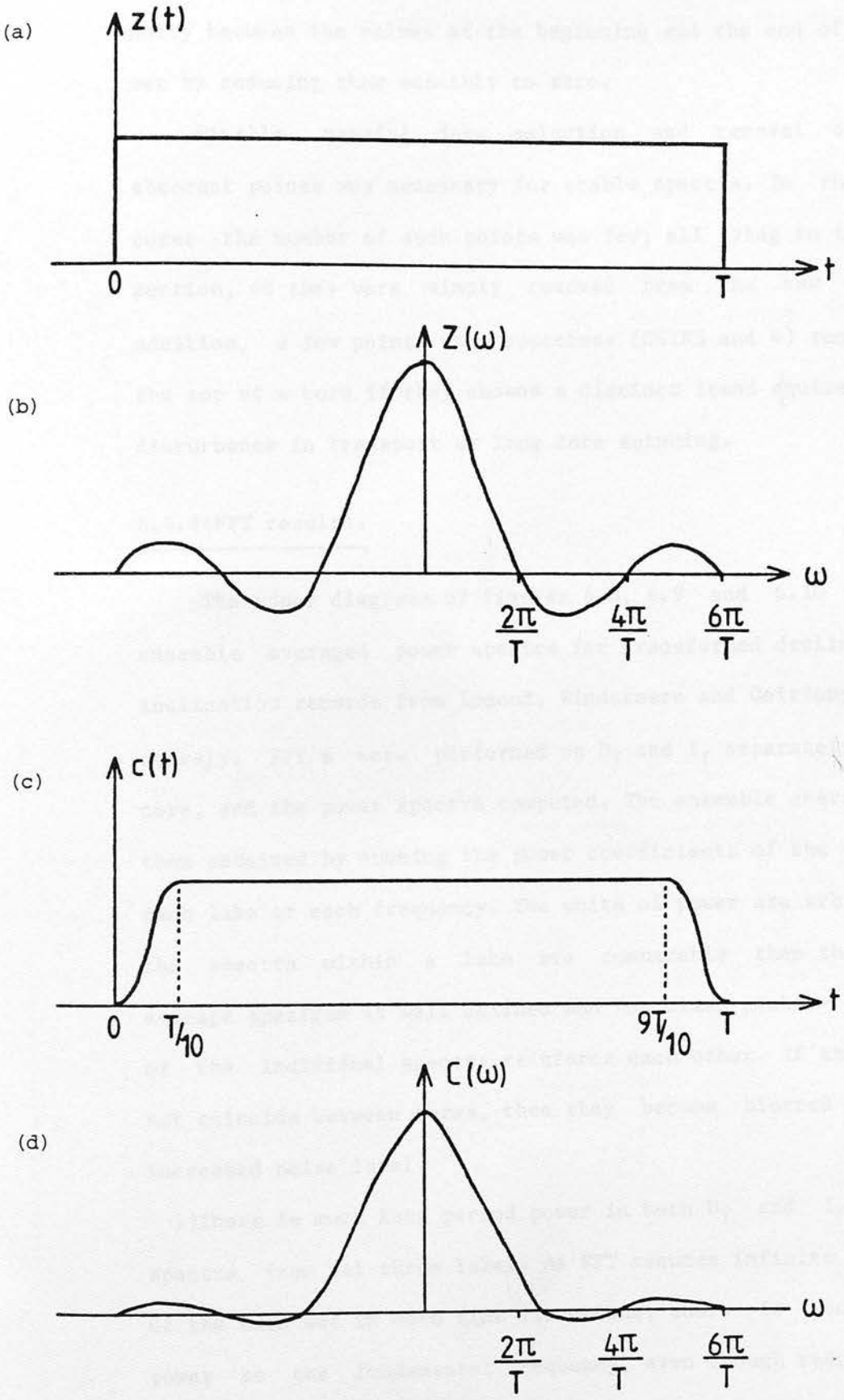


Figure 6.7 : (a) box car function and (b) its Fourier transform.

(c) cosine taper and (d) its Fourier transform.

the first and last 10% of the data set (Bingham, Godfrey and Tukey, 1967). Use of a taper also compensates for any discontinuity between the values at the beginning and the end of the data set by reducing them smoothly to zero.

Finally, careful data selection and removal of single aberrant points was necessary for stable spectra. In the Lomond cores the number of such points was few, all lying in the marine section, so they were simply removed from the raw data. In addition, a few points were sometimes (GEIR3 and 4) removed from the top of a core if they showed a distinct trend acquired due to disturbance in transport or long core spinning.

6.4.4:FFT results.

The upper diagrams of figures 6.8, 6.9 and 6.10 show the ensemble averaged power spectra for transformed declination and inclination records from Lomond, Windermere and Geirionydd respectively. FFT's were performed on $D_T$ and $I_T$ separately for each core, and the power spectra computed. The ensemble averages were then obtained by summing the power coefficients of the cores from each lake at each frequency. The units of power are arbitrary. If the spectra within a lake are comparable then the ensemble average spectrum is well defined and has clear peaks - the peaks of the individual spectra reinforce each other. If the peaks do not coincide between cores, then they become blurred into the increased noise level.

1)There is much long period power in both $D_T$ and $I_T$ in the spectra from all three lakes. As FFT assumes infinite repetition of the data set in both time directions, there is bound to be power at the fundamental frequency, even though reduced by the

Figure 6.8: Ensemble average FFT and maximum entropy FFT spectra for LLRD 1,2,3, LLRP 4.

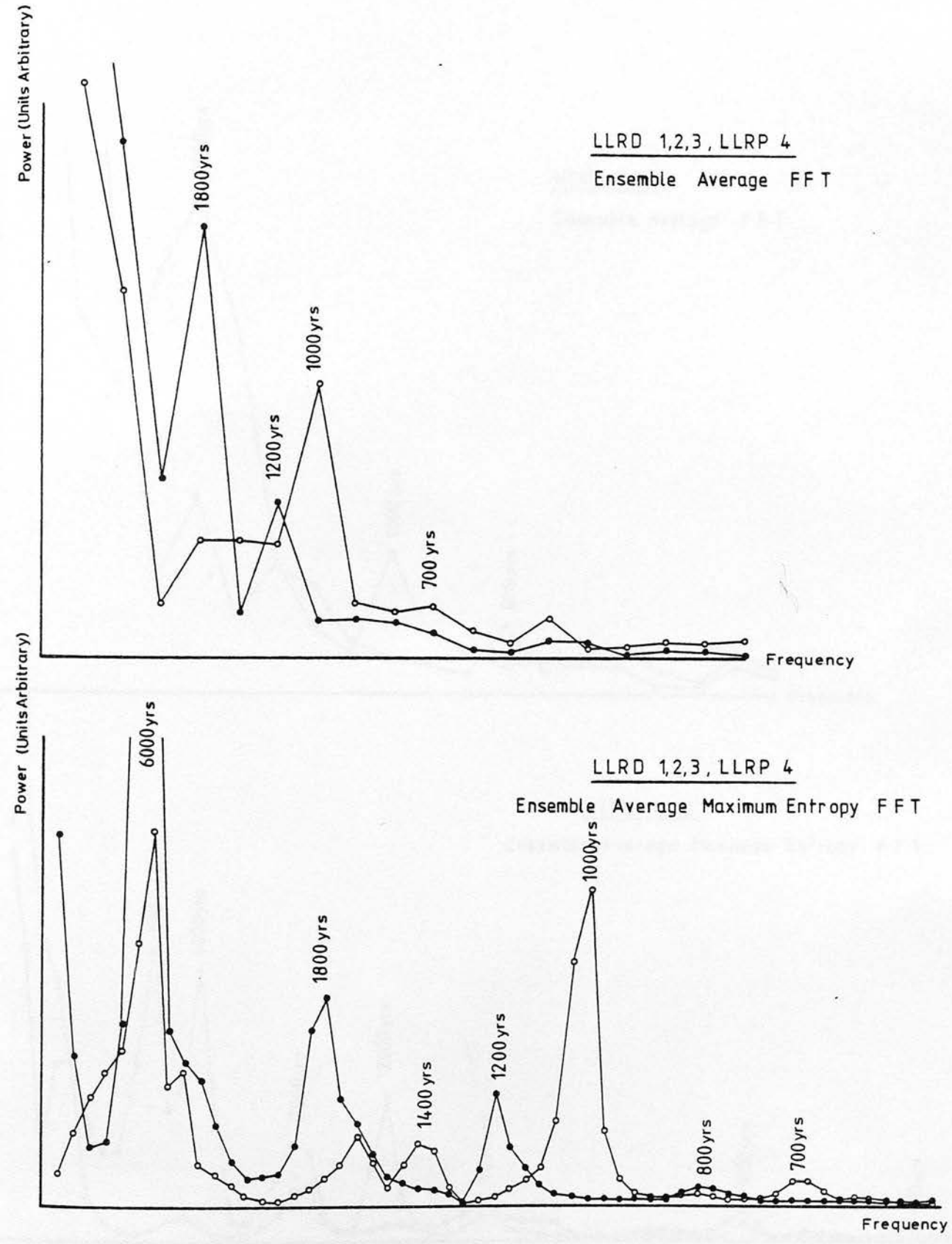

Figure 6.9: Ensemble average FFT and maximum entropy FFT spectra for WIND 1,2,3.

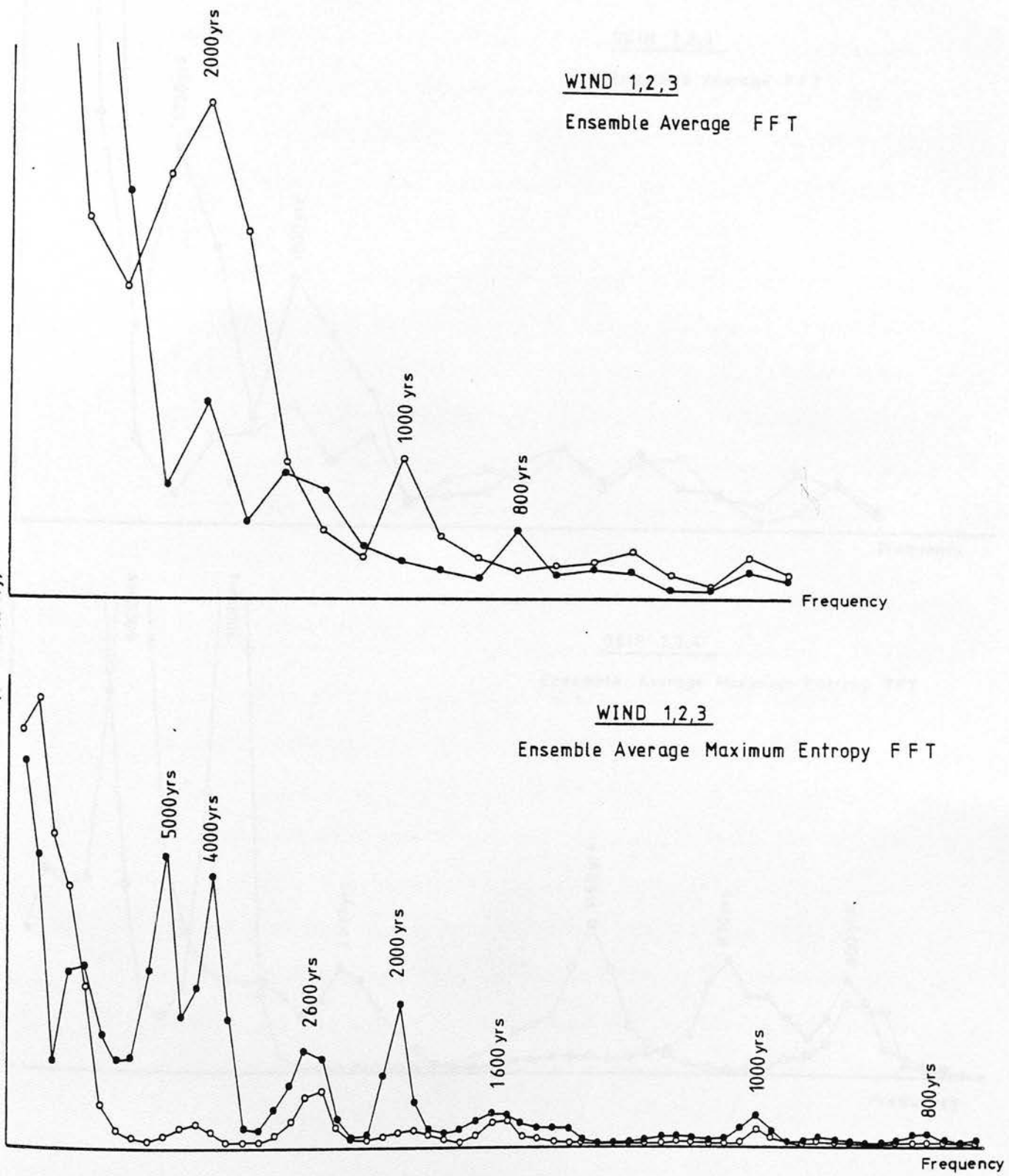

Figure 6.10: Ensemble average FFT and maximum entropy FFT spectra for GEIR 2,3,4.

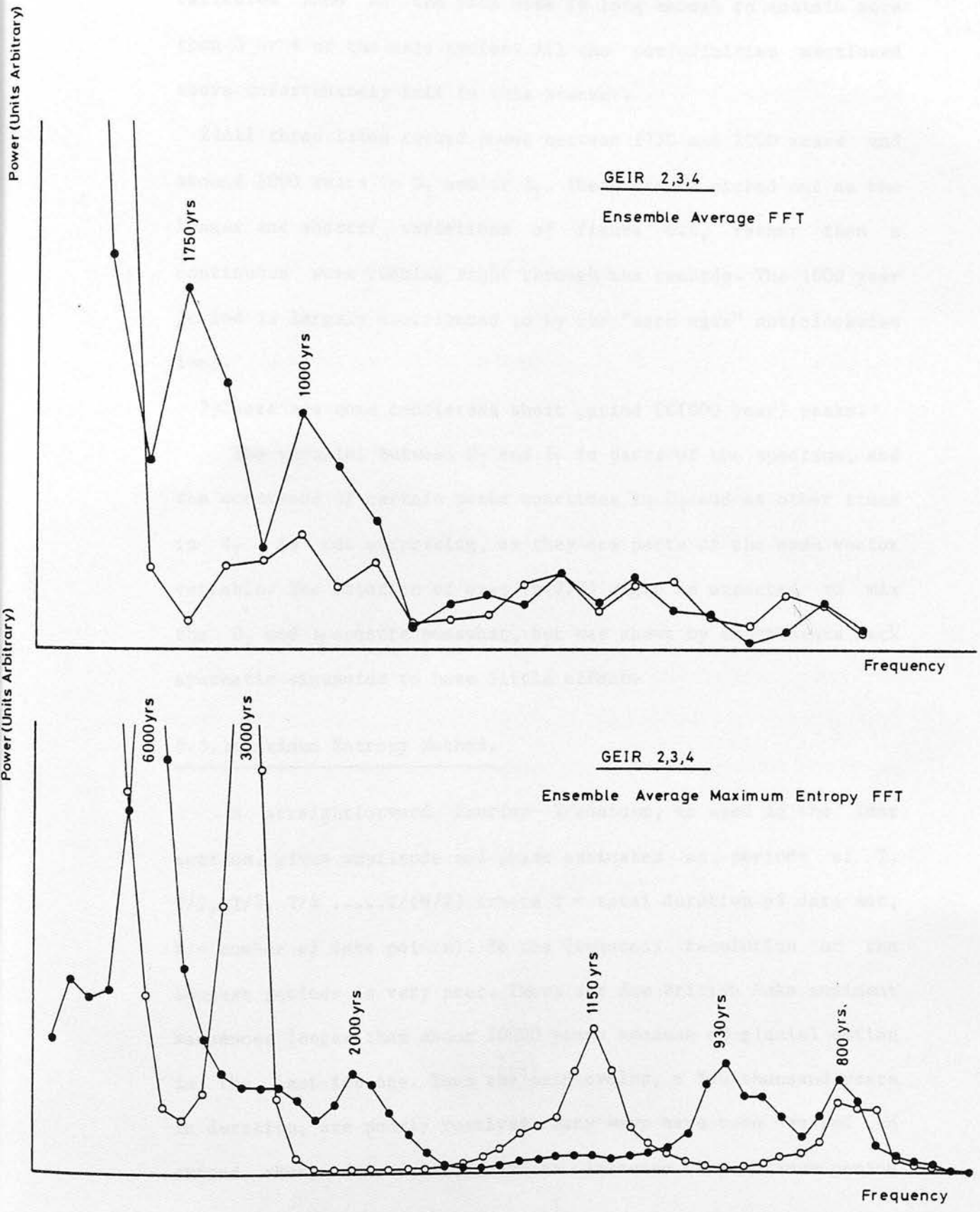

pretransform treatment. For this reason, and the lack of resolution at this end of the spectrum the long periods are not reliable. None of the data sets is long enough to contain more than 3 or 4 of the main cycles. All the periodicities mentioned above unfortunately fall in this bracket.

2)All three lakes record power between 1750 and 2000 years and around 1000 years in $D_T$ and/or $I_T$. These can be picked out as the longer and shorter variations of figure 6.4, rather than a continuous wave running right through the records. The 1000 year period is largely contributed to by the "dark ages" anticlockwise loop.

3)There are some consistent short period (<1000 year) peaks.

The parallel between $D_T$ and $I_T$ in parts of the spectrum, and the occurence of certain peaks sometimes in $D_T$ and at other times in $I_T$ is not surprising, as they are parts of the same vector variable. The rotation of axes (6.2.3) might be expected to mix the $D_T$ and $I_T$ spectra somewhat, but was shown by experiments with synthetic sinusoids to have little effect.

6.5.1:Maximum Entropy Method.

A straightforward Fourier Transform, as used in the last section, gives amplitude and phase estimates at periods of T, T/2, T/3, T/4 .....T/(N/2) (where T = total duration of data set, N = number of data points). So the frequency resolution at the longest periods is very poor. There are few British lake sediment sequences longer than about 10000 years because of glacial action in the last ice age. Thus the main cycles, a few thousand years in duration, are poorly resolved. Many ways have been devised to extend short data sets, and so increase the maximum period

estimated and give better resolution around the length of the original data set. The simplest of these is merely to add zeros, but this just causes interpolation between the spectral components previously estimated: since no new information is added, nothing extra is obtained. The most popular data adaptive method in current use is Burg's Maximum Entropy method (Burg, 1967 ). This uses the minimum amount of information (hence "Maximum Entropy") from the existing data to predict its behaviour beforehand and afterwards. The data set is normally increased to 5 times its original length: 2 times forwards and 2 times backwards. So now the periods at which spectral estimates are obtained become 5T, 5T/2, 5T/3, 5T/4 ..... 5T/(5N/2) i.e. there are many more estimates around the fundamental T. It is still dubious however, whether one should regard spectral peaks at such periods as indicative of a significant periodicity.

There is a variable parameter- the "prediction filter length" (PFL), which must be chosen and set before using the maximum entropy method. The PFL is essentially the amount of information from the original data used to compute each forward and backward prediction. Numerous ways have been suggested to obtain the optimum value of the PFL. Ulrych and Bishop (1975) develop another parameter - the "final prediction error", calculated during the maximum entropy extension, which should be minimised for an optimum PFL. However, this method has two drawbacks: it is tedious and time consuming, and it often predicts PFLs of one or two data points, which is meaningless, and in such cases one must resort to the second minimum (M.E. Evans, pers. comm.). A much simpler, purely empirical method, which can be calculated beforehand on a pocket calculator, has

recently been suggested by Berryman (1978). He lays down a number of conditions which should be satisfied by the PFL, and consequently suggests the formula $M = 2N/\ln(2N)$ (M= PFL, N= original number of data points). This function, though not uniquely satisfying the conditions layed out, is at least as reliable as other methods, and has the advantage of simplicity.

### 6.5.2:Maximum Entropy results.

The lower spectra of figures 6.8, 6.9 and 6.10 show the ensemble averaged maximum entropy spectra for the three lakes. In all three cases the relation between the upper and lower diagrams is obvious, although there is apparently much better resolution in the maximum entropy spectra. Despite this, the agreement between lakes at long periods is not as good as it is below 2000 years. The difference in the original length of the Windermere record may cause the extra long period declination peaks at 4000 and 5000 years, since there are more estimates in this region of the spectrum, but they should not be distinguished from the 6000 year peaks in Lomond and Geirionydd.

In summary, the main consistent peaks are around 1000 years, 1750- 2000 years and a long period variation, probably 5000-6000 years. These peaks occur in both $D_T$ and $I_T$ and are present in FFT and maximum entropy spectra from all three lakes. They probably do not represent continuous periodic variations running right through the 10000 year record, but single features of these time durations.

## 6.6:Spectral analysis as a complex pair.

In 1975 Denham suggested a way of obtaining a combined

spectrum of declination and inclination, and using it to gain information about the looping of the geomagnetic vector at any particular frequency.

The sequence of unit vectors along the record is projected onto a plane tangential to the unit sphere at the pole of the core mean direction. In the case of small amplitude swings this is, to a first approximation, equivalent to the Bauer plots of section 6.3.2.This projection plane is then treated as the complex plane, and a series of complex numbers input to FFT, the real and imaginary parts being approximately transformed declination and inclination respectively. When complex numbers are put into an FFT, the positive and negative frequencies in the transform assume separate significance. The balance of power between the positive and negative parts of the spectrum at a given frequency can be used to determine the sense and ellipticity of the looping of the vector at that frequency. For example, a circular, anticlockwise looping with frequency w is represented by:

$\cos(wt) + i \sin(wt) = e^{iwt}$ ; this would be caused by declination and inclination both oscillating with a frequency w, inclination leading declination by $\pi/2$. This produces a single, positive line spectrum +w. So a wholly positive spectrum implies anticlockwise looping, and conversely a negative spectrum results from clockwise, circular looping, as

$$e^{-iwt} = \cos(wt) - i \sin(wt)$$

A balanced spectrum with equal positive and negative parts is produced by linear motion. In general the ellipticity of the looping can be estimated from the ratio of positive to negative power at a frequency.

As our time series go backwards in time, the first term of

the input data being the most recent,(for data handling convenience), a positive spectrum implies clockwise motion and a negative spectrum implies anticlockwise motion of the geomagnetic vector with time. The complex pair method has the advantage of computing one spectrum for the two components, $D_T$, $I_T$, treating them as related parts of the same variable. It is also more economical in computing time and was therefore tried on some of the Lomond data.

6.6.1:Results.

The pretransform data conditioning subroutines discussed in section 6.4.3 were modified to take complex data. Maximum entropy extension was then used, as in Denham's original treatment. The spectrum for core LLRD1 between 7000 and 0 BP is shown in the lower diagram of figure 6.11. Since the plot is of power density, the power at a particular frequency is the area under the peak.

The two major peaks at 5000 and 1800 years obviously contain more positive than negative power, and represent the main clockwise looping observed in the Bauer plots. It is interesting to see the predominantly negative 1000 year peak, which is mainly contributed to by the dark ages anticlockwise loop. At shorter periods positive and negative sides of the spectrum are approximately evenly balanced, this represents the small scale loops which complicate the Bauer plots.

Since certain peaks in the above whole core spectrum were thought to derive from specific features rather than cycles throughout the record, it was decided to split the record into two sections and analyse them separately. The spectra for the sections from 3500- 0 BP and 7000-3500 BP are shown in the upper

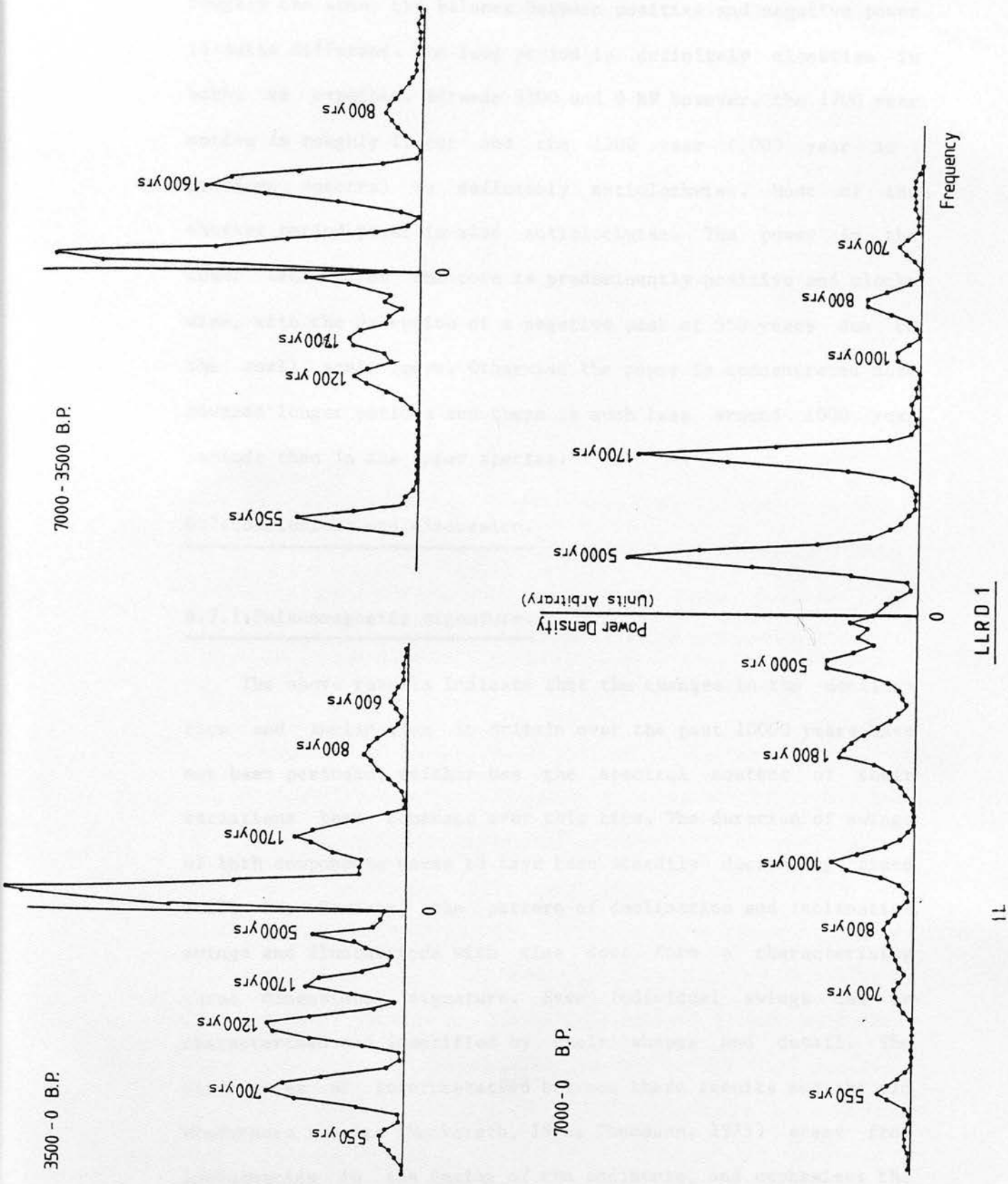


Figure 6.11 : Complex number representation maximum entropy Fourier transforms for LLRD 1.

half of figure 6.11.

Although the periodicities found in the two sections are roughly the same, the balance between positive and negative power is quite different. The long period is definitely clockwise in both, as expected. Between 3500 and 0 BP however, the 1700 year motion is roughly linear and the 1200 year (1000 year in previous spectra) is definitely anticlockwise. Most of the shorter period power is also anticlockwise. The power in the lower section of the core is predominantly positive and clockwise, with the exception of a negative peak at 550 years due to the small scale loops. Otherwise the power is concentrated more towards longer periods and there is much less around 1000 year periods than in the upper spectra.

## 6.7:Conclusions and discussion.

### 6.7.1:Palaeomagnetic signature.

The above results indicate that the changes in the declination and inclination in Britain over the past 10000 years have not been periodic, neither has the spectral content of their variations been constant over this time. The duration of swings of both components seems to have been steadily decreasing since 10000 BP. However, the pattern of declination and inclination swings and fluctuations with time does form a characterising three dimensional signature. Even individual swings can be characterised and identified by their shapes and detail. The differences of interpretation between these results and the old Windermere results (Mackereth, 1971; Thompson, 1975) stems from inadequacies in the dating of the sediments, and emphasises the

necessity of accurate, well supported age estimates. Duplicate C-14 dates are desirable on any horizon or feature, from different cores, and preferably different lakes, and whenever possible a second form of dating e.g. pollen zones, varve counting, volcanic ash bands etc., should confirm the C-14 estimates. The dating presented here is certainly more rigorous than the old Windermere dates as 1) sediments from three lakes have been dated independently in two different laboratories; and 2)on the two cores where complete suites of data have been taken, the samples are more closely spaced. It is unlikely that further dating will greatly refine the outline time scale laid down here, although when C-14 methods become available on much smaller quantities of material (Gribbin, 1979), it will be interesting to date the finer features. By comparison with the curves of figure 6.3 it should be possible to date post-Glacial sediment sequences to within 5-10%, if they carry a measurable remanence.

6.7.2:Comparison with other lacustrine and archaeomagnetic records.

Comparison of these results with other European limnic records is impeded by the lack of reliable dating control on the latter. Even so, sediment cores from Finland (Stober and Thompson, 1977), dated by pollen zone assemblages and radiocarbon, Lake Zurich(Thompson and Kelts, 1974) dated by varve sequences and pollen zones, and France and Greece (Creer et al., 1977) all carry the same basic pattern of fluctuations of 2000 - 4000 years duration. However it is impossible to say whether the finer detail is comparable, due to the variability of the recording properties of the different sediments or to small differences in the times of

the turning points of the declination and inclination swings. One can however say that the same sources have dominated the secular variation patterns over this area for the past 10000 years.

A detailed archaeomagnetic record has been produced for S.E. Europe for the period 6500 - 100 B.C. (8450-2050 BP) by Kovacheva and Veljovich (1977). (The palaeointensity curve was mentioned in chapter 4.) The similarity of the declination record is quite striking - a broad e, sharp f and multiple g. The 500 year age discrepancy found in the intensity, occurs again. The inclination curves are less similar: swings corresponding to $\delta-\varepsilon-\zeta$ are more compressed in the recent part of the record, while rather more significant swings are apparent in the older samples. The record is similar enough to the British to be predominantly affected by the same source, although another influence seems to be affecting the inclination of one or the other.

A second archaeomagnetic record, obtained by Rusakov and Zagniy (1973) for the Ukraine, extends only from 3000 - 0 BP and is detailed only between 2000 and 500 BP. However over this range a tentative correlation can also be drawn for declination swings d-e, and inclination $\beta-\gamma-\delta$.

The Japanese record of Hirooka (1971), from 1700 - 0 BP, is however quite different.The swings have different signatures, and no phase lag common to both declination and inclination (which might indicate westward drifting features) is readily apparent.

The North American lacustrine records (Lake Michigan: Creer et al., 1976a; Lake Erie: Creer et al., 1976b) do not obviously correlate with the British record either, although it is difficult to be conclusive because of inadequate dating control which is independent of the geomagnetic field.

6.7.3:Sources of the secular variation.

Creer (1977) compared secular variation records from Britain, the Black Sea, Lebanon and the North American Great Lakes, and from their differences deduced 1) that different sources dominate the non - dipole field at different sites; 2)these sources remain stationary and oscillate or pulsate in magnitude, rather than drifting westwards as originally suggested by Bullard et al. (1950). The time scales used in drawing these comparisons are however drawn up by assuming the declination and inclination variations at each site to be periodic, and deducing "periodicities" for them. Although this is a speculative approach, as mentioned in the last section, the North American and British records differ sufficiently in the number, direction and detail of declination and inclination swings to conclude that they are dominated by different non-dipole sources.

So whereas Europe and Scandinavia, as far east as Czechoslovakia and probably the Ukraine, are currently dominated by the same non-dipole sources, and have been for the past several thousand years, sites as distant as Japan and the U.S.A. appear to have different sources. (Preliminary results on cores from Iceland collected in summer 1979 also show remarkably similar features to the British records, suggesting the change in dominance occurs at a longitude west of Iceland.)

This suggestion of different sources dominating the field at different sites is quite contrary to the suggestions of Kawai et al. (1965) and Kawai and Hirooka (1967), that the secular variation is chiefly due to a wobbling of the main dipole field axis as it precesses anticlockwise around the Earth's rotation

axis. This was based on a comparison of the then existing British and Japanese archaeomagnetic records, and results from recent Icelandic lavas. Loops of short duration occur at 800, 1000, 1300 and 1800 A.D. in all or some of these records, superimposed on an overall anticlockwise looping over the 2000 year period. The British lake record, which now fills in the "dark ages" of the British archaeomagnetic record, no longer supports this model, as the only anticlockwise motion is between 1500 and 600 BP. Neither is there any indication of anticlockwise motion further back in time to support the continued existence of such a model.

Runcorn (1959) and Skiles (1970) have developed a method for inferring the direction of drift of non-dipole features of the field beneath or close to a site, from the sense in which the magnetic vector at the site rotates with time. If the vector rotates clockwise when viewed along it towards its north seeking end, the sources are inferred to drift westwards, if the rotation is anticlockwise the drift is eastwards. This is supported by the fact that most of the world's observatories are currently recording clockwise rotation and westward drift. However, the picture is not totally consistent, as four of the eight dipoles of the Alldredge-Hurwitz model moved eastwards between the best fits to the fields of 1945 and 1955.

The Bauer plots of figures 6.4, 6.5 and 6.6 show clockwise rotation for nearly the whole of the period from 10000 - 0 BP, with the exception of the anticlockwise loop from 1500 - 600 BP and a roughly linear section between 7500 and 6000 BP. This would then suggest a field drifting predominantly westwards with time over Britain, in keeping with the present day world wide

dominance of westward drift, but with a 900 year period when either 1) a different source, drifting eastward, became dominant, or 2) the dominant source reversed its direction of drift. Either form of eastward drift is difficult to incorporate into the dynamo-eddy model of the origin of the non-dipole field. This difficulty led Dodson (1979) to seek a mechanism whereby anticlockwise rotation of the vector could be produced by westward drifting sources. He showed that, if the perturbing sources are near the core/mantle boundary, they can result in certain combinations of spherical harmonic components, and certain orientations of the secular variation field with respect to the steady field, which will produce anticlockwise motion of the vector while still drifting westwards. If this mechanism alone is the cause of anticlockwise vector motion then it follows:

1) that clockwise motion would be much more common than anticlockwise. This appears to be so from the records available.

2)Anticlockwise motion would be observed much less often at high latitudes than close to the equator. This is difficult to test as insufficient data is available at high latitudes.

3)Anticlockwise motion would be accompanied by a decrease in the field intensity, whereas either an increase or decrease could accompany clockwise motion. This appears to be the case in Mono Lake (Denham, 1974), but intensity measurements on sediments are not accurate enough to be conclusive.

So, although it has been customary to associate anticlockwise looping with eastward drift of features of the non-dipole field, it is quite possible that both anticlockwise and clockwise motions are caused by a westward drifting field, which could originate from the differential rotation of the core and mantle.

In summary:

1)We need a geomagnetic field model of a number of localized sources, with different sources dominating the field at different locations.

2)The sources should be at or near the core/mantle boundary.

3)Although most models have used dipoles, the sources need not be so localized, but may be broader current loops.

4)Over the time period covered by observatory records there has been a definite westward drift of the non-dipole field. We do not need to introduce eastward drift to explain the short periods of anticlockwise motion recorded. If the sources are drifting westwards, they must also be changing in form e.g. growing and decaying, oscillating in magnitude, on a scale of hundreds or at most thousands of years, as we do not observe a time lag between secular variation patterns of sites at the same latitude and different longitude.

# CHAPTER 7:MR WILLIAM'S FIELD : A STUDY OF THE GROWTH AND MOVEMENT OF MAGNETIC MINERALS IN A DRAINAGE BASIN.

## 7.1:Introducion.

This subsidiary project was undertaken with two aims: firstly to assess different methods of surveying the magnetic properties of soils on location, and secondly, to identify and trace the passage of magnetic material into a lake from different parts of its drainage basin. The second aim leads to the examination of the magnetic minerals responsible for, and the mode of aquisition of the magnetic remanence in an unconsolidated lake sediment. The fieldwork techniques and results are discussed first, followed by laboratory experiments and analyses which include magnetic susceptibility, saturated IRM, coercivity of remanence, Curie point measurements and Mössbauer spectra.

## 7.2:Study area.

The area chosen for this project is the drainage basin of Llyn Geirionydd (figure 7.1). The palaeomagnetic properties of the lake sediment have already been discussed in previous chapters.

The lake is in a narrow, steep sided valley, formed by the north-east movement of a cwm glacier, and partially contained by moraines. It has a surface area of 0.26 $km^2$ and a catchment area of nearly 4 $km^2$, mainly south and east of the lake (figure 7.1). The local bedrock consists mainly of slates, shales and mudstones, interbedded with some volcanic ashes and lavas. The land

Figure 7.1 : Llyn Geirionydd : Land use, sampling and field work sites.

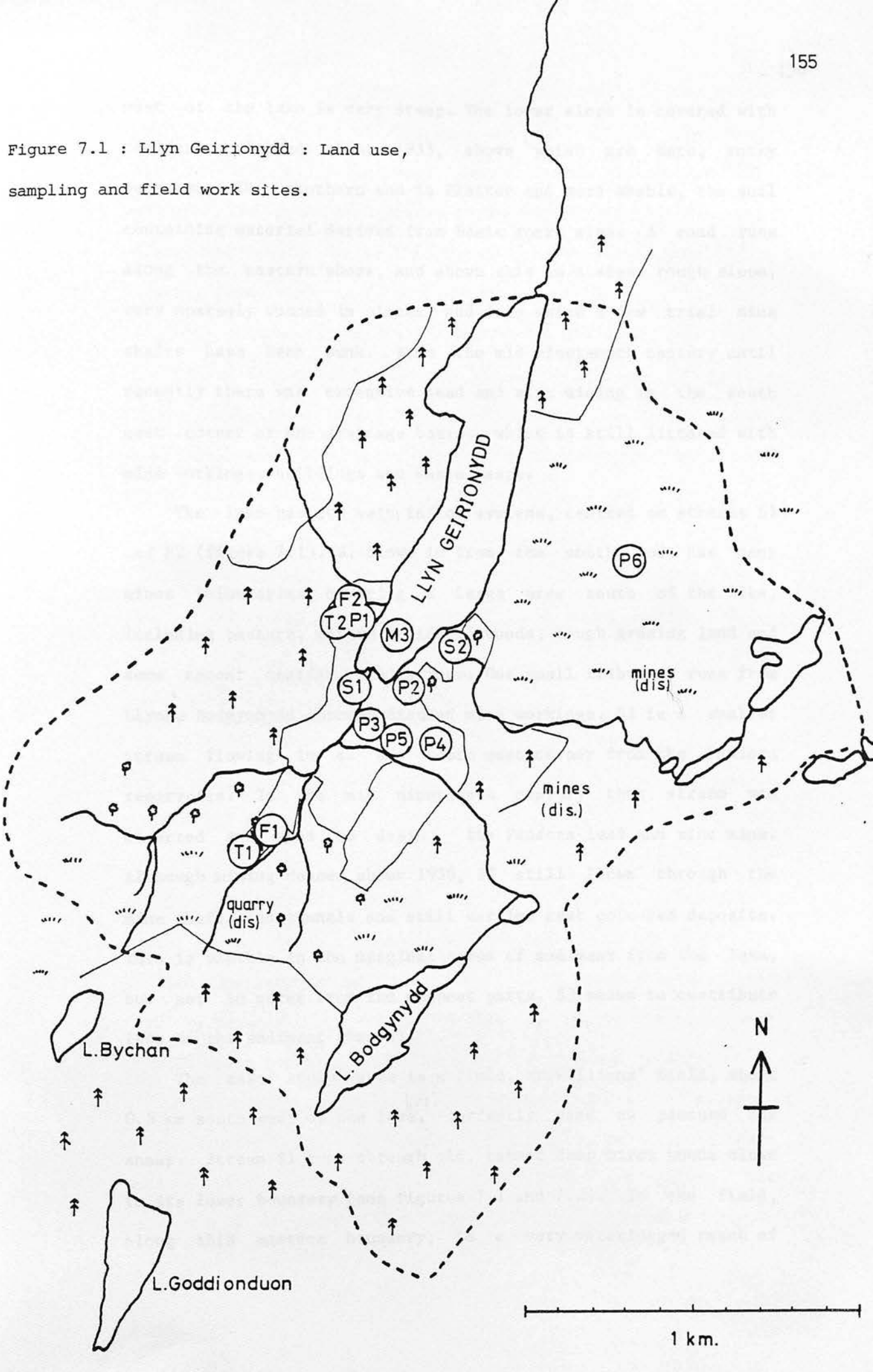

west of the lake is very steep. The lower slope is covered with conifers, planted about 1935, above which are bare, rocky outcrops. The southern end is flatter and more arable, the soil containing material derived from basic rocks also. A road runs along the eastern shore, and above this is a steep rough slope, very sparsely wooded in places, and into which a few trial mine shafts have been sunk. From the mid nineteenth century until recently there was extensive lead and zinc mining in the south east corner of the drainage basin, which is still littered with mine workings, buildings and waste heaps.

The lake has two main inflow systems, centred on streams S1 and S2 (figure 7.1). S1 flows in from the south and has many minor tributaries covering a large area south of the lake, including pasture, mature deciduous woods, rough grazing land and some recent conifer plantations. One small tributary runs from Llynau Bodgynnydd through disused mine workings. S2 is a smaller stream flowing in at the south east corner from the Pandora reservoirs. In the mid nineteenth century this stream was diverted and used to drain the Pandora lead and zinc mine. Although mining ceased about 1930, S2 still flows through the mine shafts and tunnels and still carries rust coloured deposits. This is visible in the marginal cores of sediment from the lake, but not in cores from the deepest parts. S2 seems to contribute less to the sediment than S1.

The main study area is a field, Mr.Williams' field, about 0.5 km south west of the lake, currently used as pasture for sheep. Stream S1 runs through old, rather damp birch woods close to its lower boundary (see figures 7.1 and 7.2). In the field, along this eastern boundary, is a very waterlogged patch of

heavy, grayish, well gleyed soil, colonized by rushes of the Juncus family, typical of this type of environment. The field dries out as it rises westwards towards mature, dry oak and beech woods. A level track cuts across this gradient and is now used only by the farmer, but at the beginning of the century it led to a nearby slate quarry and was heavily used.

This particular field was chosen for the main study, since it contains many of the features which, according to current theory,should show large magnetic contrasts, due to the growth, enhancement and breakdown of magnetic minerals in the soil, and their passage through the soil to the streams and eventually to the lake.

The sites of other fieldwork, and the collection of soil samples are listed briefly in table 7.1 and shown on figure 7.1.

### 7.3.1:Soil magnetism.

The following paragraphs give a simplified idea of current theories of magnetic minerals in soils. For a more extensive account see Mullins (1977).

Most British soils can be classified as podsols or brown earths. In podsols, forming on porous bedrock, deficient in bases, the ferrimagnetic oxides are leached out of the upper 'A' horizon and redeposited in the lower 'B' layer in a paramagnetic form. In brown earths, where the pH is nearer neutral, the soluble bases are washed out but the iron compounds remain.

Both podsols and brown earths are susceptible to gleying, under anaerobic, poorly drained conditions. The iron is taken into solution in the reduced form, due to lack of oxygen, but does not drain away. This gives the gley its characteristic

Table 7.1 Fieldwork & Sample collection sites.

| Site | Description | Fieldwork Details |
|---|---|---|
| F1, T1 | see text | PIM grid, PIM & PPM traverses |
| F2, T2, P1 | rough pasture, steep slope to lake, water-logged at foot of slope | PIM traverses. T2 N,S,C<br>soil profile P1 |
| P2 | exposed podsol | A & B layers sampled |
| P3, P4 | pasture, sloping | P3 topsoil at foot of slope<br>P4 topsoil at top of slope |
| P5 | mature oak woods<br>rich brown earth | v. high PIM readings<br>topsoil sample |
| P6 | remnants of old hawthorn woods on rough slope, soil beginning to form podsol | complete soil profile taken. |

green-gray tinge. On subsequent exposure to the air the iron is reprecipitated in a non- magnetic, rust coloured ferric form; the orange specks frequently seen in a gley. So gleying removes the ferrimagnetic component of the topsoil, converting it to a weakly paramagnetic form.

In 1955 Le Borgne reported extremely low magnetic susceptibility values in a gleyed soil at the foot of a steep slope, even though a priori one might expect solifluction to concentrate the heavy minerals there.

The ferrimagnetic oxides are to be found then, mainly in the top layers of brown earths. It is frequently found that the susceptibility of this topsoil is significantly higher than that of the parent sedimentary rock: hence some form of "magnetic enhancement" has occurred.

### 7.3.2:Magnetic minerals.

Table 7.2 summarizes the magnetic properties of some iron oxides and hydroxides commonly encountered in soils.

Weakly ferromagnetic and paramagnetic iron oxides and hydroxides such as haematite ($\alpha$-$Fe_2O_3$) and goethite ($\alpha$-FeO.OH) are common end products in the weathering of sedimentary rocks. During enhancement these become converted to the more strongly ferrimagnetic magnetite ($Fe_3O_4$) or maghaemite ($\gamma$-$Fe_2O_3$). Although chemically identical to the weakly magnetic haematite, and inverting to it above 350°C, maghaemite has an incomplete spinel type structure, with iron ions on two opposing sub-lattices, leading to a strong ferrimagnetic moment. Magnetite is formed by reduction of haematite, and also has a spinel structure with tetrahedrally and octahedrally co-ordinated iron ions on A and B

Table 7.2 Common magnetic minerals found in soils

| Mineral | Crystal structure | Magnetic state | Spontaneous magnetisation at R.T. ($m\ A.m^{-1}$) | Specific susceptibility (S.I.) |
|---|---|---|---|---|
| Magnetite $Fe_3O_4$ | inverse spinel ions on A+B sublattices oppositely aligned | ferrimagnetic | $4.7 \times 10^5$ | $5 \times 10^4$ |
| Maghaemite $\gamma - Fe_2O_3$ | incomplete inverse spinel | ferrimagnetic | $4.2 \times 10^5$ | $5 \times 10^4$ |
| Haematite $\alpha - Fe_2O_3$ | corundum | antiferromagnetic with weak, ferromagnetism due to canted spins | $5 \times 10^2$ | 27 |
| Goethite $\gamma$-FeO.OH | | antiferromagnetic with weak parasitic ferromagnetism | | |

lattices, and a high magnetic moment. Both magnetite and maghaemite, and a range of minerals of intermediate composition may be formed during enhancement. However, the degree of oxidation and the presence of substitutional impurities make unambiguous identification difficult.

### 7.3.3:Enhancement mechanisms.

Le Borgne(1955) has proposed two mechanisms for the magnetic enhancement of topsoil: the "heating" and the "fermentation" mechanisms. Both involve initial reduction of haematite and other weakly magnetic oxides and hydroxides to magnetite, followed by possible re-oxidation to maghaemite. (The second stage of reoxidation is not necessary for a high susceptibility, and is doubted in some cases (e.g. Longworth et al., 1979).)

The heating mechanism relies on the occurrence of forest and/or domestic fires in the area e.g. deforestation of the land for agricultural use. The burning organic compounds in the top layers cause temperature elevation in a reducing atmosphere (carbon monoxide). This reduces haematite and other oxides and hydroxides to magnetite. This may be followed by a variable amount of re-oxidation, maintaining the spinel structure and enhanced susceptibility of the minerals, as the fire cools slowly and air re-enters the system.

The fermentation mechanism makes use of the decay of organic matter in wet periods, causing anaerobic conditions, which reduce the oxides to magnetite. This would be followed in subsequent dry periods by re-oxidation towards maghaemite. Oscillations in the condition of the topsoil would then cause buildup of the ferrimagnetic mineral. For the fermentation mechanism to function

successfully the period of such oscillations must be short enough to prevent gleying, but the drainage must not be so rapid that a podsol is formed. Annual, Mediterranean-type oscillations are suggested by Tite and Linington ( 1975 ) to be ideal for the fermentation mechanism.

## 7.4:Instruments.

Two instruments were used while on fieldwork: a proton precession magnetometer (P.P.M.) and a pulse induction meter (P.I.M.). The two instruments are designed for quite different purposes, and operate in very different ways.

### 7.4.1:The Proton Precession Magnetometer.

The P.P.M. records the intensity of the ambient magnetic field at a point, by measuring the frequency of the Larmor precession of the magnetic moments of protons as they relax about the magnetic field direction after an aligning pulse. The ambient magnetic field has two components of importance: the primary, geomagnetic field, and the field caused by the induced or remanent magnetization in the bedrock, soil, or local metal objects. The first is assumed constant over the small area studied, differences in the second are recorded. If one assumes induced features to be of dipolar form, then the sensitivity of the instrument would drop away with the inverse cube of the distance from it. Small scale inhomogeneities would be picked up with the instrument held close to the ground. Holding it at a greater height would produce a smoothing over such irregularities, and a deeper sounding.

## 7.4.2:The Pulse Induction Meter.

The P.I.M. was originally built as a metal detector, but Colani and Aitken (1966), during archaeological work, have shown that, in the absence of metal objects it also responds to soil magnetism. It is an active device, a single, flat coil, 12" in diameter, acting as both transmitter and receiver. Figure 7.2 illustrates the operation. A series of 350 $\mu$ second strong, unipolar pulses are transmitted, at a rate of about 11 per second (a). The rising and trailing edges of each of these pulses induce magnetization in the surroundings, which decays with time (b). We are concerned only with the induction caused by the trailing edge. The rate of decay, or "viscosity" of this magnetization is controlled mainly by the nature and size and shape distributions of the magnetic grains in the soil; its magnitude is dependent also on the amount of magnetic mineral affected. The secondary e.m.f. (V) induced back in the coils has two components: one proportional to $dH_1/dt$, from direct coupling with the primary, and the second, proportional to $dH_2/dt$, from the field produced by this decaying viscous magnetization (c). This signal is monitored after allowing sufficient time for the direct coupling to die away. Monitoring is achieved in two sampling pulses (d); the difference in signal between the two being taken (e), to minimize the noise, particularly 50 Hz and its harmonics. The output is averaged over several cycles, and read from a meter. Since its operation involves both transmission and reception, the sensitivity of the P.I.M. is shorter ranged than for the P.P.M. - falling away as $1/d^6$ . In practice it was found necessary to hold the coils parallel and pressed close to the ground to obtain repeatable measurements. This was difficult in long grass and

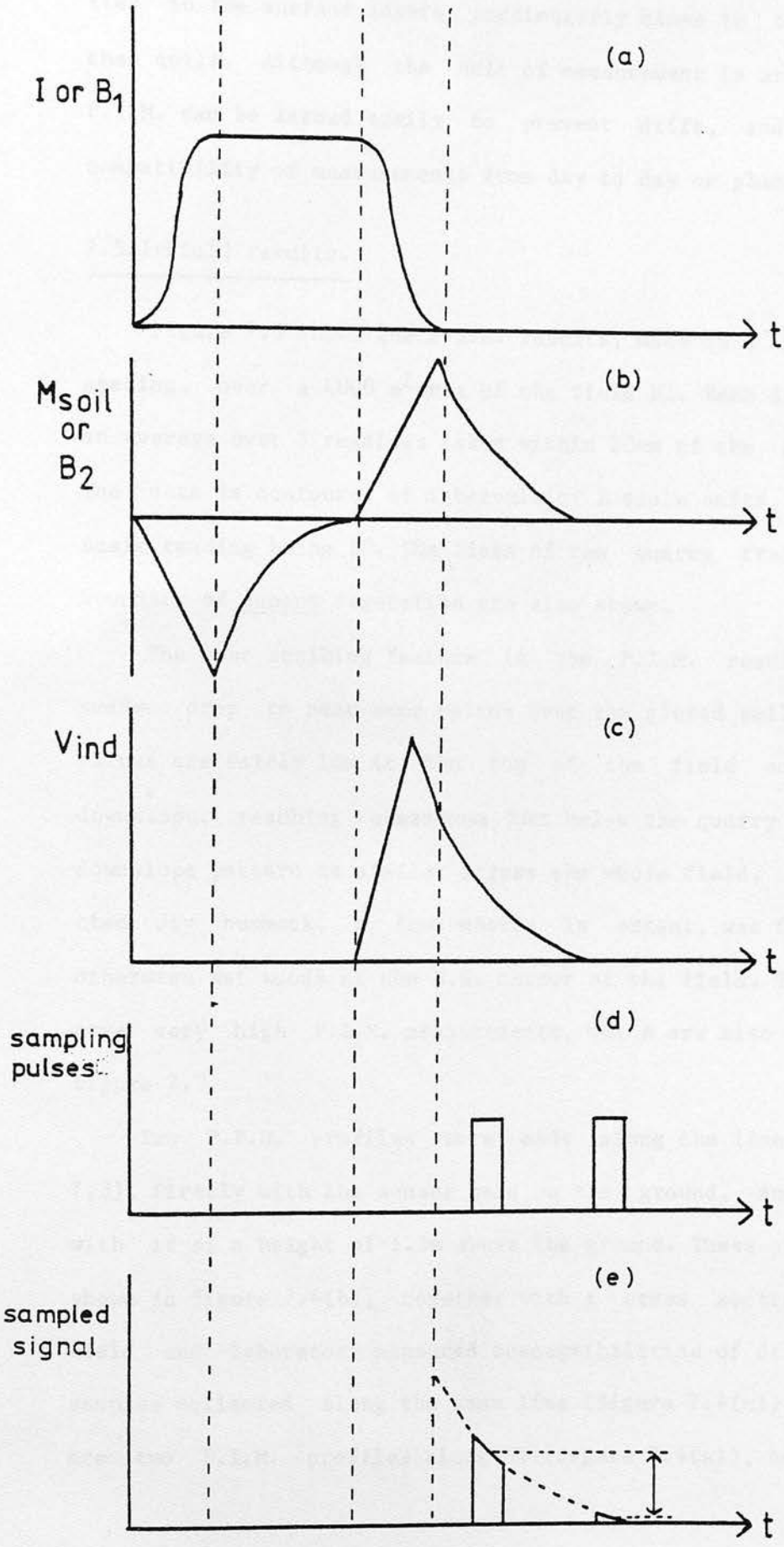


Figure 7.2 : Pulse Induction Meter (P.I.M.) operation.

rushes. The P.I.M. is very sensitive to small scale inhomogeneities in the surface layers, particularly close to the edge of the coils. Although the unit of measurement is arbitrary, the P.I.M. can be zeroed easily to prevent drift, and to ensure compatibility of measurements from day to day or place to place.

### 7.5.1:Field results.

Figure 7.3 shows the P.I.M. results, made on a grid of 5m spacing, over a 4000 $m^2$ area of the field F1. Each data point is an average over 3 readings taken within 20cm of the grid point. The data is contoured at intervals of 2 scale units, the maximum scale reading being 10. The lines of the quarry track and the boundary of Juncus vegetation are also shown.

The most striking feature in the P.I.M. results is the sudden drop to near zero values over the gleyed soil. Otherwise values are fairly low at the top of the field and increase downslope, reaching a maximum just below the quarry track. This downslope pattern is similar across the whole field. An unexpected dry hummock, a few metres in extent, was found in the otherwise wet woods at the N.E. corner of the field. This hummock gave very high P.I.M. measurements, which are also included in figure 7.3.

Two P.P.M. profiles were made along the line XY (figure 7.3), firstly with the sensor held on the ground, and secondly with it at a height of 1.5m above the ground. These profiles are shown in figure 7.4(b), together with a cross section of the field and laboratory measured susceptibilities of dried topsoil samples collected along the same line (figure 7.4(c)).Also shown are two P.I.M. profiles along XY (figure 7.4(a)), one with the

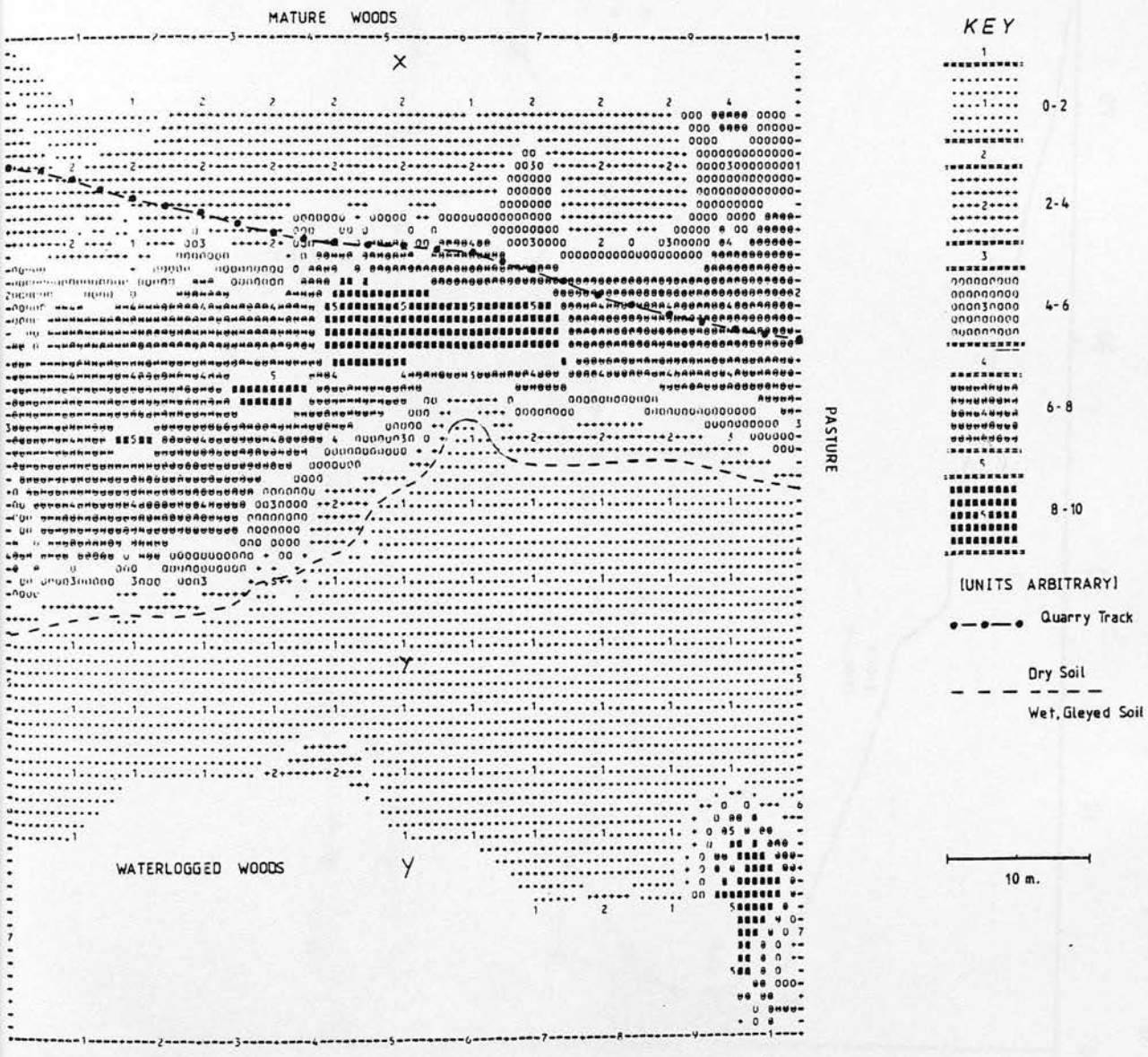


Figure 7.3 : P.I.M. results ; grid covering field F1.

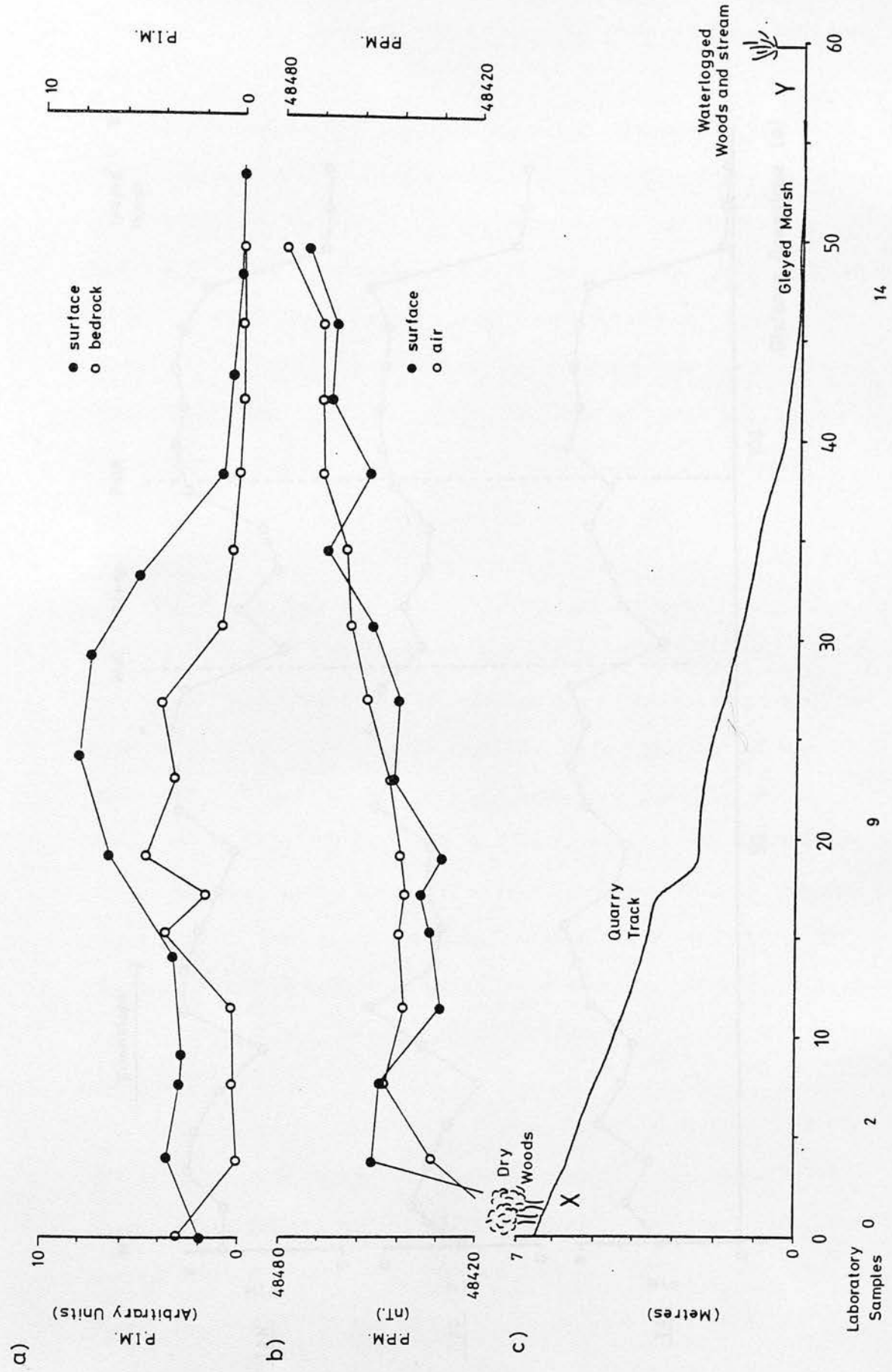


Figure 7.4 : P.I.M. and P.P.M. results and cross section of traverse T1.

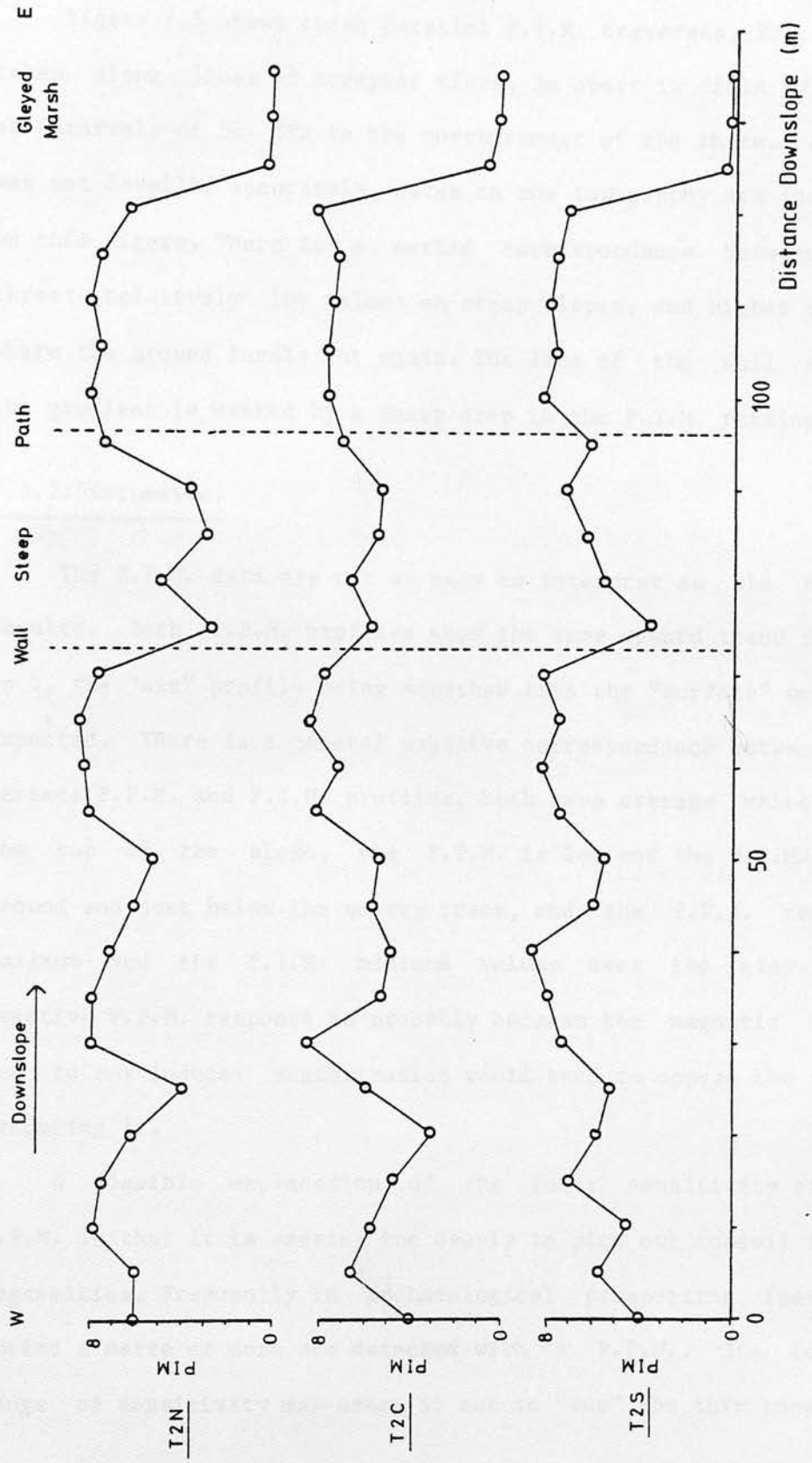


Figure 7.5 : P.I.M. traverses in field F2 : T2 N,C,S.

coils on the surface, the other with them at the bottom of a hole, dug to the bedrock, to test the contribution of the topsoil.

Figure 7.5 shows three parallel P.I.M. traverses, T2N, C, S, taken along lines of steepest slope, 5m apart in field F2, made at intervals of 5m. T2N is the northernmost of the three. As F2 was not levelled accurately, notes on the topography are included on this figure. There is a marked correspondence between the three: relatively low values on steep slopes, and higher values where the ground levels out again. The line of the wall across the gradient is marked by a sharp drop in the P.I.M. readings.

### 7.5.2:Discussion.

The P.P.M. data are not as easy to interpret as the P.I.M. results. Both P.P.M. profiles show the same upward trend from X to Y, the "air" profile being smoother than the "surface" one, as expected. There is a general negative correspondence between the surface P.P.M. and P.I.M. profiles, both have average values at the top of the slope, the P.P.M. is low and the P.I.M. high around and just below the quarry track, and the P.P.M. reaches maximum and the P.I.M. minimum values over the gley. This negative P.P.M. response is probably because the magnetic field due to any induced magnetization would tend to oppose the field producing it.

A possible explanation of the lower sensitivity of the P.P.M. is that it is sensing too deeply to pick out topsoil inhomogeneities. Frequently in archaeological prospecting features buried a metre or more are detected with a P.P.M.. Its longer range of sensitivity may cause it not to "see" the thin topsoil,

but deeper horizons - the more uniform drift and bedrock. The P.I.M.'s response at such depths is negligible.

7.5.3: Inferences from the P.I.M. results.

1)Comparison of the two P.I.M. profiles along T1 shows the topsoil to be "enhanced" magnetically with respect to the drift and bedrock. In other parts of the drainage basin also, readings were low on bedrock, and maximum values were consistently obtained in mature woods with rich brown earths. The drift in the area is mainly slates and shales, poor in magnetic minerals, the iron being present mainly as sulphides. However the lake sediment has a reasonably high susceptibility and carries a stable magnetic remanence. The minerals responsible for this could not have come unaltered from the bedrock, so must have been formed during the processes of weathering, soil development and carriage to the lake. The similaritiy in the magnetic properties of the soils and the lake sediment (section 7.6) suggests this enhancement to have taken place in the soil.

2) The P.I.M. results in F1 and F2 support Le Borgne's finding that the magnetic content is drastically lower in a gleyed soil. This support is reinforced by magnetic susceptibility measurements on dried soil samples; those from the gley were approximately 1/50 of typical values in the rest of the field (table 7.2).

3)The pattern of P.I.M. results on the slopes indicates that either a) downslope movement of the topsoil, enhanced in magnetic minerals, is producing thicker layers near the foot of the slope and so increasing the P.I.M. reading; or b) the degree of enhancement increases as the soil moves downslope, so the oldest, most magnetic soil is found at the foot. However, in F2

the maximum P.I.M. reading was recorded above the wall, which contoured across the slope, causing a noticeable accumulation of soil against it. This indicates that the depth of the enhanced topsoil does vary, and that such variations do at least contribute to the recorded differences in P.I.M. response.

### 7.5.4:Soil profiles.

The two soil profiles, P1 and P6, shown in figure 7.6 are representative of the two main soil types found around Geirionydd, which could provide magnetic minerals to the lake.

P1 (fig 7.6(a)),from site 25 on P.I.M. traverse T2C is typical of well used fields and mature woods, with a magnetically enhanced topsoil. The susceptibility peaks in the uppermost A horizon, in the this case about 25 cm deep, which merges into the less magnetic B horizon. The very weakly magnetic drift, mainly slates and shales, occurs at about 60 cm.

The second profile, P6 (figure 7.6(b)), is from near the top of the steep slope, east of the lake. This ground is now used as rough mountain pasture for sheep, but the sparse remnants of an old hawthorn wood still occur in protected areas. Much of the surrounding, more exposed ground, is wet and gleying. Leaching of the coarse, gray topsoil of P6 has obviously begun. The low susceptibility of the topsoil, with a higher value in the underlying, red B layer indicates that a podsol is forming here. Pockets of dark brown soil, possibly a buried humus layer from the time of the woods, were found at about 35 cm, within the B layer. The drift, mainly slates, again had a very low susceptibility.

A similar susceptibility pattern was seen in the podsol at

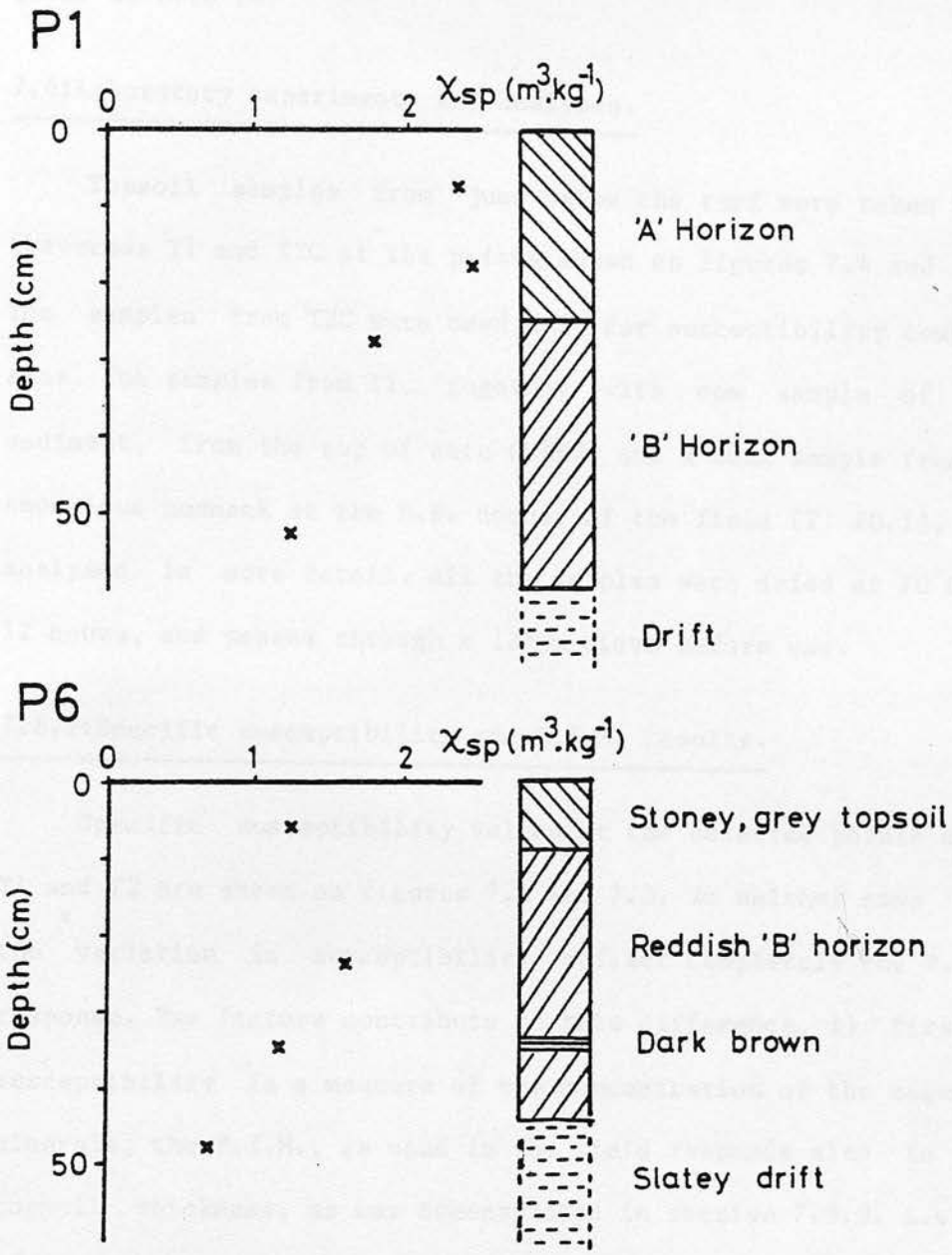


Figure 7.6 : Soil profiles P1 and P6.

site P2, although values in both A and B layers were lower than those at site P6.

## 7.6:Laboratory experiments and analyses.

Topsoil samples from just below the turf were taken along traverses T1 and T2C at the points shown on figures 7.4 and 7.5. The samples from T2C were used only for susceptibility comparisons. The samples from T1, together with one sample of lake sediment, from the top of core GEIR2, and a soil sample from the anomalous hummock at the N.E. corner of the field (T1 20.1), were analysed in more detail. All the samples were dried at 70°C for 12 hours, and passed through a 125μm sieve before use.

### 7.6.1:Specific susceptibility and P.I.M. results.

Specific susceptibility values at the selected points along T1 and T2 are shown on figures 7.4 and 7.5. In neither case does the variation in susceptibility reflect completely the P.I.M. response. Two factors contribute to this difference, 1) firstly, susceptibility is a measure of the concentration of the magnetic minerals; the P.I.M., as used in the field responds also to the topsoil thickness, as was demonstrated in section 7.5.3. i.e. to the quantity of magnetic mineral in its sensing volume. 2) As stated in section 7.4.2., the P.I.M. measures the decay rate of viscous magnetization. Therefore its largest contribution will be from those grains most easily magnetized, and least capable of retaining the magnetization. One might expect large, multidomain grains to give a large contribution, but there is insufficient energy to cause domain wall movement within them. The most important grains are those on the superparamagnetic/single domain

boundary. So the P.I.M. responds best to soils with grain size distributions peaking around this size ( 0.03 μm for spherical magnetite (Dunlop,1973), smaller for elongated grains). Superparamagnetic grains are grains of a ferrimagnetic mineral which are smaller than the critical blocking volume necessary to retain a stable magnetic moment. Although unable to contribute to a remanence their magnetic susceptibility is much higher than that of paramagnetic minerals, and also than that of bigger ferrimagnetic grains. Susceptibility, then, has contributions from both superparamagnetic and ferrimagnetic grains, but does not have the same degree of grain size selection as the P.I.M.. Unfortunately it is impossible to assess these differences, as the grain sizes of interest are so small. By simple sieving it is only possible to separate particles down to 32μm. Below this size other methods must be used, and it is very difficult to disperse the particles completely, overcoming electrostatic and surface tension forces.

### 7.6.2:Susceptibility and I.R.M.

Table 7.3 gives more detailed magnetic measurements on samples and magnetic concentrates from T1 and GEIR2. Again susceptibility and SIRM monitor different regions of a sample's grain size spectrum. Unlike susceptibility, SIRM is a remanence, and has no superparamagnetic contribution. So the ratio of SIRM to susceptibility gives an idea of the division between superparamagnetic and ferrimagnetic grains in a sample. Although there are large spreads in the susceptibility and SIRM values (0.03-5.0 x $10^{-6}$ $m^3.kg^{-1}$ and 140-40000 $Am^{-1}.kg^{-1}$ ), their ratio shows much less variation (5.2-12.5 x $10^9$ S.I.). This suggests similar fractions of ferrimagnetic and superparamagnetic grains in the

magnetic components of the samples, the variation between samples being chiefly in the overall concentration of magnetic mineral. This magnetic uniformity between the samples is also reflected in 1) the coercivity of back IRM values, $B_{CR}$, are similar for all samples except the gley (T1 14.1), and 2) the similar shapes of thermomagnetic curves obtained on magnetic concentrates from the soils. These thermomagnetic results are discussed further in the next section. The plots are essentially of the spectra of the unblocking temperatures of the magnetic particles. A marked variation in the spectrum of grains from sample to sample, would be reflected in the unblocking temperature spectrum.

### 7.6.3: Thermomagnetic curves.

Plots of saturation magnetization against temperature were made on magnetic extracts (more precisely concentrates), from a number of samples from T1 and lake sediment to obtain the Curie points of the principal magnetic minerals. The concentrates were obtained by pumping a dilute suspension of the soil through a 5mm diameter glass tube, between the poles of a 5kOe permanent magnet, at about $0.5 cm^3.s^{-1}$ . The magnetic sample adhering to the tube was collected and washed frequently, while the remainder was returned to the reservoir and recycled. Magnetic concentrates were used rather than bulk samples 1) to increase the amount of magnetic material in the tiny sample used (30mgm), 2) to remove other components of the soil, e.g. clay minerals which might react with the magnetic minerals on heating, or non magnetic iron compounds which may convert to magnetic compounds on heating. The concentration procedure may however select certain particles (e.g. small, light ones), in preference to others. So the

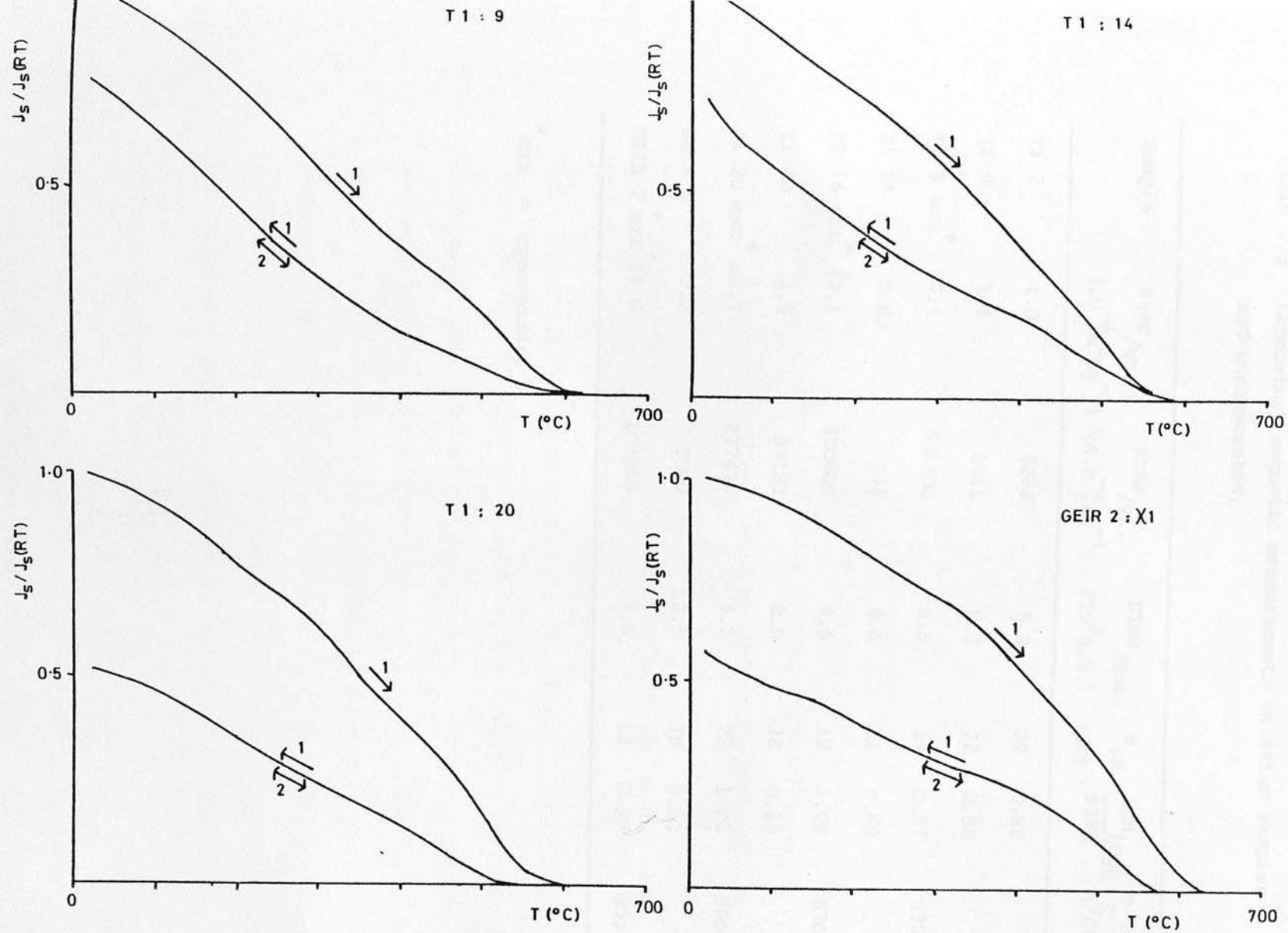


Figure 7.7: Thermomagnetic curves on magnetic concentrates from Geirionydd soils and sediment.

Table 7.3 Laboratory magnetic measurements on dried samples and concentrates.

| Sample | Susc./wt. ($10^{-6}$ $m^3.Kg^{-1}$) | SIRM/wt. ($A.m^{-1}.Kg^{-1}$) | SIRM/Susc. ($10^9$ S.I.) | $B_{cr}$ (mT) | $\frac{IRM_{100}}{SIRM}$ | $T_c$ (°C) |
|---|---|---|---|---|---|---|
| Tl 2 | 1.0 | 5268 | 5.3 | 22 | 0.88 | |
| Tl 9 | 1.5 | 8011 | 5.3 | 22 | 0.88 | |
| Tl 9 ext* | 47.6 | 308900 | 6.5 | 14 | 0.87 | 575 |
| Tl 14 | 0.03 | 138 | 4.6 | 44 | 0.69 | |
| Tl 14 ext* | 22.1 | 100600 | 4.6 | 12 | 1.00 | 570 |
| Tl 20 | 4.9 | 39192 | 8.0 | 24 | 0.82 | |
| Tl 20 ext* | 66.7 | 277490 | 4.2 | 22 | 1.02 | 580 |
| GEIR 2 | 0.2 | 2580 | 12.5 | 38 | 0.90 | |
| GEIR 2 ext* | 29.6 | 107065 | 3.6 | 12 | 0.99 | 600 |

*ext = concentrate

concentrate may not contain a representative sample of the magnetic fraction of the soil. This may be indicated by the lower coercivities ($B_{CR}$) and more variable $IRM_{100}$/SIRM ratios of the extracts, compared with the bulk samples (table 7.3). However these anomalies may also be shape effects of the tiny samples of extracts.

Thermomagnetic analysis was carried out by heating the sample in air to 700°C at a rate of about 15° C/min; in the maximum field gradient of a 500mT electromagnet. A negative feedback system counteracted the magnetic force on the sample ($\underline{M}$.gradB), due to its induced magnetization $\underline{M}$, in a field gradient gradB, and maintained the position of the sample. By monitoring the feedback current, a plot was made of the decay and growth of the induced magnetization M against temperature on an X-Y recorder.

All the samples, including the lake sediment, showed obvious main Curie points between 570°C and 600°C (figure 7.7) - close to the value of 580°C for pure magnetite, but also possible in an impure maghaemite. Also visible in all the curves is an irreversible change, resulting in a reduction of up to 50% in the room temperature value of M, after cooling. Such a change could be explained by the inversion of maghaemite to haematite at 350° C (higher if impure), and is possibly visible in some of the heating curves. M vs. T curves for second heating cycles however are invariably reversible, and show no further magnetic changes.

### 7.6.4:Mössbauer spectra.

Mössbauer spectra were performed by G.Longworth on sample T1 9 (concentrate) at both room temperature, and at 4.2K, with and

without an applied magnetic field of 4.5T. At room temperature 50% of the spectrum is in the central, superparamagnetic doublet. At the lower temperature this large superparamagnetic component becomes ferrimagnetic, and so the spectrum splits and becomes interpretable. The principal magnetic mineral is suggested to be an impure maghaemite, the ratio of iron atoms on the A and B sub-lattices being 0.32, as opposed to 0.6 in the pure form. (G.Longworth, pers.comm.)

7.6.5:Discussion.

The thermomagnetic curves suggest two magnetic phases; one which is stable to heating, has a Curie point of around 580°C and usually accounts for over 50% of the original, high field magnetization at room temperature; and a second, thermally unstable phase, which inverts to a much less magnetic phase on heating above about 350°C.

The first phase could be pure magnetite, but, if impure the Curie point would be depressed below the value observed. However, it could alternatively be an impure maghaemite. Likely impurities from the parent rock or clay minerals in the soil e.g. Na, Al, Mg, Ti, would elevate the temperature of the transition to haematite, and at the same time reduce the Curie point. ( Stacey and Banerjee, 1974, p93). Pure maghaemite has a theoretical Curie point of 675°C, found by extrapolation of Curie point data on sodium doped forms, to zero doping (Michel and Chaudron, 1935). So compositions exist for which the Curie point is reached before inversion occurs. Such a phase could be responsible for the main Curie point of 570-600°C.

The second phase could then be closer in composition to

maghaemite, so that inversion to haematite does occur before the Curie point is reached. However if one phase is close to maghaemite in composition, then the other must be even more impure, as the Mössbauer results give an average A to B site ratio of 0.32.

## 7.7:Conclusions.

1) The P.I.M. is the more sensitive and the faster of the two fieldwork instruments tried. It was able to discriminate between the richly magnetic soils, poorer soils and bedrock encountered in this field area. It also responded to variation in the thickness of magnetically enhanced topsoil. Soil profiles must however still be dug if the "magnetic stratigraphy" of the soil is required.

2) The magnetic minerals in the upper layers of magnetically rich soils appear indistinguishable from those in the lake sediment. Since the local bedrock is magnetically poor, these minerals must grow in the soils, and be transported, via the streams, to the lake sediment.

3)Evidence from Mössbauer spectra and thermomagnetic curves suggests that probably both maghaemite and magnetite are present, although both may be impure.

4)The similarities between the remanences grown in the soil and lake sediment samples, and the natural remanence of the sediment show that these minerals probably carry the stable remanence in the sediment.

# CHAPTER 8: PALAEOMAGNETIC STUDY OF SEDIMENTS FROM THE FIRTH OF CLYDE.

## 8.1: Introduction.

Continental shelf sediments, unlike those on the deep-sea floor, frequently accumulate at rates comparable to lacustrine sediments, and thus they may also carry a record of the secular variation. Bishop (1975) obtained whole core declination records on five continental shelf sediment cores from the Inner Sound of northwest Scotland. His chief aim was to aid in dating and documenting the sedimentation in the area. His palaeomagnetic records were very variable, and the correlation he has drawn with Mackereth's Windermere record is only tentative in the absence of independent dating control. There are very few other publications of palaeomagnetic secular variation records from European continental shelf sediments, although work is in progress in both Britain and Norway on North Sea sediments.

In December 1977 the chance arose to collect sediment cores in the Firth of Clyde from the R.R.S. John Murray, in collaboration with geochemists and marine biologists from Glasgow University. This chapter presents and discusses preliminary results from the cores collected.

### 8.2.1: The coring method.

A "Cambridge" type gravity corer operated by a winch from the stern of the ship was used. Normally a 12′ steel barrel, fitted with a 5cm diameter p.v.c. core liner, was used, but in rough sea only a 6′ barrel was practicable. No attempt could be

made to prevent the corer twisting during penetration, or to prevent "over-penetration", and consequent compaction of the sediment. Compaction may have occured in cores 12A and 12B, when the 6′ barrel was employed, and on retrieval the weights, above the barrel, were muddy. The sediment is held in the liner while it is being winched up by an "orange peel" core catcher inserted in the end. Unfortunately the soft, uppermost sediment was sometimes deformed as it pushed through the segments of the core catcher.

After retrieval the core liner was extracted from the barrel; some cores were brought back to Edinburgh for whole core measurement, others were opened, (as in figure 2.5), and subsampled on board. Appendix 1 includes a table of the measurements made on all the cores.

### 8.2.2:The field area and coring sites.

The Firth of Clyde and the Clyde estuary are described in detail in the N.E.R.C. publication on the area (1974). The Firth (figure 8.1) lies between the mainland of Ayrshire and the Kintyre peninsular. The River Clyde flows into it through Glasgow, and the Isle of Arran lies at its centre. Several deep sea lochs enter it from the north, the biggest being Loch Fyne. Most of the sediment in the Firth is a fine grey or brown mud, but there are coarser silts and sands off the Ayrshire coast and just south of Arran. Gair (1967) showed that the main sources of sediment material are the rivers running into the sea lochs, rather than the Clyde itself and its drainage basin. Since the main contributor to the southern basin of Loch Lomond is the Endrick, draining the Campsie Fells, east of the loch, there is

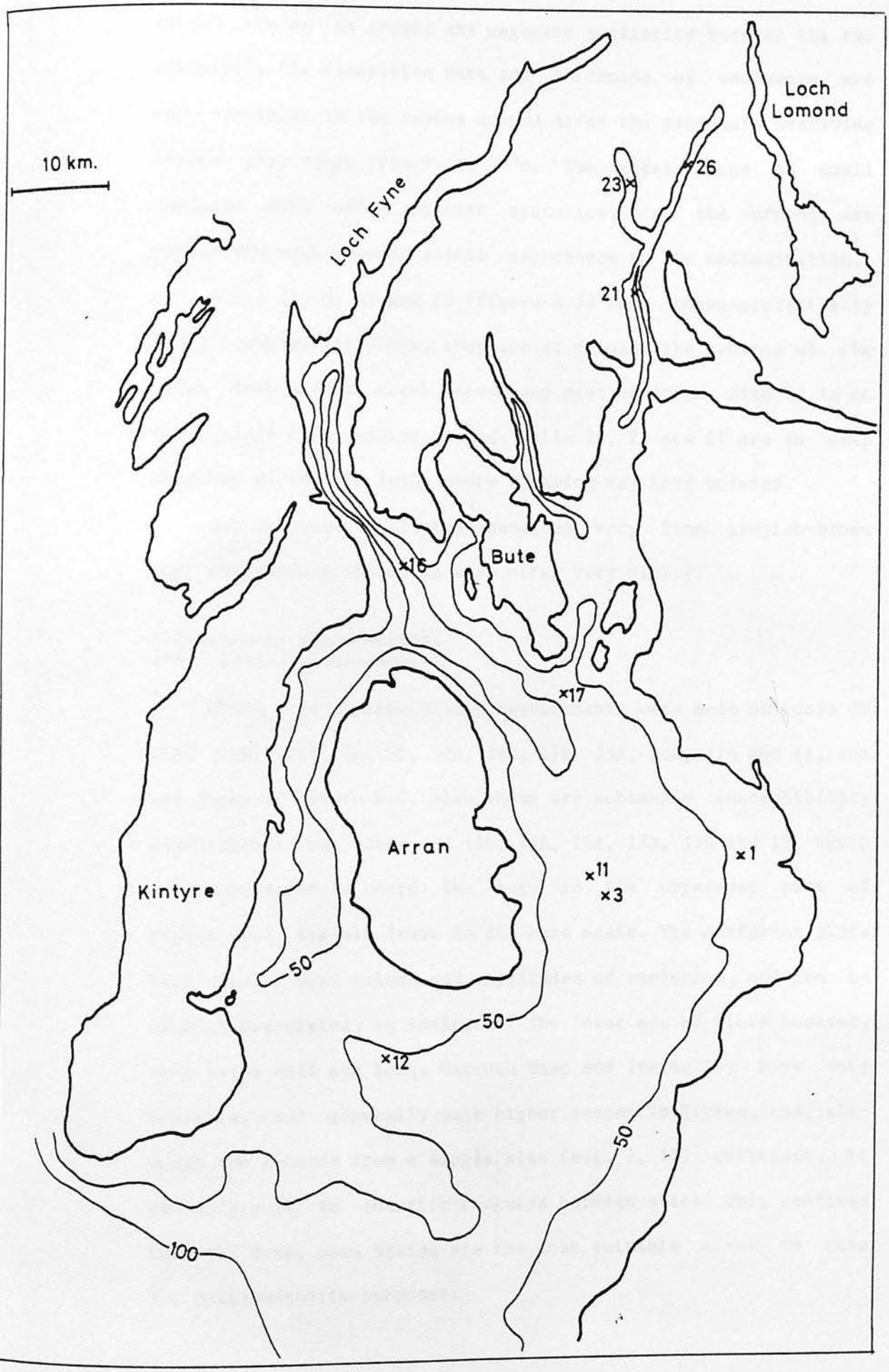


Figure 8.1 : The Firth of Clyde : bathymetry and coring sites.

little reason to expect any magnetic similarity between the two sediments. The deposition rate and thickness of sediments are very variable; in the basins around Arran the sediments overlying boulder clay range from 9 to 47m. The tidal range is small compared with other British estuaries, and the currents are relatively weak causing little disturbance to the sedimentation.

Sites 11, 3, 12 and 16 (figure 8.1) were chosen specifically for palaeomagnetic cores; they are at or near the centres of the three deep basins, north, south and east of Arran. Site 17 is on the Garroch Head dumping ground, while 26, 23 and 21 are in deep trenches of the sea lochs where slumping may have occured.

All the cores collected contained very fine greyish-brown mud; the surface sediments were often very sloppy.

## 8.3:Magnetic measurements.

Whole core susceptibility measurements were made on cores JM 11A, 11D, 11E, 3A, 3B, 12A, 16C, 17B, 23A, 26A, 21A and 1A, and are shown in figure 8.2. Also shown are subsample susceptibility measurements on cores JM 11B, 12B, 16A, 17A, 17D and 1B, which were subsampled on board. The logs in the uppermost part of figure 8.2 are all drawn to the same scale. The different plots have similar mean values and amplitudes of variation, and can be readily correlated, as indicated. The lower set of plots however, from Lochs Goil and Long, Garroch Head and Irvine Bay have very variable, but generally much higher susceptibilities, and, although the records from a single site (e.g. 1, 17) correlate, it is difficult to identify features between sites. This confirms that the deep, open basins are the most suitable sites to core for palaeomagnetic purposes.

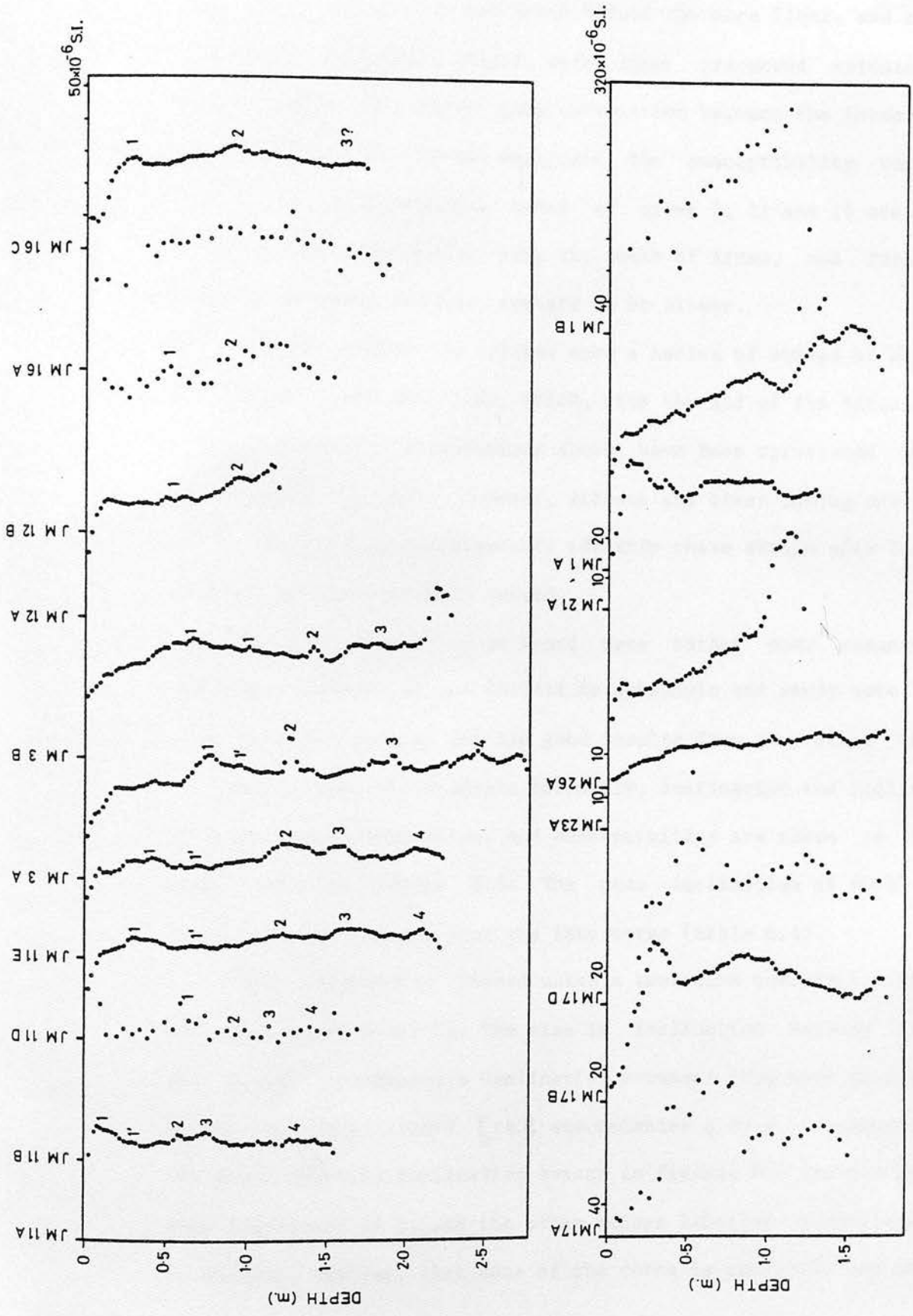


Figure 8.2 : Whole core susceptibility logs for cores JM 11A, 11D, 11E, 3A, 3B, 12A, 16C, 17B, 23A, 26A, 21A, 1A. Subsample susceptibility logs for cores JM 11B, 12B, 16A, 17A, 17D, 1B.

Figure 8.3 shows whole core remanence measurements on the sediments from the deep basins, (with the exception of core 11A, which was too fluid, and moved within the core liner, and core 11E, whose irregularly shaped core liner prevented spinning). Again, there is a fairly good correlation between the intensity logs, although they do not duplicate the susceptibility variations. The sedimentation rates at sites 3, 11 and 16 are all quite similar, but that at site 12, south of Arran, and further from the sediment sources, appears to be slower.

All the declination records show a series of swings of about $40^{\circ}$ peak - peak amplitude, which, with the aid of the intensity and susceptibility correlations above, have been correlated with one another, as shown. However, without any other dating control it is difficult to unambiguously identify these swings with features of the lake sediment record.

The cores subsampled on board gave rather poor remanence results. However, it was decided to subsample and study core 11E because of its length, and the good results from the other site 11 cores. Logs of subsample intensity, declination and inclination of natural remanences, and susceptibility are shown in the upper part of figure 8.5. The mean inclination of $61.1^{\circ}$ is comparable with values from the lake cores (table 6.1).

This inclination record makes a tentative correlation with the lake record possible. The rise in inclination between 2.30 and 2.10m accompanies a declination movement from west to east; as, in the limnic record $\zeta$ to $\varepsilon$ acccompanies g to f. Consequently the lower easterly declination swings in figures 8.3 and 8.5 have been identified as f, and the other swings labelled accordingly. It follows, however, that none of the cores is recording the 1820

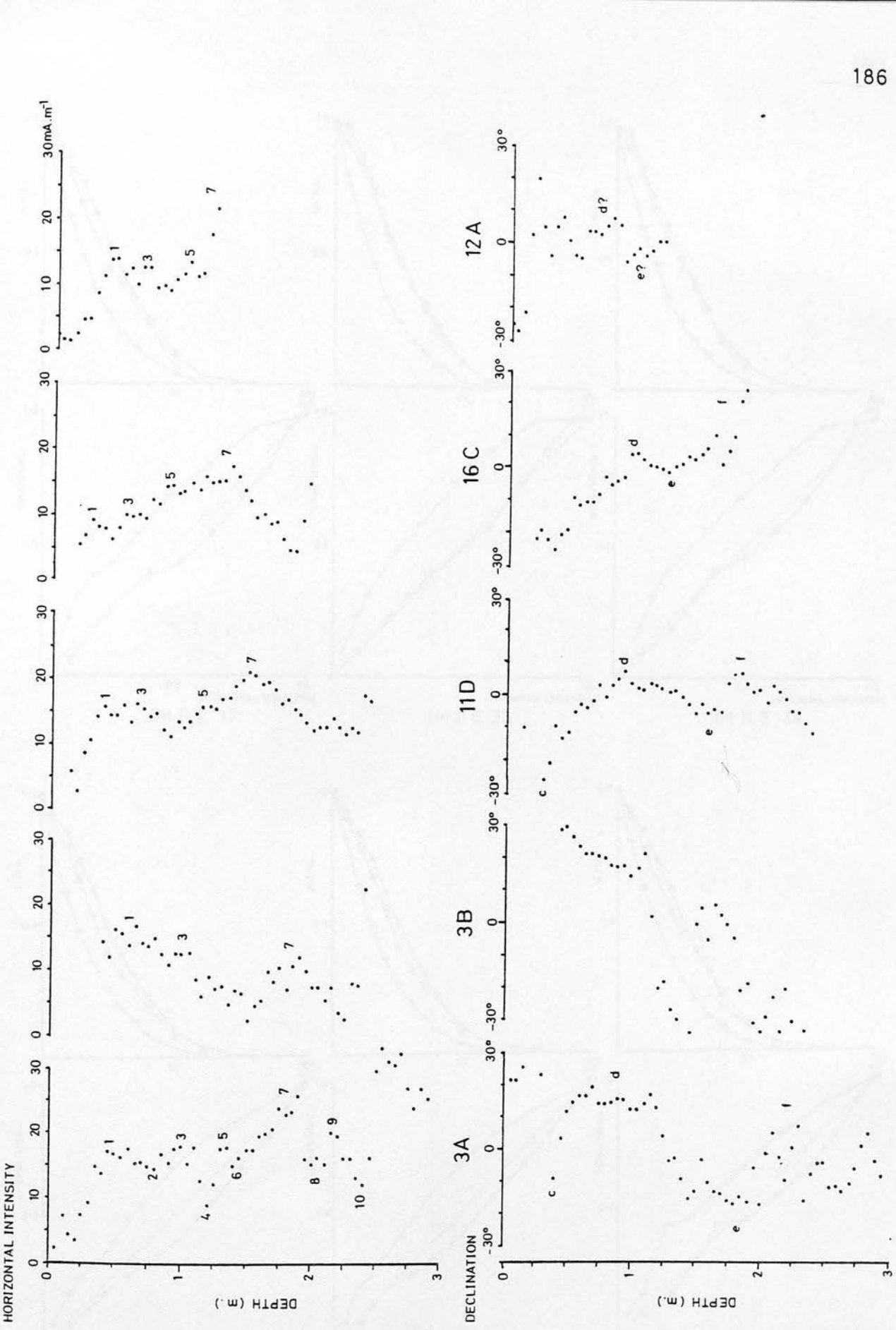


Figure 8.3 : John Murray cores : whole core horizontal remanent intensity and declination .

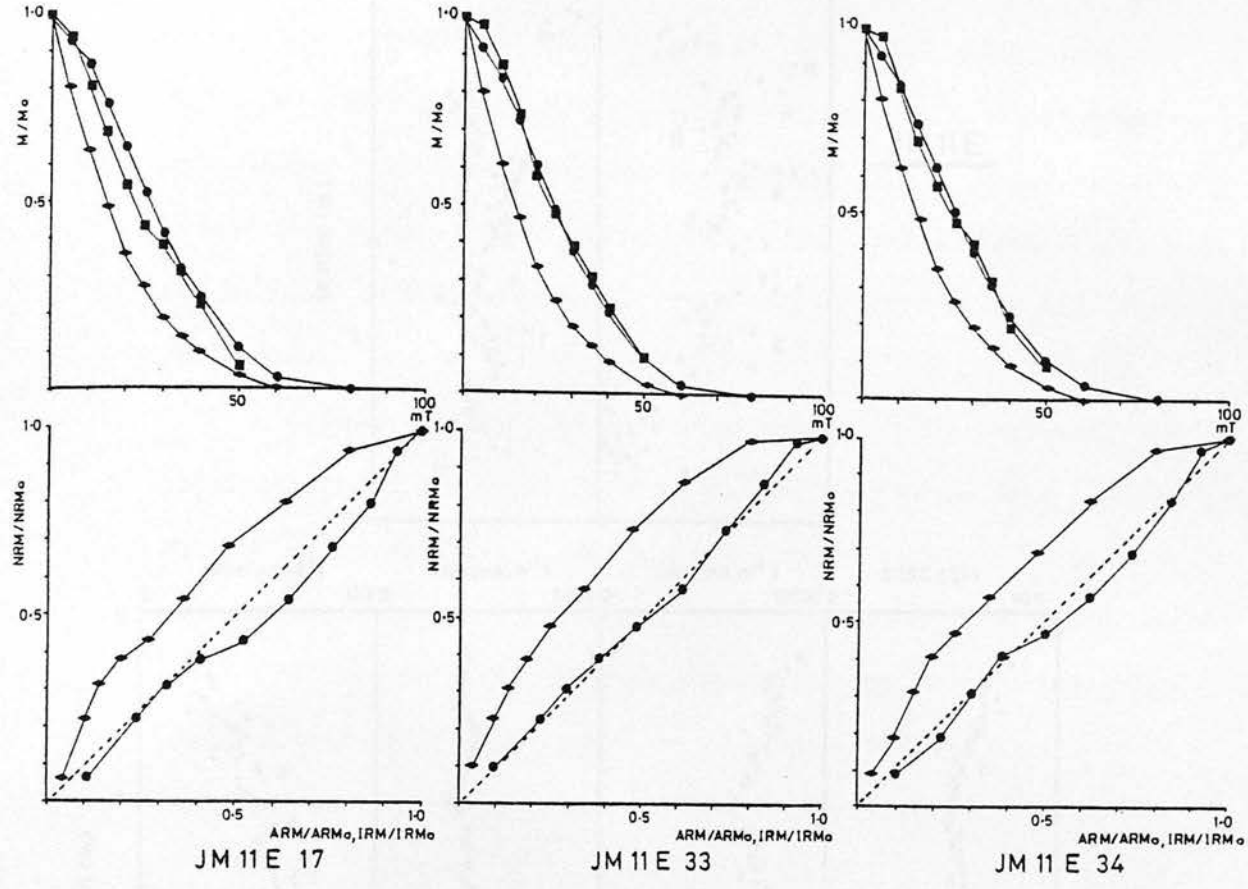


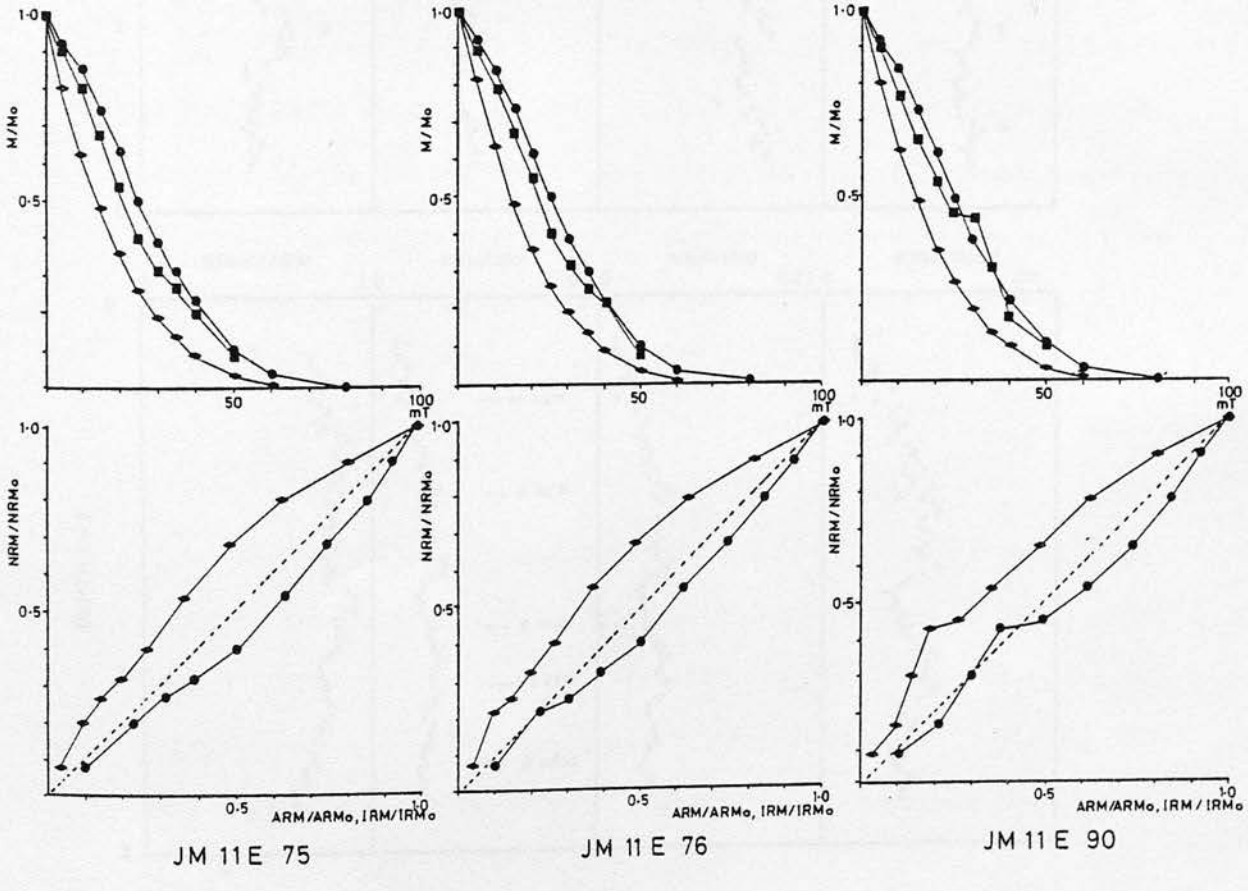


■ AF Demag. of NRM
● AF Demag. of ARM
▬ AF Demag. of IRM

● NRM/NRMo vs. ARM/ARMo
▬ NRM/NRMo vs. IRM/IRMo

Figure 8.4 : JM 11 E pilot samples : A.F. demagnetization curves for NRM, ARM and IRM.

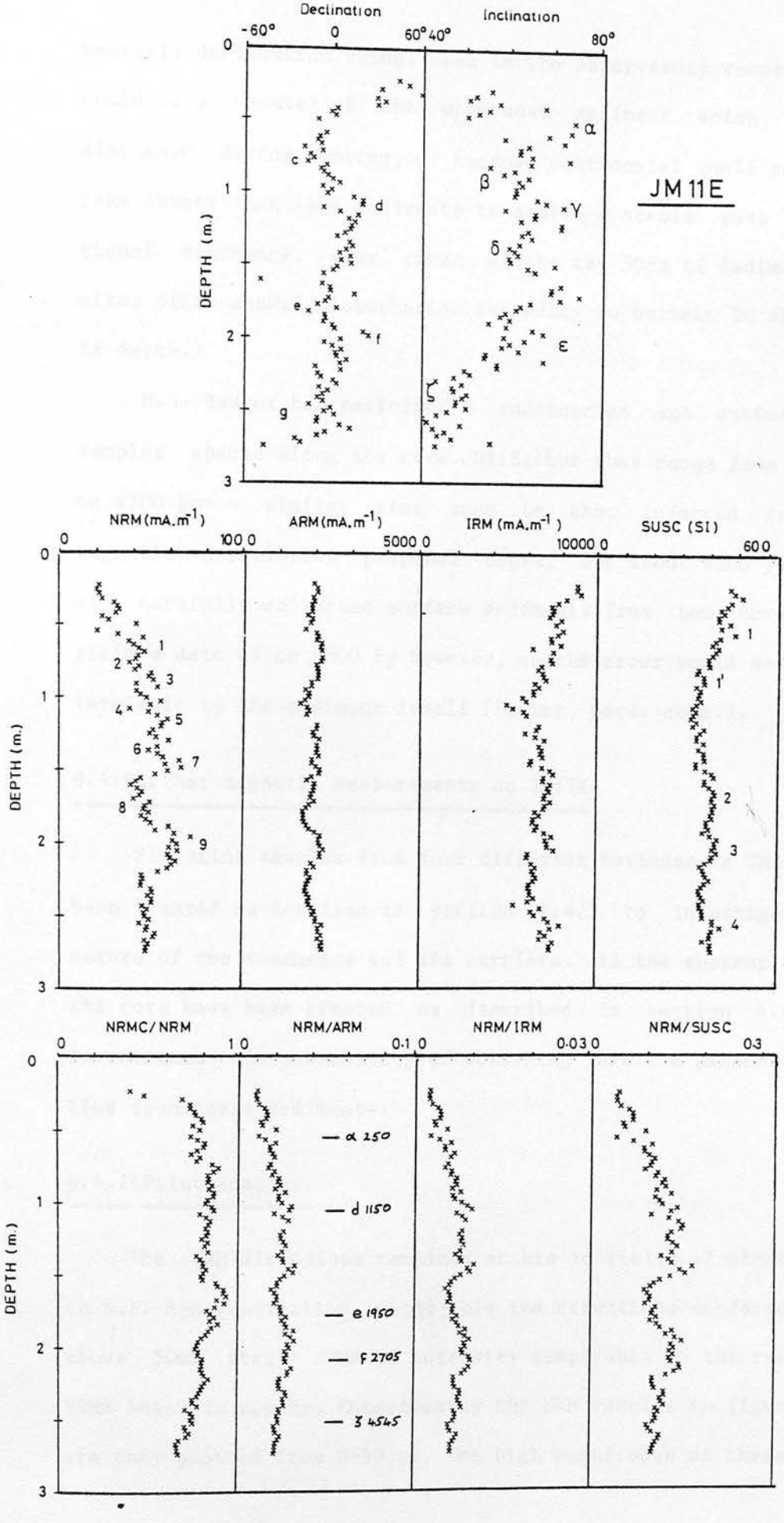


Figure 8.5 : JM 11E: Downcore plots of declination, inclination, various remanences and remanence ratios.

westerly declination swing, seen in the observatory records. This could be a result of the uppermost sediment being lost or disturbed during coring, or because continental shelf sediments take longer than lake sediments to aquire a stable post depositional remanence. (Box cores of the top 50cm of sediment at a site, often showed bioturbation extending to between 20 and 30cm in depth.)

M.S. Baxter has performed 8 radiocarbon age estimates on samples spaced along the core JM11E, but they range from 7700 bp to 4700 bp- a similar time span to that inferred from the magnetic correlation proposed above, but about 4500 years too old. Carefully collected surface sediments from box cores also yield a date of ca 4500 bp however, so the error would seem to be intrinsic to the sediment itself (Baxter, pers. comm.).

### 8.4:Further magnetic measurements on JM11E.

Six pilot samples from four different horizons in JM11E have been treated as detailed in section 4.4.1 to investigate the nature of the remanence and its carriers. All the subsamples from the core have been treated as described in section 4.4.3 to investigate the possibility of obtaining relative palaeointensities from these sediments.

#### 8.4.1:Pilot samples.

The NRM directions remained stable to fields of about 25mT, on A.F. demagnetization, above this the directions wandered, and above 50mT stray ARMs of intensity comparable to the remaining NRMs began to appear. Consequently the NRM results in figure 8.4 are only plotted from 0-50 mT. The high magnitudes of these stray

ARMs may at first sight be attributed to instrumental error. However, experiments of controlled growth of ARM show they are simply related to the magnetic composition of the sediment. In a bias field of 0.25mT, ARMs had intensities of 40 to 60 times the NRM intensities. If a linear dependance of ARM on bias field is assumed, this corresponds to 8-12 times the NRM intensity for a bias field equal to the present geomagnetic intensity. This is five times stronger than any of the lake sediments studied and accounts for the difference in behaviour during partial A.F. demagnetization.

The coercivity spectra of NRM and ARM are quite similar in all the samples, percentage differences ranging from 9.4 to 14.8, (excepting sample 90, the NRM demagnetization curve of which shows stray ARM effects at 25mT). This small difference in the coercivity spectra is insufficient to explain the large difference in intensity of the NRM and ARM. It would seem that either 1) only a small proportion of the grains capable of carrying a remanence contributes to the NRM, or 2) there is a comparatively poor degree of alignment of the grain magnetic moments in the sediment.

The intensities of the IRMs are over 100 times those of the NRMs, and as in the lake sediments, they are considerably softer than the NRMs or ARMs to A.F. demagnetization. The percentage differences between the NRM and IRM demagnetization curves averages about 20%. The modified Lowrie-Fuller test indicates then that the remanence carriers are mainly fine grained magnetite, although the lower MDFs and higher ARM intensities suggest that there are differences between these and the carriers in the lake sediments.

| JM11E | Depth (cm) | $NRM_O$ | $ARM_O$ | $IRM_O$ | $MDF_N$ | $MDF_A$ | $MDF_I$ | % diff N,ARM | % diff N,IRM | $B_{CR}$ | SUSC | $\frac{NRM}{ARM}$ | $\frac{NRM}{IRM}$ | $\frac{NRM}{SUSC}$ |
|---|---|---|---|---|---|---|---|---|---|---|---|---|---|---|
| | | ($mA.m^{-1}$) | | | (mT) | | | | | (mT) | (SI) | | | |
| 17 | 67 | 39.8 | 2322 | 6772 | 22.0 | 26.0 | 14.0 | 12.3 | 21.1 | 47.0 | 432.7 | 0.017 | 0.0059 | 0.092 |
| 33 | 105 | 48.5 | 1770 | 5306 | 24.0 | 24.0 | 14.0 | 10.3 | 23.8 | 46.0 | 352.9 | 0.027 | 0.0091 | 0.137 |
| 34 | 108 | 36.0 | 1951 | 5660 | 24.0 | 25.0 | 14.0 | 14.8 | 20.4 | 47.0 | 364.0 | 0.018 | 0.0064 | 0.099 |
| 75 | 208 | 58.2 | 2343 | 6621 | 22.0 | 25.0 | 14.0 | 9.4 | 17.9 | 47.0 | 428.0 | 0.025 | 0.0088 | 0.136 |
| 76 | 211 | 59.2 | 2333 | 6565 | 22.0 | 25.0 | 14.0 | 10.8 | 18.3 | 47.0 | 424.1 | 0.025 | 0.0090 | 0.140 |
| 90 | 244 | 40.3 | 2043 | 5826 | 22.0 | 25.0 | 14.0 | 17.3 | 21.8 | 47.0 | 390.2 | 0.020 | 0.0069 | 0.103 |

Table 8.1 : JM 11E pilot sample data

## 8.4.2: Downcore plots.

The middle and lower plots of figure 8.5 show downcore plots of various remanences and their ratios for core JM11E. Unlike Lomond and Geirionydd, the ARM pattern does not follow either the NRM or susceptibility variations completely, but has a clear signature of its own, probably reflecting changes in the concentration of remanence bearing grains, which in this case is not paralleled by the total magnetic content. The IRM log bears more resemblance to susceptibility than to the other remanences. Both IRM and susceptibility rise towards the top of the core. Thus, normalization with ARM is felt most likely to produce a palaeointensity record. Indeed, when "magnetic dates" are placed on the NRM/ARM plot, as shown, there are several features in common with the plots of figure 4.8: a rise and fall in the past 1600-1700 years, and an earlier maximum, between 2400 and 2100 BP. Although it cannot be said any more firmly that these are reflections of palaeointensity changes, these records certainly support the conclusions of chapter 4.

It is also interesting to note the NRMC/NRM plot. Again the changes in NRMC are less marked than those in NRM, and there is a negative correspondance between this plot and those indicating magnetic content. Thus NRMC/NRM might provide a good guide to the magnetic homogeneity of these sediments.

## 8.5: Discussion.

1)Continental shelf sediments can provide good palaeomagnetic records of declination, inclination and intensity of the geomagnetic field, if coring sites are selected carefully. However, the

gravity corer used in this study area was not ideal. It would also be desirable to collect longer cores, to compare with the whole of the lake sediment record.

2)The difference between the remanence carriers in continental shelf and lake sediments is worth further investigation.

3)This project has illustrated the usefullness of magnetic parameters in correlating sediment cores over distances of tens or even hundreds of kilometres. NRM, laboratory induced remanences and magnetic susceptibility are all useful in these correlations. Horizontal NRM and susceptibility can be measured rapidly without sampling or disturbing the sediment.

4)The magnetic time scale provides the most reliable method of dating these sediments at present. Radiocarbon age estimates are all systematically too old, whereas the occurrence of pollen in continental shelf sediments is very sparse.

APPENDIX 1 : CORES COLLECTED DURING THIS PROJECT.

| | core | date collected | sediment length (m.) | whole core records (figs) | sub-sample records (figs) | other work |
|---|---|---|---|---|---|---|
| LOMOND | LLRD 1 | May 1976 | 5.10 | 3.1-3.3 | 3.4,3.5 | C-14, Pollen. |
| | LLRD 2 | " | 4.70 | " | " | |
| | LLRD 3 | " | 5.35 | " | " | |
| | LLRP 4 | " | 4.75 | " | " | |
| | LLRP 5 | June 1977 | 4.00 | - | - | Records too short |
| | LLRP 6 | " | 2.70 | - | - | " " " |
| | LLRP 7 | " | 5.80 | 3.1-3.3 | - | |
| | LLRB 8 | " | 5.95 | - | - | Faulty coring process |
| | LLGU 9 | Oct 1977 | 4.35 | 3.1-3.3 | - | |
| | LLRP M1 | May 1976 | 0.96 | " | - | |
| | LLRP M2 | " | 0.88 | " | - | |
| | LLRP M3 | " | 0.85 | " | - | |
| | LLTO M4 | June 1977 | 1.10 | " | - | |
| | M5-13,15-18 | June,Oct 1977 | various | - | - | Used in other projects. |
| | LLBE M14 | Oct 1977 | 1.25 | 3.1-3.3 | - | |
| | LLGU M19 | " | 1.25 | " | - | |
| DERMERE | WIND 1 | Sept 1976 | 5.90 | 3.7-3.9 | 3.10,3.11 | C-14, Pollen. |
| | WIND 2 | " | 5.80 | " | " | |
| | WIND 3 | " | 5.95 | " | " | |
| | WIND M1 | June 1978 | 1.03 | " | - | |
| | WIND M2 | " | 1.15 | " | - | |
| | WIND M3 | " | 1.14 | " | - | |
| | WIND M4 | " | 1.11 | " | - | |

APPENDIX 1 (continued)

| | core | date collected | sediment length (m.) | whole core records (figs) | sub-sample records (figs) | other work |
|---|---|---|---|---|---|---|
| GEIRIONYDD | GEIR 1 | July 1977 | 2.60 | - | - | Short and incomplete |
| | GEIR 2 | " | 4.70 | 3.13-3.15 | 3.16,3.17 | C-14, Pollen |
| | GEIR 3 | June 1978 | 5.50 | " | " | |
| | GEIR 4 | " | 5.85 | " | " | C-14, Pollen |
| | GEIR 5 | " | 4.80 | " | - | Not yet sampled |
| | GEIR 6 | " | 5.70 | " | - | " " " |
| | GEIR 7 | " | 6.00 | " | - | " " " |
| | GEIR 8 | " | 5.90 | - | - | " " " |
| | GEIR M1 | July 1977 | 0.86 | 3.13-3.15 | - | |
| | GEIR M2 | " | 1.21 | " | - | |
| | M3-5,M7-9 | June 1978 | various | - | - | used for other studies |
| | GEIR M6 | " | 1.15 | 3.13-3.15 | - | |
| CLYDE | JM 1A | Dec 1977 | 2.10 | 8.2 | - | |
| | JM 1B | " | 1.40 | - | 8.2 | |
| | JM 3A | " | 3.12 | 8.2,8.3 | - | |
| | JM 3B | " | 2.54 | " | - | |
| | JM 11A | " | 1.76 | 8.2 | - | |
| | JM 11B | " | 1.80 | - | 8.2 | |
| | JM 11D | " | 2.64 | 8.2,8.3 | - | |
| | JM 11E | " | 2.63 | 8.2 | 8.2,8.5 | C-14 |
| | JM 12A | " | 1.32 | 8.2,8.3 | - | |
| | JM 12B | " | 1.60 | - | 8.2 | |
| | JM 16A | " | 1.95 | - | 8.2 | |
| | JM 16C | " | 2.10 | 8.2,8.3 | - | |
| | JM 17A | " | 1.65 | - | 8.2 | |
| | JM 17B | " | 2.02 | 8.2 | - | |
| | JM 17D | " | 1.75 | - | 8.2 | |

APPENDIX 1 (continued)

| | core | date collected | sediment length (m.) | whole core records (figs) | sub-sample records (figs) | other work |
|---|---|---|---|---|---|---|
| CLYDE | JM 21A | Dec 1977 | 1.60 | 8.2 | - | |
| | JM 23A | " | 2.02 | 8.2 | - | |
| | JM 26A | " | 1.43 | 8.2 | - | |

## Appendix 2. SI and CGS units.

| Quantity | SI Symbol | SI unit | CGS Symbol | CGS Unit | Conversion $\chi$ SI unit $\times$ $\chi$ = CGS unit. |
|---|---|---|---|---|---|
| permeability of free space | $\mu o$ | $H.m^{-1}$ | set = 1 | | $4\pi \times 10^{-7}$ |
| free space induction (field) | Bo | T (1$\gamma$=1nT) | H | Oe | $10^{-4}$ |
| induction in a medium | B | T | B | G | $10^{-4}$ |
| magnetic excitation | H | $Am^{-1}$ | H | Oe | $10^{3}/_{4\pi}$ |
| magnetization/unit vol. | M | $A.m^{-1}$ | I | (emu/cc $^{-1}$ (erg.Oe$^{-1}$cm$^{-3}$ | $10^{3}$ |
| (Magnetic polarization | J | T | $4\pi I$ | | $10^{-4}$) |
| susceptibility/unit vol. | $\chi$ | | $I/_{H}$ | ( G/Oe (erg.Oe$^{-2}$.cm$^{-3}$ | $4\pi$ |
| susceptibility/unit mass | $\chi_s$ | $m^3Kg^{-1}$ | | erg.Oe$^{-2}$.gm$^{-1}$ | $10^{-3} \times 4\pi$ |

The definition adopted for susceptibility (volume) is

$$\chi = \frac{M}{H} = \mu o \frac{M}{Bo}$$ dimensionless.

REFERENCES

Aitken, M.J., 1964. Archaeomagnetic results 1. Some geophysical implications. Archaeometry, 1, 43-46.

Aitken, M.J., 1970. Dating by archaeomagnetic and thermoluminescent methods. Phil. Trans. Roy. Soc. Lond., 269A, 77-88.

Alldredge, L.R. and Hurwitz, L., 1964. Radial dipoles as the source of the earth's main magnetic field. J. geophys. Res., 29, 2631-2640.

Amerigan, C., 1977. Measurement of the effect of particle size variation on the detrital remanent magnetisation to anhysteretic remanent magnetisation ratio in some abyssal sediments. Earth Planet. Sci. Lett., 36, 434-442.

Barton, C., 1978. Ph.D. Thesis, Australian National University.

Bauer, L.A., 1895. On the secular motion of a free magnetic needle. Phys. Rev., 3, 34-43.

Berryman, J.E., 1978. Choice of operator length for maximum entropy spectral analysis. Geophysics, 43, 1384-1391.

Bingham, C., Godfrey, M.D. and Tukey, J.W., 1967. Modern techniques for power spectrum estimation. I.E.E.E. Trans. Audio Electroacoust., AU-15, 56-66.

Bishop, P., 1975. The palaeomagnetism of muddy sediment cores from the Inner Sound, N.W. Scotland and the Glacial and post-Glacial history of sedimentation in the area. Earth Planet. Sci. Lett., 27, 51-56.

Blackett, P.M.S., 1947. The magnetic field of massive rotating bodies. Nature, 159, 658-666.

Bucha, V., 1970. Evidence for changes in the earth's magnetic field intensity. Phil. Trans. Roy. Soc. Lond., 269A, 47-55.

Bullard, E.C., 1949a. The magnetic field within the earth. Proc. Roy. Soc., 197A, 433-453.

Bullard, E.C., 1949b. Electromagnetic induction in a rotating sphere. Proc. Roy. Soc., 199A, 413-433.

Bullard, E.C., Freedman, C., Gellman, H. and Nixon, J., 1950, The westward drift of the earth's magnetic field. Phil. Trans. Roy. Soc. Lond., 243A, 67-90.

Bullard, E.C. and Gellman, H., 1954. Homogeneous dynamos and terrestrial magnetism. Phil. Trans. Roy. Soc. Lond., 247A, 213-278.

Burg, J.P., 1967. Maximum entropy spectral analysis. Paper presented at 37th annual Int. S.E.G. meeting Oklahoma Oct. 31,. 1967.

Clark, A.J., 1979. Magnetic dating. In press. Lond. Inst. Arch.

Clark, M., 1975. A calibration curve for radiocarbon dates. Antiquity, 49, 251-266.

Clark, M. and Thompson, R., 1978. An objective method for smoothing palaeomagnetic data. Geophys. J. R. astr. Soc., 52, 205-213.

Clegg, J.A., Almond, M. and Stubbs, P.H.S., 1954. The remanent magnetism of some sedimentary rocks in Britain. Phil. Mag., 45, 583-598.

Colani, C. and Aitken, M.J., 1966. A new type of locating device. II Field trials. Archaeometry, 9, 9-19.

Collinson, D.W., 1965. Depositional remanent magnetisation in sediments. J. geophys. Res., 70, 4663-4668.

Cook, A.H., 1973. Physics of the earth and planets. Macmillan, London.

Cooley, J.W. and Tukey, J.W., 1965. An algorithm for the machine calculation of complex Fourier series. Math. Comput., 19, 297-301.

Cox, A., 1968. Length of geomagnetic polarity intervals. J. geophys. Res., 73, 3247-3260.

Cox, A., Doell, R.R. and Dalrymple, G.B., 1964. Reversals of the earth's magnetic field. Science, 144, 1537-1543.

Creer, K.M., 1974. Geomagnetic variations for the interval 7000 25000 BP as recorded in a core of sediment from station 1474 of the Black Sea cruise of "Atlantis II". Earth Planet. Sci. Lett., 23, 34-42.

Creer, K.M., 1977. Geomagnetic secular variations during the last 25000 years: an interpretation of data obtained from rapidly deposited sediments. Geophys. J. R. astr. Soc., 48, 91-109.

Creer, K.M., Gross, D.L. and Lineback, J.A., 1976a. Origin of regional geomagnetic variations recorded by Wisconsinian and Holocene sediments from Lake Michigan, U.S.A. and Lake Windermere, England. Geol. Soc. Amer. Bull., 87, 531-540.

Creer, K.M., Anderson, T.W. and Lewis, C.F.M., 1976b. Late Quaternary geomagnetic stratigraphy recorded in Lake Erie sediments. Earth Planet. Sci. Lett., 31, 37-47.

Creer, K.M., Readman, P.W., Thompson, R., Hogg, T.E., Papamarinopoulos, S., Stober, J.C. and Turner, G., 1977. Secular variation obtained from European lake sediments. E.O.S., 58, 709.

Dagley, P., Wilson, R.L., Ade-Hall, J.M., Walker, G.P.L., Haggerty, S.E., Sigurgeirsson, T., Watkins, N.D., Smith, P.J., Edwards, J. and Grasty, R.L., 1967. Geomagnetic polarity zones for Icelandic lavas. Nature, 216, 25-29.

Denham, C.R., 1974. Counterclockwise motion of palaeomagnetic directions 24000 years ago at Mono Lake, California. J. Geomag. Geoelectr., 26, 487-498.

Denham, C.R., 1975. Spectral analysis of palaeomagnetic time series. J. geophys. Res., 80, 1897-1901.

Dickson, J.H., Stewart, D.A., Thompson, R., Turner, G., Baxter, M.S., Drndarsky, N.D. and Rose, J., 1978. Palynology, palaeomagnetism and radiometric dating of Flandrian marine andr freshwater sediments of Loch Lomond. Nature, 274, 548-553.

Dodson, R.E., 1979. Counterclockwise precession of the geomagnetic field vector and westward drift of the non dipole field. J. geophys. Res., 84, 637-644.

Drndarsky, N.D., 1976. Ph.D. thesis, University of Glasgow.

Dunn, J.R., Fuller, M., Ito, H. and Schmidt, V.A., 1971. Palaeomagnetic study of a reversal of the earth's magnetic field. Science, 172, 840-845.

Elsasser, W.M., 1946. Induction effects in terrestrial magnetism: Part I: Theory. Phys. Rev., 69, 106-116. Part II: The secular variation. Phys. Rev., 70, 202-212.

Elsasser, W.M., 1947. Induction effects in terrestrial magnetism: Part III: Electric modes. Phys. Rev., 72, 821-833.

Epp, R.J., Tukey, J.W. and Watson, G.S., 1971. Testing unit vectors for correlation. J. geophys. Res., 76, 8480-8483.

Ergin, M., Harkness, D.D. and Walton, A., 1970. Glasgow University radiocarbon measurements II. Radiocarbon, 12, 486-495.

Fisher, R.A., 1953. Dispersion on a sphere. Proc. Roy. Soc. Lond. 217A, 295-305.

Gair, ., 1967, PhD Thesis, University of Strathclyde.

Greene-Kelly, R., Chapman, S. and Pettifer, K., 1970. The preparation of thin sections of soils using polyethylene glycols. Micromorphological techniques and applications. Tech. Monogr. Soil survey. No. 2. Rothampstead experimental station. 15-24.

Gribbin, J., 1979. Making a new date with radiocarbon. New Scientist, 82, 532-534.

Harrison, C.G.A., 1966. The palaeomagnetism of deep sea sediments. J. geophys. Res., 71, 3033-3043.

Hide, R., 1967. Motions of the earth's core and mantle and variations of the main geomagnetic field. Science, 157, 55-56.

Hide, R., 1969. Interaction between the earth's liquid core and solid mantle. Nature, 222, 1055-1056.

Hide, R., 1970. On the earth's core-mantle interface. Q. J. R. Met. Soc., 96, 579-590.

Hirooka, K., 1971. Archaeomagnetic study for the past 2000 years in South West Japan. Mem. Fac. Sci. Kyoto Univ. Ser. Geol. Min., 38, 167-207.

Hogg, T.E., 1978. Ph.D. Thesis, University of Edinburgh.

Hospers, J., 1951. Remanent magnetism of rocks and the history of the geomagnetic field. Nature, 168, 1111-1112.

Howell, M., 1971. A continuous seismic profile of Windermere. Geol. J., 7, 329-334.

Ising, G., 1942. On the magnetic properties of varved clay. Ark. Mat. Astron. Fys., 29, 1-37.

Johnson, E.A., Murphy, T. and Torreson, O.W., 1948. Prehistory of the earth's magnetic field. Terr. Magn. Atmos. Elec., 53, 349-372.

Johnson, H.P., Lowrie, W. and Kent, D.V., 1975. Stability of anhysteretic remanent magnetization in fine and coarse magnetite and maghaemite particles. Geophys. J. R. astr. Soc.41, 1-10.

Johnson, H.P., Kinoshita, H. and Merrill, R.T., 1975. Rock magnetism and palaeomagnetism of some N. Pacific deep sea sediment cores. Geol. Soc. Amer. Bull., 86, 412-420.

Kawai, N., Hirooka, K. and Sasajima, S., 1965. Counterclockwise rotation of the geomagnetic dipole axis revealed in the worldwide archaeo-secular variations. Proc. Japan Acad., 41, 398-403.

Kawai, N. and Hirooka, K., 1967. Wobbling motion of the geomagnetic dipole field in historic time during these 2000 years. J. Geomag. Geoelectr., 19, 217-227.

Kent, D.V., 1973. Post depositional remanent magnetisation in deep sea sediment. Nature, 246, 32-34.

Kent, D.V., 1974. Ph.D. Thesis, University of Columbia.

King, R.F., 1955. Remanent magnetism of artificially deposited sediments. Mon. Not. Roy. Ast. Soc. Geophys. Supp., 7, 115-134.

Kono, M. and Ueno, N, 1977. Palaeointensity determination by a modified Thellier method. Phys. Earth Planet. Int., 13,305-314.

Kovacheva, M. and Veljovich, D., 1977. Geomagnetic field variations in South East Europe between 6500 and 100 years B.C.. Earth Planet. Sci. Lett., 37, 131-138.

Kusakov, O.M. and Zagniy, G.F., 1973. Archaeomagnetic secular variation study in the Ukraine and Moldavia. Archaeometry, 15, 153-157.

Laj, C., Nordemann, D. and Pomeau, Y., 1979. Correlation function analysis of geomagnetic field reversals. J. geophys. Res., 84, 4511-4515.

Le Borgne, E., 1955. Abnormal magnetic susceptibility of the top soil. Ann. Geophys., 11, 399-419.

Levi, S. and Banerjee, S.K., 1976. On the possibility of obtaining relative palaeointensities from lake sediments. Earth Planet. Sci. Lett., 29, 219-226.

Longworth, G., Becker, L.W., Thompson, R., Oldfield, F., Dearing, J.A. and Rummery, T.A., 1979, Mossbauer effect and magnetic studies of secondary magnetic oxides in soils. J. Soil Sci., 30

Lowes, F.J. and Runcorn, S.K., 1951. The analysis of the geomagnetic secular variation. Phil. Trans. Roy. Soc., 243A, 525-546.

Lowes, F.J. and Wilkinson, I., 1963. Geomagnetic dynamo: A laboratory model. Nature, 198, 1158-1160.

Lund, S. and Banerjee, S.K., 1979. Palaeosecular variations from lake sediments. Rev. Geophys. Sp. Phys. 17, 244-249

Mackereth, F.J.H., 1958. A portable core sample for lake deposits. Limnol. Oceanogr., 3, 181-191.

Mackereth, F.J.H., 1971. On the variation in the direction of the horizontal component of the remanent magnetisation in lake sediment. Earth Planet. Sci. Lett., 12, 332-338.

Malkus, W.V.R., 1963. Precessional torques as a cause of geomagnetism. J. geophys. Res., 68, 2871-2886.

Michel, A. and Chaudron, G., 1935. Etude du sesquioxide de fer cubiqe stabilise. Compte. Rend., 201, 1191.

Molyneux, L., 1971. A complete result magnetometer for measuring the remanent magnetisation of rocks. Geophys. J. R. astr. Soc., 24, 429-434.

Molyneux, L., Thompson, R., Oldfield, F. and McCallen, M.E., 1972. Rapid measurement of the remanent magnetisation of long cores of sediment. Nature, 237, 42-43.

Molyneux, L. and Thompson, R., 1973. Rapid measurement of the magnetic susceptibility of long cores of sediment. Geophys. J. R. astr. Soc., 32, 479-481.

Mullins, C., 1977. Magnetic susceptibility of the soil and its significance in soil science - a review. J. Soil Sci., 28, 223-246.

Nagata, T, Rikitake, T. and Akasi, K., 1943. The natural remanent magnetism of sedimentary rocks. Bull. earthquake res. Inst. Tokyo Univ., 31, 276-296.

Nakajima, T. and Kawai, N., 1975. Palaeomagnetism of Lake Biwa sediment. Rock magnetism and palaeogeophysics. Pub. Rock magnetism and palaeogeophysics res. group Japan., 3, 24-31.

Nesbitt, J.D., 1966. Variation of the ratio of intensity to susceptibility in red sandstones. Nature, 210, 618.

N.E.R.C. (1974). The Clyde Estuary and Firth: an assessment of present knowledge. N.E.R.C. publication. Series C No 11., May 1974.

Oberg, C.J. and Evans, M.E., 1977. Spectral analysis of quaternary palaeomagnetic data from British Columbia and its bearing on geomagnetic secular variation. Geophys. J. R. astr. Soc., 51, 691-699.

Opdyke, N.D., Ninkovich, D., Lowrie, W. and Hayes, J.D., 1972. The palaeomagnetism of two Aegean deep sea cores. Earth Planet. Sci. Lett., 14, 145-149.

Papamarinopoulos, S., 1978. Ph.D. thesis, University of Edinburgh.

Parker, R.L. and Denham, C.R., 1979. Interpolation of unit vectors. Geophys. J. R. astr. Soc., 58, 685-687.

Peddie, N.W., 1979. Current loop models of the earth's magnetic field. J. geophys. Res., 84, 4517-4523.

Runcorn, S.K., 1959. On the theory of geomagnetic secular variation. Ann. Geophys., 15, 87-92.

Runcorn, S.K., Benson, A.C., Moore, A.F. and Griffiths, D.H., 1951. Measurements of the variation with depth of the main geomagnetic field. Phil. Trans. Roy. Soc., 244A, 113-151.

Shaw, J., 1974. A new method of determining the magnitude of the palaeomagnetic field. Application to five historic lavas and five archaeological samples. Geophys. J. R. astr. Soc., 39, 133-141.

Skiles, D.D., 1970. A method of inferring the direction of drift of the geomagnetic field from palaeomagnetic data. J. Geomag. Geoelectr., 22, 441-461.

Sissons, J.B., 1967. Glacial stages and radiocarbon dates in Scotland. Scott. J. Geol., 3, 375-381.

Sissons, J.B., 1974. The Quaternary in Scotland: a review. Scott. J. Geol., 10, 311-337.

Smith, P.J., 1970. In Palaeogeophysics (ed. S.K. Runcorn) Acc. Press, London.

Snape, C., 1971. An example of anhysteretic moments being induced by alternating field demagnetisation apparatus. Geophys. J. R. astr. Soc., 23, 361-364.

Stacy, F.D., 1972. On the role of Brownian motion in the control of detrital remanent magnetisation of sediments. Pure App. Geophys., 98, 139-145.

Stacy, F.D. and Banerjee, S.K., 1974. The physical principles of rock magnetism. Elsevier, Amsterdam.

Stewart, D.A., 1978. Ph.D. thesis, University of Glasgow.

Stober, J.C. and Thompson, R., 1977. Palaeomagnetic secular variation studies of Finnish lake sediments and the carriers of remanence. Earth Planet. Sci. Lett., 37, 139-149.

Thellier, E. and Thellier, O., 1959. Sur l'intensite du champ magnetique terrestre dans le passe historique et geologique. Ann. Geophys., 15, 285-376.

Thellier, E., 1968. Geophysique tirage. In Encyclopidie de la Pleiade.

Thompson, R., 1975. Long period geomagnetic secular variation confirmed. Geophys. J. R. astr. Soc., 43, 847-859.

Thompson, R. and Kelts, K., 1974. Holocene sediments and magnetic stratigraphy from Lakes Zug and Zurich, Switzerland. Sedimentology, 21, 577-596.

Thompson, R., Battarbee, R.W., O'Sullivan, P.E. and Oldfield, F., 1975. Magnetic susceptibility of lake sediments. Limnol. Oceanogr., 20, 687-698.

Thompson, R. and Wain-Hobson, T., 1979. Palaeomagnetic and stratigraphic study of the Loch Shiel marine regression and overlying gyttja. J. Geol. Soc. Lond.,136, 383-388.

Thompson, R. and Morton, D.J., 1977. Magnetic susceptibility and particle size distribution in recent sediments of the Loch Lomond drainage basin, Scotland. J. Sed. Pet., 49, 810-812.

Tite, M.S. and Linington, R.E., 1975. The effect of climate on the magnetic susceptibility of soils. Nature, 256, 565-566.

Ulrych, T.J. and Bishop, T.N., 1975. Maximum entropy spectral analysis and autoregressive decomposition. Rev. Geophys. Space Phys., 13, 183-200.

Walker, ., 1977, PhD Thesis, University of Liverpool.

Walton, D., 1979. Geomagnetic field intensity in Athens between 2000 B.C. and A.D. 400. Nature, 277, 643-644.

Watson, G.S. and Beran, R.J., 1967. Testing a sequence of unit vectors for serial correlation. J. geophys. Res., 72, 5655-5659.

*Earth and Planetary Science Letters*, 42 (1979) 412–426




# BEHAVIOUR OF THE EARTH'S MAGNETIC FIELD AS RECORDED IN THE SEDIMENT OF LOCH LOMOND

G.M. TURNER and R. THOMPSON

*Department of Geophysics, University of Edinburgh, Edinburgh (Great Britain)*

Received June 9, 1979
Revised version received November 27, 1978

A palaeomagnetic record of geomagnetic secular variation during the last 7000 years has been obtained from the sediments of Loch Lomond, Scotland. The magnetic direction fluctuations repeat well between cores and show greater detail, especially over the last 5000 years, than other European records. A time scale has been derived from $^{14}C$ analyses on the Lomond sediment and comparison with other $^{14}C$-dated sediments. Investigation of relative palaeointensity determination methods has shown that the widely used normalization parameter of partial ARM is insensitive to even small sediment grain size fluctuations.

The new high-fidelity direction record and improved time scale show that geomagnetic field changes have not followed a simple oscillatory pattern during the last 7000 years. The record enhances the application of palaeomagnetism to dating recent sediments, as the main declination swings are now characterized by fine detail, and paired inclination data are also available. The problem of mismatching swings when correlating with other paired directional records is thus reduced.

The palaeomagnetic record agrees well with some archaeomagnetic results. It confirms the period of anticlockwise motion of the geomagnetic field vector, between 1000 and 600 years B.P., which was first documented by English archaeomagnetic investigations. Clockwise motion is shown to predominate during the remainder of the last 5500 years. The VGP path does not correlate with that of Japanese archaeomagnetic results nor North American sediment data from 2000 to 0 years B.P. This suggests that the secular changes are dominated by local non-dipole sources rather than wobbling of the main geomagnetic dipole.

## 1. Introduction

Lake sediments contribute to our understanding of recent behaviour of the geomagnetic field by extending continuously the few hundred years' record available from geomagnetic observatory data. Mackereth [1] first observed geomagnetic field changes faithfully recorded in lake sediments. Several other British sites have since been investigated [2] in order to extend the record to include inclination data and check the reproducibility of the palaeomagnetic variations. The sediments of Loch Lomond (56°N, 5°W) contain the highest quality, most detailed and most reproducible palaeomagnetic record of any lake so far investigated. The age of the sediments is assessed by $^{14}C$, pollen and $^{210}Pb$ investigations. The Lomond sediments thus provide a new, high-fidelity record of fine-scale short-term geomagnetic behaviour over the last 7000 years.

## 2. Instrumentation

### 2.1. Core collection

The deep sediments were collected using 6-m-long piston corers [3] operated by compressed air. Two different 6-m corers were used. Both obtained sediment in UPVC tubing of 60 mm external diameter and 54 mm internal diameter. The deep sediment from the northern end of the loch has a comparatively slow rate of deposition, about 0.3 mm/year, and the central part of the loch has a complicated history. So sampling for geomagnetic investigations

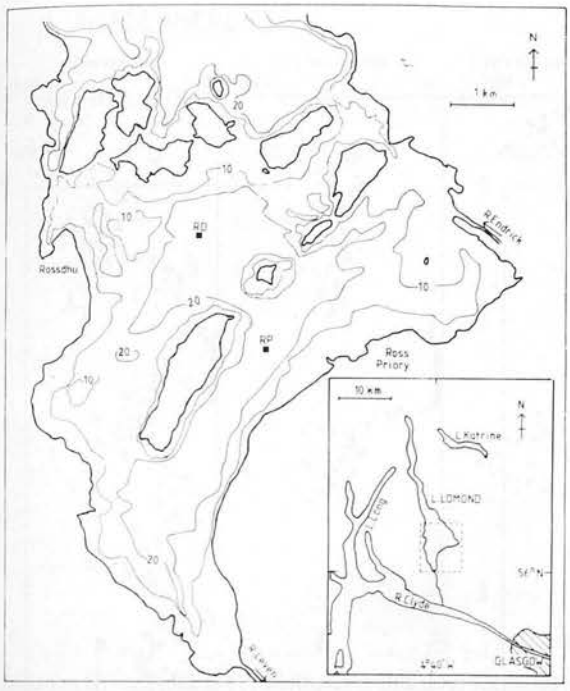


Fig. 1. South basin of Loch Lomond bathymetry (in metres) and coring sites *RP* = Ross Priory; *RD* = Rossdhu. Inset shows location in west of Scotland.

was concentrated in the wide, relatively flat-bedded, southern area (Fig. 1). One-metre Mackereth cores were collected at site *RP* by F. Oldfield. We collected 1.28-m Mackereth cores at other shallow and deep water sites. These "mini" and "midi" Mackereth cores are kept in a vertical position both during coring and transport back to the laboratory. The mud/water interface is therefore preserved in detail. In fact the Lomond sediment is so stiff that very little disturbance occurred in the 6-m cores and less than 20 mm of sediment was lost from the top of them.

### 2.2. *Magnetic measurements*

Whole core horizontal remanence measurements were made using a fluxgate magnetometer [4] and whole core susceptibility scanned using an air cored coil system [5]. The same instruments with smaller aperture sensing heads were used to analyse the 6-ml subsamples. The noise level of the magnetometer was 0.1 mA $m^{-1}$ and the susceptibility bridge had a noise level of $0.2 \times 10^{-7}$ SI units for 6-ml specimens.

Alternating field demagnetization and ARM production were carried out at a frequency of 50 Hz in a triple, inductoral driven, high-$Q$ coil capable of producing a peak alternating field of 100 mT. Isothermal remanence was produced by a conventional electromagnet with flat 55-m-diameter pole pieces.

## 3. Rossdhu and Ross Priory cores

In 1976 four 6-m and three mini cores were taken from two sites in the southern, broad, comparatively shallow basin of the loch. LLRD1, LLRD2 and LLRD3, each over 4.75 m in length, were taken from a site at 24 m depth near Rossdhu, north of the chain of islands delineating the Highland Boundary Fault. LLRP4, of similar length, and LLRPM1, LLRPM2 and LLRPM3, each about 0.8 m long, were taken from a site near Ross Priory, 2 km away and south of the islands, in 28 m of water. All four long cores have been subsampled and carefully analysed. These analyses are described in detail for one of the cores, LLRD1.

### 3.1. *Core LLRD1 description*

The core spans the time period from the last deglaciation of the loch, ca. 10,000 years B.P. [6] to the present. A simplified lithology is shown in Fig. 2a. From the base, 5.10 to 4.90 m is a band of thick, green-grey clay. From 4.90 to 3.80 m the sediment is mainly brown gyttja with occasional dark-greenish bands about 5 mm wide, and broken by another green-grey clay band from 3.92 to 3.90 m.

Between 3.80 and 3.05 m there is a distinct, clearly bounded section of much darker, very uniform sediment of lower water content. This has been identified as a marine phase of the loch, by the discovery of marine dinoflagellate cysts, exclusive to this section of core [11], and marine bivalves. Above the marine sediment is 0.25 m of very finely laminated gyttja, each band being less than 1 mm thick. The remaining 2.80 m to the top of the core is a uniform, fine-grained, dark yellowish-brown gyttja, similar to that below the marine section.

Two very light-coloured clay bands at 2.96 and

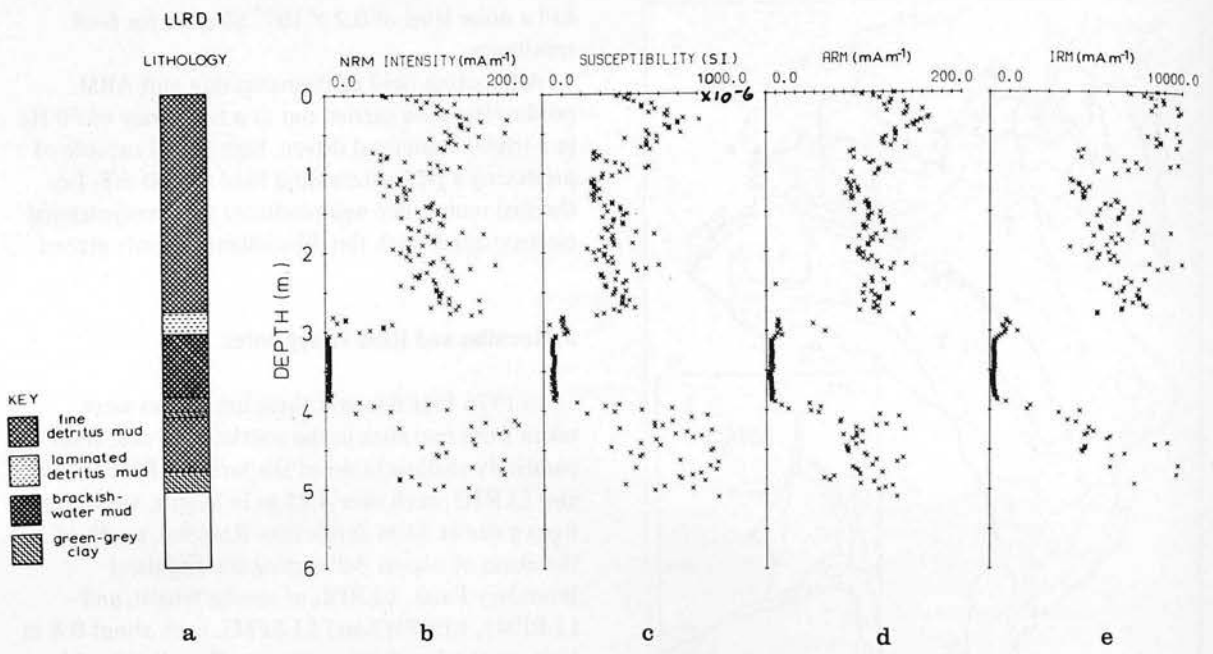


Fig. 2. Logs of (a) lithology, (b) natural remanent magnetic intensity, (c) initial reversible susceptibility, (d) anhysteretic remanent magnetization, and (e) isothermal remanent magnetization for core LLRD1.

2.02 m, each about 1 mm thick, have also been used in correlating the cores of the series.

### *3.2. Magnetic properties*

Figs. 2b, c and 3b, c show measurements of NRM intensity, magnetic susceptibility, declination and inclination on subsamples from core LLRD1. The susceptibility record shows much detail, and a high degree of variation, indicating large changes in the fractional magnetic content of the sediment. Sixteen features, maxima, minima, and points of inflection, are identified in the uppermost 3.5 m. These are used later in comparing LLRD1 with the other cores in the series.

The same 16 features are present and at the same levels in the top 3.5 m of the NRM intensity record. This similarity between NRM intensity and susceptibility is a good indication that the remanence is of detrital origin, but also shows that it is strongly dependent upon the magnetic content of the sediments, in addition to any dependence on palaeofield intensity. The NRM intensity and susceptibility are higher than in most European gyttja we have studied. The marine and freshwater sediments have different origins and magnetic properties. Both NRM intensity and susceptibility are markedly low in the marine section. They have mean values of 1 mA $m^{-1}$ and $4 \times 10^{-7}$ SI units respectively (Fig. 2b, c).

The remanence directions in the freshwater gyttja are very stable. The directions show remarkably little change throughout the whole coercivity spectrum (Fig. 4). Eight representative pilot samples were subjected to stepwise partial alternating field demagnetization in peak fields up to 95 mT. No secondary components could be detected and cleaned directional results do not differ significantly from the NRM directions. All subsamples were cleaned at 20 mT and again no changes in direction were noted. The unusual laminated sediment above the marine sequence was slightly viscous. This viscous component was removed by our standard treatment of zero field storage before NRM measurement.

Both declination and inclination logs show well-defined swings, with peak to peak amplitudes of about 45° and 15° respectively, and little scatter (Fig. 3b, c). There is slightly more scatter in the

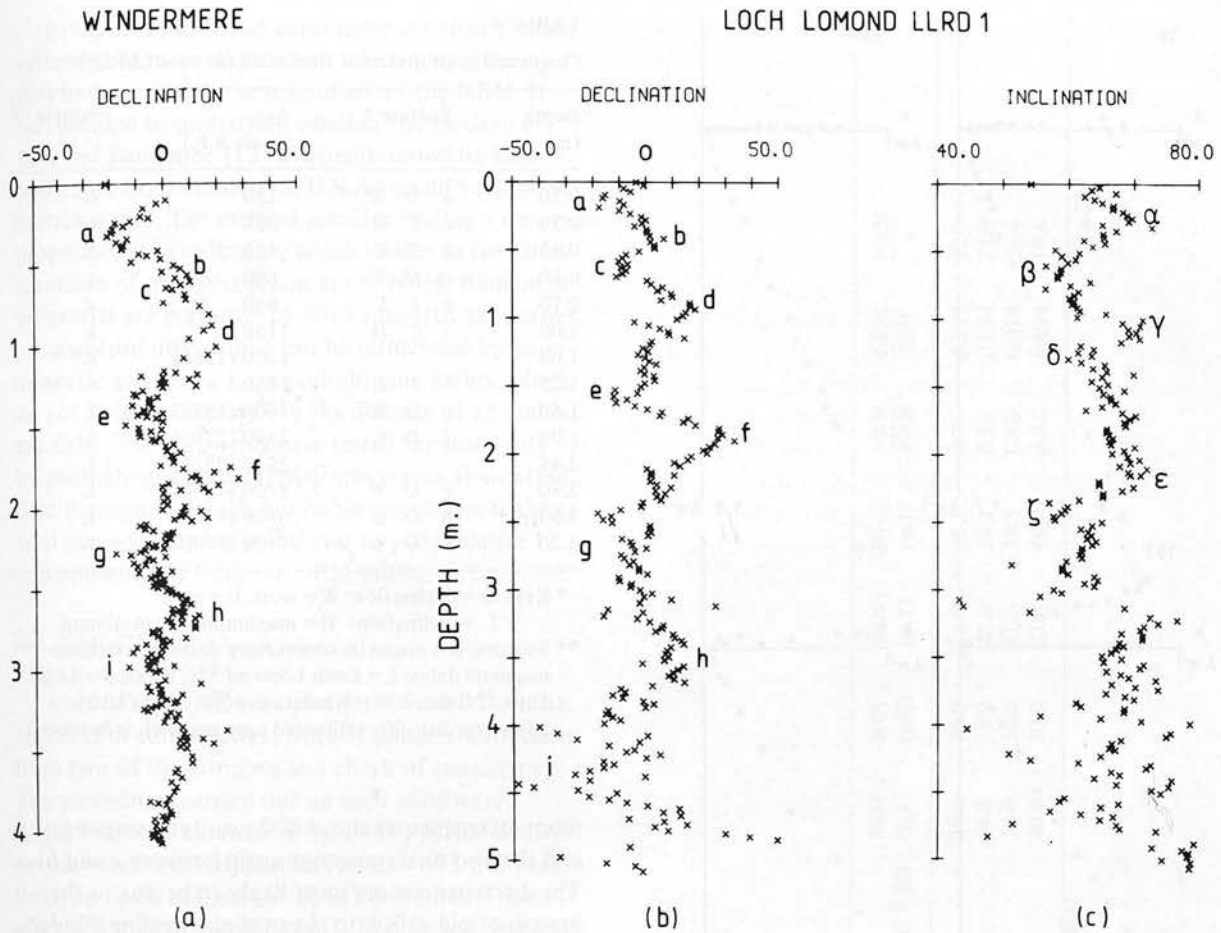


Fig. 3. (a) Palaeomagnetic relative declination log for Lake Windermere. (b), (c) Relative declination and inclination for core LLRD1.

marine sediments where the intensity is low, and below the marine, owing to sedimentological changes. The detail between major swings, and the definition of the inclination curve is clearer than has previously been recorded from British lakes, e.g. Windermere [3]. LLRD1 has a deposition rate approaching twice that of the Windermere core, and the uppermost sediments have a much lower water content. Consequently the record near the top of the core is much more clearly defined. In particular, declination swing *a-b-c* is of comparable amplitude with the other major swings, which was not apparent from Lake Windermere. Also the broad double nature of westerly swings *e* and *g* is quite distinct from the sharpness of swing *f* (Fig. 3b).

### *3.3. Dating*

A suite of $^{14}C$ age determinations have been made on core LLRD1 by Baxter and Drndarsky [7]. Baxter and Swann [8] have carried out $^{210}Pb$ dating on the companion 1-m core, LLRPM1. Also the magnetic declination and inclination swings can be compared with (1) London magnetic observatory records for the last 250 years, with (2) archaeomagnetic direction curves [9,10] extending back to 1700 years B.P., and with (3) the $^{14}C$-dated curve obtained by Mackereth [1] on Lake Windermere sediment in 1971. The correlations drawn, and ages assigned, are summarized in Table 1 and Fig. 6. Pollen analyses give further checks on the dating of Table 1 and Fig. 6. In particular, the

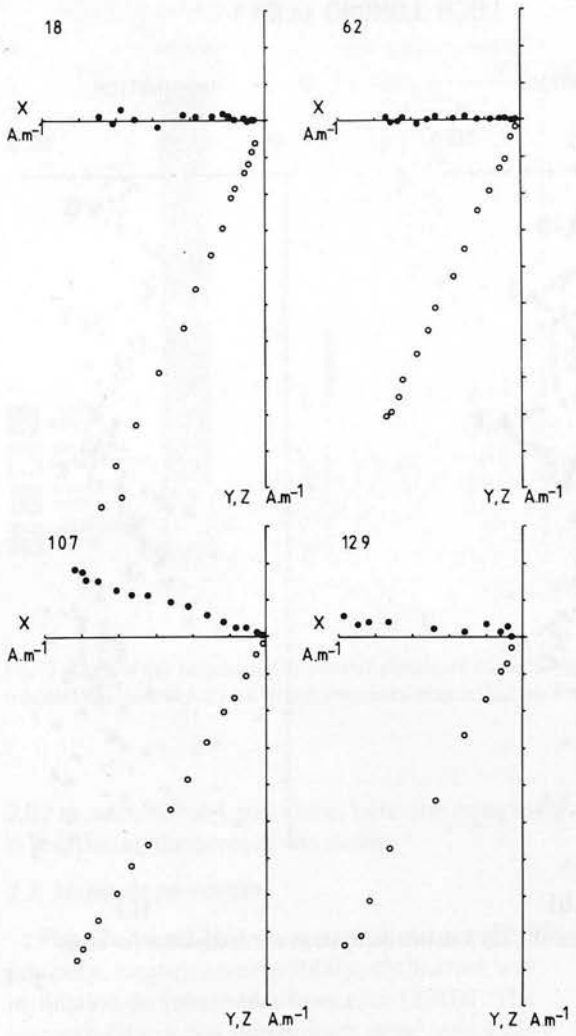


Fig. 4. Zijderveldt plots for step partial AF demagnetization of pilot samples 18, 62, 107 and 129 from core LLRD1. Closed circles represent end point of remanence vector projected on to horizontal plane; open circles projection on to north-south vertical plane. Samples 18, 62, 107, one scale division = 10 mA $m^{-1}$; sample 129, one scale division = 2 mA $m^{-1}$.

elm decline and alder rise are recognisable at 3.10 and 3.50 m, although somewhat complicated by the marine succession [11].

The radiocarbon dates do not compare well with the Windermere dates for correlated swings earlier than 1000 years B.P. The Lomond ages are generally younger than those for Windermere. There is a maximum divergence of about 800 years at swings *e* and *f*, and the two series converge again between *g* and *h*. The discrepancies are most likely to be due to the inwash of old soils into the post-elm decline Windermere sediment, producing anomalously old ages. For this reason the younger Loch Lomond dates have been used in the construction of a "preferred time scale" and sedimentation curve (Fig. 6). The $^{14}C$ dates have been calibrated against Clark's [12] bristlecone pine dendrochronological scale.

TABLE 1

Construction of preferred time scale for core LLRD 1

| Depth (m) | Feature * | Age (years B.P.) | Source ** |
|---|---|---|---|
| 0.20 | *a* D W | 150 | o |
| 0.30 | α I H | 250 | o |
| 0.45 | *b* D E | 450 | a |
| 0.60 | *c* D W | 600 | a |
| 0.70 | β I L | 650 | a |
| 1.00 | γ I H | 1150 | a |
| 1.08 | | 1300 (1265) | L |
| 1.25 | δ I L | 1650 | a |
| 1.60 | *e* D W | 2000 (1950) | L |
| 1.90 | *f* D E | 2500 (2705) | S |
| 2.45 | | 3550 (3925) | L |
| 2.70 | *g* D W | 4200 (4860) | L |
| 3.60 | *h* D E | 6300 (7165) | L |
| 4.20 | *i* D W | 7400 (8400) | W |

* Key: D = declination: W = west, E = east.
I = inclination: H = maximum, L = minimum.

** Sources: o = magnetic observatory dates; a = archaeomagnetic dates; L = Loch Lomond $^{14}C$ dates; S = Loch Shiel $^{14}C$ dates; W = Windermere $^{14}C$ dates (Libby 5568-year half-life; calibrated ages are given in brackets).

### *3.4. Relative palaeointensity determination*

Study of the ancient geomagnetic field falls into two sections, the secular variation with time of (1) the field direction and (2) the field intensity. The former is provided directly by the direction of stable remanence. However, the stable magnetic intensity of a sample depends not only on the ancient field intensity, but also on the quantity of magnetic material which carries the remanence. This second dependence must be removed in assessing palaeointensities.

In the Loch Lomond cores there are clearly large variations in magnetic content which play a strong part in determining the magnitude of the NRM. It was decided to investigate whether the method of Levi and Bannerjee [13] originally tested on lake sediments from Minnesota, U.S.A., could be applied in such a case. The method involves finding a remanent property of the sediment, which resides in the same spectrum of magnetic grains as the NRM. Remanent properties are preferred to other magnetic properties, e.g. susceptibility, which can be influenced by paramagnetic grains and large multidomain grains, which do not hold a remanence in the absence of an ambient field. The remanences are tested for suitability by comparing their coercivity spectra on alternating field demagnetization. A suitable remanence is then used as a normalizing parameter to yield relative palaeointensities from the NRM values.

### *3.5. Pilot samples*

A set of eight pilot samples was selected from six horizons in core LLRD1; pairs of samples were taken from two of the horizons as a check of consistency. The procedures carried out on each pilot were:

(1) Stepwise alternating field (AF) partial demagnetization of the NRM, at increments of 5 mT peak field, up to 50 mT, and at 10 mT increments thereafter to a maximum of 100 mT. The sample was held stationary and demagnetized consecutively in three orthogonal directions. Then to minimize any parasitic ARMs grown, due to impurities in the waveform of the coil, the final direction was reversed with the peak field halved [14].

(2) Growth of ARM in a bias field of 0.042 mT (ambient laboratory field) superimposed on and parallel to a smoothly decaying alternating field of peak value, 95 mT.

(3) Stepwise AF demagnetization of ARM, as for NRM.

(4) Growth of IRM in 100 mT direct field.

(5) Stepwise AF demagnetization of IRM, as for NRM.

The results are shown in Table 2 and plotted in Fig. 5. The ARMs were generally of the same order of magnitude as the NRMs whereas the IRMs were some 80 times larger. The NRMs and ARMs generally had similar coercivity spectra, the NRMs were slightly

TABLE 2

Pilot samples

| Sample No. | Depth (m) | NRM (mA m$^{-1}$) | ARM (mA m$^{-1}$) | IRM (mA m$^{-1}$) | $\chi$ ($\times 10^{-6}$ SI) | $MDF_N$ (mT) | $MDF_A$ (mT) | $MDF_I$ (mT) | $H_{CR}$ (mT) | $\frac{NRM}{ARM}$ | $\frac{NRM}{IRM}$ | $\frac{NRM}{\chi}$ |
|---|---|---|---|---|---|---|---|---|---|---|---|---|
| 18 | 1.177 | 113 | 150 | 10,000 | 5.0 | 26.0 | 25.0 | 18.0 | 33.5 | 0.76 | 0.011 | 22.7 |
| 62 | 2.210 | 88 | 105 | 6130 | 3.2 | 36.5 | 35.0 | 20.0 | 39.5 | 0.84 | 0.014 | 27.9 |
| 107 | 3.267 | 103 | 123 | 7600 | 3.4 | 36.0 | 36.0 | 21.0 | 38.5 | 0.83 | 0.014 | 30.4 |
| 129 | 3.788 | 19 | 60 | 1400 | 1.0 | 20.0 | 20.0 | 22.0 | 40.0 | 0.32 | 0.014 | 19.4 |

$\times(4\pi)^2$ $\div(4\pi)^2$

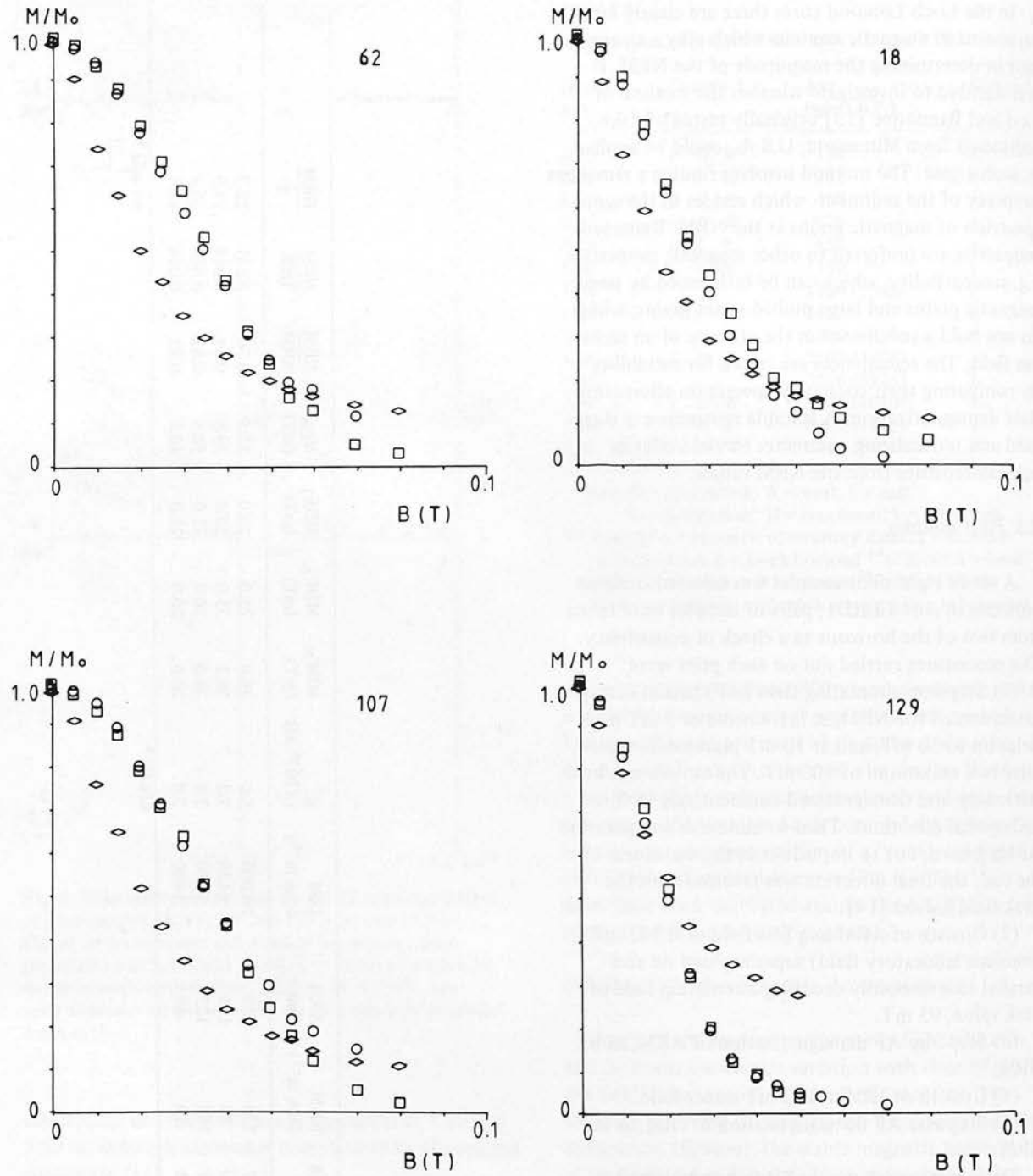


Fig. 5. Normalized partial alternating field demagnetization curves of NRM (circles), ARM (squares) and IRM (diamonds) for pilot samples of Fig. 4.

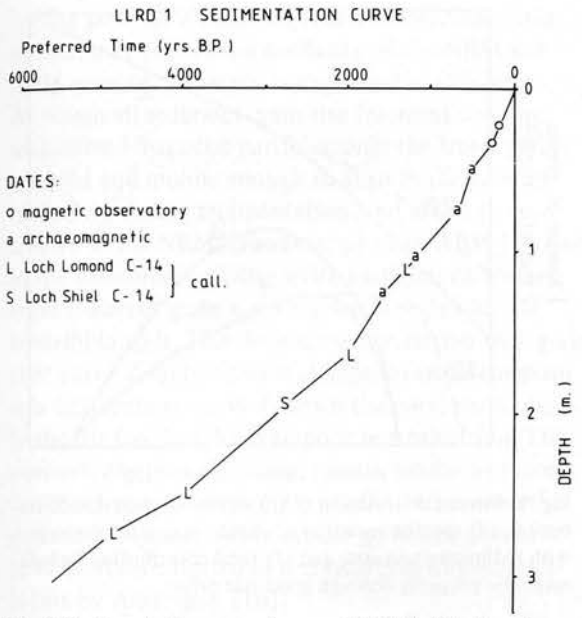


Fig. 6. Sedimentation curve for core LLRD1. "Preferred time scale" from Table 1.

harder in all cases, and the IRMs were considerably softer than both. The modified Lowrie-Fuller [15] test thus suggests the remanence carriers to be single domain.

Samples 62 and 107 characterize the remaining pilot samples not shown. The similarity of spectra in all samples, except sample 18 at the very top of the core, and sample 129 in the marine, shows that the nature of the magnetic mineral does not change significantly in the freshwater section of the core. This means that in the top 3 m the magnetic fraction is internally homogeneous, although its concentration in the sediment varies by a factor of 2.

When NRM was plotted against ARM and IRM in turn for each pilot, the ARM curve always showed a straight portion corresponding to demagnetizing fields from 0 to 40 mT. A gradient and hence unique NRM/ARM ratio could be assigned to this portion. There was, however, no such straight section to the NRM vs. IRM curves, and hence no section over which the coercivity spectra were comparable. From

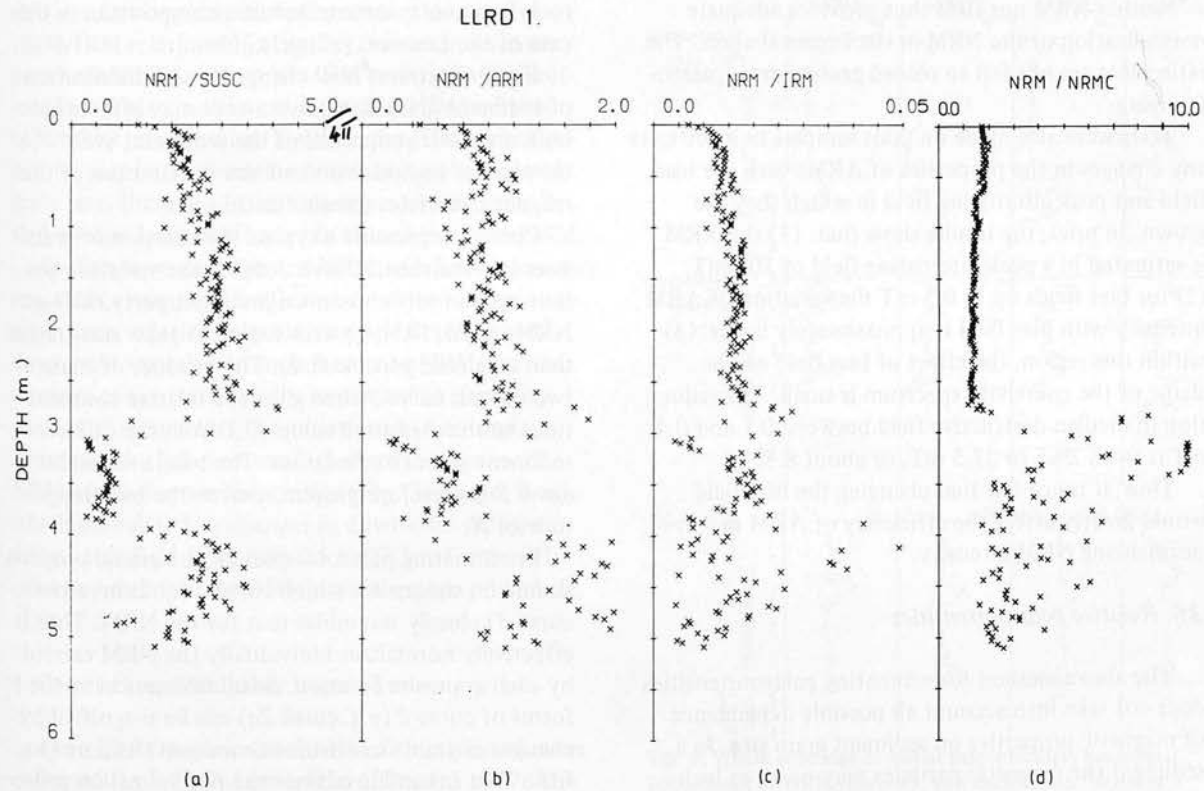


Fig. 7. Ratios of NRM to (a) initial susceptibility, (b) ARM, (c), IRM and (d) cleaned NRM vs. depth for core LLRD1.

these relationships ARM would appear to be a suitable normalizing parameter.

Following this comparison, ARMs and then IRMs were grown and measured in all the samples of the core, under the conditions described above (Fig. 2d, e). Both properties show the same trends and peak at the same horizons as NRM and susceptibility, though to different extents. Both reflect the very marked drop in magnetic concentration in the marine section. The ratios of NRM/ARM and NRM/IRM were finally calculated and plotted for the core (Fig. 7). Although ARM has an apparently suitable coercivity spectrum for the Levi and Bannerjee method, it does not appear to normalize the magnetic content completely. The same peaks are still visible in the ratio, though greatly reduced in amplitude. IRM, however, despite its unpromising coercivity spectrum, does give a deceptively smooth curve for the top 3 m of magnetically homogeneous sediment. This is perhaps a caution against using such a parameter for normalization without previously testing its suitability.

Neither ARM nor IRM thus provides adequate normalization of the NRM in the Lomond cores. The ratio plots are not felt to record geomagnetic palaeointensity.

Tests were also made on pilot samples to investigate any changes in the properties of ARMs with the bias field and peak alternating field in which they are grown. In brief, the results show that: (1) the ARM is saturated in a peak alternating field of 100 mT; (2) for bias fields up to 0.5 mT the variation of ARM intensity with bias field is approximately linear; (3) within this region, the effect of bias field on the shape of the coercivity spectrum is small. The reduction in median destructive field between 0.1 and 0.4 mT is from 29.5 to 27.5 mT, or about 8.5%.

Thus, it is not felt that changing the bias field would greatly affect the efficiency of ARM in normalizing NRM intensity.

### *3.6. Relative palaeointensities*

The above method for estimating palaeointensities does not take into account all possible dependence of magnetic properties on sediment grain size. In a sediment the magnetic particles may occur as inclusions in larger sediment grains (like currants dispersed in a bun); these larger grains being simply silt-sized rock fragments, some of basaltic composition in the case of the Lomond sediment.

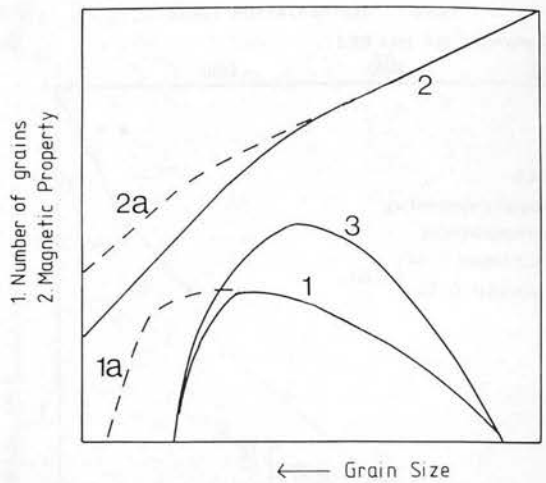


Fig. 8. Schematic variation of (*1*) sediment grain size distribution, (*2*) specific variation of chosen magnetic property with sediment grain size, and (*3*) total contribution to bulk magnetic property through grain size range.

Fig. 8 illustrates how changes in the distribution of sediment grain size down a core may affect the bulk magnetic properties of the sediment, even though the composition and size distribution of the magnetic particles remains unchanged.

Curve *1* represents a typical distribution of grain sizes in a sediment. Curve *2* shows the variation per unit mass of any chosen magnetic property, $X$ (e.g. NRM, ARM, IRM, $\chi$) with sediment grain size (rather than magnetic particle size). The product of these two curves, curve *3* then gives the relative contributions to the measured value of $X$ from the different sediment grain size fractions. The total area under curve *3* is therefore proportional to the bulk magnitude of $X$.

In estimating palaeointensities a magnetic property should be chosen for which curve *2* (and therefore curve *3*) closely resembles that for the NRM. Thus it effectively normalizes individually the NRM carried by each grain size fraction. Small differences in the forms of curve *2* (e.g. curve *2a*) can be magnified by changes in grain size distribution down the core (e.g. from *1* to *1a*) and invalidate the normalization procedure.

The poor normalization of the NRM/ARM ratio in Lomond, despite the similarity of the NRM and ARM coercivity spectra, is explained as follows. Although all sediment grain size fractions contain magnetized magnetic particles, only the finest grains are light and mobile enough to align in the geomagnetic field during sedimentation, and hence to contribute to the NRM. However, when an ARM is grown in the laboratory, all magnetite particles, no matter what sediment grain size they are included in, can contribute to it. This difference in variation with grain size, curve *2*, coupled with changes in sediment grain size distribution, curve *1*, down the core, particularly in the silt fraction, leads to poor normalization. The coercivity spectra, however, remain similar as there is little change in magnetic particle size between the grain size fractions. Very similar grain size effects have been investigated in reconstituted abyssal sediments by Amerigian [16].

The relationship between NRM and susceptibility is similar to that between NRM and ARM (Fig. 7b). This suggests that susceptibility and ARM vary with grain size in a similar manner. The smoother down-core NRM/IRM relationship (Fig. 7c), however, remains problematic. We suggest the IRM variation with sediment grain size is different from the ARM and susceptibility relationships. Further, the IRM variation is such that in combination with changes in sediment grain size, there is a fortuitous approximate cancellation so that bulk IRM varies in a similar way to NRM.

In summary, similarity of NRM and ARM coercivity spectra is alone not a sufficient condition for estimating ancient relative palaeointensities. Constancy of down-core variation in such factors as NRM/cleaned remanence are tests equally important as similarity of coercivity spectra. The variations in Lomond demonstrate that even small changes in down-core NRM/cleaned remanence ratios (Fig. 7d, upper 3 m) which are related to changes in down-core median destructive field from only 25 to 27.5 mT are sufficient to invalidate the ARM normalization procedure.

## 4. Correlations with other Lomond cores

Core LLRD1 is representative of the series of cores collected from Loch Lomond in 1976 and 1977. The importance of obtaining several correlated records, before interpreting their features as geomagnetic field changes, rather than due to local influence, has been stressed previously [17]. Correlations can be drawn on three levels: (1) between duplicate cores obtained from the same site; (2) between different sites within a lake; and (3) between different lakes, in different geographical and geological environments.

Magnetic measurements for the 6-m Rossdhu and Ross Priory cores are shown in Fig. 9. These measurements of magnetic susceptibility and the horizontal component of NRM were made on all the cores while still in the core tube. Their traces are smoother than for single sample measurements as they are slightly smoothed by the instrument response [4,5].

Susceptibility is probably the most sensitive parameter for correlation between the cores, as the Lomond records show large amplitude variations which are easily resolved in each, and these are independant of geomagnetic field changes. The 16 characteristic features previously noted in LLRD1 are visible in all

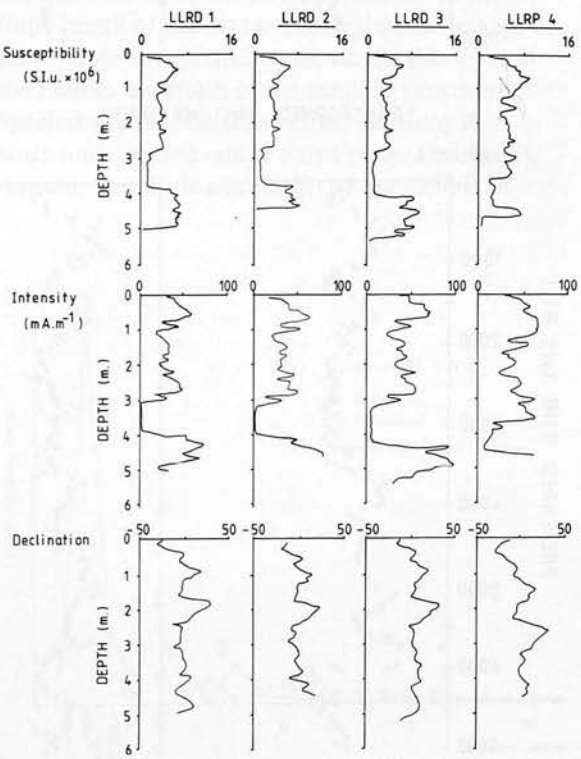


Fig. 9. Whole core logs of initial susceptibility, horizontal component of NRM intensity, and declination for cores LLRD1, -D2, -D3 and LLRP4.

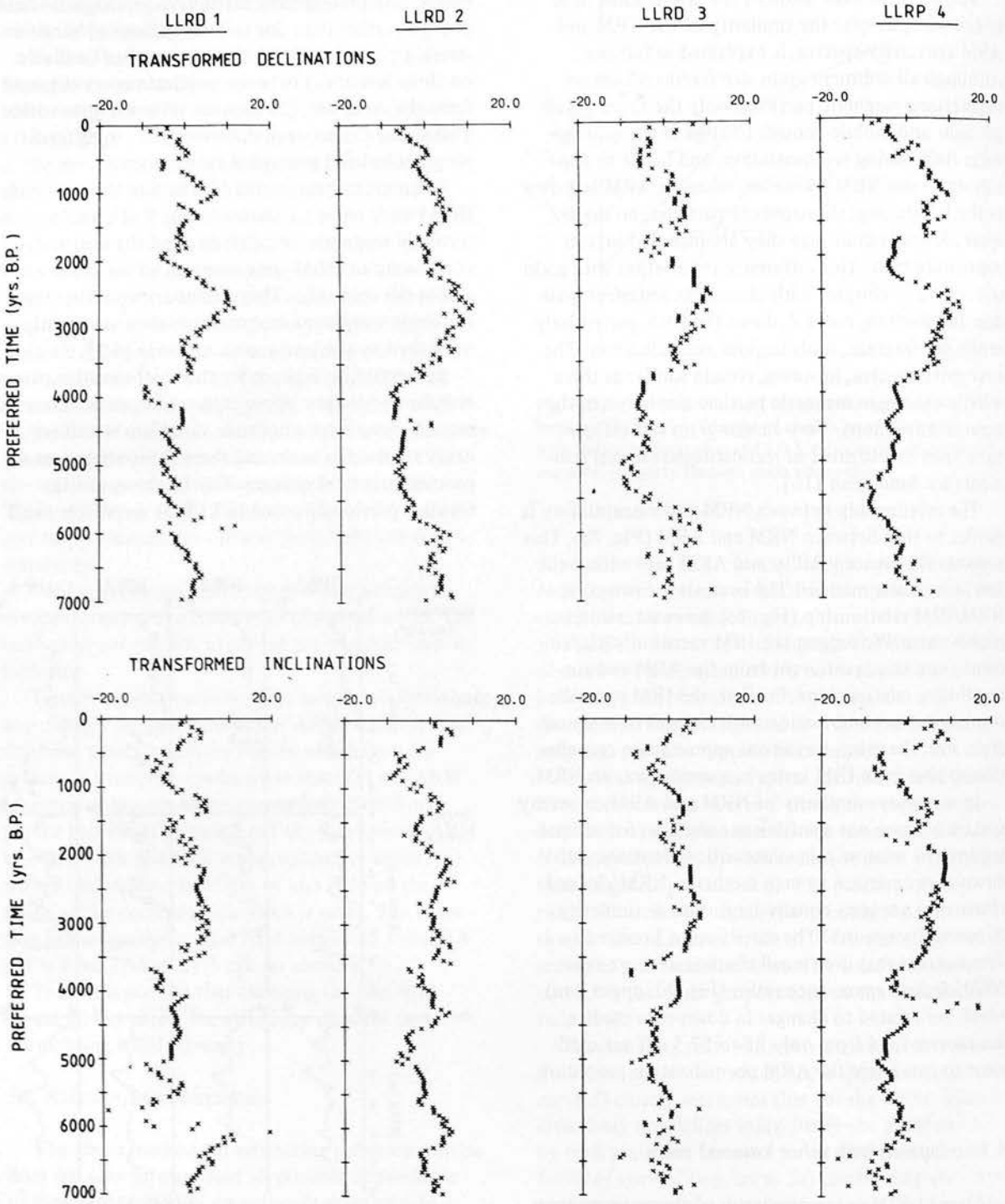


Fig. 10. "Transformed" declination and inclination logs, plotted against preferred time for cores LLRD1, -D2, -D3 and LLRP4.

four records. The two sites thus appear to have the same principal source of sediment. The features occur at the same depths in cores LLRD1, -D2, -D3, the correlation coefficient between LLRD1 and -D3 being 0.95. This implies an equal deposition rate in each of the Rossdhu cores over the time period spanned, and supports a model of spatially uniform deposition in this part of the loch. Also, when LLRD1 and LLRP4 are compared, approximately equal deposition rates are found through the core except in the top metre. The uppermost susceptibility peak is much more expanded in LLRP4, indicating a relative acceleration in sedimentation compared with LLRD1. Thus the older susceptibility features occur about 0.5 m deeper in LLRP 4 than in the LLRD cores; the marine section is between 4.50 and 3.50 m (Fig. 9). The ratio of deposition rate in LLRP4 to that in LLRD1 over the past 1000 years is calculated as 1.48. The NRM intensity and declination records support such a correlation, and also show this divergence in relative deposition rates in the uppermost sediment.

## 5. Palaeomagnetic directions and spectral analysis

The pattern of declination in the Loch Lomond sediments is very similar to that obtained by Mackereth from Lake Windermere [1]. The peak to peak declination amplitude of 40–45° in Lomond is in close agreement with the Windermere results. The scatter of directions is, however, much lower in the new Lomond results and finer-scale fluctuations are apparent. The Lomond inclination variations have peak to peak amplitudes of 10–15° in agreement with previous British data from Lough Neagh [2] and Windermere [2]. Again the signal to noise ratio is improved in the Lomond sediment and more details are visible.

With such data available, it was decided to attempt to set the correlations and results discussed above on a firmer, more quantitative basis. Firstly, the "preferred time scale" described in section 3.3 was transferred to the other three cores, using the susceptibility feature correlations. Since susceptibility variation has no dependence on geomagnetic field changes, this method preserves the independence of the four data sets. By a process of linear interpolation between the age horizons, and then by further interpolation between the data values, sets of declination and inclination values were obtained at equal intervals of time for each core. Linear interpolation was chosen to minimize the dependence introduced between the data points in the records.

Also, to remove the effect of site latitude on the relative amplitudes of variation of the declination and inclination records, the mean direction for each core was rotated to zero "transformed" declination and inclination. (The mean direction is found by averaging the direction cosines of the unit vectors formed from each declination/inclination pair.) This has the effect of roughly equalizing the amplitudes of variation. The resulting logs of "transformed" declination and inclination against "preferred time" are shown in Fig. 10.

Prior to spectral analysis, each of the records was detrended, and then a cosine taper fitted to the first and last 10% of each. These procedures reduce the amplitudes of the zero and fundamental frequencies, which would otherwise be magnified due to the finite length of the data set, and minimize leakage of power from the spectral peaks, via the side lobes in the Fourier transform of the sampling function. Spectral analysis was then carried out using R. Singleton's "mixed radix" Fast Fourier transform method. Very little adjustment of the number of

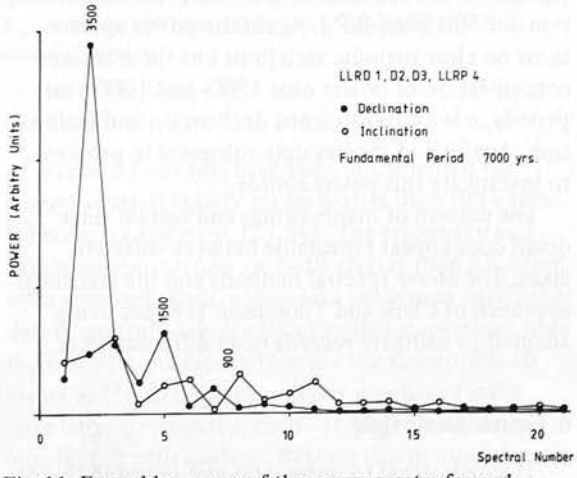


Fig. 11. Ensemble average of the power spectra formed from the transformed declinations and inclinations of four cores of Fig. 10 covering the last 7000 years.

data points is required, as this method can deal with multiples of powers of prime numbers. So a maximum of one or two points were discarded from each record.

The power spectra thus obtained for all four cores were then stacked to form the "ensemble average" over the set (Fig. 11). Since data sets of only 7000 years' length were used, little reliability is placed in the period of the major peak in both declination and inclination, only to say that there is some long-period power in both. However, the 1500-year and 1000-year peaks do rise above the noise level in both spectra, and are felt to be significant, as four independent cores were averaged in this analysis. It was originally thought that the parallelism between declination and inclination spectra might be spuriously introduced during the rotation of axes to "transformed directions". Trial runs of sinusoidal records of different periodicities, however, show very little mixing of the spectra.

Declination and inclination patterns which are repeatable between cores are taken to be reflections of past geomagnetic field changes. For example, large amplitude long-period fluctuations are visible in all the transformed declination records (Fig. 10). These fluctuations are not periodic as their durations vary from 4000 years, in the lower part of the core, to 1700 years, in the upper part. Most of the power resides in these long-period fluctuations, in both the transformed declination and inclination records (Fig. 11). Shorter time scale fluctuations are also repeatable in all four cores (e.g. the declination inflection at 3500 years B.P.). Again the power spectra show no clear periodic variations but there is some concentration of power near 1500- and 1000-year periods in both transformed declination and inclination. Analysis of shorter data subsets is in progress to investigate this power source.

The pattern of major swings and certain finer detail does appear repeatable between different lakes. The above spectral methods and the statistical approach of Clark and Thompson [18] are being adapted to compare records from different lakes.

## 6. Geomagnetic field

The high signal to noise ratio and repeatability of the Lomond record allows an analysis of the combined declination and inclination records without any need for smoothing. In Fig. 12 Bauer curves of the transformed declination and inclination are plotted. Each point represents a 40-year increment and is an average from the four cores of Fig. 10. The major trends in the Bauer curves represent the direction changes of the geomagnetic field vector with time. A general clockwise sense of motion is dominant throughout the 5500-year record shown. The only extensive period of anticlockwise motion falls between 1100 and 600 years B.P. This anticlockwise section is in good agreement with English archaeomagnetic results [19]. Such an anticlockwise motion can be explained by an eastward drift, of a field similar to that predominating today, or by a field with very different spherical harmonic components from the present-day field [19]. Changes in intensity of the non-dipole field components may also produce anticlockwise motion. Harwood and Malin [20] have pointed out that the westward drift which has been going on since at least the time of Halley, 1693, has recently been slowing down and has now virtually stopped. A relatively rapid change from eastward to westward drift around 600 years B.P., as suggested by the change in sense of motion in both the archaeomagnetic and palaeomagnetic data, is thus not unlikely.

Kawai and Hirooka [21], on the basis of a comparison of Japanese and European archaeomagnetic results, have proposed that secular variation over the last 2000 years is caused mainly by a wobbling motion of the main geocentric dipole axis around the earth's rotation axis. The Lomond data do not support this model. A gap in the English archaeomagnetic record between 1600 and 1000 years B.P. is filled by the Lomond palaeomagnetic record. During this period (Fig. 12a) the field direction lay to the east with a high inclination and changed direction slowly. The Lomond data also extend the English geomagnetic record to cover the full period of the Japanese [22] 2000-year record. Although Aitken [9] notes some broad common trends between the virtual pole positions of the English and Japanese records from 1000 years B.P. to the present, our data, for the period between 2000 and 1000 years B.P., show little similarity to the Japanese. The Japanese archaeomagnetic directions follow two smooth anticlockwise loops between 1850 and 1150 years B.P., whereas the Lomond directions follow a

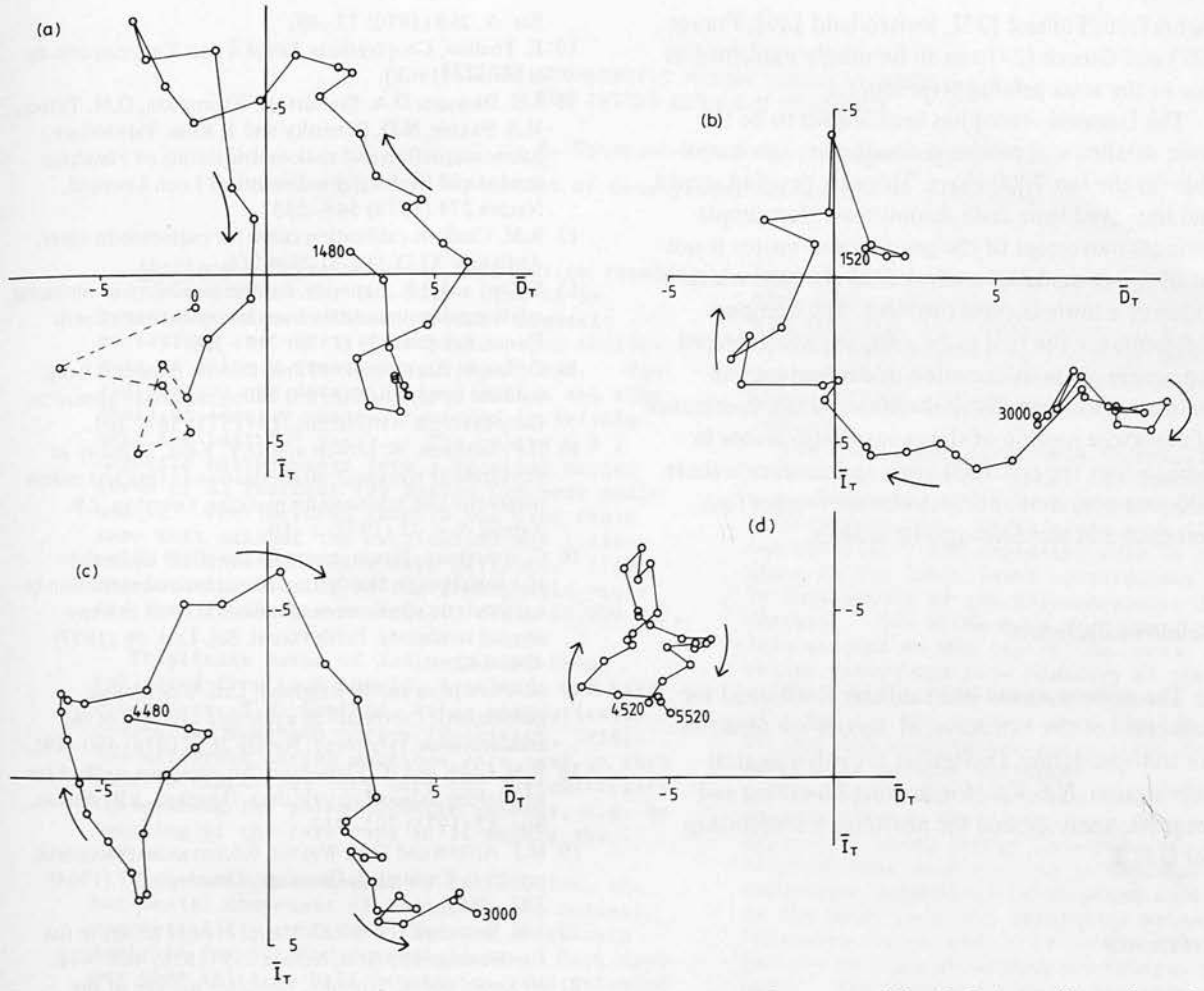


Fig. 12. Bauer plots of transformed declination and inclination averaged over the four cores of Fig. 10. Points at 40-year intervals for the time periods (a) 1500–0 years B.P., (b) 3000–1500 years B.P., (c) 4500–3000 years B.P., (d) 5500–4500 years B.P. The most recent record (dashed) is least accurately known due to coring disturbance.

clockwise path and move unusually slowly at 1600 and 1300 years B.P. We therefore attribute these geomagnetic variations, over the last 2000 years, to more localized non-dipole changes involving both westward and eastward drift, rather than to changes associated directly with the main dipole.

Comparison of British limnic palaeomagnetic records with those from other countries is a hazardous exercise on account of lack of dating controls. Although systematic errors in $^{14}C$ dating of lacustrine sediments resulting from hard-water effects, inwash of ancient carbon from old soil profiles, and inwash of graphite from tills have been documented for several years, it is only recently that their full extent is becoming apparent [23,24]. The frequency and degree of these errors are both greater than has often been assumed. Thus, unless lake sequences have other dating controls, e.g. tephra or pollen assemblage zone links to peat profiles (which are less susceptible to errors in $^{14}C$ dating), or unless a number of lakes have been investigated, their $^{14}C$ "ages" should be interpreted with caution. Bearing this in mind, fluctuations in geomagnetic direction of duration 2000–4000 years recorded in European lake sedi-

ments from Finland [25], Switzerland [26], France [27] and Greece [27] can all be simply explained as due to the same geomagnetic sources.

The Lomond record has been shown to be the most detailed and precise geomagnetic record available for the last 7000 years. This new detailed record and improved time scale demonstrate that simple periodic movement of the geomagnetic vector is not an adequate model of ancient field changes, which followed a more complex pattern. The Lomond sediments are the first to be analyzed which record repeatable phase information of declination and inclination changes. They demonstrate the dominance of clockwise motion of the geomagnetic vector in Europe over the last 5500 years and confirm a short 600-year period of anticlockwise movement first recognized in archaeomagnetic studies.

## Acknowledgements

The authors would like to thank F. Oldfield for collection of the 1-m cores, M. Baxter for facilities for isotopic dating, D. Stewart for palynological information, N.E.R.C. for funding for coring and magnetic analyses, and for providing a studentship for G.M.T.

## References

1 F.J.H. Mackereth, On the variation in direction of the horizontal component of remanent magnetization in lake sediment, Earth Planet. Sci. Lett. 12 (1971) 332–338.
2 R. Thompson, Long-period European geomagnetic secular variation confirmed, Geophys. J.R. Astron. Soc. 43 (1975) 847–859.
3 F.J.H. Mackereth, A portable core sampler for lake deposits, Limnol. Oceanogr. 3 (1958) 181.
4 L. Molyneux, R. Thompson, F. Oldfield and M.E. McCallan, Rapid measurement of the remanent magnetization of long cores of sediment, Nature 237 (1972) 42–43.
5 L. Molyneux and R. Thompson, Rapid measurement of the magnetic susceptibility of long cores of sediment, Geophys. J.R. Astron. Soc. 32 (1973) 479–481.
6 J.B. Sissons, The Quaternary in Scotland: a review, Scott. J. Geol. 10 (1974) 311–337.
7 N.D. Drndarsky, Ph.D. Thesis, University of Glasgow (1976).
8 D. Swann, Ph.D. Thesis, University of Glasgow (1978).
9 M.J. Aitken, Dating by archaeomagnetic and thermoluminescent methods, Philos. Trans. R. Soc. London, Ser. A, 269 (1970) 77–88.
10 E. Thellier, Geophysique Tirage à part Encyclopedie de la plèiade (1968).
11 J.H. Dickson, D.A. Stewart, R. Thompson, G.M. Turner, M.S. Baxter, N.D. Drnarsky and J. Rose, Palynology, palaeomagnetism and radiometric dating of Flandrian marine and freshwater sediments of Loch Lomond, Nature 274 (1978) 548–553.
12 R.M. Clark, A calibration curve for radiocarbon dates, Antiquity XLIX (1975) 251–266.
13 S. Levi and S.K. Banerjee, On the possibility of obtaining relative palaeointensities from lake sediments, Earth Planet. Sci. Lett. 29 (1976) 219–226.
14 C. Snape, An example of anhysteretic moments being induced by alternating field demagnetization apparatus, Geophys. J.R. Astron. Soc. 23 (1971) 361–364.
15 H.P. Johnson, W. Lowrie and D.V. Kent, Stability of anhysteretic remanent magnetization in fine and coarse magnetite and maghaemite particles, Geophys. J.R. Astron. Soc. 41 (1975) 1–10.
16 C. Amerigian, Measurement of the effect of particle size variation on the detrital remanent magnetization to anhysteretic remanent magnetization ratio in some abyssal sediments, Earth Planet. Sci. Lett. 36 (1977) 434–442.
17 R. Thompson and B. Berglund, Late Weichselian geomagnetic "reversal" as a possible example of the reinforcement syndrome, Nature 263 (1976) 490–491.
18 R.M. Clark and R. Thompson, An objective method for smoothing palaeomagnetic data, Geophys. J.R. Astron. Soc. 52 (1978) 205–213.
19 M.J. Aitken and G.H. Weaver, Recent archaeomagnetic results in England, J. Geomagn. Geoelectr. 17 (1964) 393–396.
20 J.M. Harwood and S.R.C. Malin, Present trends in the Earth's magnetic field, Nature 259 (1976) 469–471.
21 N. Kawai and K. Hirooka, Wobbling motion of the geomagnetic dipole field in historic time during these 2000 years, J. Geomagn. Geoelectr. 19 (1967) 217–227.
22 K. Hirooka, Archaeomagnetic study for the past 2000 years in southwest Japan, Mem. Fac. Sci., Kyoto Univ., Geol. Mineral. Ser. XXXVIII (1971) 167–207.
23 I.U. Olsson, Some problems in connection with the evaluation of $^{14}C$ dates, Geol. Fören. Stockholm Förh. 96 (1974) 311–320.
24 F. Oldfield, Lakes and their drainage basins as units of sediment based ecological study, Progr. Phys. Geogr. 1 (1977) 460–504.
25 J.C. Stober and R. Thompson, Palaeomagnetic secular variation studies of Finnish lake sediment and the carriers of remanence, Earth Planet. Sci. Lett. 37 (1977) 139–149.
26 R. Thompson and K. Kelts, Holocene sediments and magnetic stratigraphy from Lakes Zug and Zurich, Switzerland, Sedimentology 21 (1974) 577–596.
27 K.M. Creer, P.W. Readman, R. Thompson, T.E. Hogg, S. Papamarinopoulos, J.C. Stober and G. Turner, Secular variation obtained from European lake sediments, EOS 58 (1977) 709.

# BRITISH GEOMAGNETIC MASTER CURVE 10,000-0 yr B.P. FOR DATING EUROPEAN SEDIMENTS

R. Thompson and G. M. Turner

Department of Geophysics, University of Edinburgh.

Abstract. Palaeomagnetic inclination records are demonstrated for the first time to be repeatable between lakes. These magnetic variations can now be interpreted with confidence as being a true geomagnetic record. New radiocarbon age determinations refine the time scale of secular changes recorded in Britain over the last $10^4$ years. The paired D & I magnetic measurements form a detailed master curve of 23 features for dating European sediments. The improved records and time scale show that neither the declination nor inclination fluctuations have been periodic. Tight or clockwise looping of the geomagnetic vector has been dominant over Britain since 10,000 B.P.

Triplicate cores of sediment have been collected from Loch Lomond, Scotland, and Lake Windermere, N.W. England, using pneumatically controlled Mackereth corers (Mackereth, 1958). Two different coring machines were used in each lake to check that they were not systematically influencing the palaeomagnetic records, e.g. by twisting of the core tube as it enters the sediment.

Whole-core measurement of declination, the horizontal component of remanence and magnetic susceptibility confirmed that the cores were suitable for further investigation. Each core was then split in half lengthwise, and oriented sub-samples taken in 8.2 ml cubic boxes, at 2.5 cm intervals. These samples were stored in zero magnetic field prior to measurement in a slow speed spinner fluxgate magnetometer (Molyneux, 1971). Special care was taken to ensure the sediment remained fresh and did not dry out.

Finer detail and better reproducibility were recorded in declination and inclination logs (Fig. 1) from both lakes, than had previously been attained, indicating that they provide a reliable geomagnetic signature. Ten declination and 13 inclination features are identified in all the records (with the exception of the top metre of W3, which was disturbed in coring). Partial alternating field demagnetization of a representative selection of samples used in this study, up to peak fields of 90 mT, showed stable magnetization, with an average median destructive field of 25 mT in Windermere and 40 mT in Lomond. No low stability or viscous components with directions different from the NRM were detected. Thus, both the NRM and partially demagnetized remanence record the past directional changes of the geomagnetic field.

Thirty published radiocarbon age determinations and palynological age controls (Mackereth, 1971; Thompson, 1975; Dickson et al, 1978; Thompson & Wain-Hobson, 1979), from cores with palaeomagnetic records from 5 British lakes, have been used to construct a time scale summarized in Table 1 and used in plotting Fig. 1. Features a, b, c, and $\alpha$, $\beta$, $\gamma$, $\delta$, have been located on the time scale by comparison with the archaeomagnetic results of Aitken (1970) & Thellier (1968) and observatory records.

The Windermere cores were internally correlated using thin clay bands; the Lomond cores were internally correlated using magnetic susceptibility features. Thus, since both lithology and susceptibility are dependant only on the material input to the lake, these correlations are completly independent of the palaeomagnetic direction changes. The Windermere and Lomond records were then matched at the top of the cores, and at the pollen assemblage zone boundary of the Ulmus decline, which lies between magnetic features of g and l. The records were finally stretched so that the declination oscillation f-e-d also correlated between the lakes.

The calibrated time scale (Table 1) was then used to convert the depth scale into equal intervals, using linear interpolation between adjacent data points so as to minimize the dependance introduced between new data points. As the cores were not absolutely oriented a reference system had to be chosen, in which comparison of the palaeomagnetic records could be made. The records of each core were rotated ('transformed') so that its mean vector, calculated by averaging over the direction cosines, had zero declination and inclination. This reference system has the advantages that (a) equal weight is given to both the transformed declinations and inclinations and (b) smoothing methods such as that of Clark & Thompson (1978) can be adapted to process the paired data.

The major features in the new records can be recognised, with hindsight, in the original Windermere declination measurements (Fig.2). Also in the new records extra detail can be seen to be repeatable between cores. The palaeomagnetic logs show that there has been no dramatic change in the style of secular variation in Britain over the last 10,000 years.

It is clear that the fluctuations in both declination and inclination are not periodic over many cycles. For example, the duration of declination cycles steadily decreases from 4,000 to 1,700 years. The secular variations are probably built up from a number of disconnected, short, variable features associated with the growth, movement and decay of magneto-hydrodynamic centres in the Earth's core. Such a combination of features would be expected to lead to the power spectrum obtained from these records, which peaks in a spread of periods between 2,000 and 3,000 years. Bauer plots, of transformed declination against inclination, averaged over the whole suite of cores, show that the geomagnetic vector has



Paper number 9L0103.
0094-8276/79/049L-0103$01.00

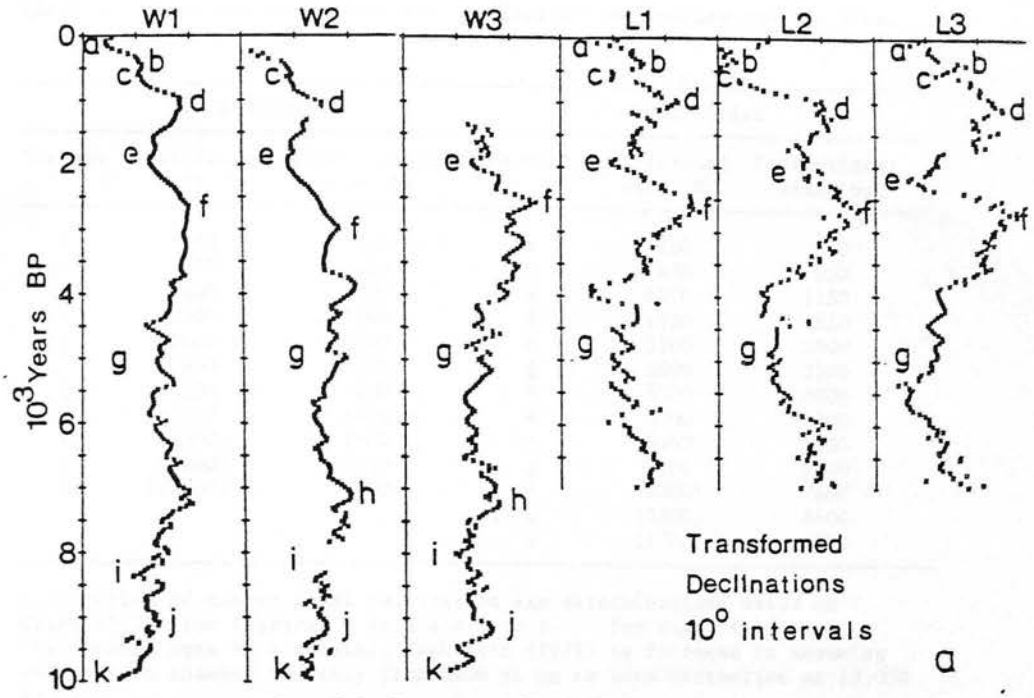


Fig. 1a. Transformed declinations plotted against preferred time for three Lake Windermere cores (W1-3) and three Loch Lomond cores (L1-3). Symbols refer to characteristic features which may be sharp (e.g. 'f') or drawn out (e.g. 'g').

moved in tight closed loops between 10,000 and 7,000 yrs B.P. This behaviour is followed by more open, clockwise looping, interrupted only by one extensive period of anticlockwise movement from 1,100 to 600 B.P. which is also seen in archaeomagnetic curves. The rate of change of direction varies considerably and the magnetic vector shows periods of unusually slow movement, for example, around 1,600 B.P.

The nature of the British variations suggests that assignment of magnetic ages by interpolation or extrapolation from major secular variat-

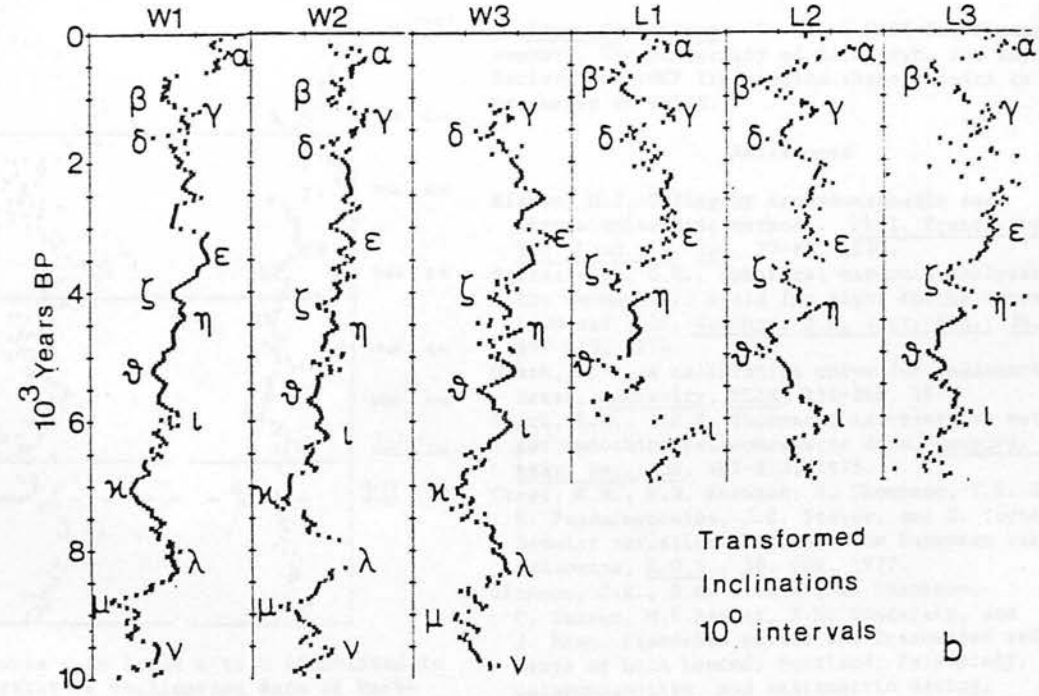


Fig. 1b. Transformed inclinations for the same six cores as Fig. 1a and the same time scale.

TABLE 1. Preferred time scale for declination and inclination features.

| Declination | | | Inclination | | |
|---|---|---|---|---|---|
| Feature | Calibrated date BP | Conventional date bp | Feature | Calibrated date BP | Conventional date bp |
| a | 150 | 150 | α | 250 | 250 |
| b | 450 | 450 | β | 650 | 650 |
| c | 600 | 600 | γ | 1150 | 1150 |
| d | 1000 | 1000 | δ | 1650 | 1650 |
| e | 2000 | 2000 | ε | 3100 | 2900 |
| f | 2600 | 2500 | ξ | 3800 | 3500 |
| g | 4900 | 4200 | η | 4300 | 3800 |
| h | 7100 | 6200 | θ | 5000 | 4300 |
| i | (8300) | 7400 | ι | 6000 | 5200 |
| j | (9100) | 8800 | χ | 7100 | 6200 |
| k | (10000) | 10000 | λ | (8300) | 7400 |
| | | | μ | (8800) | 8400 |
| | | | ν | (9700) | 9700 |

Calibration of conventional radiocarbon age determinations based on Clark (1975) for features a to h and α to χ. For older features (calibrated ages in brackets), Mackereth (1971) is followed in assuming calibration changes smoothly from 6500 yr bp to zero correction at 10,000 yr bp.

ion peaks is liable to be a hazardous exercise, but it has been attempted by Stuiver (1978). The palaeomagnetic record can, however, be used as a rapid dating tool over the last $10^4$ years by correlation of the declination features a to k and inclination features α to ν. Palaeomagnetic records from Finland (Stober and Thompson, 1977), Switzerland (Thompson and Kelts, 1974) and Greece (Creer et al., 1977) and historic records (Barraclough, 1974) suggest that the master curve of Fig. 1 will be useful over the whole area of Western Europe for the last $10^4$ years.

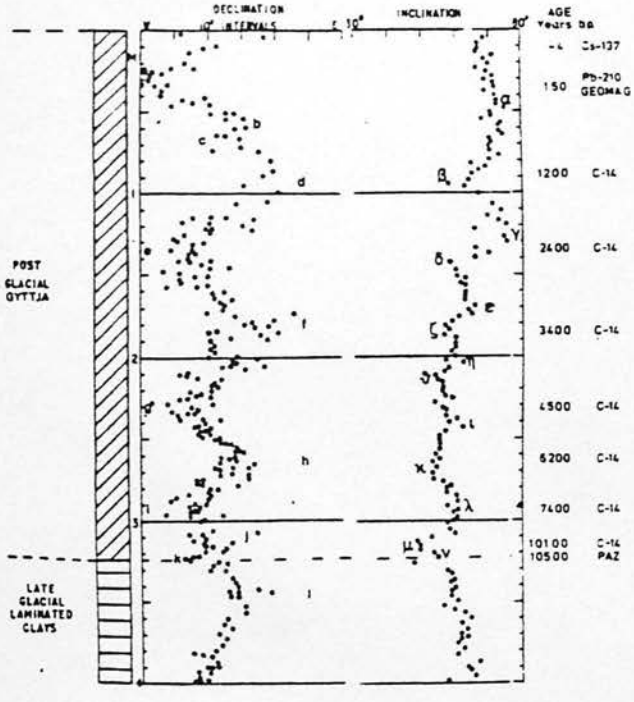


Fig. 2. Features a to l and α to ν identified in the original relative declination data of Mackereth (1971) and inclination data of Thompson (1977).

Acknowledgements. We thank NERC for financial support. The University of Edinburgh, the Royal Society and IGCP 128 enabled these results to be presented at IAS X.

References

Aitken, M.J, Dating by Archaeomagnetic and Thermoluminescent methods. Phil. Trans. Roy. Soc. Lond., A, 269, 77-88, 1970.

Barraclough, D.R., Spherical harmonic analyses of the geomagnetic field for eight epochs between 1600 and 1910, Geophys. J.R. astr. Soc., 36, 497-513, 1974.

Clark, R.M., A calibration curve for radiocarbon dates, Antiquity, XLIX, 251-266, 1975.

Clark, R.M., and R. Thompson, An objective method for smoothing palaeomagnetic data, Geophys. J.R. astr. Soc., 36, 497-513, 1975.

Creer, K.M., P.W. Readman, R. Thompson, T.E. Hogg, S. Papaminopoulos, J.C. Stober, and G. Turner, Secular variation obtained from European lake sediments, E.O.S., 58, 709, 1977.

Dickson, J.H., D.A. Stewart, R. Thompson, C. Turner, M.S.Baxter, N.D. Drndarsky, and J. Rose, Flandrian marine and freshwater sediments of Loch Lomond, Scotland; Palynology, palaeomagnetism and radiometric dating, Nature, 274, 548-553, 1978.

Mackereth, F.J.H., A portable core sampler

for lake deposits. Limnol. Oceanogr., 3, 181-191, 1958.

Mackereth, F.J.H., On the variations in direction of the horizontal component of remanent magnetization in lake sediments, Earth. Planet. Sci. Lett., 12, 332-338, 1971.

Molyneux, L., A complete results magnetometer for measuring the remanent magnetization of rocks, Geophys. J.R. astr. Soc., 24, 429-434, 1971.

Stober, J.C., and R. Thompson, Palaeomagnetic secular variation studies on Finnish lake sediment and the carriers of remanence, Earth, Planet. Sci. Lett., 139-149, 1977.

Stuiver, M., Radiocarbon timescale tested against magnetic and other dating methods, Nature, 273, 271-274, 1978.

Thellier, E., Encyclopedie de la pleiade, 326-376.

Thompson, R., Long period European geomagnetic secular variation confirmed, Geophys. J.R. astr. Soc., 43, 847-859, 1975.

Thompson, R., Stratigraphic consequences of palaeomagnetic studies of pleistocene and recent sediments, Jl. geol. Soc., Lond., 133, 51-59, 1977.

Thompson, R., and K. Kelts, Holocene sediments and magnetic stratigraphy from Lakes Zug and Zurich, Switzerland, Sedimentology, 21, 577-596, 1974.

Thompson, R., and T. Wain-Hobson, Palaeomagnetic and stratigraphic study of the Loch Shiel Marine regression and overlying gyttja, J. Geol. Soc., London (in press), 1979.

(Received October 16, 1978;
accepted January 8, 1979.)